



Computed Tomography in the Diagnosis and Treatment of Canine Tarsocrural Osteochondrosis

Ingrid Gielen

Proefschrift ter verkrijging van de graad van Doctor in de Diergeneeskundige
Wetenschappen (PhD) aan de Faculteit Diergeneeskunde, Universiteit Gent

**Promotor: Prof. Dr. H. van Bree
Co-promotor: Prof. Dr. Y. Palmers**

Vakgroep Medische Beeldvorming van de Huisdieren
Faculteit Diergeneeskunde
Universiteit Gent

Dit proefschrift draag ik op aan mijn papa, Dr. Jan Gielen

Moed is niet het ontbreken van
angst of wanhoop,
maar de kracht om die te overwinnen.

D. Steel

LIST OF ABBREVIATIONS

CL: clinical

CT: computed tomography

DFOV: display field-of-view

DJD: degenerative joint disease

dorsal plane (veterinary medicine) = coronal plane (human medicine)

3-D: three-dimensional

HU: Hounsfield units

kVp: peak kilovoltage

LTOC: lateral tarsocrural osteochondrosis

mAs: milliampereseconds

MPR: multiplanar-reformatting

MTOC: medial tarsocrural osteochondrosis

NCL: non-clinical

OA: osteoarthritis

OC: osteochondrosis

OCD: osteochondritis dissecans

ROI: region of interest

(S)FOV: (scan) field-of-view

TOC: tarsocrural osteochondrosis

transversal plane (veterinary medicine) = axial plane (human medicine)

WL: window level

WW: window width

LIST OF ABBREVIATIONS

List of abbreviations

GENERAL INTRODUCTION: Review of the literature	1
1. Computed tomography in small animals. Part 1: Technical aspects	3
Adapted from: Kompendium der Allgemeinen Veterinärchirurgie 2003; 3. Bildgebende Verfahren, c. Computertomographie, Kramer M. (ed.), Schlütersche Verlag, Hannover, Deutschland: In press. And: <i>Vlaams Diergeneeskundig Tijdschrift</i> 2003: In press.	
2. Computed tomography in small animals. Part 2: Clinical applications	25
Adapted from: Kompendium der Allgemeinen Veterinärchirurgie 2003; 3. Bildgebende Verfahren, c. Computertomographie, Kramer M. (ed.), Schlütersche Verlag, Hannover, Deutschland: In press. And: <i>Vlaams Diergeneeskundig Tijdschrift</i> 2003: In press.	
3. Tarsocrural osteochondrosis in the dog	57
AIMS OF THE STUDY	73
<u>CHAPTER 1.</u> COMPUTED TOMOGRAPHY OF THE TARSAL JOINT IN CLINICALLY NORMAL DOGS	77
Adapted from: <i>American Journal of Veterinary Research</i> 2001; 62: 1911-1915.	
<u>CHAPTER 2.</u> RADIOGRAPHIC, COMPUTED TOMOGRAPHIC AND ARTHROSCOPIC FINDINGS IN 23 DOGS WITH OSTEOCHONDROSIS OF THE TARSOCRURAL JOINT	95
Adapted from: <i>Veterinary Record</i> 2002; 150: 442-447.	

<u>CHAPTER 3.</u>	COMPUTED TOMOGRAPHY COMPARED WITH RADIOGRAPHY IN THE DIAGNOSIS OF TARSOCRURAL OSTEOCHONDROSIS OF THE LATERAL TROCHLEAR RIDGE IN THE DOG	117
	Adapted from: <i>Veterinary and Comparative Orthopaedics and Traumatology</i> 2003; Manuscript accepted for publication.	
	And: Abstract 12 th International Veterinary Radiology Association. Obihiro-Japan, August 21-25, 2000. p 29.	
	<i>Veterinary Radiology & Ultrasound</i> 2001; 42: 174.	
	Award for the best oral presentation.	
CHAPTER 4.	COMPARISON OF MORPHOLOGICAL AND CLINICAL FEATURES BETWEEN MEDIAL AND LATERAL, AND CLINICAL AND NON-CLINICAL CANINE TARSOCRURAL OSTEOCHONDROSIS LESIONS	131
	Adapted from: <i>American Journal of Veterinary Research</i> 2003; Manuscript submitted for publication.	
CHAPTER 5.	MINIMALLY INVASIVE TREATMENT OF CANINE TARSOCRURAL OSTEOCHONDROSIS: A LONG-TERM FOLLOW-UP STUDY OF 30 CASES	145
	Adapted from: <i>Veterinary Surgery</i> 2003; Manuscript submitted for publication.	
CHAPTER 6.	THE VALUE OF COMPUTED TOMOGRAPHY IN THE CLINICAL COURSE OF CANINE TARSOCRURAL OSTEOCHONDROSIS	163
	Adapted from: Abstract 9 th Annual Conference EAVDI (European Association of Veterinary Diagnostic Imaging). 24-27 th July 2002, Archena (Murcia), Spain. p 75.	
	<i>Veterinary Radiology & Ultrasound</i> 2003; 44: p 253.	
GENERAL DISCUSSION		179
SUMMARY		191
SAMENVATTING		199
DANKWOORD		207
CURRICULUM VITAE		211

GENERAL INTRODUCTION: Review of the literature

1. Computed tomography in small animals. Part 1: Technical aspects
Adapted from: Kompendium der Allgemeinen Veterinärchirurgie 2003;
3. Bildgebende Verfahren, c. Computertomographie, Kramer M. (ed.),
Schlütersche Verlag, Hannover, Deutschland and Vlaams Diergeneeskundig
Tijdschrift 2003: In press

2. Computed tomography in small animals. Part 2: Clinical applications
Adapted from: Kompendium der Allgemeinen Veterinärchirurgie 2003;
3. Bildgebende Verfahren, c. Computertomographie, Kramer M. (ed.),
Schlütersche Verlag, Hannover, Deutschland and Vlaams Diergeneeskundig
Tijdschrift 2003: In press.

3. Tarsocrural osteochondrosis in the dog

1. COMPUTED TOMOGRAPHY IN SMALL ANIMALS

Part 1: TECHNICAL ASPECTS

I. Gielen, A. Van Caelenberg, H. van Bree

Department of Medical Imaging, Faculty of Veterinary Medicine,
Ghent University, Salisburylaan 133, Merelbeke, Belgium

Adapted from:

I. Gielen, H. van Bree. Kompendium der Allgemeinen Veterinärchirurgie 2003;
3. Bildgebende Verfahren, c. Computertomographie, Kramer M. (ed.),
Schlütersche Verlag, Hannover, Deutschland: In press.

And

I. Gielen, A. Van Caelenberg, H. van Bree. Computed tomography in small
animals. Part 1: Technical aspects. Vlaams Diergeneeskundig Tijdschrift 2003: In
press.

SUMMARY

Computed tomography (CT) is a cross-sectional imaging technique using x-rays and computers that is becoming increasingly available to veterinarians. During CT scanning, an x-ray tube rotates around the patient. Multiple radiographic projections of a particular slice of tissue are made, and information from all projections is combined to create a single tomographic (slice) image. CT images provide accurate anatomic evaluation of tissue planes and regions that often cannot be visualised with conventional radiography. Compared to radiography, CT uses a wide range of grey shades which enables a high contrast resolution, very important for soft tissue discrimination. Many imaging artefacts can occur in the process of generating CT images. A good understanding of these artefacts is necessary to enable an accurate interpretation of the CT images. After the scan examination, images in other planes can be produced using computerised reformatting, which is of help in evaluating the extent of a lesion. To increase the amount of soft tissue information, contrast agents can be used. Positive contrast techniques are of greatest importance e.g. for demonstrating brain tumours. Biopsies can also be obtained under CT guidance, a procedure that can be accurately performed.

INTRODUCTION

Computed tomography (CT) is a cross-sectional imaging technique using x-rays and computers (Huygens and Baert, 1983; Hathcock and Stickle, 1993). With the discovery of x-rays in 1895, a new era of visualisation of internal body structures had begun. The discovery was almost immediately recognised and accepted for its potential as a great medical diagnostic tool. The technique has been characterised by many evolutionary improvements during the intervening 85 years. In the early 1970s a new technique of x-ray imaging had a revolutionary impact on medicine. In 1971 an x-ray scanner has been developed which produced cross-sectional images of the brain by using several different scientific concepts, some known for over 50 years (Robb, 1982). The tomographic nature of CT images provides accurate anatomic evaluation of tissue planes and regions which are often impossible to visualise with conventional radiography. The most valuable property of this new technique is its high contrast resolution. The ability to image in cross-section makes it possible to build up a three-dimensional picture which is invaluable for understanding normal anatomy and for planning surgical or radiotherapy treatment. The greatly increased tissue resolution allows differentiation between fluid and solid tissues and assessment of the internal structure of soft tissues (Dennis, 1995).

HISTORY

Already in 1963, Cormak was able to determine the absorption coefficient of x-rays through a flat object and to measure the variations in intensity of the x-ray beam in different planes. In 1967, Hounsfield had the idea that it must be possible to measure the intensity of the x-ray beam as it is sent through the body. He understood that a computer was needed to make the calculations. In 1972, Hounsfield introduced the EMI Mark I brain scanner for computerised axial transverse scanning of the head. Initially, the procedure was known as CAT scanning (Computerised Axial Tomography or Computer-Assisted Tomography), but the preferred term now is CT or Computed Tomography. This

original scanner was capable of producing a pair of cross-sectional images following a four to five minute scan time (Wortman, 1986).

The first-generation scanners used a single, narrow x-ray beam and one single detector. Hooked together, they moved in straight and parallel lines across the patient, radiation and recordings being made at the same time. At the end of the linear motion, the tube and the detector were rotated 1° and the linear motion was repeated again, in all, 180 times. With these so-called translation rotation scanners, a scan lasted 5 to 6 minutes per slice to acquire the data (Hathcock and Stickle, 1993; Wegener *et al.*, 1993).

A wide, fan-shaped x-ray beam and multiple detectors were used in the second-generation units, the so-called rotation-only scanners, allowing a larger rotation between linear motions. Scan times were reduced to less than 1 minute (Wegener *et al.*, 1993).

Third and fourth-generation units employ a rotating x-ray tube with movable or stationary detectors (Figure 1). Scan time with these units is only a few seconds.

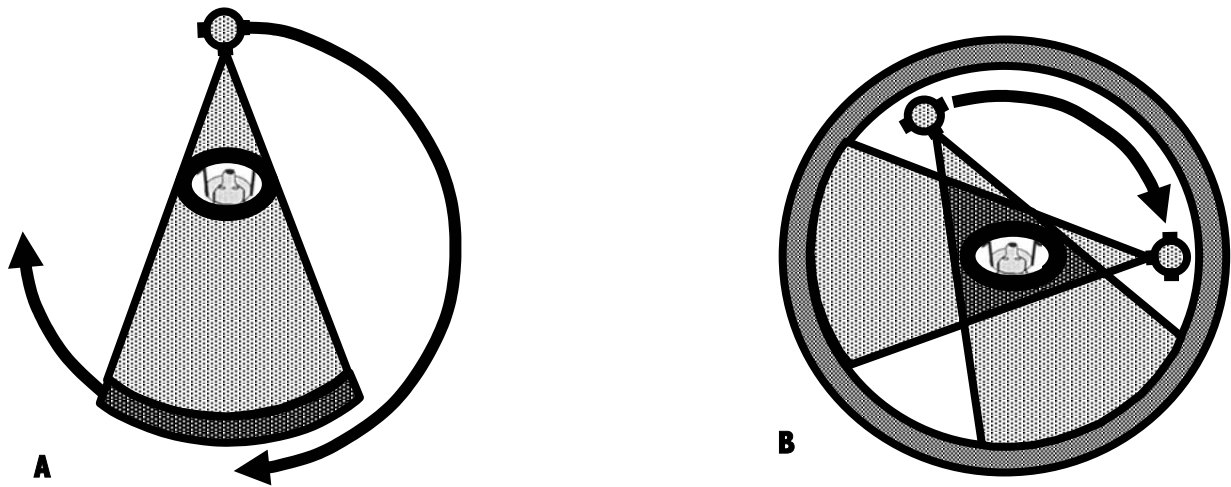


Figure 1: Rotation scanner of the third generation with movable detectors (A) and of the fourth generation with stationary detectors (B).

The fifth-generation scanners were developed primarily for high-speed scanning. With the use of spiral CT, the scan time of data acquisition has been dramatically reduced, resulting in a much quicker overall examination, which is especially important in the investigation of small animals in reducing the number of motion artefacts. Thinner slices

and faster imaging times are now possible, resulting in increased image resolution (Dennis, 1996; Seeram, 2001a).

The newest development in CT-scanners is the multislice CT or the multirow–detector CT scanners. These scanners produce multiple (2, 4 and 16) spiral acquisition slices simultaneously and gather a high data set of the scanned volume. This information can be processed in order to provide images of slices in all planes and directions. The newest multislice CT-scanners permit submillimeter collimation slice-width, and can provide an isotropic data set which allows not only an optimal in plane resolution but also an identical spatial resolution of multiplanar-reformatting (MPR) in all directions: the image voxels have equal size in all directions (Seeram, 2001b).

GENERAL PRINCIPLES OF COMPUTED TOMOGRAPHY

The CT image

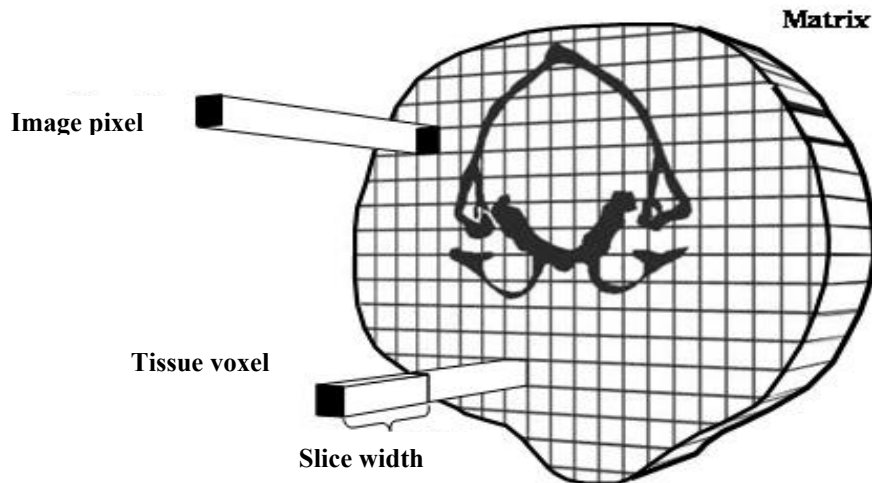


Figure 2: Composition of the CT image: the smallest square unit of a CT image is the pixel. Each pixel is a two-dimensional representation of a three-dimensional volume of tissue (voxel) from the body slice.

In classic sequential CT, multiple radiographic projections of a particular slice of tissue are made and information from all projections is combined to create a single tomographic (slice) image. A complete CT scan consists of a number of slices or images, usually

contiguous, through the area of interest. The CT image is composed of a matrix of small tiny squares, called pixels. Each pixel is a two-dimensional representation of a three-dimensional volume of tissue, the voxel. The third dimension of this volume of tissue is the thickness of the slice of the tissue (Figure 2). The matrix may vary from 256x256 to 1024x1024 pixels. The more pixels in a matrix, the less the transition between the different pixels is visible and the better the spatial resolution (Huygens and Baert, 1983; Feeney *et al.*, 2001).

The colours that are used are black, white and shades of grey. CT systems can record thousands of grey shades and separate densities ranging from air to high-density metal can be visualised. For every degree of radioabsorption of a particular tissue or object, there is a corresponding shade of grey (see ahead for window settings). Each tissue has its own characteristic attenuation coefficient (Hathcock and Stickle, 1993).

The CT process

In CT images, the shade of grey in the pixels represents the linear attenuation coefficient of the tissues in that voxel. The process of computed tomography determines this linear attenuation coefficient to make a useful image (Assheuer and Sager, 1997). Therefore, all the components of the CT equipment are used: the gantry and the patient table, the computer, the imaging computer and display console, and the camera for hard copies.

The gantry contains the x-ray tube, x-ray collimators and x-ray detector. A CT scanner's gantry can, within limits, be tilted to angle the scan plane. In the spine, for example, the scan plane has to be parallel to the intervertebral disc space. For brain examinations, the scan plane has to be transverse, i.e. perpendicular to the hard palate. In CT, the choice of peak kilovoltage (kVp) is usually limited and a high kVp technique is always used. The kVp should be increased for very thick and dense body parts to ensure adequate penetration, and for very dense objects to minimise beam hardening. Because of the limitations of thermal tube capacities with a given focal spot size, the choice of milliamperes seconds (mAs) also depends on the selected kVp. High mAs will increase image detail because it reduces image noise. When thin sections are made, an increase in mAs can compensate for otherwise very interfering image noise associated with narrow slice collimation (Seeram, 2001c).

Scan time is the time necessary for the x-ray tube to rotate around the patient while making the exposure. A longer scan time may result in improved image detail since the number of projections can be higher, but may cause motion artefacts (including respiratory motion) and can eventually cause x-ray tube heating (Stickle and Hathcock, 1993). A 3-second scan time is mostly used in our department. Effects of breathing motion are not a significant problem when scanning joints. Obviously, patient motion should be minimised by using general anaesthesia. Because CT scanners use ionising radiation, the anaesthesiologist must take the appropriate radioprotective precautions. Therefore, monitoring of the patient should be done with acoustic monitors or have displays that can be seen from a distance (Robertson, 1999). For protective reasons for all personal, the operator site is also behind a protective shield.

The patient lies horizontally on a movable table, in a way that images are transverse to the long axis of the body. First a scout view of the object is obtained by moving the table through the gantry as the x-rays are being emitted while the tube and detectors remain stationary. A scout view is similar to a plain radiograph and is in fact a digital radiograph. The scout view is used to verify patient positioning and to assist the operator in planning the number and location of slices that are required (Wortman, 1986).

During CT scanning, an x-ray tube emits the x-ray beam and rotates 360° around the patient. A first collimator, located between the tube and the patient, determines the thickness of the slice (1-10 mm). A second collimator located between the patient and the detector, also influences the slice width and limits the interference of scattered x-rays. The thinner the slice, the higher the spatial resolution, but an increased number of slices requires more scan time. Thick slices may result in small lesions remaining undetected because the attenuation information within each tomographic slice is averaged (partial volume effect). Slices of 10 mm are used when scanning the entire canine thorax or abdomen. In brain CT, 5 mm thick slices are normally used. If it is essential to image the entire object, continuous slices are required. This leads to an increased overall scanning time and tube load. Therefore, thicker slices are often chosen instead. On the other hand, there are body parts and conditions where continuous scanning is not essential. In these circumstances, scanning with a thin slice width and a few mm slice interval is often a

better alternative (Stickle and Hathcock, 1993). One must be aware of information gaps between the different sections.

Depending on the kind of tissue and the thickness of the slices, the x-ray beam is absorbed or scattered. The x-ray photons emerging from the patient are absorbed by the x-ray detectors, converted to an electrical signal, amplified and converted into a number (numeric value). This number is relative to the intensity of the beam as it emerges from the patient, and is equivalent to the attenuation. This number is processed in the computer. The x-ray tube circles around the patient and data are collected from all angles. In this way, different numbers are obtained and a mathematical method is used to determine a specific number, the CT number, for each pixel (Hathcock and Stickle, 1993). The range of these numbers assigned to the various tissues is from +1000 to -1000 Hounsfield Units (HU), where +1000 is assigned to cortical bone, -1000 to air and 0 to water. Thus the more radiopaque the tissue, the more attenuation occurs within that voxel, the higher the CT number and the whiter that area of the image. Groups of CT numbers are awarded to a particular scale of grey. The operator controls the tissue contrast. One can also choose the central grey colour (window level (WL)) and the range above and below the window (window width (WW)). When the computer receives a CT number above or below the window edge, a white or black density is outlined (Figure 3).

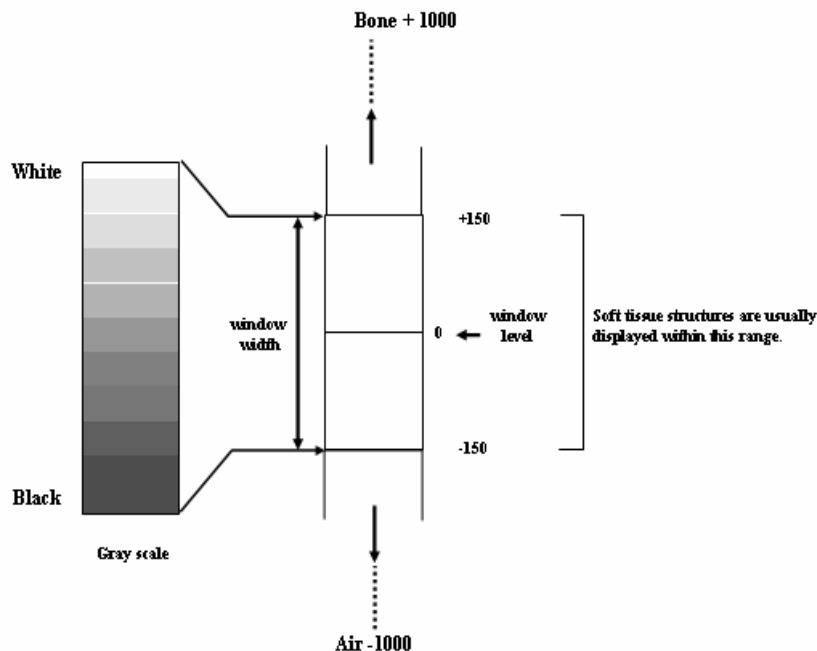


Figure 3: For the final CT image, the CT numbers of the Hounsfield scale are converted to a grey scale. In the Hounsfield scale, +1000 is assigned to cortical bone, -1000 to air and 0 to water. The central grey colour (window level) and the range above and below this window level (window width) can be chosen.

A narrow WW maximises tissue contrast between tissues with a small difference in attenuation coefficient (soft tissue window). A wide WW is selected to view bony structures so that the bones stand out from the soft tissues (bone window) (Dennis, 1996; Hathcock and Stickle, 1993; Lee *et al.*, 1999).

Artefacts

Using CT, imaging artefacts may occur. A CT artefact is defined as any discrepancy between the reconstructed CT numbers in the image and the true attenuation coefficient of the object (Hsieh, 1995). This definition implies that anything that causes an incorrect measurement of transmission readings by the detectors will result in an image artefact (Shogo *et al.*, 1995; Seeram, 2001d). Artefacts can be very confusing and degrade image quality and affect the perceptibility of detail. A good understanding of these phenomena is required to enable accurate interpretation (Seeram, 2001d).

The most common artefact seen on CT images is streaking. This artefact can have a number of causes, including patient motion, presence of a high-density object (usually metal) in the scanning field, the effect of ‘beam hardening’, ‘aliasing’, ‘edge gradient effect’ and the presence of objects out of the scan field of view (Hathcock and Stickle, 1993).

In an individual slice, the assumption is that no movement occurred during the scan. In imaging small animals, patient movement is common and can create streaking and blurring of the image (Figure 4) (Feeney *et al.*, 1991a). The computer averages the density of the pixels and is affected by misinformation caused by the motion. The severity of streak artefacts depends not only on the amount of motion but also, to some extent, on the density of the part in motion (Hathcock and Stickle, 1993).

Radiation streaks, due to an exceptionally high attenuation, arising from metal implants, gun pellets and plastic tubes can extend across the entire image (Figure 5).

‘Beam hardening’ artefacts are the result of differences in the energy of the x-ray beam that fool the mathematical algorithm. Whenever the x-ray beam travels through substantial volumes of dense bone or metal, lower energy x-rays are absorbed by the dense material. The mean energy of the resulting x-ray beam increases and the tissues on

the far side of the dense object seem to be more radiolucent than they actually are. This is due to the over-penetration of the distal tissues by the higher energy x-ray beam.

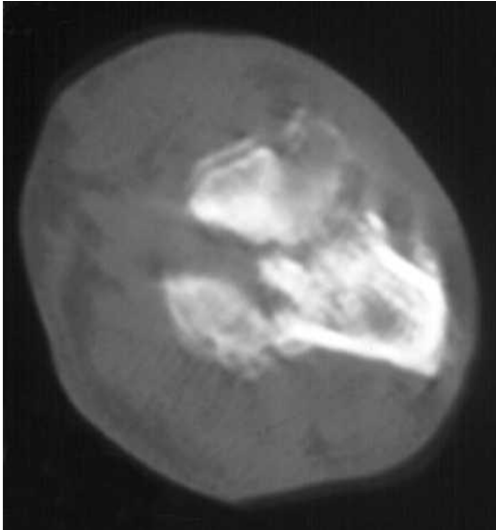


Figure 4: Motion artefact on a CT image through a pathologic elbow joint: blurring of the image due to patient movements.



Figure 5: Metal artefact due to a screw in the humeral condyle, causing streaking in the image.

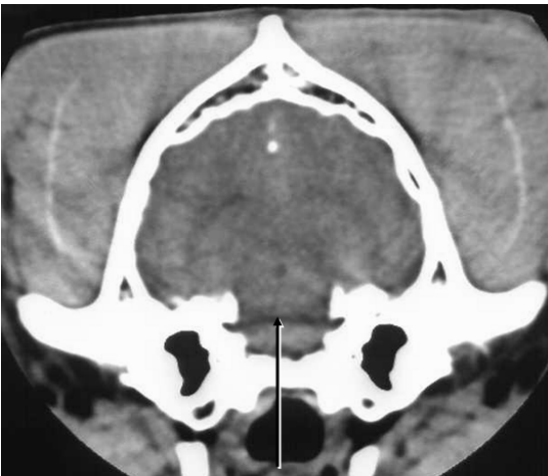


Figure 6: Between the petrous temporal bones, the area of the ventral cerebellum and brainstem appears blacker (arrow) than the rest of the brain because the beam was selectively hardened as it passed through the petrous part of the temporal bone. This artefact is referred to as beam hardening.



Figure 7: On this transverse CT scan through the frontal sinuses, aliasing artefacts are visible (arrows). These are streaks from the edges of high density structures. They may sometimes mask detail and result in misinterpretation of the image.

This phenomenon results in dark streaks in areas near high-density/low-density interfaces. This artefact is best seen in the transverse image of the brain between the petrous temporal bones (Figure 6). In the canine skull, which is relatively thicker than the human skull, lesions in the pituitary and caudal fossa of the skull may be overlooked due to beam hardening (Dennis, 1996; Feeney *et al.*, 1991a; Lee *et al.*, 1999; Seeram, 2001d). ‘Aliasing artefacts’ are streaks emanating from the edges of high-density structures, which result from inadequate sampling of the x-ray projection data. These streaks are sometimes in a pattern that may mask detail within the image (Figure 7) (Hathcock and Stickle, 1993; Lee *et al.*, 1999). The edge gradient effect consists of the creation of lucent edges or borders near very radiopaque objects such as the edges of the skull or the edges of the pelvis. These could be overestimated and misinterpreted as air instead of merely as artefacts of the image processing procedure (Feeney *et al.*, 1991a; Lee *et al.*, 1999). Objects outside the scanning field of view also cause streak artefacts. These interfere with the reference detectors or alter the x-ray beam (Hathcock and Stickle, 1993). Therefore, it is necessary to try to move any body parts which are not to be imaged out of the scan plane. It is, for example, possible to scan the canine elbow joints without superimposition of the head and neck, which significantly improves the image quality (Figure 8) (De Rycke *et al.*, 2002).



Figure 8: Positioning of a dog in lateral recumbency to scan the elbow joints (arrow) without superimposition of the head (asterisk) and neck. Interference from body parts outside the scanning field, which may cause streak artefacts, is avoided through the use of this positioning.

Ring artefacts are typical for third generation CT scanners. They occur when a channel of the detector provides input/output properties which are different from those of other channels. These artefacts are ring shaped obstructive shadows centered on the field of the view (Figure 9) (Shogo *et al.*, 1995; Lee *et al.*, 1999).

Finally, an artefact may be caused by the partial volume effect, which results from the inclusion of two different tissue densities within the thickness of the slice (Figure 10) (Feeney *et al.*, 1991a). These different densities are displayed as an average within the voxel. The CT numbers are not accurate, and at certain tissue interfaces, the margins or borders are indistinct or fuzzy. These artefacts can lead to a false impression of bony proliferation or periosteal reactions. Selecting a reduced slice thickness minimises this effect and makes it easier to show an exact value (Dennis, 1996; Shogo *et al.*, 1995).

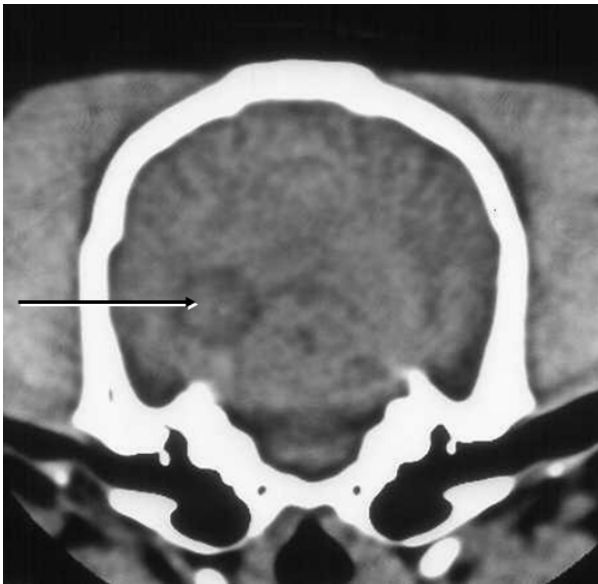


Figure 9: Image through a canine brain with ring artefact (arrow), due to a failing detector.

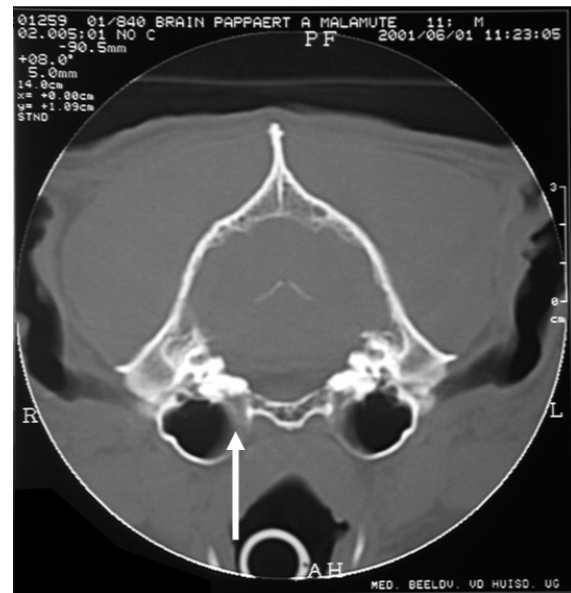


Figure 10: The partial volume effect results from the inclusion of two different tissue densities within the thickness of the slice. On this transverse slice through the head, the partial volume effect is visible at the edge of the tympanic bullae, including both air and bone tissue (arrow).

Image reconstruction

Modern CT scanners allow a choice of reconstruction algorithms to provide the optimal image, depending on the area or tissue of greatest interest (bone, soft, detail, edge and

standard). From raw scan data, it is possible to use one algorithm for the primary reconstruction and another for the secondary reconstruction. The algorithms used for reconstruction techniques are based on calibration phantoms built for humans. Therefore the optimal reconstruction for small animals can often only be established on a trial-and-error basis. For example, very small patients often result in very noisy pictures. They require different reconstruction algorithms to reduce noise.

The portion of the patient that is seen on the display monitor (display field-of-view (DFOV)) can be much smaller than the scan field-of-view (SFOV). This allows small structures to be reconstructed with relatively large size, though with sufficient detail and without degrading image quality. If one selects a DFOV which is too small or improperly centered for the area of interest, it is not necessary to do a new CT examination. If the raw data have been saved, a secondary reconstruction can be done to change the DFOV (Stickle and Hathcock, 1993; Seeram, 2001e).

After the scan examination, images in other planes can be produced using computer reformatting. Using data from the transverse slices, images are reproduced in other planes (Figure 11). It is easier to appreciate the extent of a lesion when it can be studied in multiple planes (Figure 12) (Dennis, 1996; Jeffery *et al.*, 1992).

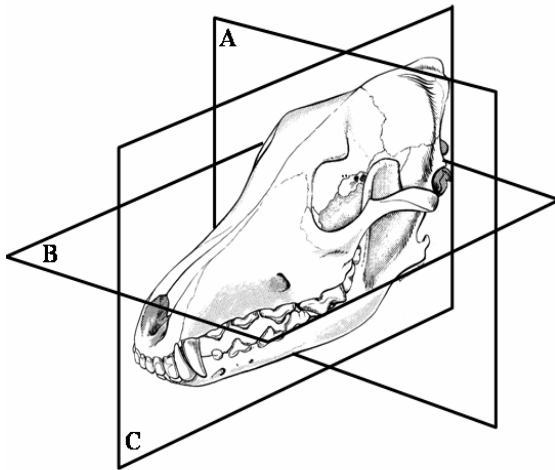


Figure 11: After the scan examination, images can be reconstructed in different planes.

- A: transverse plane**
- B: dorsal plane**
- C: sagittal plane**

Three-dimensional (3D) reconstruction is useful in selected cases for obtaining a panoramic view of a lesion and its extent of involvement, particularly in regard to bone lesions. By instructing the computer to eliminate soft-tissue CT numbers, a 3D surface

image can be produced and rotated. 3D reconstructions for bone are clearer and more useful in our field of interest (Figure 13) (Stickle and Hathcock, 1993; Seeram, 2001f). Some scanners permit different degrees of edge enhancement, which may increase sharpness (Figure 14).

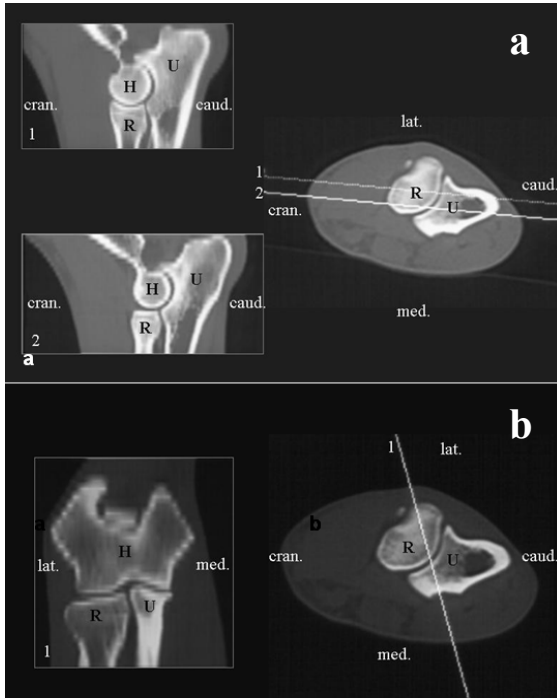


Figure 12: Using data from the transverse slices of a canine elbow joint, reconstructed images can be reproduced in sagittal (a) and dorsal (b) planes. H: humerus; R: radius; U: ulna.



Figure 13: 3-D reconstructed image of hip joints in a young dog.

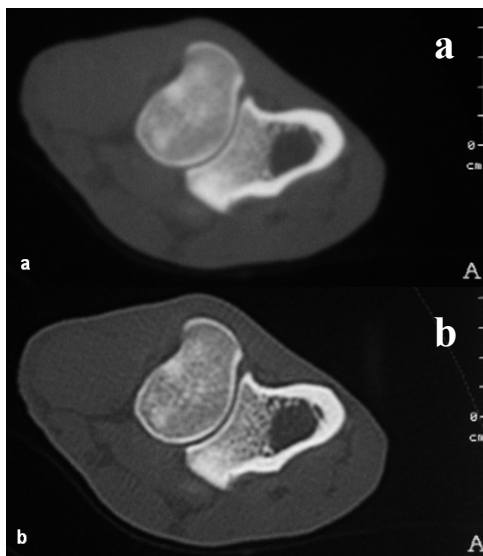


Figure 14: After the CT image is displayed on the screen, the sharpness of the image can be increased.

- a. Survey transverse image at the level of radius and ulna
- b. Same image after edge enhancement

Image interpretation

A thorough knowledge of normal anatomy is essential, certainly when dealing with cross-sectional images. Interpretation is simplified in some areas of the body by comparing to the opposite side. Straight standardised positioning produces symmetric anatomy on transverse images, making interpretation much easier (Stickle and Hathcock, 1993). The identification of structures on one transverse image can usually be accomplished simply by examining multiple adjacent transverse images. The scanned structure can be followed in relation to recognisable surrounding organs as it appears and disappears. With its image based on the differential absorption of the x-ray beam by different tissues, CT provides a far better soft tissue resolution than conventional x-rays. Lesions are detected by virtue of displacement or deformity of normal landmarks (mass effect) or by changes in tissue density due to pathological processes such as oedema, haemorrhage, necrosis, calcification and osteolysis. External landmarks and depth measurements are used to localise lesions for the purpose of biopsy, surgery or radiotherapy. Appropriate window levels and window widths are crucial for the proper interpretation of CT images and must be adapted to the tissue type and area of interest (Dennis, 1996). Image manipulation can be done after the exposure as the image is on the display screen (Figure 15). Prior to making a printed copy of the CT scan, the correct window and image contrast must be selected (Feeney *et al.*, 1991a). Regions of interest (ROI) can be selected and various data computed and displayed regarding them, including size and CT number average and range. Comparison of CT numbers between different areas on an image is sometimes useful, particularly regarding to relative differences in density (Stickle and Hathcock, 1993).

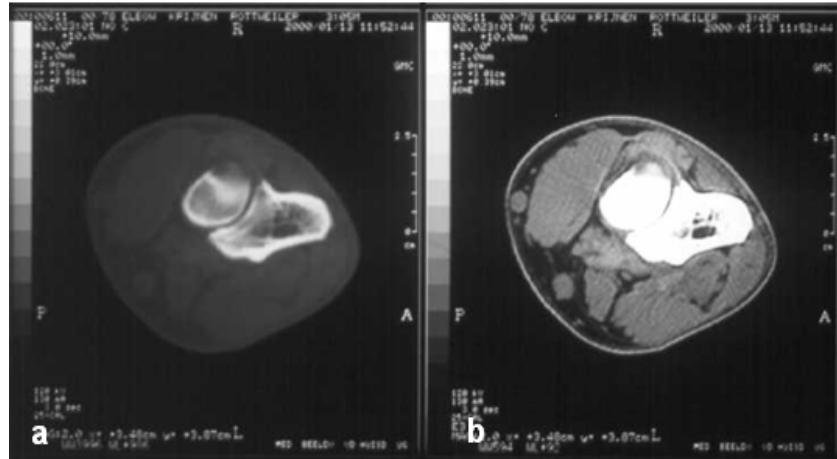


Figure 15: After the scan examination, the window level and window width can be manipulated. Using a bone window (a), the subchondral details in radius and ulna are nicely visible. On a soft tissue window (b), the details of muscles, tendons and vessels are more clearly visible.

Contrast studies

To increase the amount of soft tissue information, negative (air) and positive contrast agents, such as radiopaque iodine can be used. CT myelography, gastro-intestinal, and urogenital studies can be performed. Intravenous contrast is used to differentiate between normal and abnormal tissue (Seeram, 2001g). Positive contrast techniques are the most important tools in veterinary medicine e.g. for demonstrating brain tumours. Normally, water soluble, iodinated contrast media do not cross the intact blood-brain barrier, though where this barrier is damaged by a lesion, the contrast medium will enter in the interstitium and enhance the radioabsorption of that area. Normal brain enhances only 2-4 HU after the administration of intravenous contrast medium injection (caused by small vascular structures) (Figure 16), but the density of a lesion will increase by 20-40 HU. This enhancement reflects not only vascularity but leakage (transition) of the contrast medium in the intercellular space as well (damaged Blood Brain Barrier). This phenomenon can be useful for delineating areas of necrosis (Dennis, 1996). The use of non-ionic contrast agents is advantageous because of their lower incidence of side-effects but they are more expensive than the ionic forms. The ionic, high osmolality contrast agents are good for providing positive contrast enhancement of fluid filled cavities. They are less expensive and, in general, adverse reactions are a minimal problem in these cases and especially in veterinary medicine (Holland, 1993).



Figure 16: Plain CT image of a dog's skull (a) and corresponding image after the administration of IV contrast medium (b). The vascular structures become visible (black arrow heads) and the overall density of the brain parenchyma increases.

Contrast agents can be injected either as a bolus or as an infusion. Improved visualisation of a solid lesion in liver, spleen, or pancreas is most likely achieved by scanning during bolus effect, that is, within the first 2 minutes after injection of a contrast material bolus or during a contrast material infusion (Burgener and Hamlin, 1981).

Best opacification of the ureters was obtained with 400 and 800 mg I/kg injected as a bolus, with a constant peak at 3 minutes and durable opacification for 1 hour (Barthes, 1998).

CT guided biopsies

It is possible to obtain biopsies under CT guidance, a procedure which can be accurately performed when additional information is needed for diagnosis, staging or therapy planning. This approach can be of value for investigating mass lesions resulting from neoplasia or infections. Besides their use in the brain, CT guided biopsies in dog and cat appear to be particularly useful for lesions involving the retrobulbar space, the nasal and paranasal cavities, the vertebrae and ribs, the pelvis, and the lung and mediastinum in dog and cat. Although stereotactic devices and guidance devices improve the accuracy, free-hand techniques are commonly used. CT guided percutaneous biopsy can be performed

using a fine aspiration needle, a tru-cut needle to obtain tissue core samples, or a bone biopsy needle. When performing CT guided needle biopsies, precise needle tip localisation is an essential skill (Figure 17) (Tidwell and Johnson, 1994a).

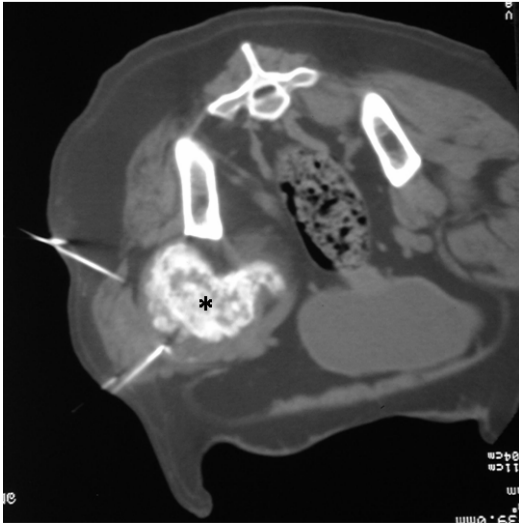


Figure 17: Transverse image of the pelvis of a dog with a calcified mass (black asterisk) ventral to the ilium. Two metallic biopsy needles are in place to perform CT guided biopsy. Note the precise location of the needle tip. The histological diagnosis was chondrosarcoma.

The retrobulbar region is directly accessible to biopsy due to the incomplete bony orbit of the dog. Care must be taken not to damage the optic nerve and the external ophthalmic artery (Penninck *et al.*, 2001). A percutaneous CT-guided needle biopsy of deep lesions such as a vertebral body or intervertebral disc can be determined in a safe and accurate way (Moore *et al.*, 2000; Risselada *et al.*, 2001).

CT guided aspiration in the thoracic cavity of lymph nodes or pulmonary masses may result in a cytological diagnosis. The administration of intravenous injection of contrast medium delineates vessels immediately adjacent to a mass. During the puncture procedure, vessels can be avoided and the safety of CT guided biopsies in the thorax can be improved (Tidwell and Johnson, 1994b).

Stereotactic devices are normally used for obtaining brain biopsies. They are rather expensive and complicated, as they have to be adaptable to the different possible skull sizes in dogs. Because most of the time the CT findings do not absolutely correlate with histological findings, biopsies are extremely useful in treatment planning (LeCouteur, 1999; Moissonnier *et al.*, 2002).

REFERENCES

- Assheuer J., Sager M. (1997). Principles of imaging techniques. In: Assheuer J., Sager M. (eds.). *MRI and CT Atlas of the Dog*, Blackwell Science Ltd, Berlin, pp. 449-453.
- Barthez P.Y., Begon D., Delisle F. (1998). Effect of contrast medium dose and image acquisition timing on ureteral opacification in the normal dog as assessed by computed tomography. *Veterinary Radiology and Ultrasound* 39, 524-527.
- Burgener F.A., Hamlin D.J. (1981). Contrast enhancement in abdominal CT: bolus vs. infusion. *American Journal of Roentgenology* 137, 351-358.
- Dennis R. (1996). An introduction to veterinary CT and MR scanning. *Veterinary Annual* 36, 16-40.
- De Rycke L.M., Gielen I.M., van Bree H., et al. (2002). Computed tomography of the elbow joint in clinically normal dogs. *American Journal of Veterinary Research* 63, 1400-1407.
- Feeney D.A., Fletcher T.F., Hardy R.M. (1991). Abdomen and pelvis. In: Mills L.E. (ed). *Atlas of Correlative Imaging Anatomy of the Normal Dog, Ultrasound and Computed Tomography*, W.B. Saunders, Philadelphia, USA, pp. 219-333.
- Grumme T., Kluge W., Kretschmar K., Roesler A. (1998). Basic physical and technical concepts. In: *Cerebral and Spinal Computed Tomography*, third edition, Blackwell Science, Berlin, Germany, pp.1-15.
- Hathcock J.T., Stickle R.L. (1993). Principles and concepts of computed tomography. *Veterinary Clinics of North America: Small Animal Practice* 23, 399-415.
- Hsieh J. (1995). Image artefacts, causes and correction. In: Goldman L.W., Fowlkes J.B. (eds.). *Medical CT and Ultrasound: Current Technology and Applications*, American Association of Physics in Medicine, USA.
- Holland, M. (1993). Contrast agents, diagnostic imaging. *Veterinary Clinics of North America: Small Animal Practice* 23, 269-277.
- Huygens W., Baert A. (1983). Axiale Computertomografie. In: *Radiologische onderzoeksmethoden*, eerste editie, Acco, Leuven, Belgium, pp 119-126.
- Jeffery N.D., Thakkar C.H., Yarrow T.G. (1992). Introduction to computed tomography of the Canine Brain. *Journal of Small Animal Practice* 33, 2-10.
- LeCouteur R.A. (1999). Current concepts in the diagnosis and treatment of brain tumours in dogs and cats. *Journal of Small Animal Practice* 40, 411-416.
- Lee S.H., Rao K.C., Zimmerman R.A. (1999). Physics and instrumentation: computed tomography. In: *Cranial MRI and CT*, fourth edition, McGraw-Hill, New York, USA, pp. 1-41.
- Moissonnier P., Devauchelle P, Delisle F, et al. (2002). Stereotactic CT-guided brain biopsy in the dog. *Journal of Small Animal Practice* 43, 115-123.
- Moore G.E., Mathey W.S., Eggers J.S., et al. (2000). Osteosarcoma in adjacent lumbar vertebrae in a dog. *Journal of the American Veterinary Medical Association* 217, 1038-1040.

- Penninck D., Daniel G.B., Brawer R., et al. (2001). Cross-sectional imaging techniques in veterinary ophthalmology. *Clinical Techniques in Small Animal Practice* 16, 22-39.
- Risselada M., Saunders J., Bhatti S., et al. (2001). CT-geleid aspiratie biopt van een geïnfecteerde tussenwervelschijf. *Vlaams Diergeneeskundig Tijdschrift* 70, 59-64.
- Robb R.A. (1982). X-ray computed tomography: an engineering synthesis of multiscientific principles. *Critical Review of Biomedical Engineering* 7, 265-333.
- Robertson S.A. (1999). Newer diagnostic and surgical techniques and their impact on anesthesia. *Veterinary Clinics of North America: Small Animal Practice* 29, 665-682.
- Seeram E. (2001a). Data acquisition concepts. In: Wilke J. (ed). *Computed Tomography: Physical Principles, Clinical Applications, and Quality Control*, second edition, W.B. Saunders, Philadelphia, USA, pp. 75-95.
- Seeram E. (2001b). Multislice spiral/helical computed tomography: physical principles and instrumentation. In: Wilke J. (ed). *Computed Tomography: Physical Principles, Clinical Applications, and Quality Control*, second edition, W.B. Saunders, Philadelphia, USA, pp. 245-265.
- Seeram E. (2001c). Computed tomography of the head, neck, and spine. In: Wilke J. (ed). *Computed Tomography: Physical Principles, Clinical Applications, and Quality Control*, second edition, W.B. Saunders, Philadelphia, USA, pp. 325-340.
- Seeram E. (2001d). Image quality. In: Wilke J. (ed). *Computed Tomography: Physical Principles, Clinical Applications, and Quality Control*, second edition, W.B. Saunders, Philadelphia, USA, pp. 173-198.
- Seeram E. (2001e). Computed tomography. In: Wilke J. (ed). *Computed Tomography: Physical Principles, Clinical Applications, and Quality Control*, second edition, W.B. Saunders, Philadelphia, USA, pp. 1-19.
- Seeram E. (2001f). Image manipulation. In: Wilke J. (ed.). *Computed Tomography: Physical Principles, Clinical Applications, and Quality Control*, second edition, W.B. Saunders, Philadelphia, USA, pp. 131-151.
- Seeram E. (2001g). Computed tomography of the body. In: Wilke J. (ed.). *Computed Tomography: Physical Principles, Clinical Applications, and Quality Control*, second edition, W.B. Saunders, Philadelphia, USA, pp. 341-163.
- Shogo A., Makoto G., Tetsuya H., et al. (1995). ABCs of CT scan. In: Shogo A. (ed). *General Electrics Medical Systems*, Tokyo, Japan, pp. 1-39.
- Stickle R.L., Hathcock J.T. (1993). Interpretation of computed tomographic images. *Veterinary Clinics of North America: Small Animal Practice*, 23, 417-429.
- Tidwell A.S., Johnson K.L. (1994a). Computed tomography-guided percutaneous biopsy: criteria for accurate needle tip identification. *Veterinary Radiology and Ultrasound* 35, 440-444.
- Tidwell A.S., Johnson K.L. (1994b). Computed tomography-guided percutaneous biopsy in the dog and cat: description of technique and preliminary evaluation in 14 patients. *Veterinary Radiology and Ultrasound* 35, 445-456.
- Wegener O.H., Fassel R., Welger D. (1993). Techniques of Computed Tomography. In: Weber S. (ed). *Whole Body Computed Tomography*, second edition, Blackwell Scientific Publications, Mass., USA, pp. 3-9.

Wortman J.A. (1986). Principles of X-ray Computed Tomography and Magnetic Resonance Imaging.
Seminars in Veterinary Medicine and Surgery (Small Animal) 1, 176-184.

2. COMPUTED TOMOGRAPHY IN SMALL ANIMALS

Part 2: CLINICAL APPLICATIONS

I. Gielen, H. van Bree

Department of Medical Imaging, Faculty of Veterinary Medicine,
Ghent University, Salisburylaan 133, Merelbeke, Belgium

Adapted from:

I. Gielen, H. van Bree. Kompendium der Allgemeinen Veterinärchirurgie 2003;
3. Bildgebende Verfahren, c. Computertomographie, Kramer M. (ed.),
Schlütersche Verlag, Hannover, Deutschland: In press.

And

I. Gielen, H. van Bree. Computed tomography in small animals. Part 2: Clinical
applications. Vlaams Diergeneeskundig Tijdschrift 2003: In press.

SUMMARY

CT is an imaging tool with many applications in various clinical disciplines that is becoming increasingly available to the veterinary profession. This imaging procedure is particularly valuable for the detection and diagnosis of brain diseases associated with mass lesions. The fact that some intracranial lesions may not be visible on CT is due to diffuse distribution, attenuation levels similar to those of the surrounding normal tissue, and minimal or absent contrast enhancement. In evaluating the localisation, extent and characterisation of lesions of the nasal cavities, paranasal sinuses, orbita, jaws, temporomandibular joints and tympanic bullae, CT is more accurate than conventional radiography. CT appears to be remarkably accurate in revealing the location, extent and origin of nasal diseases, and is superior to conventional radiography for detecting middle ear disease. In the investigation of spinal lesions in the event of doubtful radiographic and/or myelographic findings, CT is useful and can be of help in surgical planning. For the detection and description of masses, malformations and fluid collections in the thoracic cavity, CT is one of the best imaging modalities and is considered the most sensitive method for the detection of pulmonary metastases. CT of the abdomen gives excellent anatomic images of the organs and vessels, although the overall availability of ultrasound may have decreased the demand for abdominal CT studies. Skeletal CT may be helpful in clinical cases in which standard radiography is negative or inconclusive even though there is a high suspicion of pathology. In the diagnosis of fragmented coronoid process and other elbow joint pathology, CT has been proven to be superior to radiography.

INTRODUCTION

Computed tomography (CT) was introduced in the 1970s in human medicine, and since then it has become an established and important imaging procedure (Seeram, 2001). Although over the last decade CT has become more readily available to the veterinary profession, its general application is still limited. It requires animal patients to be anaesthetised for examination (Jeffery *et al.*, 1992). Another disadvantage is the cost of purchasing and maintaining the equipment. Superior soft-tissue differentiation and the absence of superimposition are the major advantages of CT over conventional x-ray techniques (Hathcock and Stickle, 1993). The predominant emphasis is the evaluation of affections of the head and central nervous system, and orthopaedic disease. Besides its use in detecting abnormalities, CT is also used for better defining the extent and severity of lesions, all these features being useful for treatment planning. A thorough knowledge of the cross-sectional anatomy is required in examining each region of the body.

BRAIN AND SKULL

In cases of trauma, fractures of the cranium can be identified easily with CT because of its great sensitivity for bony tissue (Jeffery *et al.*, 1992; Dennis, 1996).

Computed tomography is particularly valuable for the detection and diagnosis of brain diseases. The first reports of CT scanning in small animals were published in the 1980s and concerned the normal brain anatomy as seen on CT (Fike *et al.*, 1980; Fike *et al.*, 1981a; Fike *et al.*, 1984; Legrand and Carlier, 1986; Zook *et al.*, 1981; George and Smallwood, 1992) and various types of tumours in dogs and cats (Fike *et al.*, 1981b; LeCouteur *et al.*, 1981; LeCouteur *et al.*, 1983; Turrell *et al.*, 1986; Lang *et al.*, 1988). Intracranial masses and fluid-filled cavities are usually clearly demonstrated with CT (Stickle and Hathcock, 1993).

During the examination the dog is best placed in prone position with the head extended. The head should be held with cushions to maintain a straight and symmetric position. A scout view is performed in the lateral and ventrodorsal planes. The area of interest

extends from the cranial aspect of the first cervical vertebra to the cribriform plate and transverse slices are set perpendicular to the hard palate (Fike *et al.* 1981b; LeCouteur *et al.*, 1981). The scan thickness is generally 5 mm for large dogs and 2 mm for small dogs and cats (Jeffery *et al.*, 1992; Stickle and Hathcock, 1993). For brain scanning a window level of 50 Hounsfield units (HU) and a window width of 150 HU is routinely used in our department. A survey scan series is performed, followed by the IV administration of iodinated contrast medium and a second series of scans (Fike *et al.*, 1981b). The falx cerebri, the tentoria cerebelli, and the ventricular system are readily visible on survey CT images (Figure 1) (Stickle and Hathcock, 1993; Jeffery *et al.*, 1992). Intracranial mass lesions seen on CT scans are generally classified on the basis of a shift in the position of normal structures (mass effect) (Figure 2) (Fike *et al.*, 1981b; Fike *et al.* 1986).



Figure 1: Transverse CT image of the canine brain, made at the level of the fourth ventricle. The occipital region of the brain (A), tentoria cerebelli (B), cerebellum (C) and fourth ventricle (D) are easily visible on survey CT images.

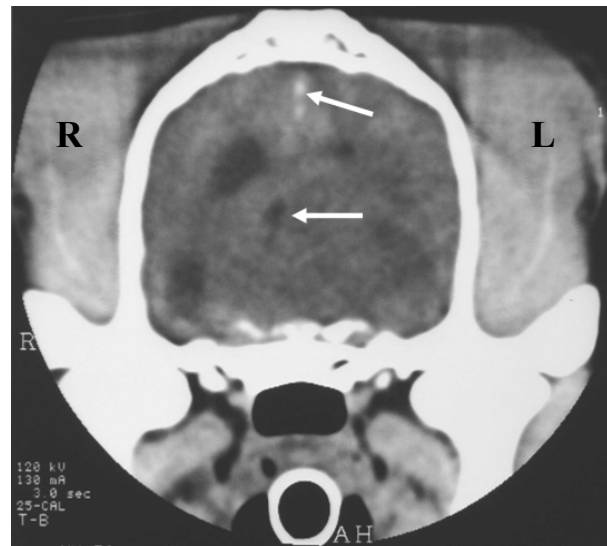


Figure 2: Pre-contrast transverse CT image of the brain of a dog showing a mass-effect. A lateral displacement of the falx cerebri (white arrow on top) and the third ventricle (white arrow in the middle) towards the right is visible. There is a shift of the midline structures, probably due to an intracranial mass in the left hemisphere.

Oedema may be visible as an area of decreased density in the brain parenchyma (Plummer *et al.*, 1992; Stickle and Hathcock, 1993). Both primary brain tumours and metastases can be identified. The visibility of intracranial lesions is enhanced on CT because of the leakage of contrast medium through a disrupted blood-brain barrier and/or

an increase in vascularity (Fike *et al.*, 1981b; Fike *et al.*, 1986). Unfortunately, different types of lesions can have virtually identical characteristics on CT, making the differentiation between neoplastic and non-neoplastic diseases impossible (Plummer *et al.*, 1992; Wolf *et al.*, 1995). Nevertheless, certain tumour types, such as meningiomas can often be recognised. These are extra-axial lesions which appear to be hyperdense compared to the brain parenchyma. They may show areas of calcification and tend to have a homogeneous enhancement with sharp demarcation from normal tissue (Figure 3) (Lang *et al.*, 1988; Turrell *et al.*, 1986; Jeffery *et al.*, 1992). In this type of tumour, hyperostosis is seen in 50% of the cats (Gordon *et al.*, 1994).

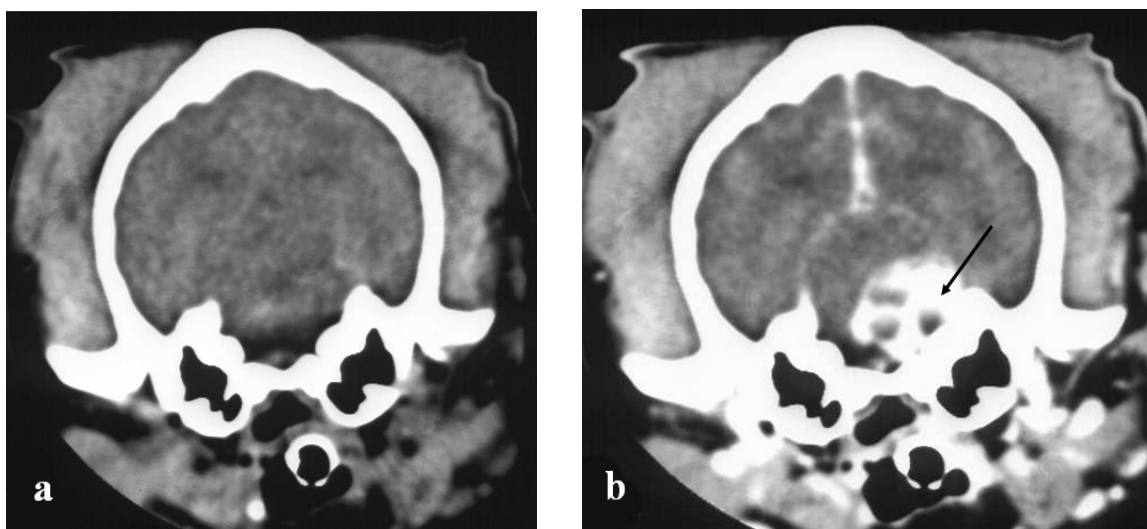


Figure 3: Representative pre- and post-contrast transverse CT scan of the brain of a dog. The pre-contrast image (a) shows a normal symmetry of the brain parenchyma. The ventricles are not enlarged and there is no mass effect. On the corresponding post-contrast scan (b), intense contrast enhancement of a mass with a broad base on the dura (black arrow) is visible. This extra-axial mass lesion is suggestive of a meningioma.

Astrocytomas and oligodendrogliomas are intra-axial lesions and typically show peripheral enhancement with central lucency or heterogeneous, non-uniform enhancement (LeCouteur *et al.*, 1981; Turrell *et al.*, 1986; Jeffery *et al.*, 1992). However, ring-enhancement is a relatively non-specific sign and a brain abscess or inflammatory disease may also exhibit this feature (Turrell *et al.*, 1986; Plummer *et al.*, 1992; Wolf *et al.*, 1995). Choroid plexus tumours typically are intra-ventricular, well defined hyperdense masses that enhance markedly after contrast administration (Figure 4).

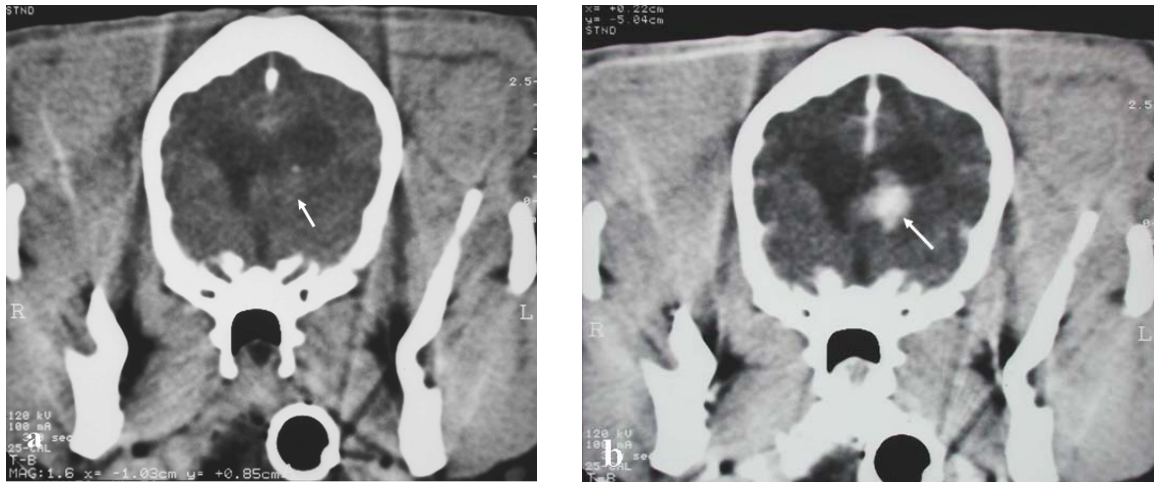


Figure 4: Pre-contrast (a) and post-contrast (b) CT scan of the canine brain at the level of the lateral ventricles. The pre-contrast image shows asymmetry and a mass-effect of the left lateral ventricle (white arrow). After intravenous contrast administration (b) a well-defined hyperdense intraventricular mass is visible. This lesion is suggestive of a choroid plexus papilloma.

Large pituitary tumours may be recognised by their location at the level of the sella turcica and typically show uniform contrast enhancement (Figure 5) (Turrel *et al.*, 1986.; Jeffery *et al.*, 1992).

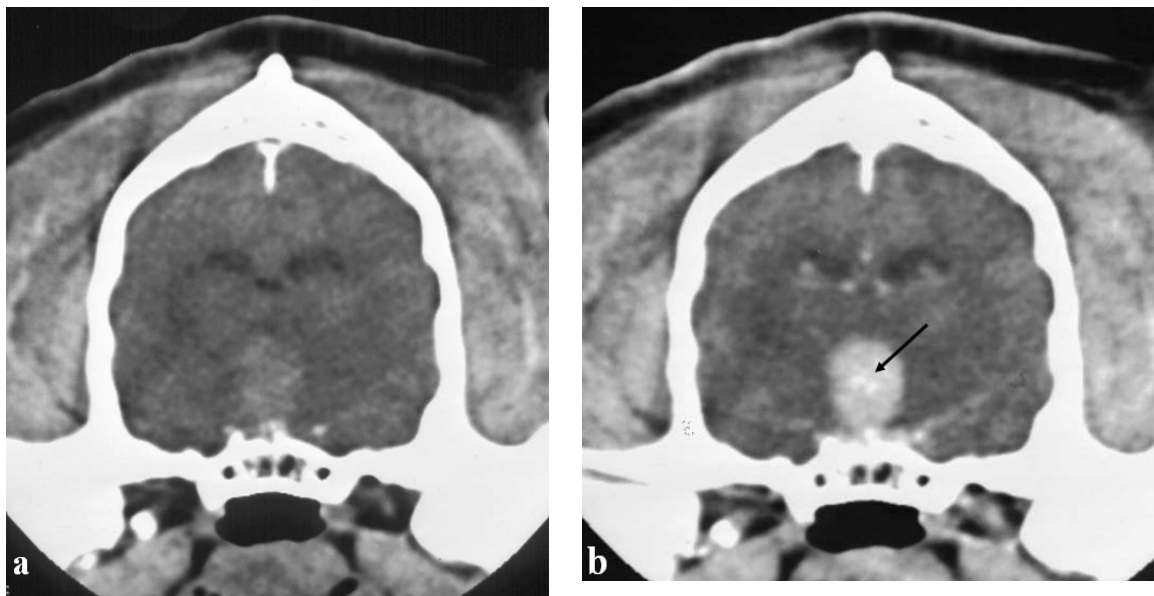


Figure 5: Tumour in a 9 year-old dog. On the non-contrast enhanced transverse scan (a), a slight hyperdense mass is visible at the midline above the pituitary fossa. Use of contrast medium (b) revealed intense, homogeneous enhancement (black arrow).

Several infectious and non-infectious inflammatory disorders can cause CT abnormalities in dogs. The presence of multifocal granulomatous lesions in more than one region of the

brain is considered to be specific for primary inflammatory disease such as granulomatous meningoencephalitis (Figure 6) (Ducoté *et al.*, 1999; Speciale, 1992; Plummer *et al.*, 1992).

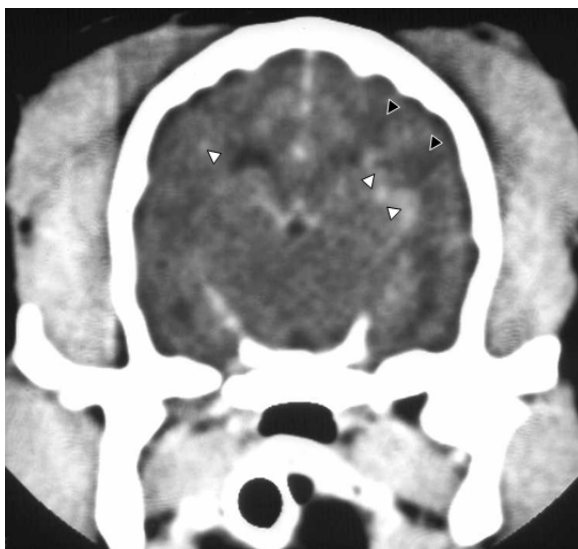


Figure 6: Transverse CT image of the brain of a patient with granulomatous meningoencephalitis, after IV administration of contrast medium. There are multifocal regions of contrast enhancement suggestive of inflammatory granulomatous foci (white arrowheads) and areas of decreased density of the brain parenchyma compatible with oedema (black arrowheads).

CT findings such as multifocal areas of decreased density have been found to be characteristic for necrotising encephalitis mostly seen in the Yorkshire Terrier (Ducoté *et al.*, 1999). Although asymmetric enlargement of the lateral ventricles is often associated with this disease, this is also a common feature in normal dogs (Dennis, 1996). Unfortunately, information about ventricle size and normal variation with regard to breed is still scarce. A recent study demonstrated a statistically significant difference between Yorkshire Terriers and German Shepherd dogs, but no age-related difference could be determined (Esteve-Ratsch, 2001).

Areas of acute haemorrhage appear as homogenous, hyperdense areas associated with oedema and mass-effect (LeCouteur *et al.*, 1981; Jeffery *et al.*, 1992; Stickle and Hathcock, 1993). Other intracranial lesions that are well visualised are those related to the fluid filled spaces of the brain. The appearance of hydrocephalus can be detected (Figure 7) and the aetiology can sometimes be demonstrated.

Some intracranial lesions may not be visible on CT probably due to diffuse distribution, attenuation similar to that of the surrounding normal tissue and minimal or absent contrast enhancement (LeCouteur, 1999).

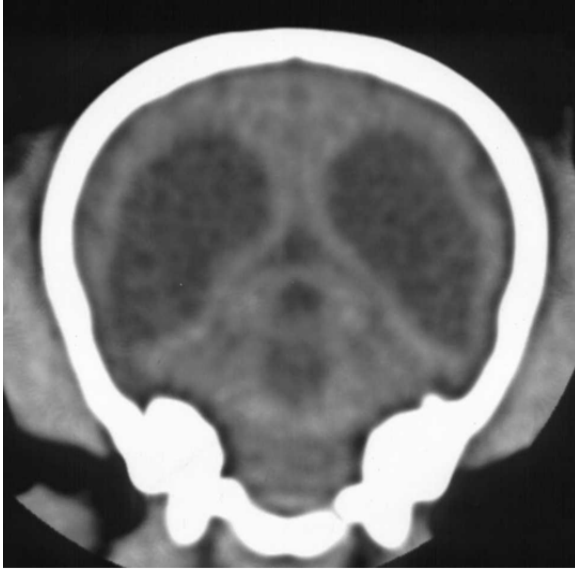


Figure 7: Transverse CT image of the brain of a dog with hydrocephalus. The complete ventricular system is enlarged and the size and shape of the fluid filled spaces of the brain are remarkable. Since the subarachnoid spaces are not obliterated, a communicating hydrocephaly is most likely.

A definitive diagnosis of intracranial diseases and lesions can only be reached by obtaining a tissue sample for histological examination. Pre-operative biopsy of a lesion may provide information needed to establish a treatment protocol and to give prognostic information to the owner. One report describes the use of CT guided free-hand needle biopsy to perform brain biopsies in dogs. The success rate was rather low due to the inadequate sample size. Clinical complications after biopsy were also reported (Harari *et al.*, 1994). The most accurate method for obtaining samples of a cerebral mass in dogs is CT-guided stereotactic biopsy. This technique uses a frame to hold the head in place while the orientation and insertion of the biopsy needle is guided using coordinates derived from imaging data. Different stereotactic CT-guided devices for dogs and cats have been modified and developed (Coffey and Lunsford, 1987; LeCouteur *et al.*, 1998; Koblik *et al.*, 1999a; Moissonnier *et al.*, 2000; Flegel *et al.*, 2002; Giroux *et al.*, 2002). With the required instrumentation, small brain lesions exceeding 6-9 mm in diameter can be biopsied (Koblik *et al.*, 1999b; Moissonnier *et al.*, 2000; Moissonnier *et al.*, 2002).

NASAL CAVITY, PARANASAL SINUSES, ORBIT, TYMPANIC BULLA

The diagnostic information obtained using CT concerning localisation, extent and characterisation of lesions of the nasal cavities, paranasal sinuses, orbit, jaws, temporomandibular joints and tympanic bulla, is more accurate than conventional radiography (Feeny *et al.*, 1991b; Stickle and Hathcock, 1993; Dennis, 1996). Patients are positioned in sternal recumbency and horizontally in the CT gantry. Symmetric positioning of the patient is critical for acquiring images in which the left and right side can be compared (Losonsky, 1997).

Commonly, multiple window levels and widths are used for the evaluation of bony and soft tissue structures (Stickle and Hathcock, 1993). All nasal structures can be made clearly visible by manipulation of the grey scale. CT appears to be remarkably accurate in revealing the location and extent of chronic nasal diseases (Codner *et al.*, 1993; Forrest, 1999, Saunders *et al.*, 2003).

All commonly seen nasal disorders have their typical CT features. The CT features of canine nasal aspergillosis are destruction of the turbinates producing cavitating lesions, and a rim of soft tissue along the frontal bone (Figure 8) (Burk, 1992a; Codner *et al.*, 1993; Schwartz, 1995; Saunders *et al.*, 2002).

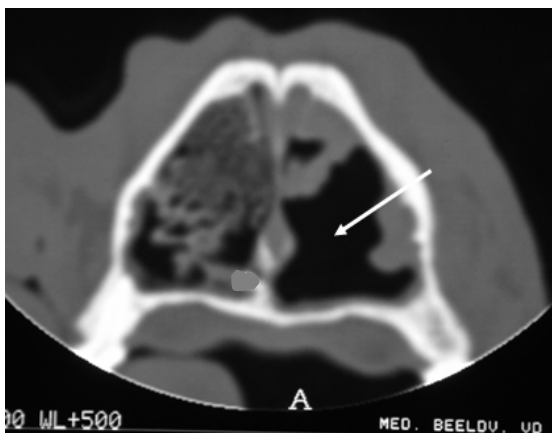


Figure 8: Transverse image of the nasal cavity illustrating nasal aspergillosis. There is a complete turbinate lysis (arrow) and mucosal thickening visible in the nasal cavity.

The CT features of nasal neoplasm include space-occupying lesions associated with bone destruction, patchy areas of increased soft-tissue density, and destruction of the ethmoid bone (Figure 9). The extent to which a nasal neoplasm has destroyed the frontal bone and

extended into the orbit can be established very accurately (Thrall *et al.*, 1989; Burk, 1992a; Park, 1992; Codner *et al.*, 1993; Schwartz, 1995). The CT features of non-specific rhinitis include non-destructive processes that spare the paranasal sinuses and affect most often both nasal cavities (Codner *et al.*, 1993).

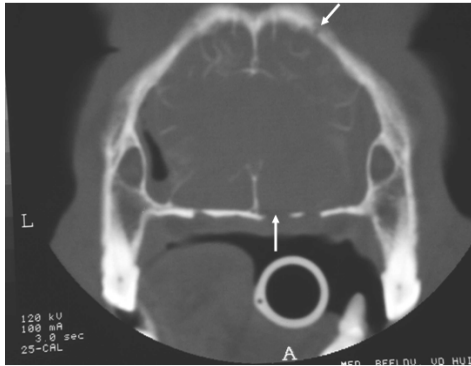


Figure 9: CT image of the nasal cavity of a dog with nasal neoplasia. A low density mass fills both sides of the nasal cavity. Nasal turbinate destruction and lysis of the nasal septum is present. Note the lytic areas in the maxilla (arrow on top) and a defect in the hard palate (vertical arrow).

CT also provides accurate information on the extension of the process for treatment, surgery planning and radiation therapy of nasal lesions (McEntee *et al.*, 1991, Codner *et al.*, 1993; Mathews *et al.*, 1996).

Studies are available on the normal nasal cavity and paranasal sinuses in the dog and cat to assist in interpretation of CT images (Burk, 1992b; Losonsky *et al.*, 1997).

Because radiographic examination rarely is conclusive in orbital diseases, CT is increasingly being used for the investigation of orbital lesions and the detection and involvement of retrobulbar masses (Figure 10) (Feeney *et al.*, 1991b; Calia *et al.*, 1994; LeCouteur *et al.*, 1982). Exophthalmus and soft tissue swelling associated with the orbit or calvaria can be evaluated using CT. Multilobular tumours and their bone involvement in the zygomatic arch and in the rostral and frontal bone can best be visualised on non-contrast CT images using a bone window (Hathcock and Newton, 2000).



Figure 10: Transverse CT scan of a dog at the level of mid-zygomatic arch. A diffuse mass is present in the right orbit (asterisk), displacing the globe laterally and rostrally.

CT provides excellent image detail of bony changes and small fractures of the temporomandibular joint in dogs and cats (Schwarz *et al.*, 2002). The IV injection of contrast medium enhancing the pathologically affected zone in the area of the mandibula or zygomatic arch was noticed in some cases seen in our department. This finding appeared useful to determine the borders of non-mineralised soft tissue masses (Figure 11).



Figure 11: Pre-contrast (a) and post-contrast (b) transverse CT image of the head of a dog. The pre-contrast image (bone window) displays lysis of the right mandibula (white arrow). On the corresponding post-contrast image (soft tissue window) peripheral enhancement of the soft tissue of the mass is clearly visible.

CT imaging allows clear visualisation of the base of the skull and tympanic bullae without superimposed structures creating confusion (Hoskinson, 1993; Seitz, 1996) and can accurately enable the diagnosis of otitis media in dogs and cats in the early stages of the condition (Hoskinson, 1993; Love, 1995; Seitz, 1996; Forrest 1999). CT can detect subtle increases in soft tissue densities (fluid or mass) in the tympanic bulla and is therefore superior to conventional radiography for detecting middle ear disease (Love *et al.*, 1995) (Figure 12). One must be aware that on CT images there is an apparent increase in thickness of the tympanic bulla wall when it is filled with fluid. A window of +2000 and a small slice thickness must be used to reduce this volume average artefact (Barthez *et al.*, 1996). CT is also valuable in evaluating the external ear canals, the inner ear, the

nasopharyngeal area and the extent of osseous bulla involvement in inflammatory polyyps in cats (Seitz, 1996).

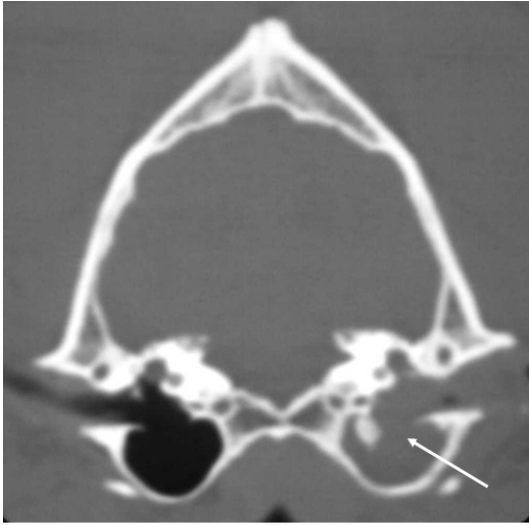


Figure 12: CT image at the mid-tympanic bulla. The tympanic bulla (white arrow) and ear canal are filled with soft tissue density. There is no osseous thickening of the wall of this tympanic bulla. The tympanic bulla at the other side is normal and filled with air.

Good knowledge of the normal anatomy of the middle and inner ear is mandatory for optimal interpretation of clinical CT images (Russo *et al.*, 2002).

SPINE

For a CT examination of the spine, the patient is positioned in sternal recumbency. Gantry tilt is used so that the scan plane through the primary site of interest is nearly perpendicular to the long axis of the spinal canal. In cats and small dogs, sagittal CT images for visualising the entire thoracic and lumbar spine can be acquired after positioning the animal in ventral recumbency across the table with the long axis of the spine transverse to the direction of table movement (Kneissl and Schedbauer, 1997). The interpretation of spinal and vertebral CT images is performed in both a bone and soft tissue window (Stickle and Hathcock, 1993).

CT examination of the spinal cord should be performed post-myelography (Drost *et al.*, 1996). CT is useful in the investigation of spinal lesions in the event of doubtful radiographic and/or myelographic findings (Stickle and Hathcock, 1993; Drost *et al.*, 1996). With CT, the localisation and extent of spinal lesions can be accurately evaluated, which is of help in surgical planning. The spinal cord, the intervertebral discs and the

vertebrae can be visualised. Spinal cord and nerve root compression can also be demonstrated (Dennis, 1996).

Spinal cord compression can be more accurately assessed with CT than with standard radiographs (Stickle and Hathcock, 1993). In spinal arachnoid cysts, CT provides additional information to myelography by improving visualisation of the caudal limits of the cyst and eventual topographic position. The degree of spinal cord compression can accurately be measured using CT (Galloway *et al.*, 1999).

CT myelography is an additional diagnostic procedure in dogs with cervical spondylomyelopathy, this technique provides extra information on the exact location and degree of compression (Sharp *et al.*, 1995). In dogs with cervical intervertebral disc protrusion, CT myelography performed pre- and postoperatively has proved also to be quite useful in planning the surgical technique and in establishing the prognosis (Hara *et al.*, 1994).

Mineralised intervertebral disc material in the vertebral canal can also be detected using CT without myelography. However, herniated disc material with soft tissue attenuation may not be visible on non-contrast images. The accuracy of CT in diagnosing and localising herniated disc material compares favourably with myelography (Olby *et al.*, 2000). The incidence and extent of acute haemorrhage in the vertebral canal can be also identified using CT. CT has proved to be superior when bony changes are involved. However, in one study, spinal cord lesions (intradural/ extramedullary and intramedullary) were less correctly classified using CT than using myelography (Drost *et al.*, 1996).

Gas between vertebrae and in the vertebral canal (the “vacuum phenomenon”), which is a sign of disc degeneration, can be identified with computed tomography (Hathcock, 1994).

CT can also be of great value in the diagnosis and evaluation of lumbosacral lesions (Feeney *et al.*, 1991c; Jones *et al.*, 1994; Jones *et al.*, 1995; Jones *et al.*, 1996; Feeney *et al.*, 1996; Ramirez and Thrall, 1998). For this examination, the dogs are positioned in dorsal recumbency with the hind limbs entering the gantry first. This position allows consistent neutralisation of lumbosacral lordosis (Jones *et al.*, 1994; Jones *et al.*, 1995). Bone remodelling, evidence of cauda equina compression, articular process joints,

sacroiliac joints and the intervertebral foramina can be evaluated without superimposition (Stickle and Hathcock, 1993; Jones *et al.*, 1995). Structures visible on CT include disc margin bulging, nerve tissue displacement, degenerative articular process joint disease and idiopathic or developmental stenosis (Figure 13) (Stickle and Hathcock, 1993; Jones *et al.*, 1996; Ramirez and Thrall, 1998).

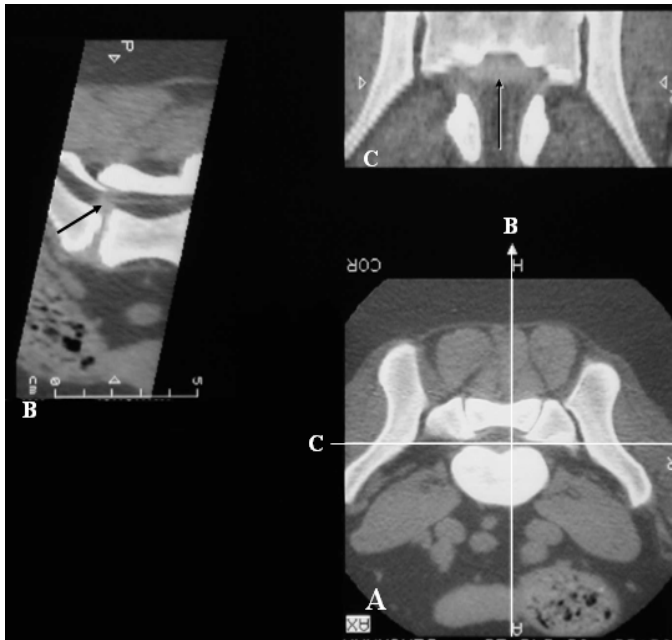


Figure 13: Transverse CT image (A) through the space between L7 and S1, displayed using a soft tissue window. Note the convex appearance of the dorsal disk margin. At the sagittal (B) and dorsal reconstructed (C) images of the same region, the disc margin bulging (black arrow) can be clearly seen.

Epidural injection of contrast medium tends to cause uneven accumulations and hinders the interpretation of CT images (Stickle and Hathcock, 1993). When using intravenous contrast, however, the positive predictive value for compressing soft tissues involving the spinal canal was quite high (Jones *et al.*, 1999). The individual L5-S3 nerve roots can be visualised and traced to the point of exit from their corresponding foramina because of the inherent contrast provided by abundant epidural fat (Jones *et al.*, 1995; Jones *et al.*, 1996). Where there is an increase in soft tissue density in the absence of epidural fat, cauda equina compression should be suspected, even if degenerative changes appear mild (Jones *et al.*, 1996). CT findings in older dogs, especially stenosis and loss of epidural fat, indicate that some lumbosacral abnormalities are clinically insignificant (Jones, 2000).

CT can also be used to define the extent of a lumbosacral plexus nerve sheath tumour in a dog. A soft tissue mass can be identified ventral to the sacrum, following the course of the lumbosacral trunk and sciatic nerve (Figure 14) (Niles *et al.*, 2001).

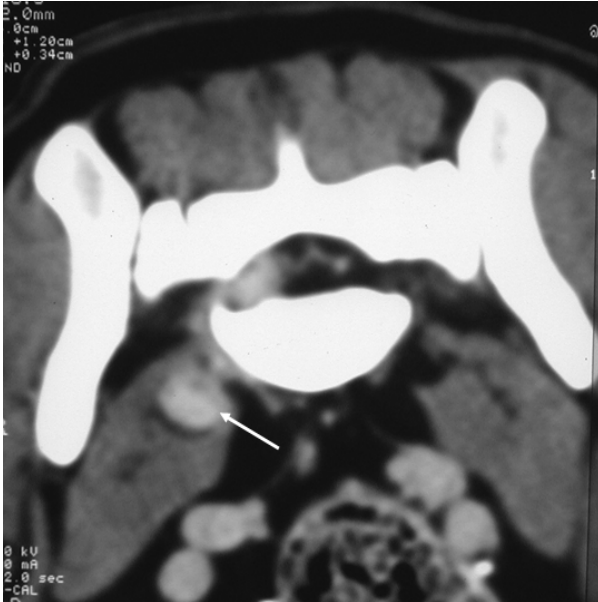


Figure 14: Post-contrast CT view of the lumbosacral region. The lumbosacral plexus is enhanced and enlarged (arrow). The tumour follows the course of the S1 component of the sciatic nerve suggesting a peripheral nerve sheath tumour.

CT provides excellent visualisation of brachial plexus tumours, but it is difficult to determine the exact origin of the nerve sheath involved. The administration of contrast medium intravenously helps to identify vascular structures (Figure 15) (McCarthy *et al.*, 1993).



Figure 15: Transverse CT view through the fourth cervical vertebra after IV administration of contrast medium. Note the subtle contrast enhancement of a 3 cm diameter mass (asterisk) representing a brachial plexus tumour.

Avulsion of the nerve roots of the brachial plexus, which can be demonstrated using CT after myelography, results in an improved prognostic assessment of brachial plexus paralysis (Forterre *et al.*, 1998).

CT anatomic studies of the normal canine spine and lumbosacral region have been described (Jones 1995; Feeney *et al.*, 1991c; Smallwood and George, 1993; Feeney *et al.* 1996).

THE THORAX

Sternal recumbency is preferable for imaging the thoracic cavity, as it allows more normal positioning of the heart and other mediastinal structures. CT images obtained in ventral recumbency can help to avoid overlooking a mass in the pulmonary parenchyma (Ahlberg *et al.*, 1985). Again, symmetrical positioning of the patient allows better visualisation and evaluation of the structures in the thorax. Breathing and cardiac pulsation are the main causes of motion artefacts. These artefacts can be suppressed using single CT slices, short scan time and artificial respiration with breathholds (Fike *et al.*, 1980).

CT is the best imaging modality for the detection and description of masses, malformations and fluid collections in the thoracic cavity (Burk, 1991; Samii *et al.*, 1998). It can be used to determine the exact size and shape of a mass, the presence of early mass mineralisation (indicating neoplastic transformation), and the occurrence of any changes in the surrounding structures (Stickle and Hathcock, 1993). Because of the high tissue-air contrast, lung structures are delineated with a very high degree of detail, especially when window width (WW) and window level (WL) are adjusted to lung tissue (-700 HU). Changes of the pleura and changes on the medial aspect of the ribs can also be evaluated (Burk, 1991). Soft tissue evaluation of the mediastinum, body wall and bone is performed using multiple window levels (Stickle and Hathcock, 1993). Thoracic masses can be differentiated from accumulations of mediastinal or pleural fluid (Feeney *et al.*, 1991d; Samii *et al.*, 1998) and can be characterised as areas of calcification, as cavitations or as solid masses (Fike *et al.*, 1980). Through the use of intravenous contrast medium, the vasculature of the mediastinum can be distinguished from structures of similar appearance on pre-contrast CT (Figure 16) (Stickle and Hathcock, 1993; Marincheck and Young, 1980).

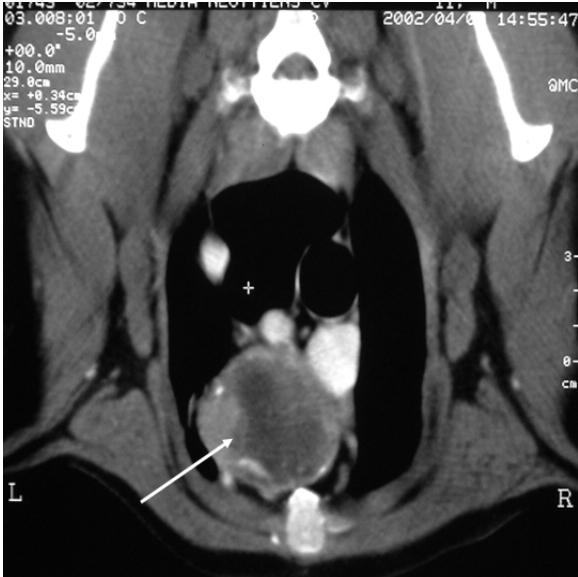


Figure 16: CT scan of the thorax after IV administration of contrast. In the cranial mediastinum a large heterogeneous enhanced mass is visible (arrow). Histological examination confirmed a thymoma.

CT is considered the most sensitive method for detecting pulmonary metastases (Figure 17), but there are limitations in the detection capacity. Lesions smaller than 5 mm are often not demonstrated, and micro-metastases, the most common type, are usually overlooked (Waters *et al.*, 1998).

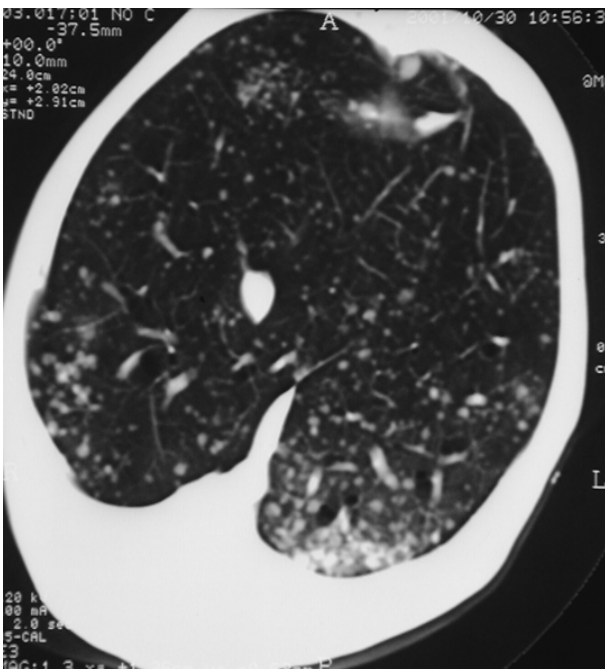


Figure 17: Computed tomography scanning of the thorax with contrast enhancement. Diffuse nodular densities in the lungs were judged to be metastatic lesions. The primary tumour was localised within the spleen.

CT enables improved detection of small pulmonary nodules and hilar or mediastinal lymphadenopathy. Large bullae and cavitated neoplasms can be revealed, but small (less than 3 mm) peripheral bullae are difficult to detect (Burk, 1991).

CT is also used to define the extent and the definition of contours of masses, information which is useful for planning surgery (Burk, 1991; Smallwood and George, 1993).

Descriptions of normal canine and feline cross-sectional anatomy of the thorax, including correlative CT images, are available (Assheuer and Sager, 1997a; Feeney *et al.*, 1991d; Fike *et al.*, 1980; Samii *et al.*, 1998; Smallwood and George, 1993; Zook *et al.*, 1989).

ABDOMEN

CT of the abdomen gives excellent anatomic images of the organs and vessels. The relative lack of CT imaging in abdominal disease in animals may be due to the need for anaesthesia and artefacts due to respiratory motion. In addition, the availability of ultrasound may have decreased the demand for CT. Abdominal images usually are evaluated using a window level of 40 and a window width of 350 to 500 (Stickle and Hathcock, 1993). Usually CT scans are requested for the purpose of better defining the relationship of a known abdominal mass to adjacent vital structures or for evaluating known or suspected lesions involving the spine and pelvic canal.

CT examination is very useful for the early detection of renal carcinomas and for differentiating between cysts and solid tumours (Figure 18) (Moe and Lium, 1997).

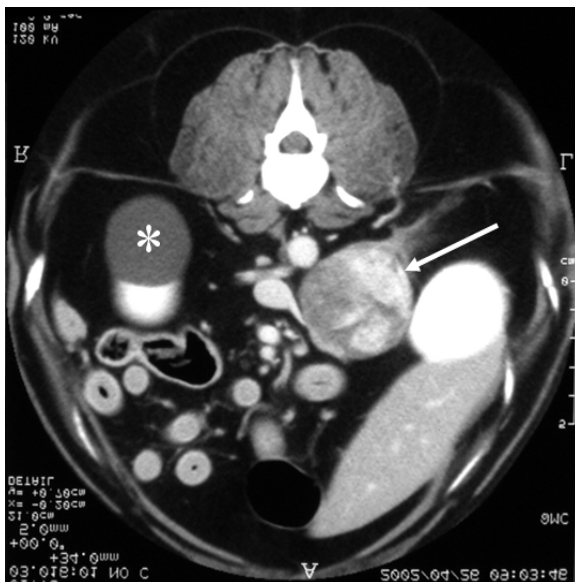


Figure 18: Computed tomography scan of the abdomen at the level of the kidneys after IV administration of contrast medium. A large cyst is occupying the dorsal part of the right kidney (asterisk). A large heterogeneous enhanced mass representing a left adrenal gland tumour is visible (white arrow).

A bolus injection of contrast medium increases the possibility of differentiating a solid vascular renal mass from an avascular cyst (Evill *et al.*, 1988; Moe and Lium, 1997; Yamazoe *et al.*, 1994).

The imaging of adrenal glands and the evaluation of the assessment of size, shape and topography of adrenal masses is another important indication for CT (Figure 18) (Bailey, 1986; Emms *et al.*, 1986; Rosenstein, 2000; Voorhout, 1990; Voorhout *et al.*, 1990).

When used to evaluate canine hyperadrenocorticism, this technique provides good differentiation between unilateral adrenal masses and bilateral adrenal gland enlargement (Emms *et al.*, 1986; Voorhout *et al.*, 1988). Fine-needle aspiration of an adrenal mass using CT guidance can be performed in dogs (Rosenstein, 2000).

CT images at maximum expiration allow a detailed view of the normal pancreatic parenchyma, whereas normal pancreatic and bile ducts cannot be visualised. The main technical problem in CT imaging of the pancreas is its demarcation from adjacent organs, especially liver, spleen, and stomach (Probst and Kneissl, 2001).

Contrast-enhanced CT offers a combination of topographic and functional assessment of the spleen and is an accurate method for diagnosing splenic torsion in a dog (Patsikas *et al.*, 2001).

It has been reported that contrast-enhanced CT is useful for the diagnosis of portosystemic shunt (Kleiter *et al.*, 1999).

Contrast enhancement is needed to differentiate mesenteric masses from normal bowel or vascular structures. The clear visualisation of gastric detail, both in the small and in the large intestine, indicates that CT could effectively be used to evaluate gastrointestinal pathology (Fike *et al.*, 1980). However, the application of CT to gastrointestinal imaging is limited in the dog. CT has great localising value, but it cannot assess dynamic activity of the bowel (Feeney *et al.*, 1991a).

Because of high contrast resolution and lack of superposition, CT is valuable for the evaluation of the ureters and the ureterovesicular junction; with IV administration of contrast medium, it also makes it possible to diagnose the presence of an ectopic ureter (Figure 19) (Barthez *et al.*, 1998).

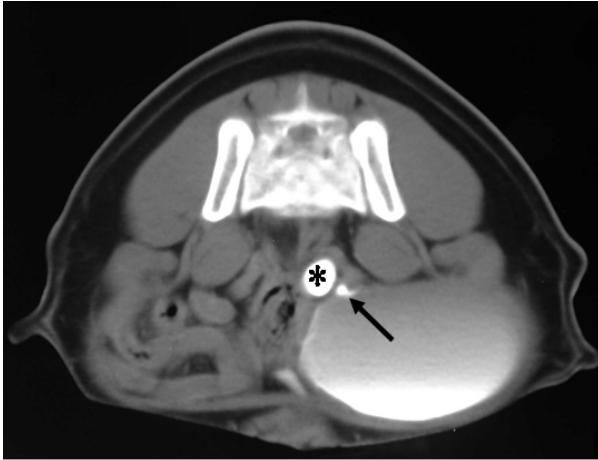


Figure 19: Post-contrast transverse CT image of the caudal abdomen. A dilated ectopic ureter is seen bypassing the vesicouretral junction (asterisk). The other ureter (black arrow) enters the bladder at its normal location.

Descriptions of the normal canine and feline cross-sectional anatomy of the abdomen and pelvis are available, with correlative CT images (Assheuer and Sager, 1997b; Feeney *et al.*, 1991a; Fike *et al.*, 1980; Samii *et al.*, 1998; Smallwood and George, 1992; Smallwood and George, 1993).

MUSCULOSKELETAL SYSTEM

CT is widely used to evaluate the musculoskeletal system in human medicine (Dalinka, 1989; Erickson, 1997; Pettersson, 1998; Feldman, 2000). It is often used for the examination of acute and chronic injuries involving the articular surfaces (Newberg, 1990; Pretorius and Fishman, 1995). Nowadays, the technique is increasingly being used by veterinarians for the diagnosis of orthopaedic disorders in small animals (Hoskinson and Tucker, 2001; van Bree *et al.*, 2002). Despite the growing availability, reports on its use in small animal orthopaedics are still infrequent (Fitch *et al.*, 1997). Skeletal CT may be helpful in clinical cases in which standard radiography is negative or inconclusive and when there is a high suspicion of pathology (Hoskinson and Tucker, 2001). Radiographic identification of the cause of lameness localised in the joints of small animals may be difficult, especially considering the complex radiographic anatomy of some joints and the superimposition of the bony structures. CT enables more detailed and specific morphological diagnosis than radiography (Kippenes and Johnston, 1998) and facilitates

the examination of complex joint structures such as the elbow and tarsus by eliminating superimposed structures (Reichle and Snaps, 1999). Osteolysis, sclerosis and new bone formation can be detected in the very early stages due to the extreme sensitivity of CT for bone and calcified tissue. CT enables the detection of density differences as low as 0.5%, as apposed to the lower limits of approximately 30% that are possible with conventional radiography (Hoskinson and Tucker 2001). Therefore CT is most accurate in evaluating the extent of an osteosarcoma in dogs prior to limb-sparing osteotomy (Davis *et al.*, 2002).

CT has been proved to be superior to radiography in the diagnosis of fragmented coronoid process of the elbow joint (Figure 20) (Carpenter, 1993; van Bree and Van Ryssen, 1994; Reichle *et al.*, 2000). Its use in the diagnosis of elbow incongruity has also been reported (Figure 21) (Gielen *et al.*, 2001).

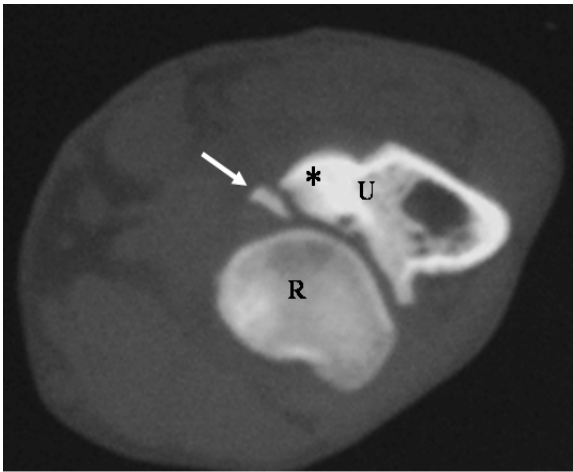


Figure 20: Transverse image of the elbow (U: ulna, R: radial head) through the area of the medial coronoid process, showing fragmentation of the medial coronoid process (arrow). There is a clear sclerosis of this part (asterisk) of the ulna.

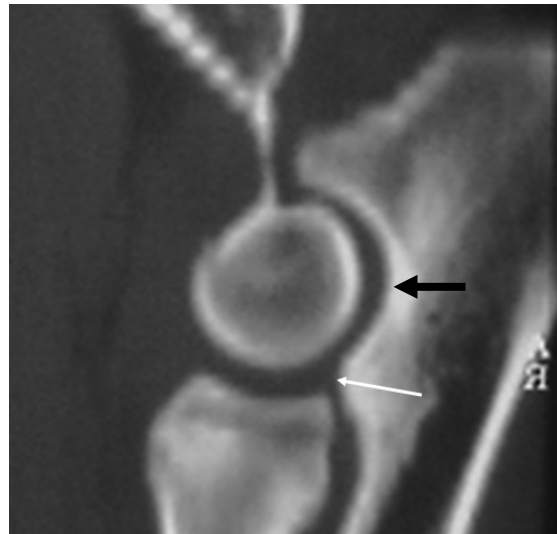


Figure 21: Sagittal reconstruction of an incongruent elbow. Note the step between radius and ulna (white arrow), as well as the abnormal shape of the trochlear notch of the ulna in the incongruent joint (black arrow).

CT is superior in the diagnosis of incomplete ossification of the humeral condyle (Figure 22) (Marcellin-Little *et al.*, 1994; Brunnberg, 2001; Meyer-Lindenberg *et al.*, 2002).

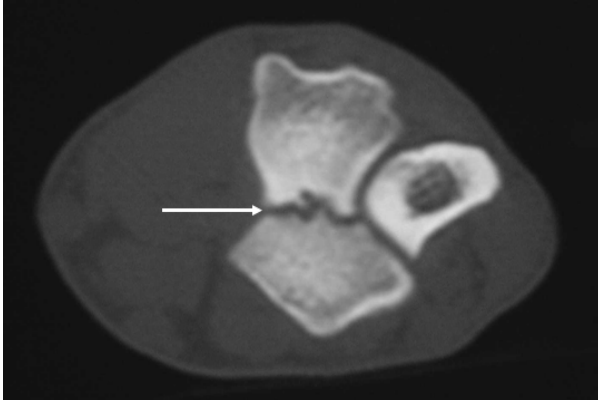


Figure 22: Transverse CT image through the humeral condyle of a dog. A radiolucent line (arrow) indicates an incomplete ossification of the humeral condyle.

In the treatment of hip dysplasia, CT can be used to check the status of the dorsal acetabular rim which is an important criterion when triple pelvic osteotomy (TPO) is being considered (van Bree *et al.*, 2002).

In addition to purely diagnostic imaging, CT is a valuable tool in orthopaedic research. For example, CT offers the ability to non-invasively quantify volume, density and angles of long bones (Markel *et al.*, 1990; Fitch *et al.*, 1996; Johnson *et al.*, 2001; Dueland *et al.*, 2001)

Conventional arthrography techniques with negative or positive contrast agents can be used in combination with CT scanning. High-resolution thin-slice arthrogram images produced by CT may demonstrate lesions undetected on standard contrast radiography (Davies and Cassar-Pullicino, 1989; Hoskinson and Tucker, 2001).

The ability to view images in several image planes may help to better delineate fracture orientation and to plan the repair process. It may also reveal articular involvement unrecognised with standard radiographs.

REFERENCES

- Ahlberg N.E., Hoppe F., Kelter U., et al. (1985). A Computed tomographic study of volume and X-ray attenuation of the lungs of Beagles in various body positions. *Veterinary Radiology* 26, 43-47.
- Assheuer J., Sager M. (1997a). The thorax. In: Assheuer J., Sager M. (eds.). *MRI and CT Atlas of the Dog*, Blackwell Science Ltd, Berlin, pp. 315-345.
- Assheuer J., Sager M. (1997b). The abdomen. In: Assheuer J., Sager M. (eds.). *MRI and CT Atlas of the Dog*, Blackwell Science Ltd, Berlin, pp. 347-403.
- Bailey M.Q. (1986). Use of X-ray computed tomography as an aid in localization of adrenal masses in the dog. *Journal of the American Veterinary Medical Association* 188, 1046-1049.
- Barthez P.Y., Koblik P.D., Hornof W.J., et al. (1996). Apparent wall thickening in fluid filled versus air filled tympanic bulla in computed tomography. *Veterinary Radiology and Ultrasound* 37, 95-98.
- Barthez P.Y., Begon D., Delisle.F. (1998): Effect of contrast medium dose and image acquisition timing on ureteral opacification in the normal dog as assessed by computed tomography. *Veterinary Radiology and Ultrasound* 39, 524-527.
- Brunnberg L., Pauls J., Burger M., et al. (2001). „Interkondyläre“, nicht dislozierte Humerusfraktur beim Hund. *Kleintierpraxis* 46, 783-792.
- Burk R.L. (1991). Computed tomography of thoracic diseases in dogs. *Journal of the American Veterinary Medical Association* 199, 617-621.
- Burk R.L. (1992a). Computed tomographic imaging of nasal disease in 100 dogs. *Veterinary Radiology and Ultrasound* 33, 177-180.
- Burk, R.L. (1992b). Computed tomographic anatomy of the canine nasal passages. *Veterinary Radiology and Ultrasound* 33, 170-176.
- Calia C.M., Kirschner S.E., Bear K.E., et al. (1994). Computed tomography scan for the evaluation of orbital diseases in dogs and cats. *Veterinary and Comparative Ophthalmology* 4, 24-30.
- Carpenter L., Schwarz P., Lowry J., et al. (1993). Comparison of radiologic imaging techniques for diagnosis of fragmented medial coronoid process of the cubital joint in dogs. *Journal of the American Veterinary Medical Association* 203, 78-83.
- Codner E.C., Lurus A.G., Miller J.B., et al. (1993). Comparison of computed tomography with radiography as a noninvasive diagnostic technique for chronic nasal disease in dogs. *Journal of the American Veterinary Medical Association* 202, 1106-1110.
- Coffey R.J., Lunsford L.D. (1987). Animal research stereotactic instrument modified for computed tomographic guidance. *Applied Neurophysiology* 50, 81-86.
- Dalinka M.K., Kricun M.E., Zlatkin M.B., et al. (1989). Modern diagnostic imaging in joint disease. *American Journal of Roentgenology* 152, 229-240.
- Davies A.M., Cassar-Pullicino V.N. (1989). Demonstration of osteochondritis dissecans of the talus by coronal computed tomographic arthrography. *British Journal of Radiology* 62, 1050-1055.

- Davis G.J., Kapatkin A.S., Craig L.E., et al. (2002). Comparison of radiography, computed tomography, and magnetic resonance imaging for evaluation of appendicular osteosarcoma in dogs. *Journal of the American Veterinary Medical Association* 220, 1171-1176.
- Dennis R. (1996). An introduction to veterinary CT and MR scanning. *Veterinary Annual* 36, 16-40.
- Ducoté J.M., Johnson K.E., Dewey C.W., et al. (1999). Computed tomography of necrotizing meningoencephalitis in 3 Yorkshire Terriers. *Veterinary Radiology and Ultrasound* 40, 617-621.
- Dueland R.T., Adams W.M., Fialkowski J.P., et al. (2001). Effects of pubic symphysiodesis in dysplastic puppies. *Veterinary Surgery* 30, 201-217.
- Drost W.T., Love N.E., Berry C.R. (1996). Comparison of radiography, myelography and computed tomography for the evaluation of canine vertebral and spinal cord tumours in sixteen dogs. *Veterinary Radiology and Ultrasound* 37, 28-33.
- Emms S.G., Wordmann J.A., Johnston D.E., et al. (1986). Evaluation of canine hyperadrenocorticism, using computed tomography. *Journal of the American Veterinary Medical Association* 189, 432-439.
- Erickson S. (1997). High-resolution imaging of the musculoskeletal system. *Radiology* 205, 593-618.
- Esteve-Ratsch B, Kneissl S, Gabler C. (2001). Comparative evaluation of the ventricles in the Yorkshire terrier and the German Shepherd dog using low-field MRI. *Veterinary Radiology and Ultrasound* 42, 410-413.
- Evill C.A., Wilcox J., Hassam R.M., et al. (1988). Examination of the nephrographic potential of iotrol by computed tomography. *Investigative Radiology* 23, 216-220.
- Feeney D.A., Fletcher T.F., Hardy R.M. (1991a). Abdomen and pelvis. In: Mills L.E. (ed.). *Atlas of Correlative Imaging Anatomy of the Normal Dog, Ultrasound and Computed Tomography*, W.B. Saunders Company, Philadelphia, USA, pp. 219-333.
- Feeney D.A., Fletcher T.F., Hardy R.M. (1991b). Head and Neck. In: Mills L.E. (ed.). *Atlas of Correlative Imaging Anatomy of the Normal Dog, Ultrasound and Computed Tomography*, W.B. Saunders Company, Philadelphia, USA, pp. 4-87.
- Feeney D.A., Fletcher T.F., Hardy R.M. (1991c). Spine. In: Mills L.E. (ed.). *Atlas of Correlative Imaging Anatomy of the Normal Dog, Ultrasound and Computed Tomography*, W.B. Saunders Company, Philadelphia, USA, pp. 89-151.
- Feeney D.A., Fletcher T.F., Hardy R.M. (1991d). Thorax. In: Mills L.E. (ed.). *Atlas of Correlative Imaging Anatomy of the Normal Dog, Ultrasound and Computed Tomography*, W.B. Saunders Company, Philadelphia, USA, pp. 153-210.
- Feeney D.A., Evers P., Fletcher T.F., et al. (1996). Computed tomography of the normal canine lumbosacral spine: a morphologic perspective. *Veterinary Radiology and Ultrasound* 37, 399-411.
- Feldman. (2000). Musculoskeletal radiology: Then and now. *Radiology* 216, 309-316.
- Fike J.R., Zook B.C., Davis D.O., et al. (1980). Canine anatomy as assessed by computerised tomography. *American Journal of Veterinary Research* 41, 1823-1832.
- Fike J.R., LeCouteur R.A., Cann C.E. (1981a). Anatomy of the canine brain using high resolution computed tomography. *Veterinary Radiology* 22, 236-243.

- Fike J.R., LeCouteur R.A., Cann C.E., et al. (1981b). Computerised tomography of brain tumours of the rostral and middle fossas in the dog. *American Journal of Veterinary Research* 42, 275-281.
- Fike J.R., LeCouteur R.A., Cann C.E. (1984). Anatomy of the canine orbital region, multiplanar imaging by CT. *Veterinary Radiology* 25, 32-36.
- Fike J.R., Cann C.E., Turowski K., et al. (1986). Differentiation of neoplastic from non-neoplastic lesions in dog brain using quantitative CT. *Veterinary Radiology* 27, 121-128.
- Fitch R.B., Hathcock J.T., Montgomery R.D. (1996). Radiographic and computed tomographic evaluation of the canine intercondylar fossa in normal stifles and after notchplasty in stable and unstable stifles. *Veterinary Radiology and Ultrasound* 37, 266-274.
- Fitch R.B., Wilson E.R., Hathcock J.T., et al. (1997). Radiographic, computed tomographic and magnetic resonance imaging evaluation of a chronic long digital extensor tendon avulsion in a dog. *Veterinary Radiology and Ultrasound* 38, 177-181.
- Flegel T., Podell M., March P.A., et al. (2002). Use of a disposable real-time CT stereotactic navigator device for minimally invasive dog brain biopsy through a mini-burr hole. *American Journal of Neuroradiology* 23, 1160-1163.
- Forrest L.J. (1999). The head: excluding the brain and orbit. *Clinical Techniques in Small Animal Practice* 14, 170-176.
- Forterre F., Gutmannsbauer B., Schmahl W., et al. (1998). CT-Myelographie zur Diagnose des Plexus-brachialis-Abrisse beim Kleintier. *Tierärztliche Praxis* 26, 322-329.
- Galloway A.M., Curtis N.C., Sommerlad S.F., et al. (1999). Correlative imaging findings in seven dogs and one cat with spinal arachnoid cysts. *Veterinary Radiology and Ultrasound* 40, 445-452.
- George T.F., Smallwood J.E. (1992). Anatomic atlas for computed tomography in the mesaticephalic dog: head and neck. *Veterinary Radiology and Ultrasound* 33, 217-240.
- Gielen I., Van Ryssen B., Buijtelts J., et al. Canine elbow incongruity evaluated with computerised tomography (ct), radiography and arthroscopy. *Proceedings European Association of Veterinary Diagnostic Imaging annual conference*, Paris, July 18-21st 2001, p 22.
- Giroux A., Jones J.C., Bohn J.H., et al. (2002). A new device for stereotactic CT-guided biopsy of the canine brain: design, construction, and needle placement accuracy. *Veterinary Radiology and Ultrasound* 43, 229-236.
- Gordon L.E., Thacher C., Matthiesen D.T., et al. (1994). Results of craniotomy for the treatment of cerebral meningioma in 42 cats. *Veterinary surgery* 23, 94-100.
- Hara Y., Tagawa M., Ejima H., et al. (1994). Usefulness of computed tomography after myelography for surgery on dogs with cervical intervertebral disc protrusion. *Journal of Veterinary Medical Science* 56, 791-794.
- Harari J., Moore M. M., Leathers C.W., et al. (1994). Computed tomographic-guided free-hand needle biopsy of brain tumours in dogs. *Progress in Veterinary Neurology* 4, 41-44.
- Hathcock J.T. (1994). Vacuum phenomenon of the canine spine: CT findings in 3 patients. *Veterinary Radiology and Ultrasound* 35, 285-289.
- Hathcock J.T., Stickle R.L. (1993). Principles and concepts of computed tomography. *Veterinary Clinics of North America: Small Animal Practice* 23, 399-415.

- Hathcock J.T., Newton J.C. (2000). Computed tomographic characteristics of multilobular tumour of bone involving the cranium in 7 dogs and zygomatic arch in 2 dogs. *Veterinary Radiology and Ultrasound* 41, 214-217.
- Hoskinson J.J. (1993). Imaging techniques in the diagnosis of middle ear disease. *Seminars in Veterinary Medicine and Surgery (Small Animal)* 8, 10-16.
- Hoskinson J.J., Tucker R.L. (2001). Diagnostic imaging of lameness in small animals. *Veterinary Clinics of North America: Small Animal Practice* 31, 165-180.
- Jeffery N.D., Thakkar C.H., Yarrow T.G. (1992). Introduction to Computed Tomography of the Canine Brain. *Journal of Small Animal Practice* 33, 2-10.
- Johnson A.L., Probst C.W., DeCamp C.E., et al. (2001). Comparison of trochlear block recession and trochlear wedge recession for canine patellar luxation using a cadaver model. *Veterinary Surgery* 30, 140-150.
- Jones J.C., Wilson M.E., Bartels J.E. (1994). A review of high resolution computed tomography and a proposed technique for regional examination of the canine lumbosacral spine. *Veterinary Radiology and Ultrasound* 35, 339-346.
- Jones J.C., Cartee R.E., Bartels J.E. (1995). Computed tomographic anatomy of the canine lumbosacral spine. *Veterinary Radiology and Ultrasound* 36, 91-99.
- Jones J.C., Sorjonen D.C., Simpson S.T., et al. (1996). Comparison between computed tomographic and surgical findings in nine large breed dogs with lumbosacral stenosis. *Veterinary Radiology and Ultrasound* 37, 247-256.
- Jones J.C., Shires P.K., Inzana K.D., et al. (1999). Evaluation of canine lumbosacral stenosis using intravenous contrast-enhanced computed tomography. *Veterinary Radiology and Ultrasound* 40, 108-114, 1999.
- Jones J.C., Inzana K.D. (2000). Subclinical CT abnormalities in the lumbosacral spine of older large breed dogs. *Veterinary Radiology and Ultrasound* 41, 19-26.
- Kippenes H., Johnston G. (1998). Diagnostic imaging of osteochondrosis. *Veterinary Clinics of North America: Small Animal Practice* 28, 137-160.
- Kleiter M., Henninger W., Hirt R., et al. (1999). Portosystemischer Shunt bei einem Hund- Diagnosestellung mit Hilfe der Computertomographie. *Tierärztliche Monatschrift* 86, 64-70.
- Kneissl S., Schedlbauer B. (1997). Sagittal computed tomography of the feline spine. *Veterinary Radiology and Ultrasound* 38, 282-283.
- Koblik P.D., LeCouteur R.A., Higgings R.J., et al. (1999a). Modification and application of a Pelorus Mark III stereotactic system for CT-guided brain biopsy in 50 dogs. *Veterinary Radiology and Ultrasound* 40, 424-433.
- Koblik P. D., LeCouteur R.A., Higgings R. J., et al. (1999b). CT-guided brain biopsy using a modified Pelorus Mark III stereotactic system : experience with 50 dogs. *Veterinary Radiology and Ultrasound* 40, 434-440.
- Lang J., Huber P., Vandeveld M. (1988). Erfahrungen mit der Computertomographie in der Kleintierneurologie. *Schweizer Archiv für Tierheilkunde* 130, 167-183.

- LeCouteur R.A., Fike J.R., Cann C.E., et al. (1981) Computed tomography of brain tumours in the caudal fossa of the dog. *Veterinary Radiology* 22, 244-251.
- LeCouteur R.A., Fike J.R., Scagliotti R.H., et al (1982). Computed tomography of orbital tumours in the dog. *The Journal of the American Veterinary Medical Association* 180, 910-913.
- LeCouteur R.A., Fike J.R., Cann C.E., et al. (1983). X-ray computed tomography of brain tumours in cats. *Journal of the American Veterinary Medical Association* 183, 301-305.
- LeCouteur R.A., Koblik P.D., Higgings R.J., et al. (1998). Computed tomography-guided stereotactic brain biopsy in 25 dogs and 10 cats using the Pelorus mark III biopsy system. *Journal of Veterinary Internal Medicine* 12, 207.
- LeCouteur R.A. (1999). Current concepts in the diagnosis and treatment of brain tumours in dogs and cats. *Journal of Small Animal Practice* 40, 411-416.
- Legrand J.J., Carlier B. (1986). Examen tomodensitométrique de l'encéphale du chien I. Conduite de l'examen et repères anatomiques. *Revue de Médecine Vétérinaire* 137, 193-203.
- Losonsky J.M., Abbott L.C., Kuriashkin I.V. (1997). Computed tomography of the normal feline nasal cavity and paranasal sinuses. *Veterinary Radiology and Ultrasound* 38, 251-258.
- Love N.E., Kramer R.W., Spodnick G.J., et al. (1995). Radiographic and computed tomographic evaluation of otitis media in the dog. *Veterinary Radiology and Ultrasound* 36, 375-379.
- Marcelin-Little D.J., De Young D.J., Ferris K.K. (1994). Incomplete ossification of the humeral condyle in spaniels. *Veterinary Surgery* 23, 475-487.
- Marincek B., Young S.W. (1980). Computed tomography of spontaneous canine neoplasms. *Veterinary Radiology* 21, 181-184.
- Markel M.D., Winkenheiser M.A., Morin R.L., et al. (1990). Non-invasive measurement of the material properties of bone healing with quantitative computed tomography, magnetic resonance imaging, single photon absorptiometry, and dual energy x-ray absorptiometry. *Veterinary Surgery* 19, 71-80.
- Mathews K.G., Koblik P.D., Richardson E.F., et al. (1996). Computed Tomographic Assessment of Noninvasive Intranasal Infusions in Dogs With Fungal Rhinitis. *Veterinary Surgery* 25, 309-319.
- McCarthy R.J., Feeney D.A., Lipowitz A.J. (1993). Preoperative diagnosis of tumours of the brachial plexus by use of computed tomography in three dogs. *Journal of the American Veterinary Medical Association* 202, 291-294.
- McEntee M.C., Page R.L., Heidner G.L., et al. (1991). A retrospective study of 27 dogs with intranasal neoplasms treated with cobalt radiation. *Veterinary Radiology* 32, 135-139.
- Meyer-Lindenberg A., Heinen V., Fehr M., Nolte I. (2002). Incomplete ossification of the humeral condyle as the cause of lameness in dogs. *Veterinary Journal of Comparative Orthopaedics and Traumatology* 15, 187-194.
- Moe L., Lium B. (1997). Computed tomography of hereditary multifocal renal cystadenocarcinomas in German Shepard dogs. *Veterinary Radiology and Ultrasound* 38, 335-343.
- Moissonnier P., Bordeau W., Delisle F., et al. (2000). Accuracy testing of a new stereotactic CT-guided brain biopsy device in the dog. *Research in Veterinary Science* 68, 243-247.

- Moissonnier P., Devauchelle P, Delisle F, et al. (2002). Stereotactic CT-guided brain biopsy in the dog. *Journal of Small Animal Practice* 43, 115-123.
- Moore G.E., Mathey W.S., Eggers J.S., et al. (2000). Osteosarcoma in adjacent lumbar vertebrae in a dog. *Journal of the American Veterinary Medical Association* 217, 1038-1040.
- Newberg A.H. (1990). Computed tomography of joint injuries. *Radiologic Clinics of North America* 28, 445-460.
- Niles J.D., Dyce J., Mattoon J.S. (2001). Computed tomography for the diagnosis of a lumbosacral nerve sheath tumour and management by hemipelvectomy. *Journal of Small Animal Practice* 42, 248-252.
- Olby N.J., Munana K.R., Sharp N.J., et al. (2000). The computed tomographic appearance of acute thoracolumbar intervertebral disc herniations in dogs. *Veterinary Radiology and Ultrasound* 41, 396-402.
- Park R.D., Beck E.R., LeCouteur R.A. (1992). Comparison of computed tomography and radiography for detecting changes induced by malignant nasal neoplasia in dogs. *Journal of the American Veterinary Medical Association* 201, 1720-1724.
- Patsikas M.N., Rallis T., Kladakis S.E., et al. (2001). Computed tomography diagnosis of isolated splenic torsion in a dog. *Veterinary Radiology and Ultrasound* 42, 235-237.
- Pettersson H., Resnick D. (1998). Musculoskeletal imaging. *Radiology* 208, 561-562.
- Plummer S.B., Wheeler S.J., Thrall D.E., et al. (1992). Computed tomography of primary inflammatory brain disorders in dogs and cats. *Veterinary Radiology and Ultrasound* 33, 307-312.
- Pretorius E.S., Fishman E.K. (1995). Helical (spiral) CT of the musculoskeletal system. *Radiologic Clinics of North America* 33, 949-978.
- Probst A., Kneissl S. (2001). Computed tomographic anatomy of the canine pancreas. *Veterinary Radiology and Ultrasound* 42, 226-230.
- Ramirez O., Thrall D.E. (1998). A review of imaging techniques for canine cauda equina syndrome. *Veterinary Radiology and Ultrasound* 39, 283-296.
- Reichle J.K., Snaps F.R. (1999). The elbow. *Clinical Techniques in Small Animal Practice* 14, 177-186.
- Reichle J.K., Park R.D., Bahr A.M. (2000). Computed tomographic findings of dogs with cubital joint lameness. *Veterinary Radiology and Ultrasound* 41, 125-30.
- Rosenstein D.S. (2000). Diagnostic imaging in canine pheochromocytoma. *Veterinary Radiology and Ultrasound* 41, 499-506.
- Russo M., Covelli E.M., Meomartino L., et al. (2002). Computed tomographic anatomy of the canine inner and middle ear. *Veterinary Radiology and Ultrasound* 43, 22-26.
- Samii V.F., Biller D.S., Koblik P.D. (1998). Normal cross-sectional anatomy of the feline thorax and abdomen: comparison of computed tomography and cadaver anatomy. *Veterinary Radiology and Ultrasound* 39, 504-511.
- Saunders J.H., Zonderland J., Clercx C., et al. (2002). Computed tomographic findings in 35 dogs with nasal aspergillosis. *Veterinary Radiology and Ultrasound* 43, 5-9.

- Saunders J.H., van Bree H., Gielen I., de Rooster H. (2003). Computed tomography in dogs with chronic nasal disease. *Vet Radiology and Ultrasound*, accepted for publication.
- Schwarz T. (1995). Comparison of sensitivity and specificity of conventional x-ray and computed tomography (CT) in nasal tumours and mycoses in dogs. *Veterinary Radiology and Ultrasound* 33, 428-433.
- Schwarz T., Weller R., Dickie A.M., et al. (2002). Imaging of the canine and feline temporomandibular joint: a review. *Veterinary Radiology and Ultrasound* 43, 85-97.
- Seeram E. (2001). Computed tomography. In: Wilke J. (ed). *Computed Tomography: Physical Principles, Clinical Applications, and Quality Control*, second edition, W.B. Saunders, Philadelphia, USA, pp. 1-19.
- Seitz S.E., Losonsky J.M., Marretta S.M. (1996). Computed tomographic appearance of inflammatory polyps in three cats. *Veterinary Radiology and Ultrasound* 37, 99-104.
- Sharp N.J.H., Cofone M., Robertson I.D., et al. (1995). Computed tomography in the evaluation of caudal cervical spondylomyelopathy of the Doberman Pinscher. *Veterinary Radiology and Ultrasound* 36, 100-108.
- Smallwood J.E., George T.F. (1992). Anatomic atlas for computed tomographic findings in the mesaticephalic dog: caudal abdomen and pelvis. *Veterinary Radiology and Ultrasound* 33, 143-167.
- Smallwood J.E., George T.F. (1993). Anatomic atlas for computed tomography in the mesaticephalic dog: thorax and cranial abdomen. *Veterinary Radiology and Ultrasound* 34, 65-84.
- Speciale J., Van Winckle T.J., Steinberg S.A., et al. (1992). Computed tomography in the diagnosis of focal granulomatous meningoencephalitis: Retrospective evaluation of three cases. *Journal of the American Animal Hospital Association* 28, 327-332.
- Stickle R.L., Hathcock JT. (1993). Interpretation of Computed Tomographic Images. *Veterinary Clinics of North America: Small Animal Practice* 23, 417-429.
- Thrall D.E., Robertson I.D., McLeod D.A., et al. (1989). A comparison of radiographic and computed tomography findings in 31 dogs with malignant nasal cavity tumours. *Veterinary Radiology* 30, 59-66.
- Turrell J.M., Fike J.R., LeCouteur, R.A., et al. (1986). Computed tomography characteristics of primary brain tumours in 50 dogs. *Journal of the American Veterinary Medical Association* 188, 851-856.
- van Bree H., Van Ryssen, B. (1994). Diagnostic imaging of the canine elbow including radiology, arthroscopy and computed tomography (CT). Oral Abstracts, 10th IRVA Meeting. *Veterinary Radiology and Ultrasound* 35, p 248, nr 069.
- van Bree H., Gielen I., Van Ryssen B., et al. (2002). Comparative joint imaging in small animals. *The European Journal of Companion Animal Practice* 12, 25-36.
- Voorhout G., Stalp R., Lubberink A.A.M.A. (1988). Computed tomography in the diagnosis of hyperadrenocorticism not suppressible by dexamethazone. *Journal of the American Veterinary Medical Association* 192, 641-646.
- Voorhout G (1990). X-ray computed tomography, nefrotomography, and ultrasonography of the adrenal glands of healthy dogs. *American Journal of Veterinary Research* 51, 625-631.

- Voorhout G., Stalp R., Rijnberk A. et al. (1990). Assessment of survey radiography and comparison with x-ray computed tomography for detection of hyperfunctioning adrenocortical tumours in dogs. *Journal of American Veterinary Medical Association* 196, 1799-1803.
- Waters D.J., Coakley F.V., Cohen M.D., et al. (1998). The detection of pulmonary metastases by helical CT: a clinicopathologic study in dogs. *Journal of Computerised Assisted Tomography* 22, 235-240.
- Wolf M., Pedroia V., Higgings R.J., et al. (1995). Intracranial ring enhancing lesions in dogs: a correlative CT scanning and neuropathologic study. *Veterinary Radiology and Ultrasound* 36, 16-20.
- Yamazoe K., Ohashi F., Kadosawa T., et al. (1994). Computed tomography on renal masses in dogs and cats. *Journal of Veterinary Medical Science* 56, 813-816.
- Zook B.C., Hitzelberg R.A., Fike J.R., et al. (1981). Anatomy of the Beagle in cross-section: head and neck. *American Journal of Veterinary Research* 42, 844-849.

3. TARSOCRURAL OSTEOCHONDROSIS IN THE DOG

INTRODUCTION

The designation “osteochondrosis” (OC) is used to describe a heterogeneous group of disorders involving both cartilage and bone in humans and a variety of animal species. Lesions of OC are highly prevalent in pigs, horses, large breed dogs, and poultry but do not always result in clinical signs. The radiographic picture is dominated by fragmentation, collapse, sclerosis, and sometimes reactive bone formation.

There is considerable confusion regarding the term “osteochondrosis” as a consequence of historically changed concepts on definition and pathogenesis.¹

Traditionally, osteochondrosis has been used to describe a group of disorders with predilection for the immature skeleton and involvement of an epiphysis, apophysis, or epiphysoid bone. On the other hand, in clinical practice osteochondrosis is sometimes used to describe degenerative changes which may be a consequence of the lesions involving the immature skeleton.²

Initially, vascular insufficiency with osteonecrosis was postulated as the common pathogenesis. However, this concept has been put to rest and other more generalised factors have been suggested. In the developing epiphysis, the rapidly developing central nucleus of bone within the cartilage is especially vulnerable to mechanical pressure, superimposed on hormonal or nutritional changes, hence the often bilateral appearance of the lesions. Genetic factors have been recognised. Trauma has been suggested as an initiating or aggravating factor with epiphyseal irregularity and fragmentation during periods of accelerated growth.² In veterinary medicine, osteochondrosis in the epiphysis is thought to develop as a disturbance in the ossification of epiphyseal or articular cartilage into subchondral bone. As a consequence, the cartilage thickens and the deeper layers are not sufficiently nourished and become weaker. This stage is usually not accompanied by lameness. When an osteochondral flap or fragment is formed, clinical signs are usually present.^{3,4,5} In a later stage, synovitis and degenerative changes may develop leading to arthrosis.

Osteochondrosis is diagnosed more frequently in males than in females, and especially in fast growing dogs of large and giant breeds. In a considerable percentage of the affected dogs, the condition is bilateral. Osteochondrosis can affect different/several joints but is diagnosed most frequently in the elbow and shoulder, and to a much lesser degree in the tarsocrural and stifle joint.^{6, 7, 8, 9, 10, 11, 12, 13}

TARSOCRURAL OSTEOCHONDROSIS IN THE DOG

In the dog, osteochondrosis with osteochondral fragments at the level of the tarsocrural joint is a well known but rather uncommon cause of hind limb lameness: it comprises 9% of all cases of osteochondrosis with osteochondral fragments. The tarsocrural joint is the third most commonly affected joint. The osteochondral defect can involve the medial or the lateral trochlear ridge of the talus and results in instability, pain, lameness, and progressive degenerative joint disease (DJD).¹⁴ Early cases reported involvement of the medial ridge of the talus; later reports described lesions in the lateral ridge as well. The delay in recognition of these lateral ridge lesions may have been due to the lesion in this location being more difficult to recognise radiographically.¹⁵

Tarsocrural osteochondral (TOC) lesions usually affect large breeds. Rottweilers and Labrador Retrievers are most frequently reported to be affected and the Australian Cattle dog, Bull Terrier and Bullmastiff have been over-represented. Atypical of OC with fragmentation in other sites, male and female dogs are almost equally affected.^{14, 16, 17} Approximately 50% of reported cases of TOC with fragmentation are bilateral,^{17, 18} although clinical lameness is rarely symmetrical.^{19, 20, 21}

The age at the time of presentation ranges from 4 months to 4 years, with a mean age of 7 months although affected dogs often develop clinical signs by 4 to 5 months of age. Most of the patients have a consistent weight-bearing lameness. In chronic cases this can progress to an intermittent non-weight-bearing lameness. The affected hock joint is often held in hyperextension (Fig. 1).



Figure 1: Typical posture of a dog with tarsocrural osteochondrosis. Notice the hyperextension of the affected tarsal joint (arrow).

Muscle atrophy is often present in chronic cases. Palpation of the affected hock demonstrates synovial effusion, which is detected as a fluctuant swelling most easily palpated immediately caudodistal to the malleoli. In more chronic cases, the joint capsule becomes thickened, and the range of motion is decreased, especially in flexion. Full flexion or extension of the

affected hock joint may be painful. Crepitus may be elicited as the affected joint is moved through the range of motion.²²

The most common location for the osteochondral lesions is the medial trochlear ridge of the talus. Involvement of the lateral trochlear ridge is less common and occurs in 25% of the cases.^{16, 17, 20, 23, 24} Fragmentation of the medial malleolus has also been described with and without TOC.²⁵ Rottweilers have been reported to have a higher incidence of lateral trochlear ridge involvement than other breeds.¹⁸ The location on the trochlear ridge is different for both conditions: in OC of the lateral ridge, the dorsal, dorsoproximal, or proximal part can be affected,^{26, 27} while in OC of the medial ridge, lesions occur mostly on the plantar (i.e. proximal) part.¹⁷

The diagnosis of TOC is not always obvious and exploratory arthrotomy is advocated as a reasonable diagnostic option by some authors,^{14, 17, 28} but is somewhat drastic and should be considered as the last resort.

Although a very detailed study on the radiographic anatomy of the canine tarsocrural joint exists,²⁹ the radiographic evaluation of this region remains difficult due to superimposition of the distal tibia, fibula and calcaneus. The complexity of the tarsocrural joint (Fig. 2), especially in the young dog, is such that even with an adequate number of appropriate projections, subtle changes involving both ridges of the talar trochlea can be missed.

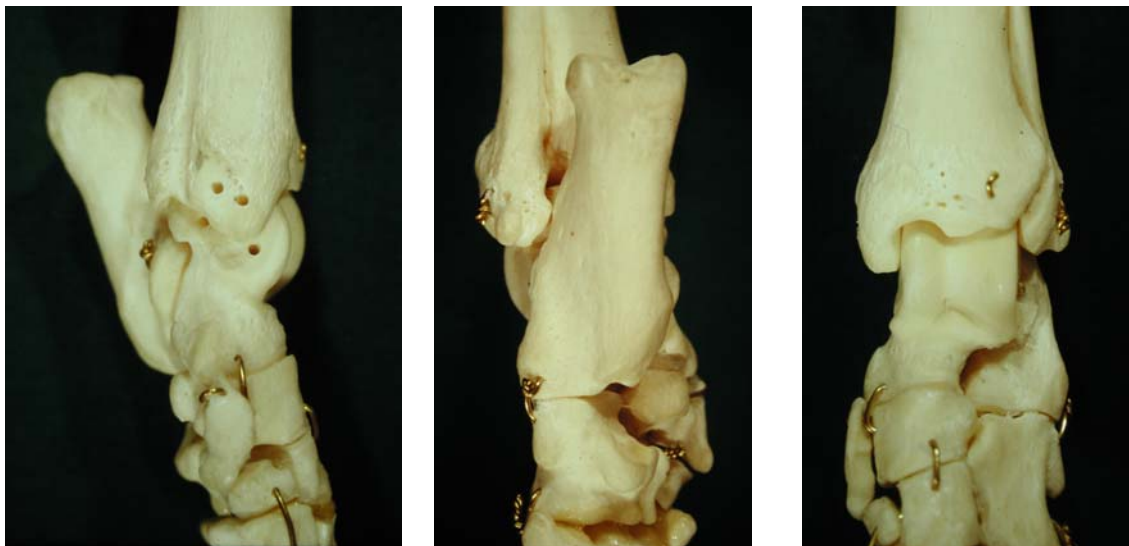


Figure 2: The tarsocrural joint is a complex joint with a lot of superimposition of bony structures making the radiographic evaluation of this region difficult.

The radiographic diagnosis of TOC can often be challenging. Excellent technique and positioning of the patient are essential for the radiographic visualisation of the lesions. Several

projections are proposed including the fully extended and fully flexed mediolateral, the plantarodorsal, the plantaromedial-dorsolateral and plantarolateral-dorsomedial, and a flexed dorsoplantar skyline view (Fig. 3).^{14, 29, 30}



Figure 3 : Radiographic protocol to examine a canine tarsal joint including the fully extended (a) and fully flexed mediolateral (b), the plantarodorsal (c), the flexed dorsoplantar skyline (d), and a plantarolateral-dorsomedial (e) and plantaromedial-dorsolateral (f) view.

Most lesions of the medial trochlear ridge can be identified on the standard plantarodorsal radiograph (Fig. 4).¹⁷



Figure 4: Plantarodorsal view of a medial TOC. Notice the enlarged joint space and the associated osteochondral fragment (arrow).

Especially the radiographic diagnosis of osteochondrosis on the lateral ridge can be difficult due to the complexity of the tarsocrural joint and the superimposition of the different bony structures. The fragments are best seen in the plantaromedial-dorsolateral oblique projection (Fig. 5), and in the fully flexed and extended mediolateral projections (Fig. 6).^{20, 26} The flexed dorsoplantar skyline projection can also be useful (Fig. 7).^{14, 21, 30}



Figure 5: Plantaromedial-dorsolateral oblique projection of a lateral TOC. Notice the defect in the lateral ridge and the fragment (arrow).



Figure 6: Flexed mediolateral projection of a lateral tarsocrural TOC. Notice the fragment (arrow).



Figure 7: Flexed dorsoplantar skyline projection of a lateral TOC. Notice the defect in the lateral ridge and the displaced fragment (arrow).

The radiographic appearance of TOC is variable and depends on the chronicity of the process and the location and extent of the lesion. Radiographic lesions vary from subchondral bony defects with associated sclerosis to mineralised flaps or osteochondral fragments. These fragments can comprise a substantial portion of the involved trochlear ridge. The OC defects may not be visible on the standard radiographic views. Degenerative changes, including subchondral sclerosis of the articulating surfaces of the tibia and osteophyte formation, are frequently present (Fig. 8).^{19, 20, 21, 24, 28, 29, 31, 32}



Figure 8: Degenerative changes, including subchondral sclerosis of the articulating surfaces of the tibia and osteophyte formation can be seen on this mediolateral (a) and dorsoplantar (b) view of a chronic case of medial TOC (arrows).

The major differential diagnosis includes dogs with post-traumatic changes in the tarsocrural joint in which the appearance of the secondary changes is similar to those that develop in the joint with an osteochondral lesion. If the DJD changes are extensive, visualisation of the contour of the trochlear ridges and identification of the osteochondral lesion is more difficult.¹⁵

Diagnostic and surgical arthroscopy of the human tarsus is considered safe, accurate and minimally invasive.^{33, 34, 35, 36, 37}

In the dog, arthroscopic techniques for evaluation of the hock joint have been described³⁸ and applied in clinical cases.^{27, 39} The technique proved to be minimally invasive while ensuring excellent visualisation of the medial and lateral trochlear ridge. It provided additional information about the extent and localisation of the lesions, allowing surgical removal of the fragment via a mini-arthrotomy.⁴⁰

In humans, OC lesions are also found in the medial or lateral aspect of the talus and although plain radiographs are usually sufficient to make the diagnosis, computed tomography is beneficial, in pre-operative planning, for accurately determining the size and location of the

lesion.⁴¹ In human beings, lateral lesions are usually traumatic in origin and are thought to be true transchondral fractures, whereas the medial lesions may have been the result of other factors.⁴² In the dog traumatic fragmentation of the lateral talar ridge is also postulated. These fragments are thought to be avulsion fractures of the short lateral collateral ligaments associated with relatively large loose fragments situated proximally. Any possible relation between osteochondrosis and these avulsion fractures could not be evaluated.⁴³

In humans, the usefulness of magnetic resonance imaging (MRI) has been documented for identifying the location of a suspected lesion and for predicting the integrity of the cartilage surface of tarsal osteochondral lesions.⁴⁴ A low intensity area on T1-weighted images strongly suggests the presence of an osteochondral lesion and is used for early as well as for definitive diagnosis of occult lesions.⁴⁵ On T2-weighted images, distinction between partially detached and fully unattached fragments is possible on the basis of a high signal fluid interface between the osteochondral fragment and the subchondral talar bed.^{44, 45} Disappearance and/or decreasing size of these signals suggests healing of these lesions on follow-up.⁴⁵

In humans, arthrography using iodinated contrast medium followed by CT (arthro-CT) is an excellent technique to detect intra-articular loose bodies and to evaluate the degree of detachment of the OC fragment. Arthro-CT images also permits to early depict contour defects and irregularities of the surface of the articular cartilage.^{46, 47} This technique is only rarely used in imaging of small animal joints (Fig. 9).

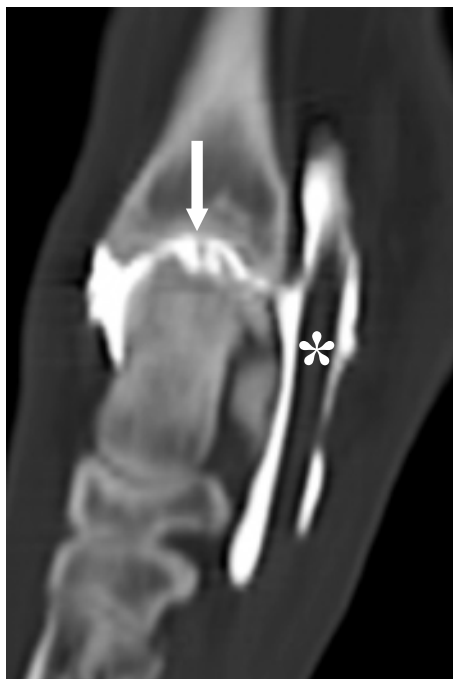


Figure 9: Sagittal image of an arthro-CT of a dog with an OC lesion of the medial talar ridge. By the injection of the contrast medium a high signal fluid interface between the OC fragment and the subchondral talar bed is noticed (white arrow). This finding suggests that the fragment is completely detached but not displaced. Also the deep flexor tendon (white asterisk) is surrounded by hyperdense fluid representing its tendon sheath communicating with the joint space.

In humans a four-stage classification system, called the “Berndt and Harty” classification, has been widely accepted to classify TOC lesions^{36, 48} and is used to determine the therapeutic regime in talar dome lesions. This classification system is based on radiographic findings but other classification systems, based on magnetic resonance imaging (MRI) and CT scanning all correlate well with this original classification system. This classification system classifies the lesion into 4 different stages depending on the status of the trochlear ridge and the associated fragment: Stage I - a subchondral bone lesion without an associated fragment; Stage II - a partially detached OC fragment; Stage III - a completely detached OC fragment remaining in the crater; and Stage IV- a complete detached and displaced fragment.^{36, 48}

Computed tomography (CT) is more available to veterinarians these days but it is only rarely used for the diagnosis of orthopaedic disorders in small animals.^{49, 50} A few reports exist on the use of CT in the imaging of ulnar fragmented coronoid processes.^{51, 52, 53} CT offers several advantages over conventional radiography including elimination of superimposed structures, thereby decreasing the complexity of the image. CT images can also be displayed in different grey scale formats, which can enhance visualisation of specific structures, and the images can be reconstructed in multiple anatomic planes.⁵⁴ These features could provide useful additional information, not only in diagnosing OC in complex joints like the tarsocrural joint, but also in identifying the exact extent and location of the lesion which is necessary for the selection of an appropriate surgical approach.²¹

In human beings, successful arthroscopic treatment of OC with fragmentation of the talus has been reported. However, depending on the appearance of the lesion, arthrotomy may be required to perform the procedure thoroughly.⁵⁵ The reported results are better than in the dog. The overall success rate in humans is about 85 to 90%.^{36, 56} The reason for this difference is probably due to the fact that these lesions are diagnosed in an earlier phase than in the dog. Another reason could be the different treatment used in men depending on the stage of the lesions. Stage III and IV lesions are treated with reduction and fixation with absorbable pins in the acute stage⁵⁷ although long-term studies regarding their outcome are lacking.⁵⁸ This technique should result in less joint incongruity and instability.⁵⁸ Studies in men have also shown better results with earlier treatment.⁵⁹ Postoperatively patients are sent to physiotherapy to regain range of motion and strength⁶⁰ which also could influence the final outcome.

Treatment options for canine TOC include conservative treatment (restricted exercise, weight management and medical treatment) and surgery. The choice to be made remains controversial. One report claims that removal of OC fragments from the medial talar trochlea

does not improve prognosis compared to conservative treatment.¹⁹ Another study found that only 25% of the treated joints had attained full function post-surgically, and that DJD changes had progressed in all joints.²⁴ Another report concluded, after a review of the literature, that surgical treatment was preferable to conservative treatment since the overall treatment response is better after surgery.¹⁷ Early surgical removal of the fragment is providing the best results.¹⁹ Waiting decreases the chances of a good result because of the progress of DJD.⁶¹ The same authors claim that dogs older than 1 year should probably be treated conservatively.⁶¹

Surgical treatment consists of OC fragment removal, with or without curettage of the defect, to allow healing by outgrowth of fibrocartilage from the underlying subchondral bone.^{62, 63}

Surgical removal of the fragment may be performed by invasive surgery (cutting collateral ligaments, osteotomy malleolus); less invasive²¹ minimal exposure techniques for both lateral and medial locations, and minimally invasive techniques (arthroscopy or mini-arthrotomy).^{39,}

⁴⁰ Several authors suggest that the re-attachment of OC fragments would be preferable to removal^{19, 21, 64, 65} especially when the lateral talar ridge is involved by traumatic fragmentation with avulsion of the short collateral ligaments.⁴³ Re-attachment of these fragments may be less successful because of degenerative changes in the fragment and an imperfect “fit” of the fragment in the subchondral bone defect.²⁴

Generally, the prognosis for full use of the affected limb is stated to be poor^{7, 22} whatever treatment has been performed.

REFERENCES

1. Ekman S and Carlson CS. The pathophysiology of osteochondrosis. *Vet Clin North Am: Small Anim Pract* 1998, 28, 17-32.
2. Resnick D. Osteochondroses. In: *Diagnosis of bone and joint disorders*. Eds. Bralow L & Wright G. Saunders Company, New York, 4th ed, 2002, 3686-3741.
3. Olsson SE, Reiland S. The nature of osteochondrosis in animals. *Acta Radiol (Suppl)* 1978, 358, 299-306.
4. Olsson SE. Pathophysiology, morphology, and clinical signs of osteochondrosis (chondrosis) in the dog. In: *Pathophysiology of small animal surgery*. Ed M.J. Bojrab. Lea & Febiger, Philadelphia, 1981, 604-617.
5. Lenehan TM, Van Sickle DC. Canine osteochondrosis. In: *Textbook of small animal orthopedics*. Eds CD Newton and DM Nunamaker. JB Lippincott Co, Philadelphia, 1985, 981-997.
6. Alexander JW, Richardson DC, Selcer BA. Osteochondritis dissecans of the elbow, stifle, and hock - a review. *J Am Anim Hosp Assoc* 1981, 17, 51-56.
7. Smith CW. Osteochondrosis in the dog - Diagnosis, Treatment, and Prognosis. *Can Pract* 1991, 16, 15-22.
8. Fox SM, Walker AM. Identifying and treating the primary manifestations of osteochondrosis of the elbow. *Vet Med* 1993, 2, 132-146.
9. Leighton RL. Osteochondritis dissecans of the shoulder joint of the dog. *Vet Clin of North Am: Small Anim Pract* 1971, 1, 391-401.
10. Montgomery RD, Milton JL, Henderson, RA, et al. Osteochondritis dissecans of the canine stifle. *Compend Cont Educ Pract* 1989, 11, 1199-1210.
11. Johnston SP. Osteochondritis dissecans of the humeral head. *Vet Clin North Am: Small Anim Pract* 1998, 28, 33-49.
12. Boulay JP. Fragmented medial coronoid process of the ulna in the dog. *Vet Clin North Am: Small Anim Pract* 1998, 28, 51-74.
13. Harari J. Osteochondrosis of the femur. *Vet Clin North Am: Small Anim Pract* 1998, 28, 87-94.
14. Fitch RB, Beale BS. Osteochondrosis of the canine tibiotarsal joint. *Vet Clin North Am: Small Anim Pract* 1998, 28, 95-113.
15. Morgan JP, Wind A, Davidson AP. Osteochondrosis of the talus. In: *Hereditary bone and joint disease in the dog: Osteochondroses-Hip dysplasia-Elbow dysplasia*. Eds JP Morgan, A Wind and AP Davidson. Schlutersche GmbH, Hannover 2000, 239-245.
16. Van Ryssen B, van Bree H, Verschooten F. Osteochondritis dissecans of the tarsal joint in the dog: a review. *Vlaams Diergeneesk Tijdsch* 1991, 60, 197-202.
17. Montgomery RD, Hathcock JT, Milton JL, et al. Osteochondritis dissecans of the canine tarsal joint. *Compend Cont Educ Pract Vet* 1994, 16, 835-845.
18. Weinstein MJ., Mongil CM., Rhodes WH, et al. Orthopedic conditions of the Rottweiler – Part II. *Compend Cont Educ Pract Vet* 1995, 17, 925-939.
19. Smith MM, Vasseur PB, Morgan JP. Clinical evaluation of dogs after surgical and nonsurgical management of osteochondritis dissecans of the talus. *J Am Vet Med Assoc* 1985, 187, 31.
20. Wisner ER, Berry CR, Morgan JP, et al. Osteochondrosis of the lateral trochlear ridge of the talus in seven rottweiler dogs. *Vet Surg* 1990, 19, 435-439.

21. Beale BS, Goring RL, Herrington J, et al. A prospective evaluation of four surgical approaches to the talus of the dog used in the treatment of osteochondritis dissecans. *J Am Anim Hosp Assoc* 1991, 27, 221-229.
22. Bloomberg MS, Lewis DD. Osteochondrosis of sporting and working dogs. In: *Canine sports medicine and surgery*. Eds MS Bloomberg, JF Dee and RA Taylor. WB Saunders Company, Philadelphia, 1998, 234-250.
23. Denny HR. Osteochondritis dissecans of the hock joint in the dog. *Vet Annual* 1981, 21, 224-228.
24. Breur GJ, Spaulding KA, Braden TD. Osteochondritis dissecans of the medial trochlear ridge of the talus in the dog. *Vet Compar Orthop Traum* 1989, 4, 168-176.
25. Newell SM, Mahaffey MB, Aron DN. Fragmentation of the medial malleolus of dogs with and without tarsal osteochondrosis. *Vet Radiol & Ultrasound* 1994, 1, 5-9.
26. Carlisle CH, Robins GM, Reynolds KM. Radiographic signs of osteochondritis dissecans of the lateral ridge of the trochlea talus in the dog. *J Small Anim Pract* 1990, 31, 280-286.
27. Van Ryssen B, van Bree H. Arthroscopic evaluation of osteochondrosis lesions in the canine hock joint: a review of two cases. *J Am Anim Hosp Assoc* 1992, 28, 295-299.
28. Johnson KA, Howlett CR, Pettit GD. Osteochondrosis in the hock joints in dogs. *J Am Anim Hosp Assoc* 1980, 16, 103-113.
29. Carlisle CH, Reynolds KM. Radiographic anatomy of the tarsocrural joint of the dog. *J Small Anim Pract* 1990, 31, 273-279.
30. Miyabayashi T, Biller, D S, Manley P A, et al. Use of a flexed dorsoplantar radiographic view of the tarsocrural joint to evaluate lameness in two dogs. *J Am Vet Med Assoc* 1991, 199, 598-600.
31. Rosenblum GP, Robins GM, Carlisle CH. Osteochondritis dissecans of the tibio-tarsal joint in the dog. *J Small Anim Pract* 1978, 19, 759-767.
32. Aron DN, Mahaffey MB, Rowland GN. Free chondral fragment involving the lateral trochlear ridge of the talus in a dog. *J Am Vet Med Assoc* 1985, 186, 1095-1096.
33. Baker CL, Andrews JR, Ryan JB. Arthroscopic treatment of transchondral talar dome fractures. *Arthroscopy: J Arthrosc Rel Surg* 1986, 2, 82-87.
34. Guhl JF. Osteochondritis dissecans. In: *Ankle arthroscopy. Pathology and surgical techniques*. Ed Guhl JF. Slack Incorp, New Jersey 1988, 95-106.
35. Ferkel R D, Fischer S P. Progress in ankle arthroscopy. *Clin Orthop Rel Res* 1989, 240, 210-220.
36. Baker C L, Morales RW. Arthroscopic treatment of transchondral talar dome fractures: A long-term follow-up study. *Arthroscopy: J Arthrosc Rel Surg* 1999, 15, 197-202.
37. Schuman L, Struijs PA, van Dijk CN. Arthroscopic treatment for osteochondral defects of the talus. Results at follow-up at 2 to 11 years. *J Bone Joint Surg* 2002, 84B, 364-368.
38. Van Ryssen B, van Bree H, Vyt Ph. Arthroscopy of the canine hock joint. *J Am Anim Hosp Assoc* 1993, 29, 107-115.
39. Cook JL, Tomlinson JL, Stoll MR, et al. Arthroscopic removal and curettage of osteochondrosis lesions on the lateral and medial trochlear ridges of the talus in two dogs. *J Am Anim Hosp Assoc* 2001, 37, 75-80.
40. van Bree H, Van Ryssen B. Diagnostic and Surgical Arthroscopy in Osteochondrosis Lesions. *Vet Clin North Am: Small Anim Pract* 1998, 28, 161-189.
41. Zinman C, Reis ND. Osteochondritis dissecans of the talus: use of the high resolution computed tomography scanner. *Acta Orthop Scand* 1982, 53, 697-700.

42. Canale ST, Belding RH. Osteochondral lesions of the talus. *J Bone Joint Surg* 1980, 62A, 97-102.
43. Sjöström L, Håkanson N. Traumatic injuries associated with the short collateral ligaments of the talocrural joint of the dog. *J Small Anim Pract* 1994, 35, 163-168.
44. Schenk RC, Goodnight JM. Current concept review: Osteochondrosis dissecans. *J Bone Joint Surg* 1996, 78A, 439-456.
45. Higashiyama I, Kumai T, Takakura Y, et al. Follow-up study of MRI for osteochondral lesion of the talus. *Foot Ankle Int* 2000, 21, 127-133.
46. Heare MM, Gillespy T, III, and E. S. Bittar. Direct coronal computed tomography arthrography of osteochondritis dissecans of the talus. *Skeletal Radiol* 1988, 17, 187-189.
47. Ragozzino A, Rossi G, Esposito S, et al. Computerized tomography of osteochondral diseases of the talus dome. *Radiol. Med. (Torino)* 1996, 92, 682-686.
48. Berndt AL, Harty M. Transchondral fractures (osteochondritis dissecans) of the talus. *J Bone Joint Surg* 1959, 41A, 988-1020.
49. Stickle R.L., Hathcock JT. Interpretation of Computed Tomographic Images. *Vet Clin North Am: Small Anim Pract* 1993, 23, 417-429.
50. Kippenes H, Johnston, G. Diagnostic imaging of osteochondrosis. *Vet Clin North Am: Small Anim Pract* 1998, 28, 137-160.
51. Carpenter L, Schwarz P, Lowry J et al. Comparison of radiologic imaging techniques for diagnosis of fragmented medial coronoid process of the cubital joint in dogs. *J Am Vet Med Assoc* 1993, 203, 78-83.
52. van Bree H, Van Ryssen, B. Diagnostic Imaging of the Canine Elbow including Radiology, Arthroscopy and Computed Tomography (CT). Oral Abstracts, 10th IRVA Meeting. *Vet Radiol & Ultrasound* 1994, 35, 4, p 248, nr 069.
53. Reichle JK, Park RD, Bahr AM. Computed tomographic findings of dogs with cubital joint lameness. *Vet Radiol & Ultrasound* 2000, 41, 125-30
54. Drost WT, Love NE, Berry CR. Comparison of radiography, myelography and computed tomography for the evaluation of canine vertebral and spinal cord tumors in sixteen dogs. *Vet Radiol & Ultrasound* 1996, 37, 28-33.
55. Seil R, Rupp S, Pape D, et al. Approach to open treatment of osteochondral lesions of the talus. *Orthopade* 2001, 30, 47-52.
56. Tol JL, Struijs PA, Bossuyt PM, et al. Treatment strategies in osteochondral defects of the talar dome: a systematic review. *Foot Ankle Int.* 2000, 21, 119-126.
57. Simpson MB. Talar osteochondral injuries in athletes. *Operat Techn Sports Med* 2001, 9, 8-13.
58. Farmer JM, Martin DF, Boles CA, et al. Chondral and osteochondral injuries. Diagnosis and management. *Clin Sports Med.* 2001, 20, 299-320.
59. Pettine KA, Morrey BF. Osteochondral fractures of the talus. *J Bone Joint Surg* 1987, 69B, 89-92.
60. Ogilvie-Harris DJ, Sarrosa EA. Arthroscopic treatment of osteochondritis dissecans of the talus. *Arthroscopy: J Arthrosc Rel Surg* 1999, 15, 805-808.
61. Brinker W, Piermattei D, Flo G. Fractures and other orthopedic injuries of the tarsus, metatarsus and phalanges. In: *Handbook of Small Animal Orthopedics and Fracture Repair.* WB Saunders, Philadelphia, 1997, 607-655.

62. Olsson SE. Osteochondrosis in the dog. In: Current veterinary therapy VII. Ed Kirk RW. WB Saunders, Philadelphia, 1980, 807-815.
63. Olson NC, Mostosky UV, Flo GL, et al. Osteochondritis dissecans of the tarsocrural joint in three canine siblings. J Am Vet Med Assoc 1980, 176, 635-637.
64. van Ee RT, Gibson K, Roberts ED. Osteochondritis dissecans of the lateral ridge of the talus in a dog. J Am Vet Med Assoc 1988, 193, 1284-1286.
65. Dew TL, Martin RA. Functional, radiographic, and histologic assessment of healing of autogenous osteochondral grafts and full-thickness cartilage defects in the talus of dogs. Am J Vet Res 1992, 53, 2141-2152.

1. Since no data are available on computed tomography (CT) of the canine tarsus, the first aim of this study was to provide a technical protocol for CT examination of the canine tarsal joint and a detailed description of the normal canine tarsus as revealed by CT.
2. The purpose of the second part of this study was to evaluate and compare the findings of CT, radiography and arthroscopy in tarsocrural osteochondrosis (TOC), and to establish a classification system comparable to the one used in man based on these findings.
3. In the tarsocrural joint, OC can affect both, the medial and the lateral talar ridge. Radiographic diagnosis of lateral TOC is particularly compromised by supplementary superimposition of the calcaneus. As CT allows inspection of the talar ridges without superimposition of any bony structures, the capabilities of CT in diagnosing lateral TOC were compared with those of radiography.
4. A different aetiology for lateral and medial TOC has been proposed. The first aim of this study was to evaluate whether significant differences exist between medial and lateral TOC. Although 50% of the reported cases of TOC are bilateral, clinical lameness is rarely symmetrical. The second aim was to evaluate the differences between clinical and non-clinical lesions in dogs showing bilateral medial TOC.
5. The aim of the fifth part of this study was to evaluate the long-term results of minimally invasive treatment of TOC in the dog and the use of CT findings in its preoperative planning.
6. The aim of the last part of this study was to evaluate if a correlation between morphological data obtained by CT and clinical data, and the long-term functional outcome could be demonstrated.

**COMPUTED TOMOGRAPHY OF THE TARSAL JOINT IN CLINICALLY
NORMAL DOGS**

I. Gielen¹, L. De Rycke¹, H. van Bree¹, P. Simoens²

Departments of Medical Imaging¹ and Morphology², Faculty of Veterinary Medicine,
Ghent University, Salisburylaan 133, Merelbeke, Belgium

Adapted from:

I. Gielen, L. De Rycke, H. van Bree, P. Simoens. Computed tomography of the tarsal joint in clinically normal dogs. *American Journal of Veterinary Research* 2001; 62: 1911-1915.

SUMMARY

Objective—To use computed tomography to provide a detailed description of tarsal joint structures in clinically normal dogs.

Animals—Six normal adult mixed-breed dogs weighing 25 to 35 kg and one 12-month-old Bullmastiff weighing 65 kg.

Procedure—To perform computed tomography (CT) of both tarsal regions, dogs were anaesthetised and placed in ventral recumbency. One- and 2-mm contiguous slices were obtained, using a third generation CT scanner. Individual images were reviewed, using bone (window width = 3500 Hounsfield units; window level = 500 Hounsfield units) and soft tissue (window width = 400 Hounsfield units; window level = 66 Hounsfield units) settings. After euthanasia, the hind limbs from the Bullmastiff were removed and frozen at -18° C. Tarsal joints were sectioned into approximately 1-mm thick slab sections using a cryomicrotome. Anatomic sections were photographed and compared with the corresponding CT images. Computed tomographic reconstructions of the tarsocrural joint were created in sagittal and dorsal planes.

Results—Structures on the CT images were matched with structures in the corresponding anatomic sections. The entire tarsocrural joint surface could be evaluated on the reconstructed images in the sagittal and dorsal planes.

Conclusions and Clinical Relevance—CT images provide full anatomic detail of the bony structures of the tarsal joint in dogs. Tendons and large blood vessels can also be evaluated. These results could be used as a basis for evaluation of computed tomographic images of dogs with tarsal joint injuries.

INTRODUCTION

The tarsal joint in dogs is a compound and complex joint, and although there is a detailed study¹ on its radiographic anatomy, radiographic evaluation of this region remains difficult because of superimposition of various bony structures, including the distal portion of the tibia and fibula, talus, calcaneus, tarsal, and metatarsal bones. Therefore, the radiographic diagnosis of tarsal lesions, including tarsocrural osteochondrosis (TOC), can be challenging, and arthrotomy has been advocated as a reasonable diagnostic option by some authors.²⁻⁵ CT offers several advantages over conventional radiography, including the following: elimination of superimposed structures, thereby decreasing the complexity of the image; variation in grey scale formats, which can enhance observation of specific structures; and reconstruction of multiple anatomic planes.⁶

In humans medicine, CT is indicated in situations where detailed information is needed to make a precise diagnosis or to define a tarsal injury more accurately.⁷⁻⁹ In instances of complex intra-articular fractures, subchondral bone sclerosis, and other subchondral bone lesions such as TOC, CT is a useful expedient for the diagnosis and may indicate the exact size and location of the lesion.

To provide accurate interpretation of CT images and to recognise abnormalities that may be found, knowledge of the anatomy of the tarsal joint in clinically normal dogs is a prerequisite. The aim of the study presented here was to provide a detailed description of the tarsal joint in clinically normal dogs, as revealed by use of CT.

MATERIALS AND METHODS

Animals

Six healthy adult mixed-breed dogs weighing 25 to 35 kg and one 12-month-old Bullmastiff weighing 65 kg were used for our study. Prior to the study, tarsal joints of each dog were physically and radiographically examined. The following 6 radiographic views were obtained: 2 mediolateral views (1 in flexion, 1 in extension), 1 dorsoplantar

view, 1 dorsoproximal-dorsodistal view, and 2 oblique views. No abnormalities were found on any radiograph.

Computed tomography

Dogs were sedated using medetomidine hydrochloride^a (40 to 50 µg/kg of body weight, IM), and anaesthetised with thiopental sodium^b (8 mg/kg, IV). After intubation, anaesthesia was maintained with halothane. Dogs were positioned in ventral recumbency on the CT scanning table with the tarsal joints in extension (Fig 1). This position allows a perfect symmetry and comparison of both tarsi at the same level.

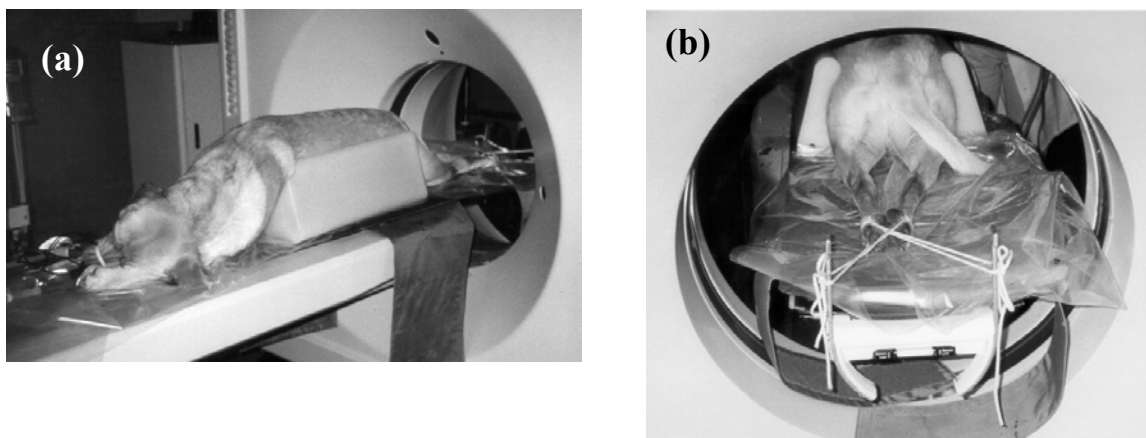


Figure 1: For CT examination of the tarsal joints, the dog is positioned in ventral recumbency (a) with the tarsal joints in extension and symmetrically positioned (b) thus allowing comparison of both tarsi at the same level.

A lateral survey view was obtained, using a third generation CT scanner^c to confirm correct positioning. On a plantarodorsal survey view, CT scans were performed from the distal portion of the tibia and fibula to the proximally located metatarsal bones and parallel to the tarsocrural joint space.

Two-millimeter thick contiguous views were obtained from the most proximal part of the calcaneus to 1 cm distal to the tarsometatarsal joint. However, in the region of the tarsocrural joint, 1-mm thick contiguous views were obtained. Individual images were reviewed using a bone setting (window width = 3500 Hounsfield units; window level = 500 Hounsfield units) and a soft tissue setting (window width = 400 Hounsfield units;

window level = 66 Hounsfield units). Settings for the CT image technique were as follows 120 kVp and 100 mA. Image acquisition time was approximately 10 minutes. Images from all 6 dogs were formatted on x-ray film^d and evaluated.

Comparison of CT and anatomic images

All 6 dogs recovered from anaesthesia. The Bullmastiff was euthanised after CT for reasons unrelated to orthopaedic conditions. After euthanasia, the hind limbs were removed and frozen at -18° C with the tarsal joints in extension. The tarsal joints from the distal portion of the tibia and fibula to the distal portion of the talus and calcaneus were embedded in carboxymethylcellulose and sectioned into approximately 1-mm-thick slab sections, using a large specimen cryomicrotome.^e All anatomic sections were photographed and matched with a corresponding CT image (bone setting) on the basis of appearance. From this collection, 12 representative matched pairs of the right tarsal joint were selected from proximal to distal regions. Bony structures and soft tissues were identified on the anatomic sections by comparing all features with a dissected tarsal joint of a large-breed dog that had been euthanised. The identified structures were subsequently located on the corresponding CT images (both bone and soft tissue settings) and afterwards, the list of identified structures was evaluated on the CT images of the 6 other dogs. The nomenclature used for designating all structures was in accordance with official anatomic terms.¹⁰ Computed tomography-based reconstructions of the tarsocrural joint in a sagittal and dorsal plane were made to determine whether an evaluation of the entire joint surface could be performed without superimposition of any bony structures.

RESULTS

The plantarodorsal survey view of the 17 selected levels of the right tarsal joint of the Bullmastiff was obtained (Fig 2). Computed tomographic images (bone and soft tissue settings) and the cut surface of the corresponding anatomic sections of the right tarsal joint of the Bullmastiff were compared (Fig 3 and 4).

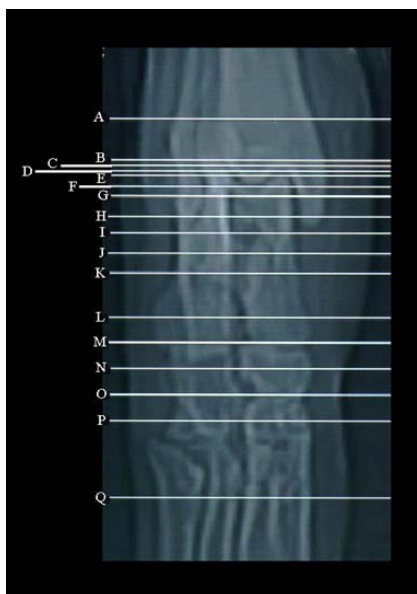


Figure 2: Plantarodorsal survey view of the tarsal joint of a clinically normal dog indicating the levels (A through Q) at which computed tomographic (CT) images were obtained.

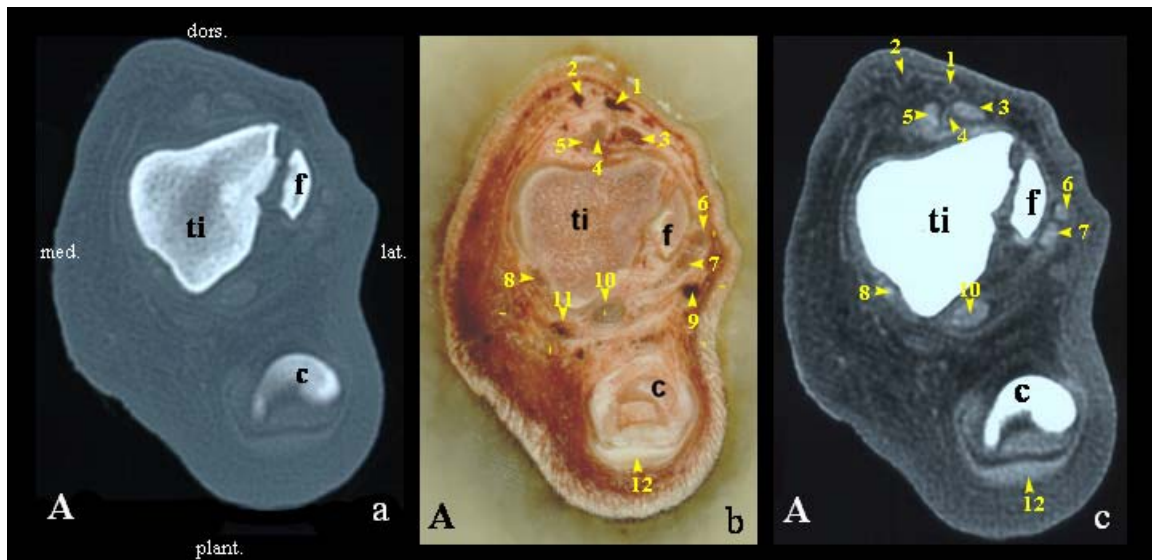
Several bony, tendinous, and vascular structures were visible on the proximally located anatomic sections (Fig. 3, rows A through E). Osseous structures included the distal portion of the tibia and fibula with the pertaining malleoli, the talus and trochlea tali ridges, and the tuber calcanei. Additionally, tendons of 7 muscles could be identified on the anatomic sections. Five major blood vessels (4 veins and 1 artery) were readily visible on all sections. All of these structures were also visible on the soft tissue-setting CT images except for the rami caudales of the vena saphena lateralis and vena saphena medialis. On the bone setting CT images, only the previously mentioned bony structures could be identified.

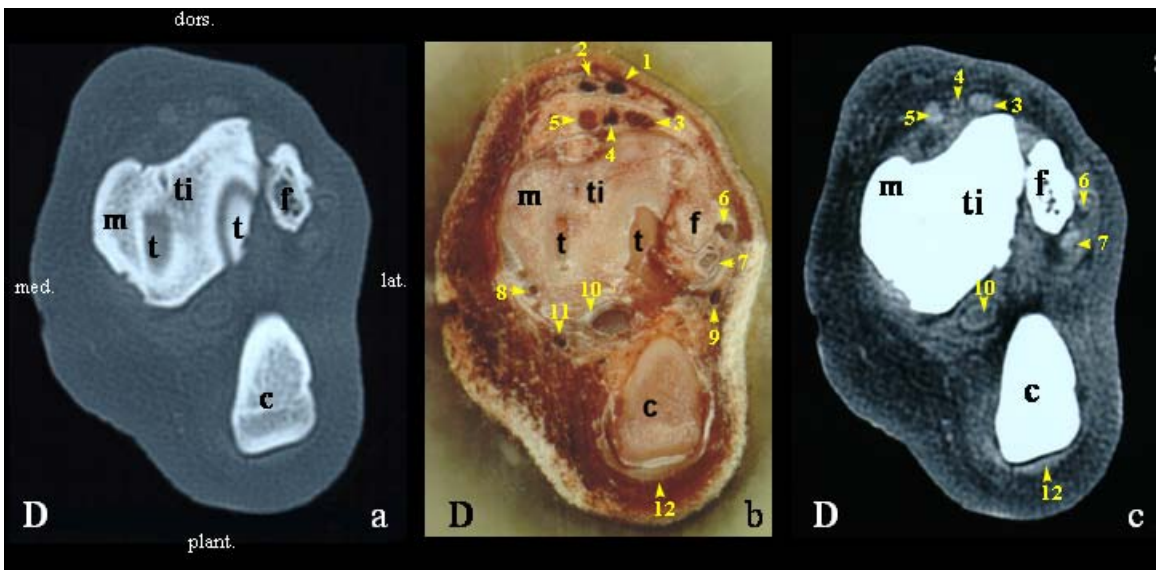
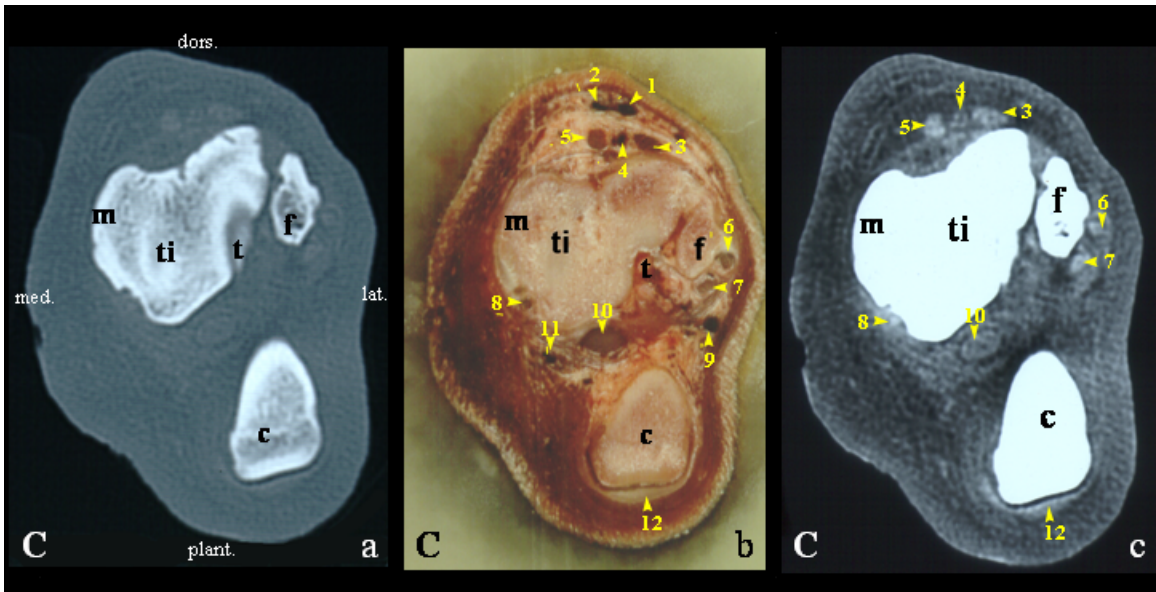
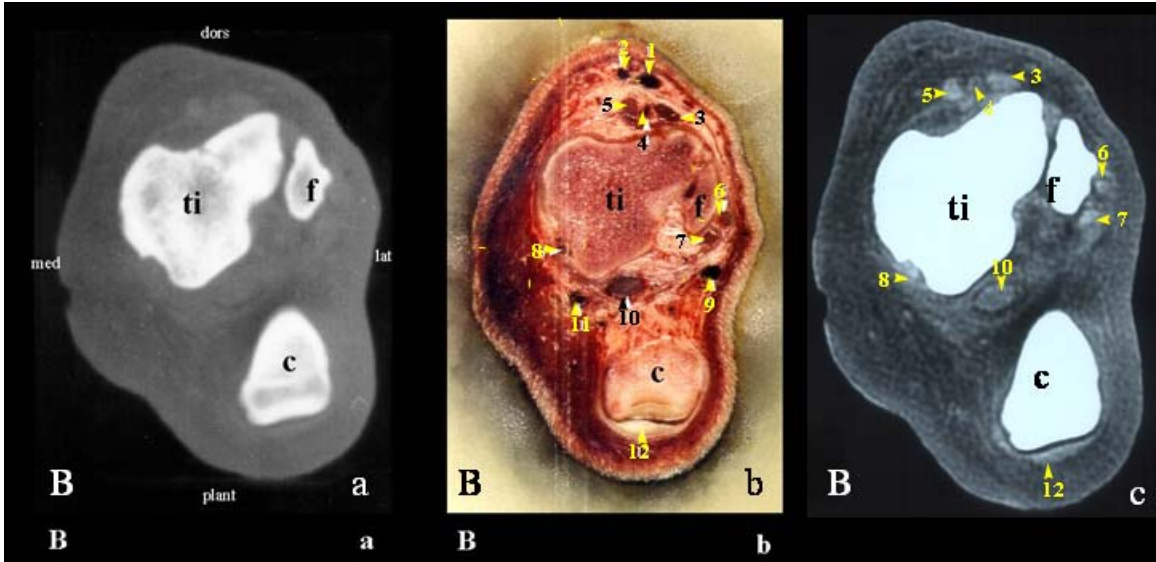
On the distally located anatomic sections (Fig 3, rows F through L), bony structures that could be identified included the distal portion of the tibia and fibula with the pertaining malleoli,, the talus and calcaneus with a prominent sustentaculum tali, or the collum tali and calcaneus. Soft-tissue structures were almost identical to those described for the proximally located anatomic sections, except that the tendons of the peroneus longus muscle and extensor digitorum lateralis muscle crossed over and, therefore changed positions, the talocalcaneous interosseous ligament was visible, and the extensor digitorum brevis muscle was observed. Distally, the dorsal region of anatomic sections of the tarsal joint contained only a single superficial vein, formed by the fusion of the rami craniales of the saphena lateralis vein and the saphena medialis vein. Except for the

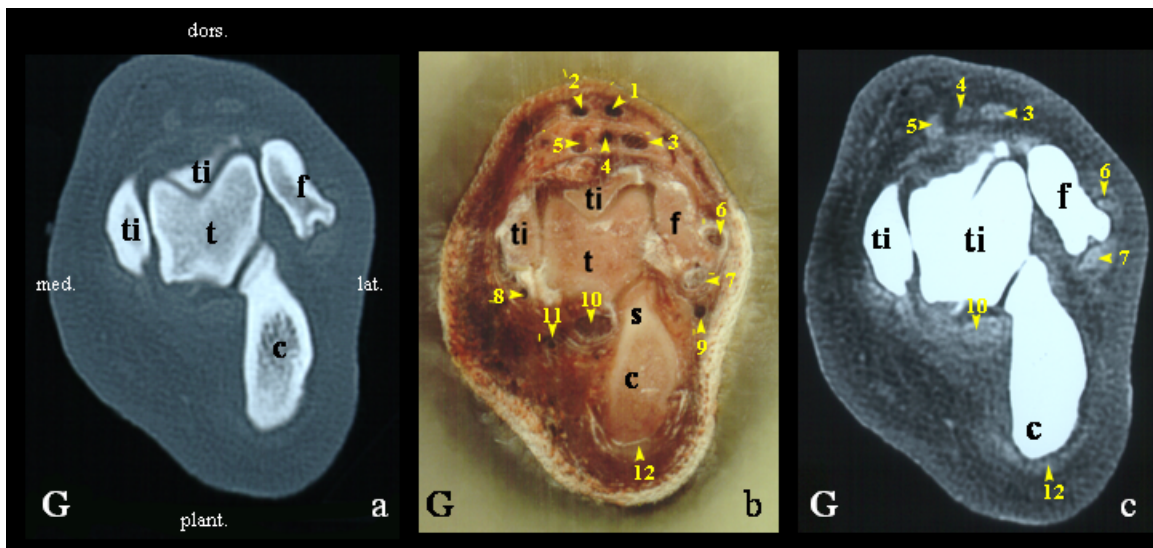
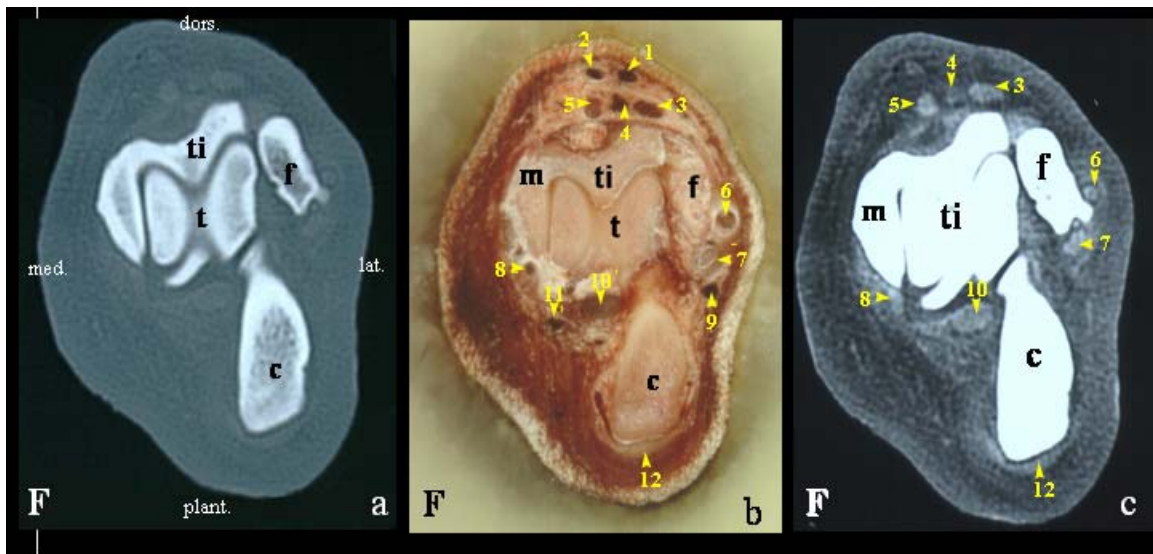
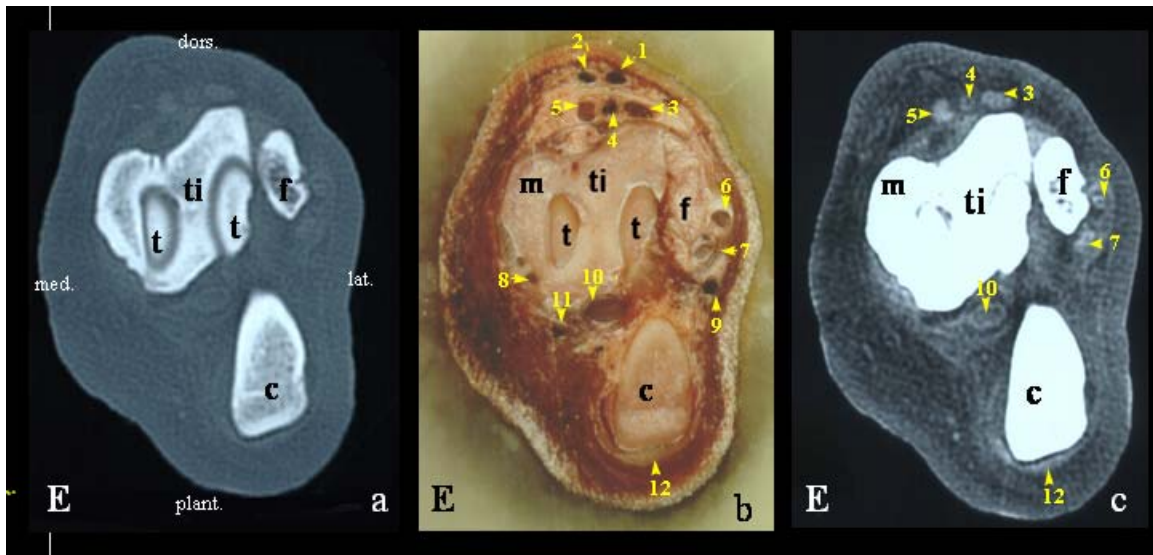
extensor digitorum brevis muscle, these osseous and soft-tissue structures were also visible on the soft-tissue setting CT images. In contrast with the more proximal anatomic sections, the rami caudales of the saphena lateralis and saphena medialis veins could be located. On the bone-setting CT images, all bony structures seen on the anatomic sections could be identified.

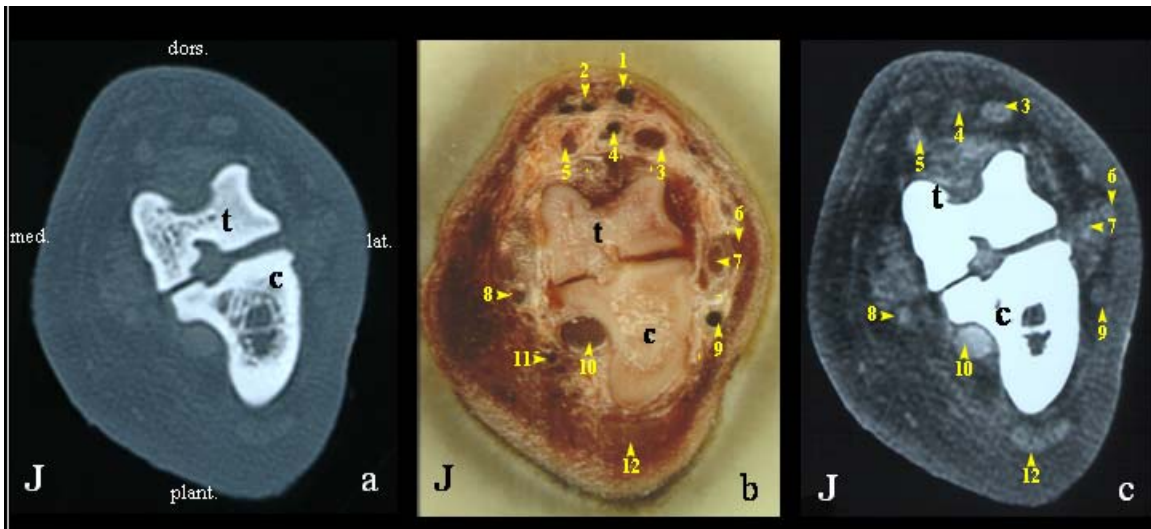
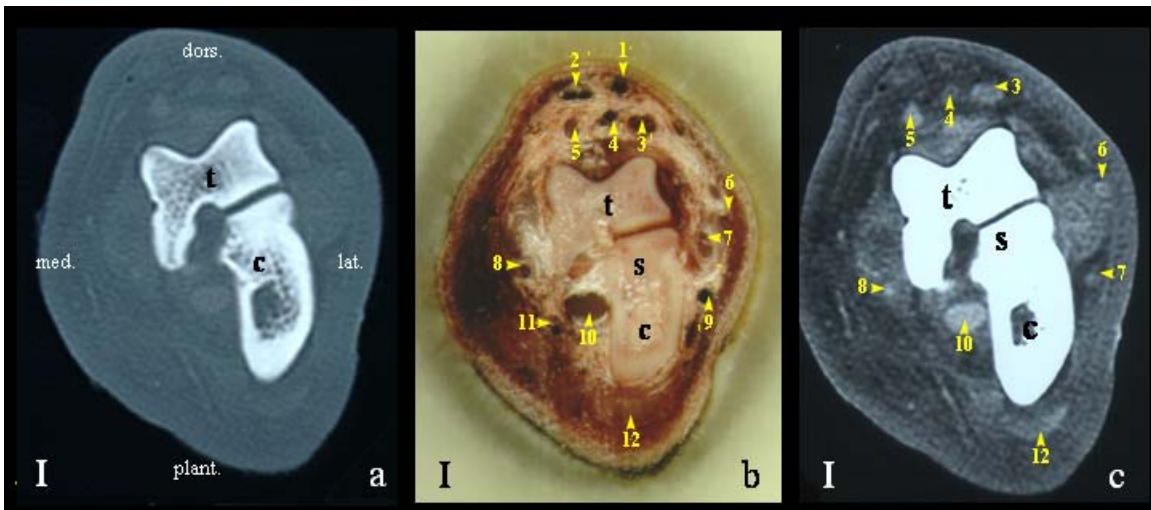
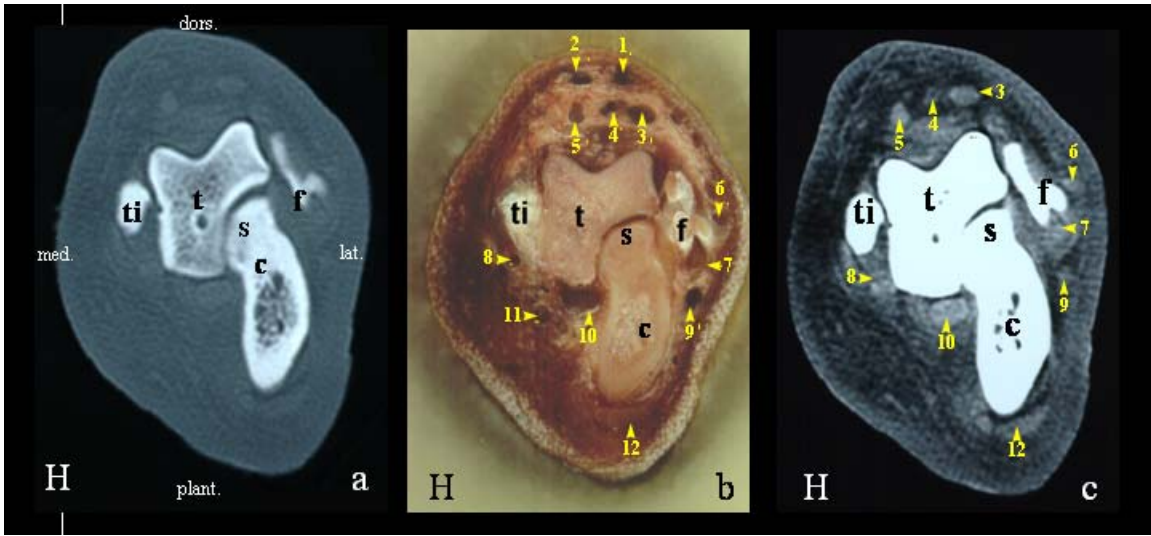
Figure 3: Transverse CT images and photographs of the corresponding anatomic sections of the tarsal joint of a clinically normal dog. Images (left, bone image; middle, anatomic section; right, soft tissue image) were obtained at levels A through L as illustrated in figure 2. (plant = plantar, med = medial, lat = lateral, dors = dorsal)

1 = Ramus cranialis of the vena saphena lateralis. 2 = Ramus cranialis of the vena saphena medialis. 3 = Extensor digitorum longus muscle. 4 = Tibialis cranialis artery. 5 = Tibialis cranialis muscle. 6 = Peroneus (fibularis) longus muscle. 7 = Extensor digitorum lateralis muscle. 8 = Flexor digitorum medialis muscle. 9 = Ramus caudalis of the vena saphena lateralis. 10 = Flexor digitorum lateralis muscle. 11 = Ramus caudalis of the vena saphena medialis. 12 = Flexor digitorum superficialis muscle. 13 = Extensor digitorum brevis muscle. 14 = Talocalcaneal interosseous ligament (*ligamentum talocalcaneum interosseum*). c = Calcaneus. f = Fibula. m = Malleolus medialis. s = sustentaculum tali. se = Os tarsale secundum. t = Talus. ti = Tibia.









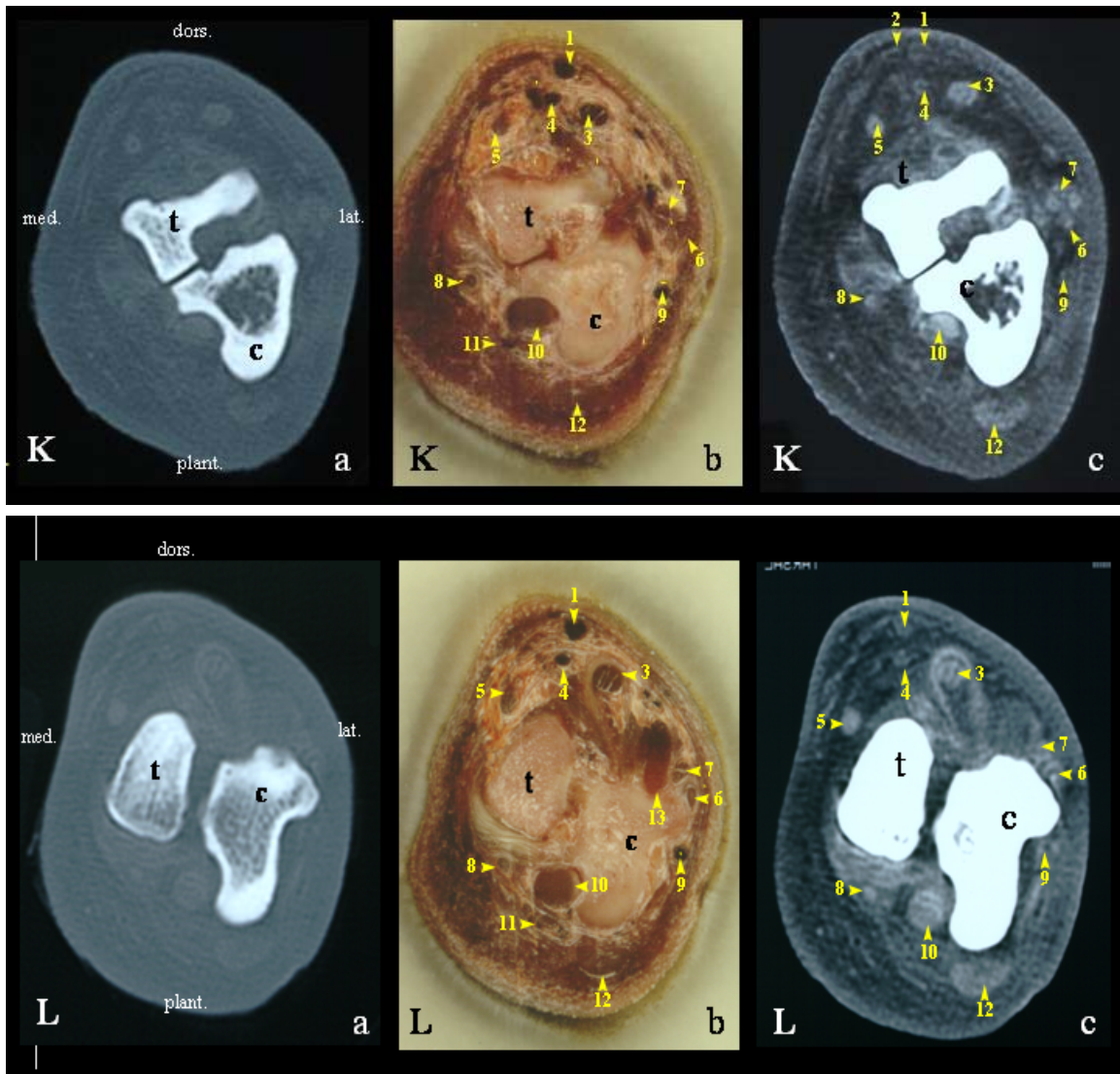


Figure 3: Transverse CT images and photographs of the corresponding anatomic sections of the tarsal joint a clinically normal dog. Images (left, bone image; middle, anatomic section; right, soft tissue image) were obtained at levels A through L as illustrated in figure 2. (plant = Plantar. med = Medial. lat = Lateral. dors = Dorsal)

1 = Ramus cranialis of the vena saphena lateralis. 2 = Ramus cranialis of the vena saphena medialis. 3 = Extensor digitorum longus muscle. 4 = Tibialis cranialis artery. 5 = Tibialis cranialis muscle. 6 = Peroneus (fibularis) longus muscle. 7 = Extensor digitorum lateralis muscle. 8 = Flexor digitorum medialis muscle. 9 = Ramus caudalis of the vena saphena lateralis. 10 = Flexor digitorum lateralis muscle. 11 = Ramus caudalis of the vena saphena medialis. 12 = Flexor digitorum superficialis muscle. 13 = Extensor digitorum brevis muscle. 14 = Talocalcaneal interosseous ligament (*ligamentum talocalcaneum interosseum*). c = Calcaneus. f = Fibula. m = Malleolus medialis. s = sustentaculum tali. se = Os tarsale secundum. t = Talus. ti = Tibia.

Analysis of CT images made at the most distal levels (Fig 4) revealed the talus, calcaneus, and os tarsi centrale; the os tarsi centrale and os tarsale quartum; the os tarsale secundum, tertium, and quartum; the os tarsale primum, secundum, tertium, and quartum; or metatarsals II, III, IV, and V.

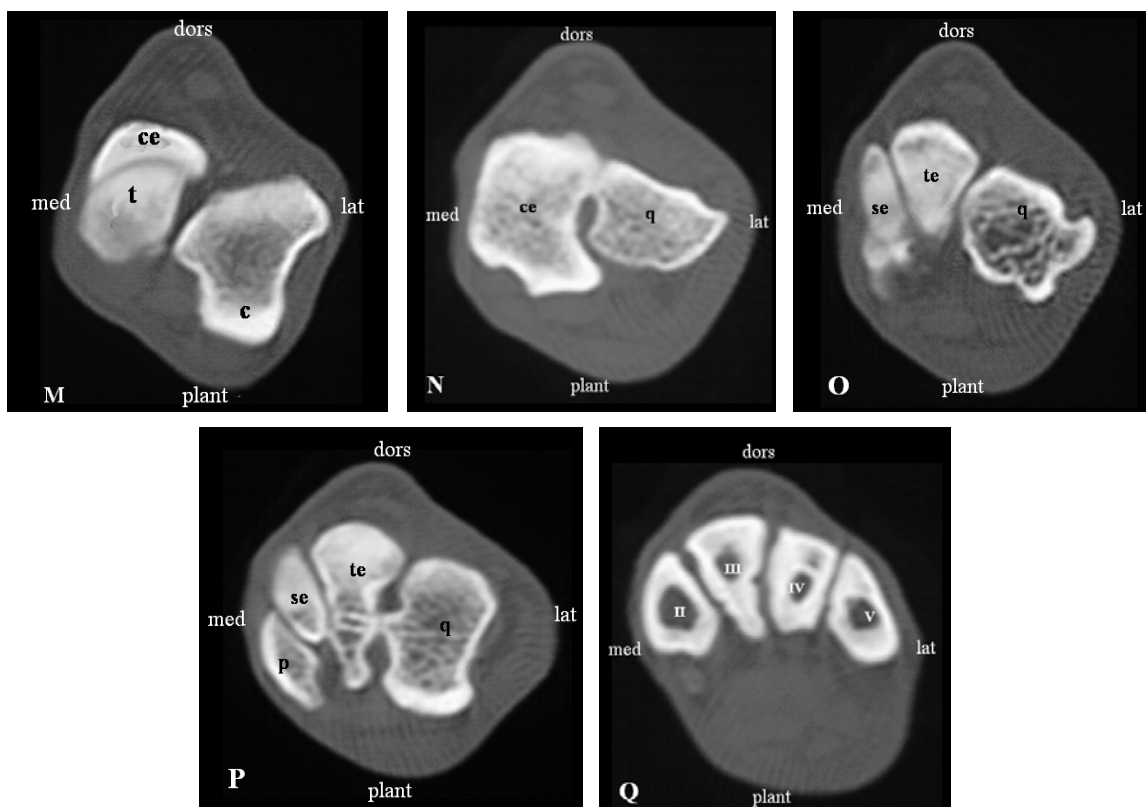


Figure 4: Transverse CT images (bone setting) of the tarsal joint of a clinically normal dog. Images were obtained at levels M through Q as illustrated in figure 2.

ce = Os tarsi centrale. p = Os tarsale primum. q = Os tarsale quartum. se = Os tarsale secundum. te = Os tarsale tertium. II = Os metatarsale secundum. III = Os metatarsale tertium. IV = Os metatarsale quartum. V = Os metatarsale quintum.

Sagittal, dorsal and three-dimensional (3-D) reconstructions were made of the right tarsocrural joint of the Bullmastiff (Fig 5). The sagittal images allowed a thorough evaluation of the lateral and medial part of the tarsocrural joint including the lateral and medial ridge. On the dorsal reconstructions, the tarsocrural joint could be evaluated from the dorsal to plantar surface in detail.

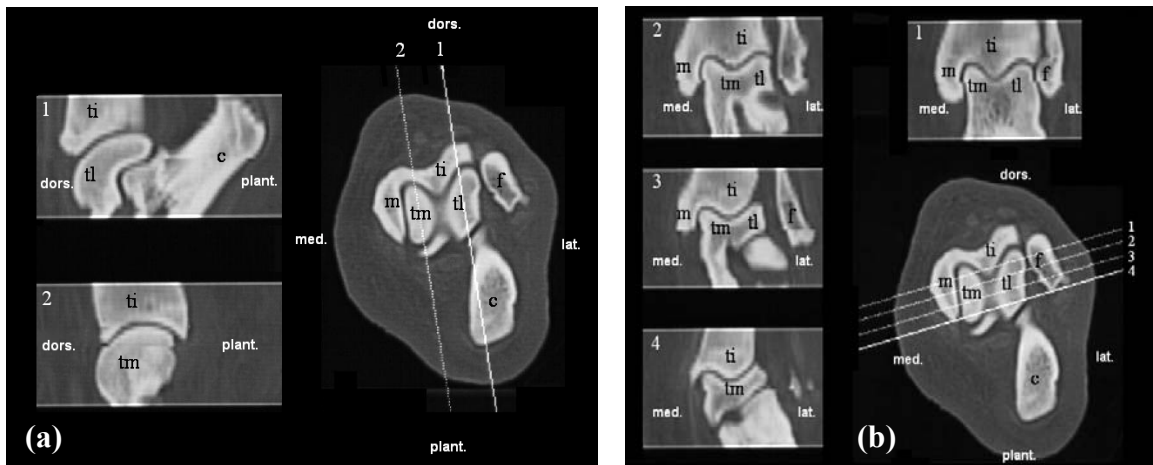
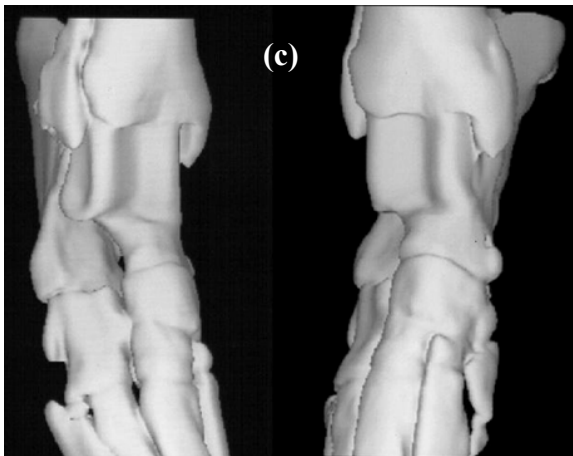


Figure 5: Sagittal (a), dorsal (b) and 3-D (c) reconstructions from CT images of the right tarsocrural joint of a Bullmastiff, euthanised for reasons unrelated to the musculoskeletal system.

tl = Lateral ridge of talus. tm = medial ridge of talus. See figure 3 for remainder of key.



For the other 6 dogs, all osseous structures mentioned for the Bullmastiff could be seen on the bone-setting CT images. Similarly, all bony, tendinous, and vascular structures that could be identified on the soft tissue-setting CT images of the Bullmastiff were also noticed on the soft-tissue setting CT images of the 6 mixed-breed dogs. Additionally, in 4 dogs, the rami craniales of the saphena lateralis and saphena medialis veins were distinct, and in 1 of these dogs, the rami caudales of both veins were also visible. In another dog, however, the tendons of the peroneus longus and extensor digitorum longus muscles could not be identified.

DISCUSSION

Although some information on CT of the tarsal joint in dogs exists,¹¹ a detailed description of imaging in clinically normal dogs is lacking. The results of our study indicate that not only is a detailed evaluation of the bony structures of the tarsal joint in dogs possible but that, by adjusting the window and making use of the varying grey scale formats, many soft tissues, including tendons and major vascular structures, can be viewed as well. The complexity of the radiographic image caused by superimposition of bony structures can be overcome by studying the axial CT images of the tarsal joint, although some familiarisation with this type of imaging is necessary. By studying the sagittal and dorsal reconstructions, the entire tarsocrural joint surface (i.e., the lateral and medial tarsal ridge and also the dorsal and plantar surfaces) can be evaluated. These results suggest that CT could be of use in the diagnosis of TOC, especially when the lateral ridge is involved and superimposition of the calcaneus over the lateral tarsocrural compartment hinders fragment detection. Moreover, CT could be of use in determining the therapeutic strategy for TOC.

Using CT, the exact localisation, size, and number of fragments may be determined in dogs with TOC. The location of the fragments on the trochlear ridge, especially on the lateral part, can be diverse, but this information is useful for the orthopaedic surgeon who wants to use a minimal exposure technique to remove the fragments.^{1,12} A disruption of the collateral ligament complex following an arthrotomy could create post-surgical instability and, thus, may compromise the long-term prognosis of affected dogs following surgical treatment.¹³ For arthroscopic treatment of these lesions, exact location is prerequisite knowledge, because various arthroscopic approaches must be performed depending on the location of the fragments. The number and size of the fragments is also important information for determining whether fragments should be removed or repaired. Osteoarthritic changes may progress because of instability or incongruity of the joint following removal of a large fragment.¹⁴ Several authors^{2,13,15,16} suggest that the reattachment of OC fragments would be preferable to removal, especially when the

lateral talar ridge is involved and traumatic fragmentation with avulsion of the short collateral ligaments has been identified.

Computed tomography could also be of use in instances of complex tarsal fractures where the same problem of superimposition of the surrounding bony structures exists and could provide information contributing to adequate treatment. Another application for CT of the tarsal joint is for detection of subchondral sclerosis, which can be done by measuring the difference in density between cortical and spongy bone. In instances of sclerosis, the density of the spongy bone is increased. Changes in cortical thickness can also be measured.

Computed tomography is becoming more readily available to veterinarians than in the past and is becoming more commonly used for the diagnosis of orthopaedic disorders in small animals.^{17,18} Major disadvantages of the technique include cost and the need for general anaesthesia. The examination time is, with the type of scanner used in our study, about 10 minutes, which is acceptable. Obtaining 6 radiographic views of the tarsal joint is more time consuming, and in some countries, general anaesthesia is obligatory for radiation safety reasons.¹ If access to additional software for multiplanar reconstruction is not available, evaluation is limited to the axial images. This requires more time to evaluate the true extent of possible lesions. Still, the information gained from only the transverse images is worthwhile.

^aDomitor, Orion Corporation, Espoo, Finland.

^bPentothal, Abott Laboratories, North Chicago, Ill.

^cCT-scanner Pace Plus, GE Medical Systems, Milwaukee, Wis.

^dFuji Photo Film Co., Ltd., Tokyo, Japan.

^eJung Cryomacrocut CM 3600, Leica Microsystems Nussloch GmbH, Nussloch, Germany.

REFERENCES

1. Carlisle CH., Reynolds KM. Radiographic anatomy of the tarsocrural joint of the dog. *J Small Anim Pract* 1990; 31:273–279.
2. Beale BS, Goring RL, Herrington J, Dee J, Conrad K. A prospective evaluation of four surgical approaches to the talus of the dog used in the treatment of osteochondritis dissecans. *J Am Anim Hosp Assoc* 1991; 27:221–229.
3. Fitch RB, Beale BS. Osteochondrosis of the canine tibiotarsal joint. *Vet Clin North Am, Small Anim Pract* 1998; 28:95–113.
4. Johnson KA, Howlett CR, Pettit GD. Osteochondrosis in the hock joint in dogs. *J Am Anim Hosp Assoc* 1980; 16:103–113.
5. Montgomery RD, Hathcock JT, Milton JL, Fitch RB. Osteochondritis dissecans of the canine tarsal joint. *Compend Cont Educ Pract Vet* 1994; 16:835–845.
6. Drost WT, Love NE, Berry CR. Comparison of radiography, myelography and computed tomography for the evaluation of canine vertebral and spinal cord tumors in sixteen dogs. *Vet Radiol & Ultrasound* 1996; 37:28–33.
7. Newberg AH. Computed tomography of joint injuries. *Radiol Clin North Am* 1990; 28:445–460.
8. Zinman C, Reis ND. Osteochondritis dissecans of the talus : use of the high resolution Computed Tomography Scanner. *Acta Orthop Scand* 1982; 53:697–700.
9. Zinman C, Wolfson N, Reis ND. Osteochondritis dissecans of the dome of the talus. *J Bone Joint Surg* 1988; 70:1017–1019.
10. World Association of Veterinary Anatomists (WAVA). In: *Nomina Anatomica Veterinaria*, 4th ed. Zurich and Ithaca, N.Y: International Committee on Veterinary Gross Anatomical Nomenclature, 1994; 1-198.
11. Assheuer J, Sager M. Tarsal joint and paw. In: Assheuer J, Sager M., *MRI and CT atlas of the dog*. Berlin: Blackwell Science, 1997; 288–295.
12. Van Ryssen B, van Bree H. Arthroscopic evaluation of osteochondrosis lesions in the canine hock joint: a review of two cases. *J Am Anim Hosp Assoc* 1992; 28:295–299.
13. Smith M, Vasseur P, Morgan J. Clinical evaluation of dogs after surgical and nonsurgical management of osteochondritis dissecans of the talus. *J Am Anim Hosp Assoc* 1985; 187:31–35.
14. Brinker WO, Piermattei DL, Flo GL. Diagnosis and Treatment of Orthopedic Conditions of the Hindlimb. In: Brinker WO, Piermattei DL, Flo GL, 3rd ed. *Small animal orthopedics and fracture repair*. Philadelphia, Pennsylvania: WB Saunders Co, 1997; 607–655.
15. Van Ee T, Gibson K, Roberts E. Osteochondritis dissecans of the lateral ridge of the talus in a dog. *J Am Vet Med Assoc* 1988; 193:1284–1286.
16. Sjöström L, Håkanson N. Traumatic injuries associated with the short lateral collateral ligaments of the talocrural joint of the dog. *J Small Anim Pract* 1994; 35:163–168.

17. Stickle RL, Hathcock JT. Interpretation of computed tomographic images. *Vet Clin North Am Small Anim Pract* 1993; 23: 417–435.
18. Kippenes H, Johnston G. Diagnostic imaging of osteochondrosis. *Vet Clin North Am Small Anim Pract* 1998; 28:137–160.

**RADIOGRAPHIC, COMPUTED TOMOGRAPHIC AND ARTHROSCOPIC
FINDINGS IN 23 DOGS WITH OSTEOCHONDROSIS OF THE
TARSOCRURAL JOINT**

I. Gielen, H. van Bree, B. Van Ryssen, T. De Clercq, H. De Rooster

Department of Medical Imaging, Faculty of Veterinary Medicine,
Ghent University, Salisburylaan 133, Merelbeke, Belgium

Adapted from:

Radiographic, computed tomographic, and arthroscopic findings in 23 dogs with osteochondrosis of the tarsocrural joint. *Veterinary Record* 2002; 150: 442-447.

SUMMARY

Twenty-three dogs with osteochondrosis (OC) of the tarsocrural joint were evaluated by radiography, computed tomography (CT) and arthroscopy. The radiographic examination included an extended and flexed mediolateral, a plantarodorsal, a flexed dorsoplantar skyline view, and a plantaromedial-dorsolateral and a plantarolateral-dorsomedial view (two oblique views). The CT examination was carried out in ventral recumbency and 1-mm slices were taken with a bone window setting; 31 lesions were identified in the 46 joints examined. The arthroscopic exploration used either a plantar or a dorsal puncture, depending on the site of the lesion.

In six cases the lateral, and in 17 cases the medial trochlear ridge was involved. Although the survey radiographs were sufficient to make the diagnosis, the CT examination helped to determine the exact site, and the number and size of the fragments of bone. A four-stage classification system comparable to the one used in man was established.

Arthroscopy provided information about synovial inflammation and damage to the joint cartilage, and made it possible to remove fragments of bone from one-third of the cases.

INTRODUCTION

In the dog, osteochondrosis (OC) of the tarsocrural joint is a well known but uncommon cause of hindlimb lameness, it constitutes 9% of all cases of OC. The tarsocrural joint is the third most commonly affected joint (Montgomery and others 1994, Fitch and Beale 1998). The disease usually affects large breeds, Rottweilers and Labrador Retrievers being most frequently affected. The age at which the condition causes clinical signs ranges from four months to four years, with a mean age of seven months. Male and female dogs are almost equally affected (Montgomery and others 1994, Van Ryssen and van Bree 1997, Fitch and Beale 1998), and approximately 50% of the reported cases of tarsocrural osteochondrosis (TOC) are bilateral (Montgomery and others 1994, Weinstein and others 1995). The most common site of the TOC lesions is the medial trochlear ridge of the talus (Denny 1981, Van Ryssen and others 1991); the lateral trochlear ridge is less commonly involved and affects 25% of the cases (Breur and others 1989, Wisner and others 1990, Montgomery and others 1994). The lateral trochlear ridge has been reported to be involved more often in Rottweilers than in other breeds (Weinstein and others 1995, Fitch and Beale 1998).

In the human beings, several conditions are grouped under the heading of OC; including osteochondral fractures, osteonecrosis, accessory centres of ossification, osteochondrosis, and hereditary epiphyseal dysplasia (Schenk and Goodnight 1996).

In men, lesions of OC are also found on the medial or lateral aspect of the talus. Although survey radiographs are usually sufficient to make the diagnosis, CT is valuable for determining the size and location of the lesion accurately (Zinman and Reis 1982) and for evaluating the effects of treatment (Zinman and others 1988). In human beings, a four-stage classification system, called the "Berndt and Harty" classification, has been widely accepted for classifying the lesions (Berndt and Harty 1959, Baker and Morales 1999) and is used to determine the therapeutic regimen for lesions of the talar dome. This classification system is based on radiographic findings but other classification systems, based on magnetic resonance imaging (MRI) and CT scanning, correlate well with the radiographic one (Baker and Morales 1999).

In dogs, the diagnosis of TOC is not always obvious and exploratory arthrotomy is recommended by some authors as a reasonable diagnostic option (Johnson and others

1980, Montgomery and others 1994, Fitch and Beale 1998); however, it is a invasive technique which should be considered as the last resort. It has been reported that the disruption of the collateral ligament complex as a result of an arthrotomy could render the joint unstable (Smith and others 1985).

The technique of CT is becoming more available to veterinarians but is rarely used for the diagnosis of orthopaedic disorders in small animals (Stickle and Hathcock 1993, Kippenes and Johnston 1998). It has several advantages over conventional radiography: it eliminates the superimposition of different structures, thereby decreasing the complexity of the image; the images can be displayed in different grey-scale formats, which can enhance visualisation of specific structures; and they can be reconstructed in multiple anatomic planes (Drost and others 1996). Having these features, CT could provide useful additional information, not only in diagnosing OC in complex joints like the tarsocrural joint, but also in identifying the exact site and extent of the lesion, so that an appropriate surgical approach could be selected (Beale and others 1991).

The aim of this study was to evaluate the findings of CT, radiography and arthroscopy in 23 dogs with TOC, and on the basis of these findings to establish a classification system comparable to the system used in human beings.

MATERIALS AND METHODS

Dogs

The breed and sex of the 23 dogs are given in Table 1. To be included each dog had to have adequately documented clinical records, a complete radiographic and CT study of both tarsocrural joints, and an arthroscopic study of the clinically affected joints. The age range was 5 months to 4 years with a mean of 20 months, and 11 of the dogs were more than 12 months old. Their body-weights ranged from 20 to 60 kg with a mean of 33 kg. When the condition was diagnosed they had been lame for from 3 weeks to 2 years, with a mean of 6 months. Seven of the dogs were affected bilaterally but only two of them were bilaterally lame when they were first examined.

The final diagnosis was based on the identification by CT of a subchondral defect or a bony fragment associated with either the medial or lateral trochlear ridge.

Radiographic examination

After the physical examination, both tarsocrural joints of every animal were examined radiographically while each dog was sedated with a combination of droperidol (0.25 mg/kg) and fentanyl (0.005 mg/kg) (Thalamonal; Janssen Cilag).

Using a table-top technique, an extended and flexed mediolateral, a flexed dorsoplantar skyline projection, a plantarodorsal and a plantaromedial-dorsolateral and plantarolateral-dorsomedial (two oblique views) (Fig 1), were taken with a 300 mA, 150 kVp x-ray unit (HFG 350-30KW Varian; X-ray Equipment Verachtert) with a focal film distance of 100 cm; the kVp setting was between 50 and 55. Orthochromatic film (Super HR-E 30 Fuji Medical X-ray Film 100 NIF; Fuji Photo Film) was used in combination with rare earth intensifying screens (FG-3; Fuji Photo film).



Figure 1: Projections used in the radiographic protocol for tarsal examination.
a: extended view; b: flexed view; c: plantarodorsal view; d: flexed dorsoplantar skyline view; e: plantarolateral-dorsomedial view; f: plantaromedial-dorsolateral view of a normal tarsal joint.

Each joint was evaluated for signs of soft tissue swelling and degenerative joint disease (periarticular bone formation of the distal tibia and talus). Each projection was evaluated for the involvement of the trochlear ridge (increased joint space over the ridge of the

talus, reduced height of the ridge, discontinuity of the delineation of the ridge) and of isolated bony fragments. If fragments could be identified, attempts were made to establish their exact location, size and number. Other associated radiographic findings, including the presence of ossified joint mice, apparent lysis and/or fragmentation of the medial malleolus of the tibia and lateral malleolus of the fibula, were also recorded.

CT examination

After the radiographic examination, a CT examination was carried out under general anaesthesia, induced with 8 mg/kg thiopental (Pentothal; Abbott Laboratories) administered intravenously, and maintained with halothane (1 to 1.5 %) (Fluothane; Zeneca). A third-generation CT scanner (CT-scanner Pace Plus; GE Medical Systems America) was used. The dogs were positioned in ventral recumbency with the scan plane approximately parallel to the tarsocrural joint space. The right and left limbs were scanned simultaneously, taking care that they were parallel and that both tarsocrural joints were in the same scan plane. Dorsoventral and lateral scout projection images were acquired to verify that the joints were positioned symmetrically and to annotate the image. Slices, 1 mm thick, were acquired at 120 kVp and 300 mAs. Reconstructions were made by using a bone algorithm. They were displayed with a bone window setting, the window width ranging from 2500 to 3500 CT units, and the window level ranging from 500 to 800 CT units. The time taken to acquire the images was approximately 10 minutes, and the images were printed on x-ray film (Fuji Medical Dry Imaging Film 100 NIF; Fuji Photo Film).

The CT images were evaluated for the involvement of the trochlear ridge (defect with or without visible fragment). Thereafter, different CT images were reconstructed in multiple anatomical planes in order to evaluate the integrity and/or the eventual involvement of the joint surface. The exact location, number and size of any fragments were determined. To describe the exact location of the TOC lesions, a map (Fig 2) was used in which the medial and lateral trochlear ridges were divided into a proximal, a dorsal and a distal area. Each area was subdivided into a medial (or lateral), and a central area. If a lesion involved both the medial (and lateral) and central area it was considered to involve the whole ridge.

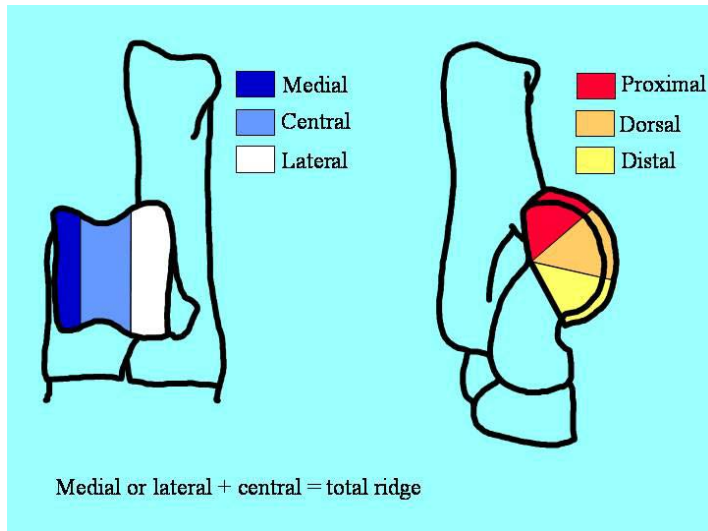


Figure 2: Diagram showing the anatomical positions of the different TOC lesions in dogs.

Other associated findings, including the presence of ossified joint mice, apparent lysis and/or fragmentation of the medial malleolus of the tibia and lateral malleolus of the fibula, were also recorded. Each joint was also evaluated for signs of degenerative joint disease (new bone formation in the distal aspect of the tibia and fibula, in the plantarodistal region of the talus and in the medial and lateral region of the calcaneus).

Arthroscopic examination

The clinically affected joints were examined arthroscopically by the method described by Van Ryssen and others (1993) while the dogs were still anaesthetised and after evaluating the radiographic and CT procedures. The CT mapping was used as a guide to determine the puncture sites. During the arthroscopic examination, the status of the synovial membrane, the articular cartilage and the visibility of the fragments were evaluated. The synovitis was classified as either moderate or severe. In a joint with moderate synovitis, the synovial villi were moderately enlarged, had a simple form, and did not fill up the joint space completely, so joint structures were still visible. In a joint with severe synovitis, the synovial villi were greatly enlarged, had a more complex form and filled up the joint space completely, covering most of the joint structures. The articular cartilage was evaluated for signs of irregularity or erosion. The visibility of any fragments was evaluated for signs of irregularity or erosion. The visibility of any fragments was classified as good, moderate or poor. With good visibility all the fragments could be visualised arthroscopically; when visibility was moderate, a fracture or fissure line was visible but the complete fragment could not be visualised; when visibility was poor no

fragment or fissure line could be visualised. If they were visible, the fragments were removed or via a mini-arthrotomy (van Bree and Van Ryssen 1998). The subchondral bone was not curetted but the joint was lavaged with Ringer's solution. The OC fragments removed from eight joints were examined histologically.

Evaluation of the findings

At the end of the study, the radiographic and CT findings were compared in terms of exact localisation of the trochlear defect and the visibility of the fragments.

A four-stage classification system comparable to the Berndt and Hardy system was established (Table 2). It classified the lesion into four different stages depending on the status of the trochlear ridge and the associated fragment: stage I, a subchondral bone defect without an associated fragment; stage II, a partially detached OC fragment; stage III, a completely detached OC fragment remaining in the crater; and stage IV, a completely detached and displaced OC fragment (Berndt and Harty 1959, Baker and Morales 1999).

TABLE 1: Breed and sex distribution of 23 dogs with OC of the tarsocrural joint

Breed	Male	Female	Total
Labrador Retriever	1	7	8
Rottweiler	4	3	7
Golden Retriever	1	2	3
Staffordshire Bull Terrier	1		1
Bull Terrier	1		1
Pitbull	1		1
Irish Wolfhound	1		1
Chow chow	1		1
Total	11	12	23

TABLE 2: Distribution of 30 TOC lesions in 23 dogs based on the “Berndt and Harty” classification

Stage	Description	Number of lesions	
		Medial	Lateral
I	Small compressed area of subchondral bone	4	
II	Partially detached osteochondral fragment	6	
III	Completely detached, non-displaced osteochondral fragment	5	1
IV	Displaced osteochondral fragment	7	7

TABLE 3: Radiographic findings in 23 dogs (31 joints) with OC of the tarsocrural joint

Projection	Mlext	Miflex	PD	PLDM	PMDL	Skyline
Ridge involvement	18	21	19	24	14	13
Fragment visible	5	18	16	19	9	5
Location determined	13	21	3	6	5	5
Size determined	6	7	6	12	6	5
Fragmentation Med Malleolus*			7	4	1	7
Other findings	3	4	5	2	2	3

Mlext = extended mediolateral; **Miflex** = flexed mediolateral; **PD** = plantarodorsal; **PMDL** = plantaromedial-dorsolateral; **PLDM** = plantarolateral-dorsomedial; **Skyline** = flexed; dorsoplantar skyline projection

* Visible in one joint without an associated trochlear ridge lesion

RESULTS

Radiographic findings

Radiographic lesions were found in 31 of the 46 tarsocrural joints examined (Table 3). There were bilateral trochlear ridge lesions in 7 of the 23 dogs and in one of them the medial malleolus in the contralateral joint was fragmented without an associated trochlear ridge lesion. In 6 dogs, 2 of them with bilateral lesions, the lateral ridge was involved. There was soft tissue swelling in 24 of the 31 joints affected. In 24 of the 31 joints, there was evidence of degenerative joint disease. In 27 of the 31 joints there was radiographic

evidence of trochlear ridge involvement but a fragment could be demonstrated in only 20 of them. The dorsoplantar skyline projection helped to identify the fragments in 5 of 8 joints with lateral trochlear ridge involvement. In these cases, the plantaromedial-dorsolateral projection was also useful in evaluating the degree of joint involvement. Medial fragments could be identified most accurately on the flexed mediolateral, the plantarodorsal and the plantarolateral-dorsomedial projections. The exact location and extent of the lesions were difficult to determine. The flexed mediolateral view was the most accurate in localising the fragment. The location of the lesion could be estimated approximately from the radiographs of 21 joints. The size of the fragment could be determined in 13 cases, and varied from 2 to 13 mm. The number of fragments could not be determined with certainty.

In 7 joints the medial malleolus was fragmented and in 6 of them the trochlear ridge was also involved.

Other associated radiographic findings included visible joint mice in 6 cases, a lucent area within the medial malleolus of one case, a lucency within the lateral malleolus of the fibula of 1 case and fragmentation of the lateral malleolus of the fibula of another case.

CT findings

CT lesions were found in 31 of the 46 tarsocrural joints examined (Table 4). There were bilateral trochlear ridge lesions in 7 dogs and in 1 of them the medial malleolus in the contralateral joint was fragmented without an associated trochlear ridge lesion. In 6 dogs, 2 of them with bilateral lesions, the lateral ridge was involved. In 29 of the 31 joints there was evidence of degenerative joint disease.

In 9 of the dogs, fragmentation of the medial malleolus was associated with medial OC. In the joint in which the medial malleolus was fragmented without associated trochlear involvement, there were CT signs of degenerative joint disease. In 1 joint in which there was only irregularity of the medial trochlear ridge, and another joint in which the joint surface was only minimally involved, there were no signs of degenerative joint disease. In 30 cases there was clear evidence of trochlear ridge involvement, either medial or lateral. In 4 cases the defect in the medial trochlear ridge was not associated with a fragment, but in the 26 other joints, fragments could be detected. The fragments could be measured in all but 2 joints in which the pieces were too small to be measured. The size

of the fragments varied from 1 to 15 mm. In 8 joints only one fragment could be detected but in 18 cases there were more than two fragments, and one joint had 7 different fragments (Table 4).

TABLE 4: Computed tomographic findings in 23 dogs (31 joints) with osteochondrosis of the tarsocrural joint

Ridge involvement	30
Defect without fragment	4
Fragment visible	26
Location	
Medial	22
Lateral	8
Size determined	24*
Number determined	
One fragment	8
More than one fragment	18
Involvement of joint surface	30
Fragmentation medial malleolus	9 ⁺
Other findings	
Joint Mice	5
Lucent area medial malleolus	1
Fragmentation lateral malleolus fibula	1
Osteolysis lateral malleolus fibula	2

* In two multiple small fragments

+ One without trochlear ridge lesions

The exact location (Fig 2) and extent of the defect could be determined in all 30 trochlear ridge lesions, by using a combination of the transverse scans and reconstructed images in different anatomical planes (Fig 3 and 4; Table 5). Other associated CT findings included visible joint mice in 5 cases, a lucent area within the medial malleolus of 1 case, and a lucency within the lateral malleolus of the fibula of 2 cases, and fragmentation of the lateral malleolus of the fibula of 1 case. One joint mouse detected radiographically appeared on CT to be a case of fragmentation of the medial malleolus.

The location and distribution of the 30 lesions based on the “Berndt and Harty” classification are shown in Table 2. There were 4 stage I lesions (a subchondral bone defect), 6 stage II lesions (partially detached fragments), 6 stage III lesions (completely detached but non-displaced fragments), and 14 stage IV lesion (displaced OC fragments).

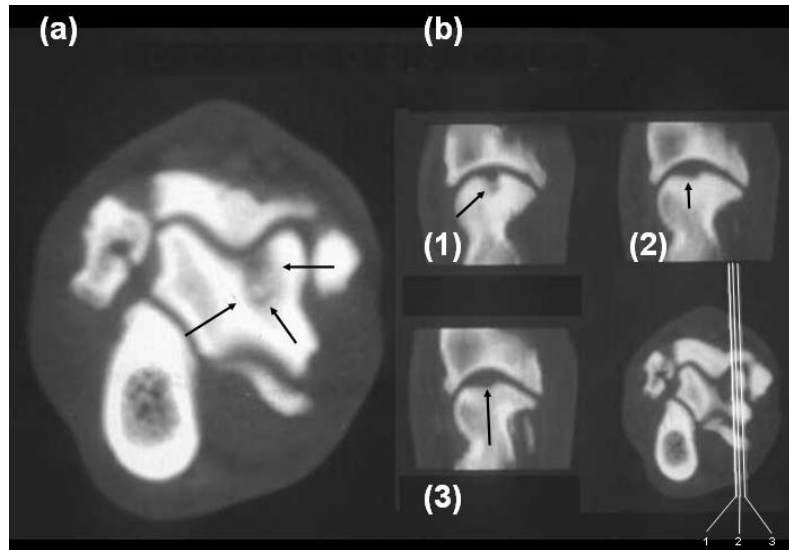


Figure 3: Transverse scan and reconstructed images of a left tarsus with an OC lesion on the medial trochlear ridge of the talus.

a: Transverse scan at the level of the talus. The black arrows show the defect of the central part between the lateral and medial ridge. Two small fragments are visible in the centre of the hypodense defect. The lesion is localised in the dorsocentral part of the talus. The fragments are partially detached: stage II lesion using the “Berndt and Harty” classification.

b: Sagittal reconstructed images were made at three different levels (1 to 3), and the black arrows show the defect.

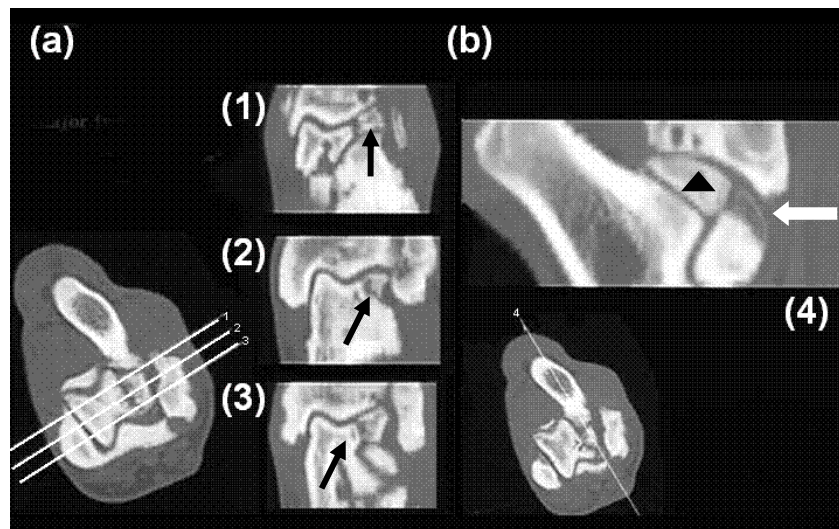


Figure 4: Transverse scan and reconstructed images of a left tarsus with a OC lesion on the lateral trochlear ridge of the talus. Two major fragments are present on the lateral trochlear ridge.

a: On this transverse scan of the left tarsocrural joint, a large fragment is visible. It is localised on the proximal part and the total ridge (=central + lateral) is involved. Three reconstructions are made in the dorsal plane (1 to 3) and the black arrows show the defect. The fragment is completely detached and non-displaced: stage III lesion using the “Berndt and Harty” classification.

b: A smaller, hypodense, dorsal fragment is visible on the more distal transverse scan. On the sagittal reconstructed image (4), the large fragment (proximal total ridge) (black triangle) and the smaller fragment (dorsolateral) (white arrow) are visible. Both fragments are a stage III lesion using the “Berndt and Harty” classification.

TABLE 5: Location of 30 TOC lesions in 23 dogs observed by computed tomography

Location	Medial	22	Lateral*	8
	Proximo-medial	3	Proximo-lateral	4
	-central	2	-central	0
	-total ridge	3	-total ridge	1
	Dorso-medial	6	Dorso-lateral	4
	-central	6	-central	0
	-total ridge	2	-total ridge	0
	Disto-medial	0	Disto-lateral	0
	-central	0	-central	0
	-total ridge	0	-total ridge	1

*In 2 joints with lateral ridge involvement there were 2 major fragments at different locations.

Comparison between radiographic and CT findings

The number of lesions identified on radiographically and by CT was the same, but more signs or degenerative joint disease could be seen by CT than on radiographs (29 versus 25) and the lesions usually looked more severe by CT. Trochlear ridge involvement could be better evaluated on CT scans than on the radiographs (30 versus 27) and the extent of lesions could be accurately mapped and evaluated by CT. By CT, 26 of the trochlear defects were associated with a visible fragment, compared with 20 by radiography, and the site, size and number of the fragments could be assessed more accurately.

Fragmentation of the medial malleolus could be evaluated better by CT than by radiography (9 cases compared with 7 cases) and one more case of lucency within the lateral malleolus was identified on CT. One joint mouse detected radiographically appeared by CT to be a case of fragmentation of the medial malleolus.

In general, more fragments could be detected by CT than on conventional radiographs and they could be evaluated more accurately.

Arthroscopic findings

All the 25 clinically affected joints were examined arthroscopically (Table 6, Fig 5a and b) a plantar puncture was used in 22 joints in which the medial ridge was involved, and a

dorsal puncture was used in 3 joints in which the lateral trochlear ridge was involved. Synovitis associated with extensive hypertrophied and hypervascular synovial villi was visible in all joints. In 19 joints the synovitis was severe and in several cases prevented the fragments from being visualised. It was sometimes difficult to position the arthroscope so as to avoid the synovial villi. In 17 joints the fragments could be visualised arthroscopically and in 11 of them they could be visualised well; in 3 of these 11 joints the fragments involved the lateral trochlear ridge and in 8 they originated from the medial area of the medial ridge; 2 of these fragments appeared completely cartilaginous and were not visible on CT, where they appeared as a crater or defect in the medial ridge. In these 11 cases, the extent of the lesion and the involvement of the joint surface could be evaluated well. In 6 joints only a moderate view of the fragments could be obtained owing either to the extensive synovitis or to the unfavourable position of the lesion. In 8 of the 25 joints, the fragments could be removed arthroscopically. In 12 of the joints the fragments were too big to be removed arthroscopically but they could be removed by extending the arthroscopic procedure into a mini-arthrotomy, thus causing minimal trauma to the soft tissues. One fragment was not seen arthroscopically, but it could be removed by a mini-arthrotomy after its position had been determined accurately by CT.

In 8 of the joints no fragments could be visualised arthroscopically. On CT, 4 of these defects were localised centrally on the medial ridge (and were treated by a mini-arthrotomy); in 2 the defect appeared not to be associated with a fragment, and eburnation of the subchondral bone could be detected arthroscopically. A third lesion appeared as a comminuted fragment on CT. These three joints were treated by thorough flushing of the tarsocrural joint. A fragment originating from the distal part of the lateral ridge was not visible arthroscopically, probably owing to its location, and a large fragment on the lateral trochlear ridge was not visible owing to the extensive synovitis.

The eight fragments examined histologically showed changes compatible with OC. There was a localised proliferation on the articular cartilage, which had been dissected by an eosinophilic necrotic fissure. Margins of exposed osseous tissue were covered by an early ingrowth of mesenchymal tissue, which had differentiated into fibrocartilage.

TABLE 6: Arthroscopic findings and treatment of 25 TOC lesions in 23 dogs

Puncture site	
Plantar	22
Dorsal	3
Findings:	
Synovitis	
moderate	6
severe	19
Cartilage erosions/eburnation	4
Visibility of the fragment	
no	8
moderate	6
good	11
Treatment:	
Arthroscopically	8
Mini-arthrotomy	13
Conservative	4

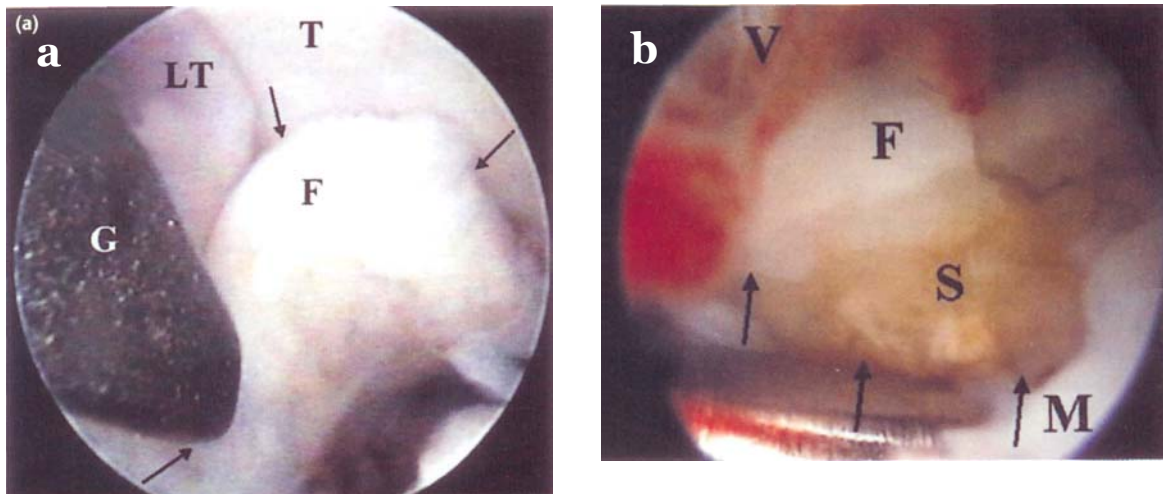


Figure 5: Arthroscopic view of (a) the dorsal part of a left tarsocrural joint, showing the treatment of OC of the lateral trochlear ridge of the talus, (b) plantar part of a left hock joint, showing OC of the medial trochlear ridge of the talus. T: distal part of the tibia. LT: lateral trochlear ridge of the talus; F: osteochondral fragment (indicated by arrows) containing cartilage and subchondral bone; G: grasping forceps; V: inflamed synovial villi; F: osteochondral fragment (indicated by arrows); S: subchondral bone showing erosion; M: medial trochlear ridge of the talus.

DISCUSSION

In TOC, either the medial or lateral trochlear ridge can be involved. In OC of the lateral ridge, the dorsal, dorsoproximal, or proximal part can be affected (Carlisle and others 1990, Van Ryssen and van Bree 1992), whereas in OC of the medial ridge the lesions occur on the plantar part (Montgomery and others 1994).

The radiographic anatomy of the canine tarsocrural joint has been described in detail by Carlisle and Reynolds (1990) but, nevertheless, the radiographic evaluation of the joint remains difficult owing to the superimposition of the distal tibia, fibula and calcaneus. It can often be difficult to diagnose TOC radiographically, and good technique and accurate positioning are essential for the radiographic visualisation of the lesions. Several projections have been proposed, including the fully extended and fully flexed mediolateral, the plantarodorsal, the plantaromedial-dorsolateral and plantarolateral-dorsomedial, and a flexed dorsoplantar skyline view (Carlisle and Reynolds 1990, Miyabayashi and others 1991, Fitch and Beale 1998). Most lesions of the medial trochlear ridge can be identified on the standard dorsoplantar radiograph (Montgomery and others 1994) but the results of this study show that the plantarolateral-dorsomedial view can also be useful. The radiographic diagnosis of lateral OC is often difficult owing to the complexity of the tarsocrural joint and the superimposition of the different bony structures. The fragments are best visualised in the plantaromedial-dorsolateral oblique projection, and in the fully flexed and extended mediolateral projections (Carlisle and others 1990). The flexed dorsoplantar skyline projection can also be useful (Beale and others 1991, Miyabayashi and others 1991, Fitch and Beale 1998).

The complexity of the tarsocrural joint, especially in young dog, is such that even with an adequate number of appropriate projections, subtle changes involving both ridges of the trochlea tali can be missed. It is therefore necessary in most of the cases to complete the protocol to get maximum radiographic information. Even with the adequate number of projections, little information may be obtained about the exact position, number and size of the fragments, and in most cases it is not possible to determine to what extent the joint surface has been involved.

Because CT avoids superimposition by surrounding bony structures it gives a better general view of the lesion. The use of CT in this study made it possible to determine the

exact location, size and number of all the fragments, valuable information for a surgeon wishing to treat the lesion. The exact location of the lesion is of interest if one wants to use a minimally invasive technique like arthroscopy to determine the best puncture site. Its exact size is important because in some cases the fragments of the talus are so big that their removal results in joint instability (Brinker and others 1997); in such cases, a better solution could be to fix the fragments. It is possible that CT could predict the potential incongruity of the joint after the removal of the fragments, and suggest the appropriate therapeutic strategy, as is done in human medicine (Zinman and Reis 1982; Zinman and others 1988). CT revealed more fragments than survey radiology, and in more than 75% of the cases more than 2 fragments were present. When using a minimal exposure technique or arthroscopy it is possible to miss smaller fragments as a result of the limited overview, a failure which may explain the relatively poor outcome after the surgical treatment of some cases. A medial malleolus osteotomy gives a better overview and visualisation of the lesions but results in a post-surgical instability (Smith and others 1985).

One potential limitation of this study is the lack of an independent “gold standard” by which the results of radiology and CT could be compared objectively. However, CT constantly revealed more lesions than radiology, and the size and location of the lesions could be evaluated more accurately by CT than on radiographs. The results are in agreement with the results of studies in human beings, for whom CT was valuable in revealing the exact location and size of the OC lesions and in guiding a surgical and arthroscopic approach (Zinman and others, 1988).

In human beings, diagnostic and surgical arthroscopy of the tarsus is considered safe, accurate and minimally invasive (Baker and others 1986, Guhl 1988, Ferkel and Fischer 1989, Baker and Morales 1999). In dogs, arthroscopic techniques for the evaluation of the hock joint have been described by Van Ryssen and others (1993) and applied in clinical cases (Van Ryssen and van Bree 1992). The technique proved to be minimally invasive and gave excellent visualisation of the medial and lateral trochlear ridge, provided information about the extent and localisation of the lesions, and made it possible to remove the fragment surgically through a mini-arthrotomy (van Bree and Van Ryssen 1998). However, in the experience of the authors, arthroscopy of the tarsocrural joint remains a difficult procedure because of the associated synovitis and the small size of the

joint space that collapses very easily. As a result, arthroscopy will not always be helpful in the diagnosis of TOC. However, in cases in which good visualisation can be obtained, the lesions can be inspected in detail and the intra-articular view is superior to the view obtained through a mini-arthrotomy. The results of the CT examination can be used to determine the puncture site for the arthroscopic examination. In this study, only 17 fragments could be visualised by arthroscopy, owing to the extensive synovial inflammation and/or the disadvantageous position of the fragments. Fragments at the medial side of the medial trochlear ridge could be seen easily.

It was shown that a classification system, comparable with the “Berndt and Harty” classification in human beings, could be applied to dogs, and that it appeared to be useful for describing the lesions in a standardised way. However, it remains to be established whether it can influence the therapeutic regimen applied to cases of OC of the tarsocrural joint in dogs.

REFERENCES

- BAKER, C. L., ANDREWS, J. R. & RYAN, J. B. (1986) *Arthroscopy: The Journal of Arthroscopic and Related Surgery* **2**, 82
- BAKER, C. L. & MORALES, R.W. (1999) *Arthroscopy: The Journal of Arthroscopic and Related Surgery* **15**, 197
- BEALE, B. S., GORING, R. L., HERRINGTON, J., DEE, J. & CONRAD, K. (1991) *Journal of the American Animal Hospital Association* **27**, 221
- BERNDT, A.L. & HARTY, M. (1959) *Journal of Bone and Joint Surgery* **41-A**, 988
- BREUR, G. J., SPAULDING, K. A. & BRADEN T. D. (1989) *Veterinary and Comparative Orthopaedics and Traumatology* **4**, 168
- BRINKER, W., PIERMATTEI, D. & FLO, G. (1997). *Handbook of Small Animal Orthopedics and Fracture Repair*. W.B. Saunders, Philadelphia. p. 607
- CARLISLE, C. H. & REYNOLDS, K. M. (1990) *Journal of Small Animal Practice* **31**, 273
- CARLISLE, C. H., ROBINS, G. M. & REYNOLDS, K. M. (1990) *Journal of Small Animal Practice* **31**, 280
- DENNY, H. R. (1981). *The Veterinary Annual* **21**, p.224
- DROST, W. T., LOVE N, E. & BERRY, C.R. (1996) *Veterinary Radiology & Ultrasound* **37**, 28
- FERKEL, R. D. & FISCHER, S. P. (1989) *Clinical Orthopedics and Related Research* **240**, 210
- FITCH, R. B. & BEALE, B. S. (1998) *Veterinary Clinics of North America: Small Animal Practice* **28**, 95
- GUHL, J. F. (1988) *Ankle arthroscopy. Pathology and surgical techniques*, Slack Incorporated, New Jersey, USA, p. 95
- JOHNSON, K. A., HOWLETT, C. R. & PETTIT, G. D. (1980) *Journal of the American Animal Hospital Association* **16**, 103
- KIPPENES, H. & JOHNSTON, G. (1998) *Veterinary Clinics of North America: Small Animal Practice* **28**, 137
- MIYABAYASHI, T., BILLER, D. S., MANLEY, P. A. & MATUSHEK, K. J. (1991) *Journal of the American Veterinary Medical Association* **199**, 598
- MONTGOMERY, R. D., HATHCOCK, J. T., MILTON, J. L. & FITCH, R. B. (1994) *Compendium on Continuing Education for the Practising Veterinarian* **16**, 835
- SCHENCK, R.C. & GOODNIGHT, J.M. (1996) *The Journal of Bone and Joint Surgery* **78:3**, 439
- SMITH, M., VASSEUR, P. & MORGAN, J. (1985) *Journal of the American Veterinary Medical Association* **187**, 31
- STICKLE, R. L. & HATHCOCK, J. T. (1993) *Veterinary Clinics of North America: Small Animal Practice* **23**, 417
- VAN BREE, H. & VAN RYSSSEN, B. (1998). *Veterinary Clinics of North America: Small Animal Practice*

28, 161

VAN RYSSSEN, B., VAN BREE, H. & VERSCHOOTEN F. (1991) *Vlaams Diergeneeskundig Tijdschrift* **60**, 197

VAN RYSSSEN, B. & VAN BREE, H. (1992) *Journal of the American Animal Hospital Association* **28**, 295

VAN RYSSSEN, B., VAN BREE, H. & VYT, PH. (1993) *Journal of the American Animal Hospital Association* **29**, 107

VAN RYSSSEN, B. & VAN BREE, H. (1997) *Veterinary Record* **140**, 360

WEINSTEIN, M.J., MONGIL, C.M., RHODES, W.H. & SMITH, G.K. (1995) *Compendium on Continuing Education for the Practising Veterinarian* **17**, 925

WISNER, E. R., BERRY, C. R., MORGAN, J. P., POOL, R. R., WIND, A. P. & VASSEUR, P. B. (1990) *Veterinary Surgery* **19**, 435

ZINMAN, C. & REIS, N.D. (1982). *Acta Orthopaedica Scandinavica* **53**, 697

ZINMAN, C., WOLFSON, N. & REIS, N.D. (1988). *The Journal of Bone and Joint Surgery* **79-A**, 1017

**COMPUTED TOMOGRAPHY COMPARED WITH RADIOGRAPHY IN THE
DIAGNOSIS OF TARSOCRURAL OSTEOCHONDROSIS OF THE LATERAL
TROCHLEAR RIDGE IN THE DOG**

I. Gielen, H. van Bree

Department of Medical Imaging, Faculty of Veterinary Medicine,
Ghent University, Salisburyaan 133, Merelbeke, Belgium

Adapted from:

The Veterinary and Comparative Orthopaedics and Traumatology, accepted, 2003.

and

I. Gielen, B. Van Ryssen, H. van Bree. The use of computed tomography (CT) in tarsocrural OCD in the lateral ridge of the dog. Abstract 12th Meeting International Veterinary Radiology Association. Obihiro-Japan, August 21-25, 2000. p 29.
Veterinary Radiology & Ultrasound (2001) 42, 1: 174.
Award for the best oral presentation.

SUMMARY

Computed tomography (CT) allows the inspection of the talar ridges without superimposition of any bony structures. In this retrospective study in 11 tarsal joints with lateral tarsocrural osteochondrosis (TOC), the value of CT with radiography in the diagnosis was compared. The flexed dorsoplantar skyline and the plantarolateral-dorsomedial (lateral oblique) projection were the most successful views to detect the OC defect (in 7 out of 11). Radiography failed to detect the fragment in 3 out of the 11 OC lesions whereas with the help of CT in all cases the fragments could be visualised and exactly localised. In 6 joints 2 fragments, and in 5 only 1 fragment was detected. This information is of use when minimally invasive techniques are used to treat the lesions. The conclusion of this study was that CT is superior to radiography to diagnose lateral TOC in the dog.

INTRODUCTION

Osteochondrosis (OC) is a term to indicate a developmental joint and bone disease in humans and a variety of animal species. There is considerable confusion regarding the definition and pathogenesis of OC. It is a disturbance in subchondral bone ossification, due to genetic, developmental, and environmental (trauma, nutrition) factors (9). In the dog, tarsocrural osteochondrosis (TOC) is a well known but uncommon cause of hind limb lameness and comprises 9% of all OC cases. The tarsocrural joint is the third most commonly affected joint. The OC defect can involve the medial or the lateral trochlear ridge of the talus and results in instability, pain, lameness, and progressive degenerative joint disease (DJD) (10).

The most common location for the TOC lesions is the medial trochlear ridge of the talus. Involvement of the lateral trochlear ridge is less common and occurs in 25% of the cases (5, 8, 15, 23, 26). Especially the radiographic diagnosis of lateral TOC can be difficult due to the complexity of the tarsocrural joint and the superimposition of the different bony structures. Lateral fragments are best seen on the plantaromedial-dorsolateral oblique projection, and in the fully flexed and extended mediolateral projections (7). The flexed dorsoplantar skyline projection can also be useful (3, 10, 17).

In humans, OC lesions are found in the medial or lateral aspect of the talus as well and although plain radiographs are usually sufficient to make the diagnosis, computed tomography (CT) is beneficial, in preoperative planning, for an accurate determination of the size and location of the lesion (18, 27) and for evaluating the follow-up after treatment (28).

CT enables a detailed examination of the canine tarsocrural joint surface (11) and enables to determine the exact location, the size and number of fragments in TOC (12).

The aim of this study was to compare the value of CT with radiography in the diagnosis of lateral TOC in the dog.

MATERIAL AND METHODS

Eleven joints (8 dogs) with TOC of the lateral trochlear ridge were used for this retrospective study. Criteria to be included in this report were, besides adequately documented clinical records, a complete radiographic study (including an extended and flexed mediolateral, a flexed

dorsoplantar skyline projection, a plantarodorsal and two oblique views: a plantaromedial-dorsolateral and plantarolateral-dorsomedial), and a CT study of both tarsocrural joints (including transverse scans of the tarsocrural region, and dorsal and sagittal reconstructions of both talar ridges). Both tarsal joints of each dog were scanned simultaneously using a recently published protocol (12). Final diagnosis was based on identification by CT of a subchondral defect or a bony fragment associated with the lateral trochlear ridge.

After the radiographic examination, each projection was blindly evaluated by one single examiner (HvB) for the presence of trochlear ridge involvement (increased joint space over the ridge of the talus, reduced height of the ridge, discontinuity of the delineation of the ridge) and of an isolated bony OC fragment.

After the CT examination the images were blindly interpreted by one single examiner (IG). The transverse CT images were evaluated for trochlear ridge involvement (defect with or without visible fragment). Thereafter, different CT images were reconstructed in multiple anatomic planes in order to evaluate the integrity and/or the eventual involvement of the joint surface. If fragments were visible, their exact location and number were determined. The CT size of the defect and associated fragment was evaluated using a four-grade classification system; no evidence of a defect (0), small defect (1), moderately sized defect (2), and large defect (3). To describe the exact location of the tarsocrural lesions, a map (12) was used in which the lateral trochlear ridge was divided in a proximal, a dorsal and a distal area (Fig 1).

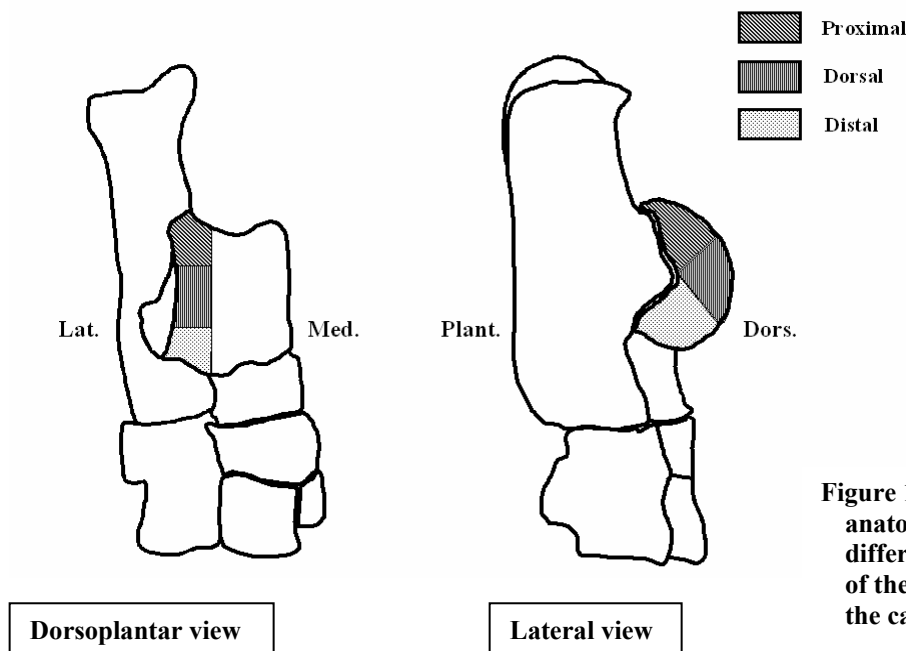


Figure 1: Diagram showing the anatomical positions of the different osteochondrosis lesions of the lateral trochlear ridge of the canine tarsocrural joint.

Also a four-stage classification system comparable to the Berndt and Hardy system was established (12). This classification system classifies the lesion into four different stages depending on the status of the trochlear ridge and the associated fragment: Stage I - a subchondral bone defect without an associated fragment; Stage II - a partially detached osteochondral fragment; Stage III - a completely detached osteochondral fragment remaining in the crater; and Stage IV- a completely detached and displaced fragment (2, 4).

After the completion of the study the radiographic and CT findings were compared regarding the visibility of the TOC fragments and the involvement of the trochlear ridge.

RESULTS

Four of the 8 dogs were female. The age range was 6 to 12 months with a mean of 9.6 months and their weight ranged from 22 to 60 kg with a mean of 34 kg (Table 1).

Table 1: Breed, gender, age, and weight distribution of 8 dogs (11 joints) with lateral TOC

Breed	Gender	Age (months)	Weight (kg)	Duration lameness	
				(months)	Trauma?
Golden Retriever	F	8	22	2	Y
Golden Retriever	F	6	27	1	Y
Golden Retriever	F	11	35	1	Y
Rottweiler	M	11	35	4	N
Rottweiler	F	7	29	1	Y
Irish Wolfhound	M	12	60	4	Y
Chow Chow	M	12	22	2	N
Mastino	M	8	45	5	N

Duration of lameness at the time of diagnosis ranged from 1 to 5 months with a mean of 2.7 months. Three dogs were bilaterally affected but only one of these was bilaterally lame at the time of presentation. In 5 of the 8 dogs, there was a history of trauma before the onset of the lameness.

After completion of the complete radiographic study (Table 2), in 10 out of the 11 joints trochlear ridge involvement could be diagnosed.

Table 2: Radiographic and CT evaluation of 11 joints

No	CT loc	B-H	CT size	Ext ml	Flex ml	Pd	D45°L-	D45°M-	Skyline	TOTAL
							PLMO	PLLO		
1	Prox	IV	3	-	+	+	+	+	+	5
2	Prox	III	3	+	+	-	+	+	+	5
3	Prox	IV	2	-	-	-	-	+	+	2
4	Dist	III	2	-	-	-	-	+	-	1
5	Prox	IV	2	-	+	-	+	-	+	3
5'	Prox	IV	3	-	+	-	+	+	+	4
6	Dors	IV	1	-	-	-	-	-	-	0
6'	Dors	IV	1	-	-	-	-	-	-	0
7	Prox	IV	3	+	+	+	+	+	+	6
8	Prox	II	1	-	-	-	-	-	-	0
8'	Prox	II	1	-	-	-	-	+	+	2
TOTAL				2	5	2	5	7	7	28

CT loc = CT localisation: Prox = proximal; Dors = dorsal; Dist = distal.

B-H = "Berndt and Harty" classification I to IV.

CT size = grading system ranging from 0 to 3

Ext ml = Extended mediolateral projection.

Flex ml = Flexed mediolateral projection.

Pd = Extended dorsoplantar projection.

D45°L-PLMO = Plantaromedial-dorsolateral (medial oblique).

D45°M-PLLO = Plantarolateral-dorsomedial (lateral oblique).

Skyline = Flexed dorsoplantar skyline projection.

+ = radiographic diagnosis of lateral TOC possible

- = radiographic diagnosis of lateral TOC not possible

One joint looked radiographically normal. The TOC fragment could be detected on only 28 out of 66 radiographic projections. In only 1 joint the fragment was visible on all 6 standard projections and in 3 it could not be detected on any of the six views, although in 2 out of 3 joints trochlear ridge involvement could be seen. In 2 joints the fragment was visible on 5 of the 6 standard projections, in 1 joint on 4 of the six views, in 1 joint on 3, in 2 joints on 2, and in 1 on 1 view out of 6. The flexed dorsoplantar skyline and the plantarolateral-dorsomedial (lateral oblique) projection were the most successful views to detect the TOC defect (in 7 out of 11). The extended mediolateral (Fig 2a) and the extended dorsoplantar projection were the less successful views (2 out of 11). On the flexed mediolateral (Fig 2b) and the plantaromedial-dorsolateral (medial oblique) view the TOC defect could be detected in 5 out of the eleven joints.

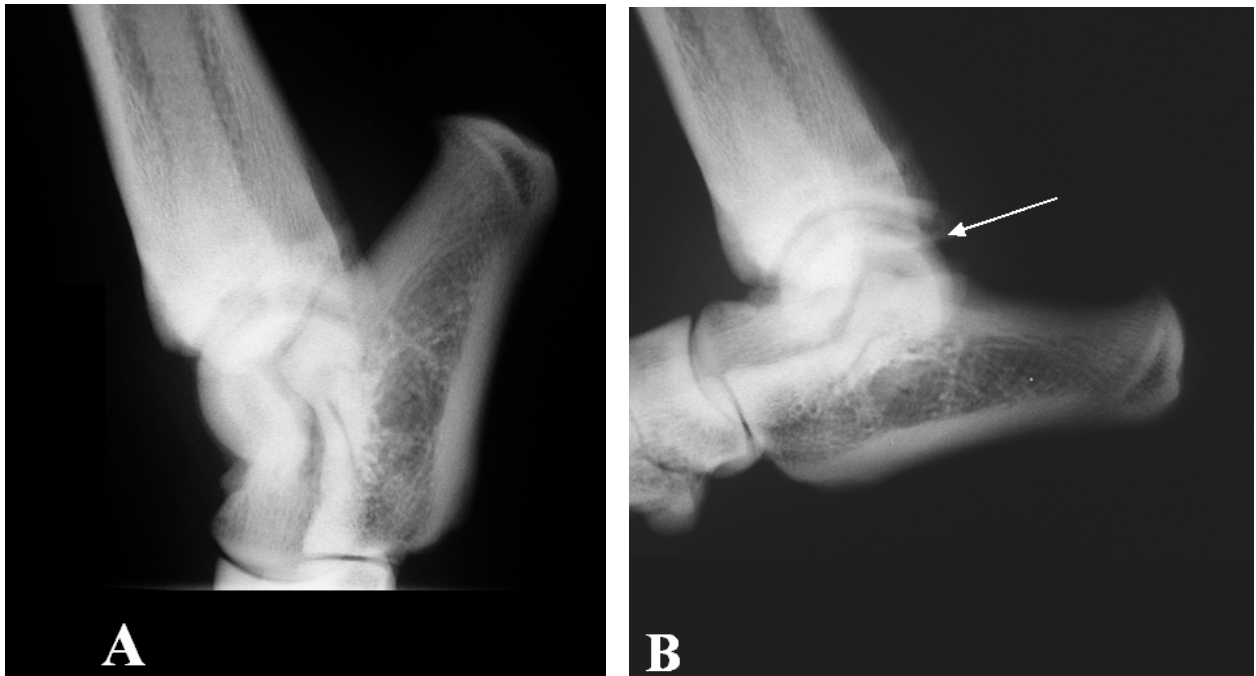


Figure 2: Mediolateral extended (A) and flexed (B) radiographic view of the tarsal joint. On the extended projection the irregular articular surface of the talus is visible. On this view the incidence of a fragment can not be identified. The flexed projection shows a fragment (white arrow) on the proximal part of the lateral trochlear ridge of the talus.

In all but 1 joint radiographically degenerative joint disease was present.

On CT, in the 11 joints 1 or 2 fragments could be detected. In 6 joints 2 fragments, and in 5 only 1 fragment was detected. The exact location and extent of the defect could be determined in all 11 lateral trochlear ridge lesions, using a combination of the transverse scans and reconstructed images in dorsal and sagittal planes (Table 2). In 8 out of 11 the defect was located on the proximal area of the lateral trochlear ridge (Fig. 3), in 2 on the dorsal (Fig 4), and in 1 on the distal area (Fig 5). Most of the lesions could be classified as “Berndt-Harty” IV (7 out of 11). Two lesions were classified as “Berndt-Harty” III, and 2 as “Berndt-Harty” II lesions. Four of the 11 defects were graded as small (1), 3 as moderately sized (2), and 4 as large (3). The 3 out of 11 fragments not detected on any of the 6 radiographic projections were small. The 4 large defects were detected on more than 4 views out of 6. The large defect detected on all 6 views was a complete detached and displaced fragment (“Berndt and Harty” IV lesion). The moderately sized defects were seen on less than 4 views.

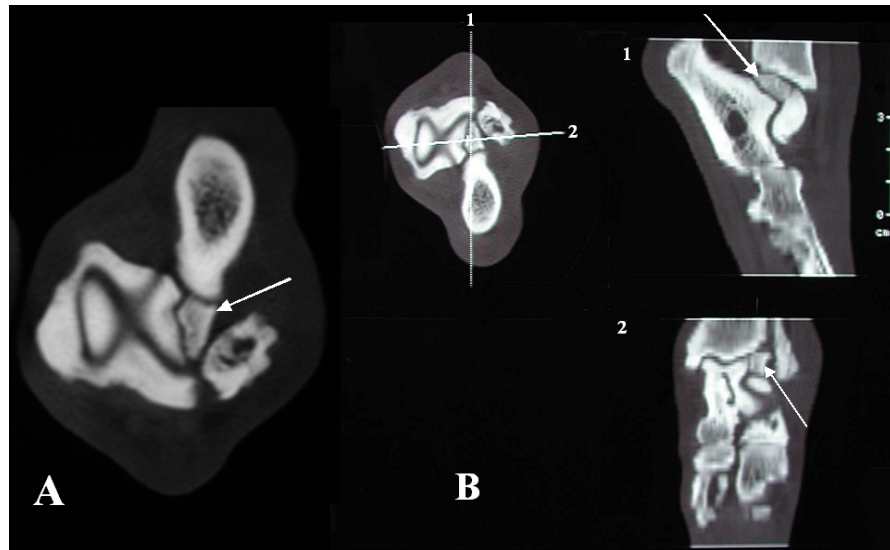


Figure 3: Transverse CT scan (A) and reconstructed images (B) of a right tarsus with an osteochondrosis lesion of the proximal part of the lateral trochlear ridge of the talus. The white arrow, on the transverse scan, shows the detached large fragment. Sagittal (1) and dorsal (2) reconstructed images show the fragment on the proximal part of the lateral ridge (white arrow). This proximal lesion is staged as a “Berndt and Harty” stage III lesion.

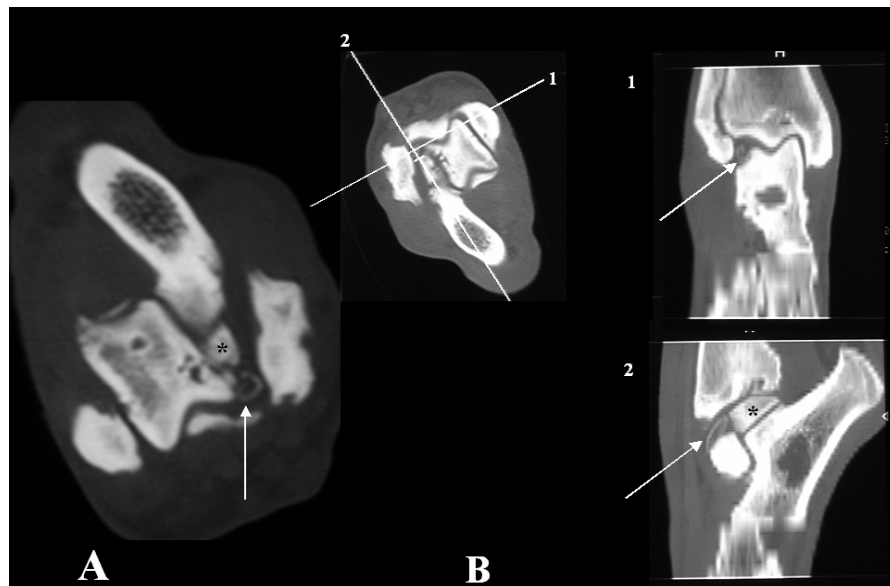


Figure 4: Transverse CT scan (A) and reconstructed images (B) of a right tarsus demonstrating a fragment on the proximal and dorsal part of the lateral talar trochlear ridge. On the transverse scan, two fragments are present on the lateral trochlear ridge. One fragment is localised in the proximal part (asterisk) and a hypodense fragment is visible on the dorsal part (white arrow). On the dorsal reconstructed image (1), the hypodense fragment on the dorsal part of the lateral ridge is demonstrated (white arrow). On the sagittal reconstructed image (2), the smaller hypodense fragment on the dorsal part (white arrow) and the fragment on the proximal part (asterisk) are visible. Using the Berndt-Harty classification, both fragments are classified as stage III lesions.

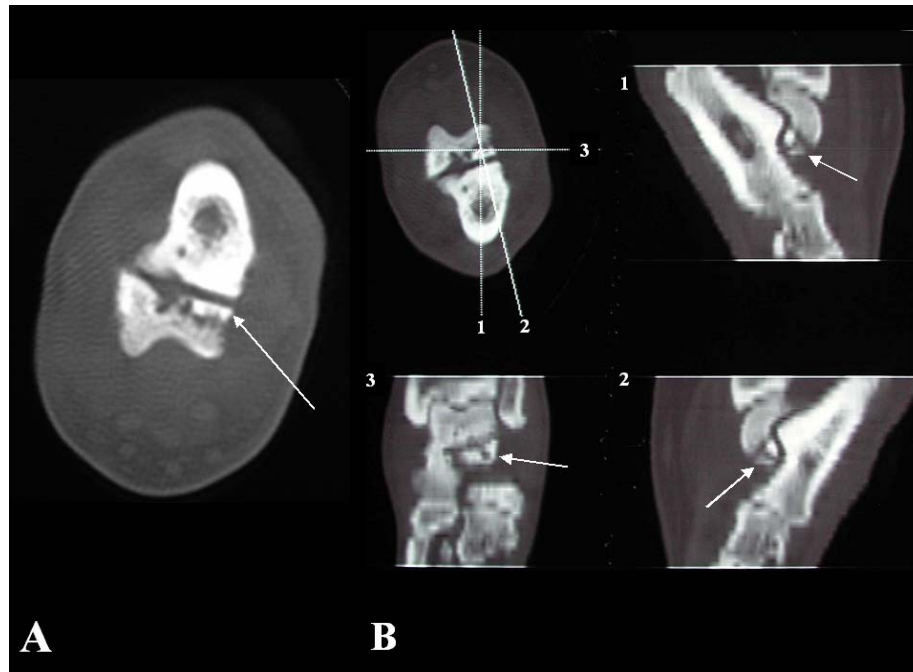


Figure 5: Transverse CT scan (A) and reconstructed images (B) of a right tarsus with an osteochondrosis lesion of on the distal part of the lateral trochlear ridge. On the transverse scan, a fragment is localised on the distal part of the lateral ridge (white arrow). Sagittal reconstructions (1, 2) demonstrate two detached fragments distally (white arrows). On the dorsal reconstructed image (3) two fragments (white arrow) are visible on the distal part of the lateral ridge. Both fragments are stage III lesion using the “Berndt and Harty” classification.

DISCUSSION

Although Rottweilers have been reported to have greater lateral trochlear ridge involvement than other breeds (25), in this study only 2 out of the 8 dogs were Rottweilers. Three Golden Retrievers and also 3 other breeds were affected. As a consequence in any young large breed dog with a hind leg lameness localised within the tarsocrural joint, a suspicion of TOC involving the lateral ridge can arise.

Although a very detailed study on the radiographic anatomy of the canine tarsocrural joint exists (6), the radiographic evaluation of this region remains difficult due to superimposition of the distal tibia, fibula and calcaneus. Especially the radiographic diagnosis of lateral TOC can often be challenging due to the complexity of the tarsocrural joint and the superimposition of the different bony structures. Because of this difficulty in diagnosis there has been a delay in recognition of these lateral ridge lesions (16). An excellent technique and positioning of the

patient are essential for the radiographic visualisation of the lesions. Several projections are proposed including the fully extended and fully flexed mediolateral, the plantarodorsal, the plantaromedial-dorsolateral and plantarolateral-dorsomedial, and a flexed dorsoplantar skyline view (6, 10, 17).

In this study, in only 1 joint the fragment was visible on all 6 radiographic views, and in 3 cases the fragments could not be seen on any of the projections made, which means that in 27% of these joints it was impossible to make a definite diagnosis of lateral tarsocrural OC. Although exploratory arthrotomy is recommended by some authors as a reasonable diagnostic option (10, 13, 15), this is an invasive technique with associated morbidity. If the radiographic examination is limited to only two standard projections (extended mediolateral and extended dorsoplantar projection) the definite diagnosis would be missed in 8 out of 11 cases. Only 3 out of the 4 large fragments could be detected. This suggests that in dogs suspected of having lateral TOC at least the proposed 6 views have to be made (7, 10, 17).

Not surprisingly, the results of this study prove that CT is superior compared to radiography in the definite diagnosis of lateral TOC. CT avoids superimposition by surrounding bony structures and consequently assures a better overview of these lesions. One potential limitation of this study is the lack of an independent “gold standard” by which the results of radiology and CT could be compared objectively. However, CT constantly revealed more lesions than radiology, and the size and location of the lesions could be evaluated more accurately by CT than on radiographs. The results are in agreement with the results of studies in human beings, for whom CT was valuable in revealing the exact location and size of the OC lesions (28) and remains the imaging technique of choice when delineation of a bone fragment is desired (22). Therefore, we can assume that using CT, in all affected joints all fragments were visible and could be exactly localised. This information is of interest to the surgeon who wants to treat the lesion. Its exact location is of interest if one wants to use a minimally invasive technique such as arthroscopy to determine the best approach to access the lesion. The exact number of fragments is also important when using a minimal exposure technique or arthroscopy because due to the limited overview it is possible to miss smaller fragments. The disadvantages of CT include the need for general anaesthesia, the limited access to-, and the high cost of the equipment. The actual CT imaging time of about 10 minutes is probably shorter than the time it takes to complete a radiographic examination including 6 views.

Although it has been reported that in TOC of the lateral ridge, the dorsal, dorsoproximal, or proximal part can be affected (7, 24), most lesions in this study were localised in the proximal part of the lateral ridge.

In the human literature, several conditions are grouped under the heading of OC; these include osteochondral fractures, osteonecrosis, accessory centres of ossification, osteochondrosis, and hereditary epiphyseal dysplasia (9, 19). The aetiology and pathogenesis of talar OC in humans remain controversial. In humans OC lesions are also found on the medial or lateral aspect of the talus. Most investigators now believe trauma to be the main cause and necrosis the consequence (18). Subsequent series have supported a traumatic aetiology for most osteochondral lesions of the talus, ranging from 75% to 100% for lateral lesions and 18% to 80% for medial lesions (22). No proof exists for a traumatic aetiology for TOC in the dog, although traumatic fragmentation of the lateral talar ridge is reported as well (1, 20). In the present study, in 5 out of the 8 dogs a history of trauma was present. It has been reported that some of these lateral lesions are thought to be avulsion fractures of the short lateral collateral ligaments associated with relatively large loose fragments situated proximally. Any possible relation between OC and these avulsion fractures could not be evaluated (20). In this series 3 out of the 11 lesions were situated in the dorsal or distal part of the lateral ridge which is not the site where the short lateral collateral ligaments attaches to the bone.

With the growing availability of CT to veterinarians (14, 21) this technique can be efficiently used for the diagnosis of lateral TOC as CT has been proven to be superior for making the diagnosis.

REFERENCES

1. Aron DN, Mahaffey MB, Rowland GN. Free chondral fragment involving the lateral trochlear ridge of talus in a dog. *J Am Vet Med Assoc* 1985; 186: 1095-1096.
2. Baker C L, Morales RW. Arthroscopic treatment of transchondral talar dome fractures: Along-term follow-up study. *Arthroscopy: J Arthrosc Rel Surg* 1999; 15: 197-202.
3. Beale BS, Goring RL, Herrington J, Dee J, Conrad K. A prospective evaluation of four surgical approaches to the talus of the dog used in the treatment of osteochondritis dissecans. *J Am Anim Hosp Assoc* 1991; 27: 221-229.
4. Berndt AL, Hartly M. Transchondral fractures (osteochondritis dissecans) of the talus. *J Bone Joint Surg* 1959; 41A: 988-1020.
5. Breur GJ, Spaulding KA, Braden TD. Osteochondritis dissecans of the medial trochlear ridge of the talus in the dog. *Vet Comp Orthop Traumatol* 1989; 4: 168-176.
6. Carlisle CH, Reynolds KM. Radiographic anatomy of the tarsocrural joint of the dog. *J Small Anim Pract* 1990; 31: 273-279.
7. Carlisle CH, Robins GM, Reynolds KM. Radiographic signs of osteochondritis dissecans of the lateral ridge of the trochlear talus in the dog. *J Small Anim Pract* 1990; 31: 280-286.
8. Denny HR. Osteochondritis dissecans of the hock joint in the dog. *Vet Annual* 1981; 21:224-228.
9. Ekman S and Carlson CS. The pathophysiology of osteochondrosis. *Vet Clin North Am: Small Anim Pract* 1998; 28: 17-32.
10. Fitch RB, Beale BS. Osteochondrosis of the canine tibiotarsal joint. *Vet Clin North Am: Small Anim Pract* 1998; 28: 95-113.
11. Gielen IM, De Rycke LM, van Bree HJ, Simoens PJ. Computed tomography of the tarsal joint in clinically normal dogs. *Am J Vet Res* 2001; 62: 1911-1915.
12. Gielen I, van Bree H, Van Ryssen B, De Clercq T, De Rooster H. Radiographic, computed tomographic and arthroscopic findings in 23 dogs with osteochondrosis of the tarsocrural joint. *Vet Rec* 2002; 150: 442-447.
13. Johnson KA, Howlett CR, Pettit GD. Osteochondrosis in the hock joint in dogs. *J Am Anim Hosp Assoc* 1980; 16: 103-113.
14. Kippenes H, Johnston G. Diagnostic imaging of osteochondrosis. *Vet Clin North Am: Small Anim Pract* 1998; 28: 137-160.
15. Montgomery RD, Hathcock JT, Milton JL, Fitch RB. Osteochondritis dissecans of the canine tarsal joint. *Comp Cont Ed Pract Vet* 1994; 16: 835-845.
16. Morgan JP, Wind A, Davidson AP. Osteochondrosis of the talus. In: Hereditary bone and joint disease in the dog: Osteochondroses-Hip dysplasia-Elbow dysplasia. JP Morgan, A Wind and AP Davidson (eds). Schlutersche GmbH, Hannover 2000, 239-245.
17. Miyabayashi T, Biller DS, Manley PA, Matushek KJ. Use of a flexed dorsoplantar radiographic view of the talocrural joint to evaluate lameness in two dogs. *J Am Vet Med Assoc* 1991; 199: 598-600.
18. Ogilvie-Harris DJ, Sarrosa EA. Arthroscopic treatment of osteochondritis dissecans of the talus. *Arthroscopy: J Arthrosc Rel Surg* 1999; 15: 805-808.

19. Schenck RC, Goodnight JM. Current concept review: Osteochondritis dissecans. *J Bone Joint Surg* 1996; 78A: 439-456.
20. Sjöström L, Håkanson N. Traumatic injuries associated with the short collateral ligaments of the talocrural joint of the dog. *J Small Anim Pract* 1994; 35: 163-168.
21. Stickle R.L., Hathcock JT. Interpretation of Computed Tomographic Images. *Vet Clin North Am: Small Anim Pract* 1993; 23: 417-429.
22. Stone. Osteochondral Lesions of the Talar Dome. *J Am Acad Orthop Surg* 1996; 4: 63-73.
23. Van Ryssen B, van Bree H, Verschooten F: Osteochondritis dissecans of the tarsal joint in the dog: a review. *Vlaams Diergeneesk Tijdsch* 1991; 60: 197-2002.
24. Van Ryssen B, van Bree H: Arthroscopic evaluation of osteochondrosis lesions in the canine hock joint: a review of two cases. *J Am Anim Hosp Assoc* 1992; 28: 295-299.
25. Weinstein MJ, Mongil CM, Rhodes WH, Smith GK. Orthopedic conditions of the Rottweiler – Part II. *Comp Cont Ed Pract Vet* 1995; 17: 925-939.
26. Wisner ER, Berry CR, Morgan JP, Pool RR, Wind AP, Vasseur PB. Osteochondrosis of the lateral trochlear ridge of the talus in seven Rottweiler dogs. *Vet Surg* 1990; 19: 435-439.
27. Zinman C, Reis ND. Osteochondritis dissecans of the talus : use of the high resolution Computed Tomography Scanner. *Acta Orthop Scand* 1982; 53: 697-700.
28. Zinman C, Wolfson N, Reis ND. Osteochondritis dissecans of the dome of the talus. *J Bone Joint Surg* 1988; 70: 1017-1019.

**COMPARISON OF MORPHOLOGICAL AND CLINICAL FEATURES
BETWEEN MEDIAL AND LATERAL, AND CLINICAL AND NON-CLINICAL
CANINE TARSOCRURAL OSTEOCHONDROSIS LESIONS**

I. Gielen, H. van Bree, F. Coopman

Department of Medical Imaging, Faculty of Veterinary Medicine,
Ghent University, Salisburylaan 133, Merelbeke, Belgium

Adapted from:

American Journal of Veterinary Research, submitted.

SUMMARY

Objective- To evaluate whether significant differences exist between medial (MTOC) and lateral (LTOC) tarsocrural osteochondrosis (TOC) and between clinical and non-clinical lesions in dogs affected with bilateral MTOC. This was done by comparing the morphological data of the lesions obtained by computed tomography (CT), the clinical features of the affected dogs, and the severity of radiographic degenerative joint disease (DJD) at the time of presentation.

Animals- Forty-nine joints (35 dogs) with TOC were considered.

Procedure- Clinical data (breed, age, gender, weight, duration of clinical symptoms) were registered. All 49 TOC defects were measured (length, width and depth) using the CT software. Comparable to studies in man, volume (= length x width x depth) and surface (= length x width) of the defect were used to compare the size of the different defects. The radiographs of the affected tarsocrural joints were evaluated for DJD. Data of LTOC - and MTOC defects, and clinical and non-clinical MTOC lesions were statistically evaluated.

Results- Dogs with LTOC lesions were significantly younger than those with MTOC lesions and the duration of lameness prior to admittance to the clinic was shorter. LTOC lesions were significantly larger than the MTOC lesions and clinical lesions were larger than non-clinical lesions. The difference in length between clinical and non-clinical MTOC lesions was of statistical significance.

Conclusions and Clinical Relevance- The results support the view of some authors that LTOC has a different aetiology than MTOC and therefore they have to be considered as different disorders. Comparable to humans, a traumatic fragmentation of the lateral talar ridge could be the cause of the OC lesions. There is probably a correlation between the size of tarsocrural lesions and the symptoms of pain and lameness.

INTRODUCTION

Osteochondrosis (OC) is a developmental joint and bone disease in humans and a variety of animal species.¹ Tarsocrural OC (TOC) has been reported in several species, including dogs, horses, cattle, pigs and humans and was first reported in the dog in 1975.² It occurs less frequently in the tarsocrural joint than in the elbow or shoulder joint and accounts for 9% of all canine OC cases.^{3,4}

The most common location for the TOC lesions is the medial trochlear ridge of the talus. Involvement of the lateral trochlear ridge is less common and occurs in 25% of the cases.^{3,5,6,7,8} Rottweilers have been reported to have greater lateral trochlear ridge involvement than other breeds.⁹

The only morphological difference reported between medial tarsocrural osteochondrosis (MTOC) and lateral tarsocrural osteochondrosis (LTOC) lesions is the difference in location on the trochlear ridge. In OC of the lateral ridge, the dorsal, dorsoproximal, or proximal part can be affected,^{10,11} contrary to OC of the medial ridge, mostly located on the plantar part (i.e. proximal).³ Approximately 50% of reported cases of TOC are bilateral,^{3,9} although clinical lameness is rarely symmetrical.^{8,12}

CT enables determination of the exact location, the size and number of TOC fragments.^{13,}

14

The aim of this study was to evaluate eventual significant differences between MTOC and LTOC by comparing the morphological data of the lesions obtained by CT (size, site, location, “Berndt-Harty” classification, and number of fragments), the clinical features of the affected dogs (breed, age, gender, weight, and duration of symptoms), and the severity of radiographic degenerative joint disease (DJD) at the time of presentation. The morphological CT data between clinical and non-clinical MTOC lesions were compared as well in a group of bilaterally affected dogs showing unilateral lameness.

MATERIAL AND METHODS

Data-collection

Forty-nine joints (35 dogs) with TOC were studied. Clinical data (breed, age, gender, weight, duration of clinical symptoms) were registered. A complete radiographic and CT study of both tarsocrural joints (including transverse scans of the tarsocrural region and reconstructions of both talar ridges) were performed. The location of the TOC lesions was classified according to the CT findings described in a previous study.¹⁴ The exact location of the TOC lesions was mapped: the medial and lateral trochlear ridges were divided in a proximal, a dorsal and a distal area (Fig 1).

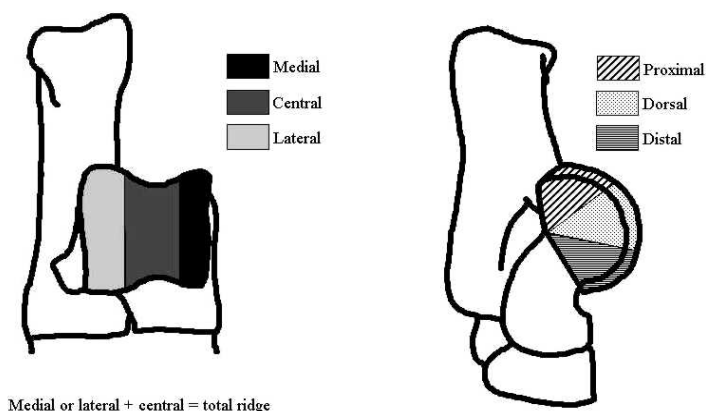


Figure 1: Diagram showing the anatomical positions of the different OC lesions of the lateral and medial trochlear ridge of the canine tarsocrural joint.

All 49 TOC defects were measured – length (L), width (W), and depth (D) – using the CT software (Fig 2). The surface (= length x width) and volume (= length x width x depth) were used to compare the sizes of the various defects. Similar to a method used in humans¹⁵ and in a previous study,¹⁶ all measurements were related to the cross-section of the talus, just below the ridges (Fig 3). This allowed dogs of various body weights and sizes to be compared. This new set of data is referred to as relative length (L-rel), relative width (W-rel), relative depth (D-rel), relative surface (Surf-rel), and relative volume (Vol-rel).

The lesions were classified according to the four-stage “Berndt and Harty” classification system used in man.¹⁴ This classification system depends on the status of the trochlear

ridge and the associated fragment: Stage I - a subchondral bone defect without an associated bony fragment; Stage II - a partially detached osteochondral fragment; Stage III - a completely detached osteochondral fragment remaining in the crater; and Stage IV - a completely detached and displaced fragment.^{17, 18} The number of fragments on CT was recorded as well.

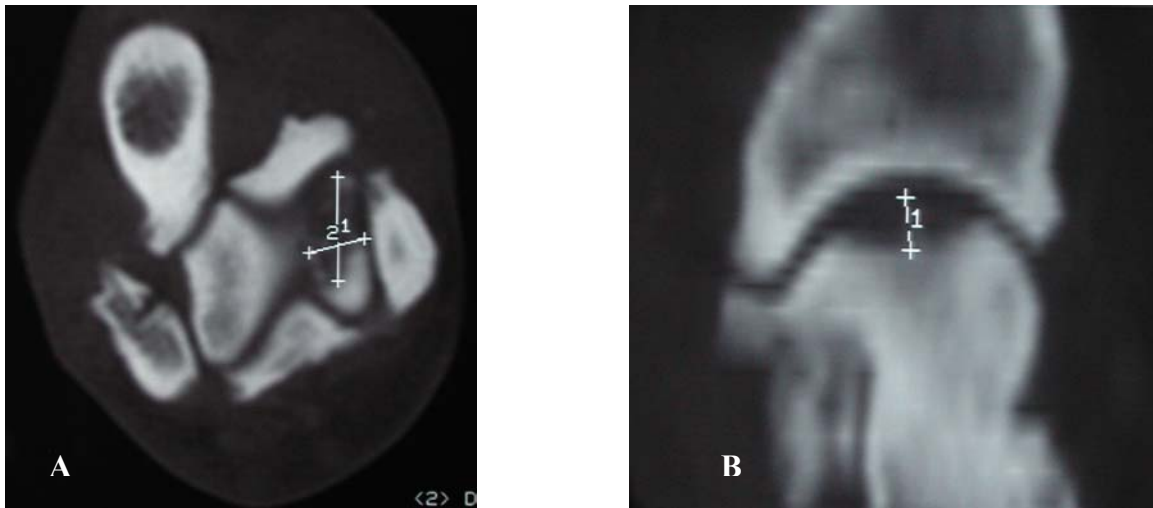


Figure 2. CT measurements:

1A: Transverse CT image through the right tarsocrural joint of a dog with an OCD defect involving the medial tarsal ridge. Using the CT software the length (L) (1) and width (W) (2) of the defect are measured.

1B: Sagittal reconstruction through the medial ridge of the talus of the same joint. On this image the depth (D) (1) of the defect is measured.

After these measurements, the length, depth and width of the defect are multiplied with one another to estimate its volume.



Figure 3. CT measurements:

All measurements (L, W, and D) were related to the cross section of the talus (1), just below the ridges allowing dogs of various body weights and sizes to be compared.

The radiographs of the affected tarsocrural joints were evaluated for DJD: the presence and size of osteophytes and subchondral sclerosis. The severity of DJD was evaluated using a four-grade classification system; no evidence of degenerative changes (0), minimal degenerative changes: early osteophyte production and subchondral sclerosis (1), moderate degenerative changes: osteophyte production and bone remodelling (2), and severe degenerative changes: excessive osteophyte production and bone remodelling (3). Subjective assessment of osteophyte formation and subchondral sclerosis was performed, using normal radiographs for comparison.¹⁹

Lesions were considered as clinical if they were associated with a visible lameness.

Statistical analysis

SPSS 11.0 for Windows was used to explore and analyse the data and correlations were calculated. Differences were looked for between the data of MTOC - and LTOC lesions. Because differences in age (mean; $p < 0.05$ and standard deviation) exist between the lateral and medial type, the independent samples Student T – test on age corrected data was used to compare the means between both types. Between both types, no significant differences were found for weight or gender, and no further corrections were needed. Differences between the data of clinical (CL) and non-clinical lesions (NCL) were compared using only the data of the dogs with bilateral MTOC lesions but with unilateral lameness ($n = 7$). A paired samples T – test was used.

RESULTS

The breed and gender of the 35 dogs are outlined in table 1. Twenty dogs were male, 15 female. Their age ranged from 5 to 48 months with a mean of 18 months; 16 dogs were older than 12 months. Body weight ranged from 11 to 60 kg with a mean of 32 kg. Duration of lameness ranged from 1 to 24 months with a mean of 6 months. Thirteen dogs were bilaterally affected and four of these were bilaterally lame and bilaterally treated. In 28 dogs, the lesions were localised on the medial talar ridge and in 8 on the lateral ridge. One dog with bilateral involvement of the lateral ridge had a unilateral MTOC lesion as well. MTOC was seen in 38 joints, LTOC in 11 joints (Table 2). Forty

affected joints showed lameness while 9 affected joints did not. Seven dogs with bilateral affections had MTOC (Table 3), 2 of them LTOC.

Table 1: Breed and sex distribution of 35 dogs (49 joints) with TOC

Breed	Male	Female	Total	Med	Lat	Uni	Bi
Labrador Retriever	4	7	11	11		6	5
Rottweiler	5	3	8	6	2	6	2
Golden Retriever		3	3		3	3	
Staffordshire Bull Terrier	1	1	2	2			2
Bull Terrier	2		2	2		2	
Bull Mastiff	1	1	2	2		1	1
Pitbull	1		1	1			1
Irish Wolfhound	1		1		1	1	
Chow Chow	1		1		1		1
Kings Poodle	1		1	1		1	
Beagle	1		1	1		1	
Belgian Shepherd	1		1	1		1	
Mastino*	1		1	1	1	1	1
Total	20	15	35	28	8	23	13

Med = medial tarsal ridge involvement.

Lat = lateral tarsal ridge involvement.

Uni = unilateral OC lesions.

Bi = bilateral OC lesions.

* = Dog with bilateral lateral OC + one medial lesion.

Table 2: Data of medial TOC (n = 38) and lateral TOC lesions (n = 11).

	Medial OC (n = 38)	Lateral OC (n = 11)
Age of the dogs (months)	19 ± 5	10 ± 2 *
Weight (kg)	31 ± 8	34 ± 12
Duration of lameness (months)	6 ± 5	3 ± 2
Length (L) (mm)	5.89 ± 2.64	8.73 ± 6.68
Width (W) (mm)	3.92 ± 1.26	4.45 ± 1.92
Depth (D) (mm)	4.58 ± 1.35	6.55 ± 3.21 **
Surface (LxW) (mm ²)	25.83 ± 18.03	48.09 ± 49.34 *
Volume (LxWxD) (mm ³)	131.58 ± 113.37	421.91 ± 505.47 **
Relative length (L-rel)	28.7 ± 12.6	40.4 ± 29.0
Relative width (W-rel)	19.1 ± 5.7	21.0 ± 9.6
Relative depth (D-rel)	22.5 ± 7.0	31.1 ± 15.5 *
Relative surface (Surf-rel)	1.2 ± 0.8	2.2 ± 2.1 *
Relative volume (Vol-rel)	6.3 ± 4.9	19.4 ± 21.5 **

* = p < 0.05; ** = p < 0.01

Table 3: Paired data (14 joints) of 7 dogs with medial TOC (bilateral involvement, unilateral lameness)

	Clinical lesions	Non-clinical lesions
Length (L) (mm)	5.43 ± 1.40	4.14 ± 1.86 *
Width (W) (mm)	3.71 ± 0.49	3.57 ± 0.98
Depth (D) (mm)	5.00 ± 1.53	4.57 ± 1.72
Surface (LxW) (mm²)	20.43 ± 6.83	16.00 ± 11.31
Volume (LxWxD) (mm³)	109.14 ± 65.23	80.57 ± 75.80
Relative length (L-rel)	28.07 ± 7.13	21.22 ± 9.10 *
Relative width (W-rel)	19.35 ± 3.71	18.35 ± 4.68
Relative depth (D-rel)	25.89 ± 7.75	23.66 ± 9.10
Relative surface (Surf-rel)	1.06 ± 0.36	0.81 ± 0.56
Relative volume (Vol-rel)	5.63 ± 3.20	4.09 ± 3.76

* = $p < 0.05$

Correlations were found between age and period of lameness ($r = 0.33$; $p < 0.05$), preoperative arthrosis ($r = 0.49$; $p < 0.05$) and number of fragments ($r = -0.33$; $p < 0.05$). Weight has a correlation with length, surface and volume of the defect of 0, 4 ($p < 0.01$) and with W-rel, Surf-rel and Vol-rel of between 0.3 to 0.35 ($p < 0.05$).

Dogs with LTOC were significantly ($p < 0.05$) younger (10 ± 2 months) than dogs with MTOC (19 ± 5 months). Dogs with LTOC had been lame for a shorter time (3 ± 2 months) than dogs with MTOC (6 ± 5 months), although the difference was not statistically significant. Mean values of depth, volume (LWD), and Vol-rel ($p < 0.01$) and mean values of surface (LW), depth – rel, surf-rel ($p < 0.05$) of the LTOC defects were significantly larger than MTOC defects. Other measures were not significantly different between both types, although LTOC defects were always larger than MTOC defects (Table 2). The other measurements showed no differences.

MTOC defects of clinically affected joints showed a significant ($p < 0.05$) difference in the mean of L (5.43 versus 4.14 mm) and L-rel (28.07 versus 21.22) compared to MTOC defects of non clinical joints. For LW (16.00 versus 20.43 mm²), LWD (80.57 versus 109.14 mm³), D-rel (23.66 versus 25.89) and Vol-rel (4.09 versus 5.63) mean differences were found with the clinical joint showing the larger defect (Table 3), but not statistically significant.

DISCUSSION

The aim of this study was to evaluate whether significant differences existed between MTOC and LTOC and to compare the morphological CT data between clinical and non-clinical MTOC lesions.

Statistically significant differences in clinical and morphological features have been found between LTOC and MTOC. Dogs with lateral lesions were younger than those with medial lesions and, although not statistically relevant, the duration of lameness was shorter. LTOC lesions are significantly larger than the MTOC lesions. All of these results supported the view of some authors that LTOC has a different aetiology than MTOC and should therefore be considered as a different disorder. A traumatic fragmentation of the lateral talar ridge was proposed as cause of the TOC lesions.^{20, 21} Some of these fragments were considered to be avulsion fractures of the short lateral collateral ligaments associated with relatively large loose fragments situated proximally.²¹

A negative correlation was found between the age of the dog and the number of TOC fragments. In older dogs, fewer fragments were counted. Whether age was correlated to the type of TOC (LTOC or MTOC) was statistically uncertain. However, age was less likely responsible for the type of TOC. The variation in size of the LTOC defects was larger than for the MTOC defects and indicates that LTOC and MTOC are different anomalies of the tarsocrural joint. The MTOC seemed to create defects that are more limited and less variable in shape than the LTOC defects. These findings correspond well with the literature. Osteochondral fractures may occur both in humans and animals. They are characterised by a sudden onset of pain and lameness and a history of trauma, and are different from (inherited) osteochondrosis.^{22, 23, 24, 25} In humans, OC lesions are found on the medial or lateral aspect of the talus. Lateral lesions are usually considered to be true transchondral fractures, whereas the medial lesions may have been the result of other factors.²⁶ Subsequent studies have supported a traumatic aetiology for most osteochondral lesions of the talus, ranging from 75% to 100% for lateral lesions and 18% to 80% for medial lesions.²⁷ In dogs with LTOC the history of trauma is not always assessed objectively.²⁸ The larger size of the LTOC fragments might explain the faster

progress of DJD in LTOC than in MTOC, because of the increased instability or incongruity of the joint following surgical removal of these larger fragments.²⁹ In the tarsocrural joint the reported incidence of bilateral OC is approximately 50%.^{3,9} Lameness, however, in these cases is said to be rarely symmetrical.^{8, 12, 30} In this study, 30% of the dogs presented with bilateral lesions were bilaterally lame which is more than reported in the literature. In dogs with bilateral defects but unilateral lameness, the lameness was present in the joint with the largest defects. This might be explained by the fact that larger defects cause more incongruity and instability than smaller ones. Lameness is most commonly associated with pain but mechanical alterations may be superimposed. Congruity of a joint is important to assure joint stability, but subluxation, associated with poor joint congruity, induces joint capsule inflammation and stimulation of nociceptors in the joint capsule and ligaments.³¹ In a study in canine shoulder OC, the size of the lesions correlated significantly with the presence of clinical signs of pain and lameness. Clinical lesions were significantly larger than non-clinical lesions.¹⁶ In this study, similar results were found, confirming the importance of the size of joint lesions on lameness. However the radiographic signs of DJD were not significantly different between the clinical and non-clinical lesions. The difference in the associated synovitis could explain the difference in symptoms as well. To conclude, MTOC and LTOC are considered to be different types of tarsocrural joint disease. The numerical values and differences in morphological and clinical features are too different to be from the same disease. Lameness is closely correlated to the size of the TOC defects in the affected tarsocrural joint. Unilateral lameness does not exclude defects in the other tarsocrural joint and investigation of both joints should always be done.

REFERENCES

1. Ekman S, Carlson CS. The pathophysiology of osteochondrosis. *Vet Clin North Am Small Anim Pract* 1998; 28: 17- 32.
2. Olsson SE. Lameness in the dog: A review of lesions causing osteoarthritis of the shoulder, elbow, hip, stifle and hock joints, in *Proceedings* from the American Animal Hospital Association, Cleveland, Ohio, 1975; 42: 363.
3. Montgomery RD, Hathcock JT, Milton JL, et al. Osteochondritis dissecans of the canine tarsal joint. *Comp Cont Ed Pract Vet* 1994; 16: 835-845.
4. Fitch RB, Beale BS. Osteochondrosis of the canine tibiotarsal joint. *Vet Clin North Am Small Anim Pract* 1998; 28: 95-113.
5. Denny HR. Osteochondritis dissecans of the hock joint in the dog. *Vet Annual* 1981; 21: 224-228.
6. Breur GJ, Spaulding KA, Braden TD. Osteochondritis dissecans of the medial trochlear ridge of the talus in the dog. *Vet Comp Orthop Traumatol* 1989; 4: 168-176.
7. Van Ryssen B, van Bree H, Verschooten F: Osteochondritis dissecans of the tarsal joint in the dog: a review. *Vlaams Diergeneesk Tijdsch* 1991; 60: 197-2002.
8. Wisner ER, Berry CR, Morgan JP, et al. Osteochondrosis of the lateral trochlear ridge of the talus in seven Rottweiler dogs. *Vet Surg* 1990; 19: 435-439.
9. Weinstein MJ, Mongil CM, Rhodes WH, et al. Orthopedic conditions of the Rottweiler – Part II. *Comp Cont Ed Pract Vet* 1995; 17: 925-939.
10. Carlisle CH, Robins GM, Reynolds KM. Radiographic signs of osteochondritis dissecans of the lateral ridge of the trochlear talus in the dog. *J Small Anim Pract* 1990; 31: 280-286.
11. Van Ryssen B, van Bree H. Arthroscopic evaluation of osteochondrosis lesions in the canine hock joint: a review of two cases. *J Am Anim Hosp Assoc* 1992; 28: 295-299.
12. Beale BS, Goring RL, Herrington J, et al. A prospective evaluation of four surgical approaches to the talus of the dog used in the treatment of osteochondritis dissecans. *J Am Anim Hosp Assoc* 1991; 27: 221-229.
13. Gielen IM, De Rycke LM, van Bree HJ, et al. Computed tomography of the tarsal joint in clinically normal dogs. *Am J Vet Res* 2001; 62: 1911-1915.
14. Gielen I, van Bree H, Van Ryssen B, et al. Radiographic, computed tomographic and arthroscopic findings in 23 dogs with osteochondrosis of the tarsocrural joint. *Vet Rec* 2002; 150: 442-447.
15. Lotke PA, Ecker ML. Current concept review: Osteonecrosis of the knee. *J Bone Joint Surg* 1988; 70A: 470-473.
16. van Bree H. Evaluation of subchondral lesion size in osteochondrosis of the scapulohumeral joint in dogs. *J Am Vet Med Assoc* 1994; 204: 1472-1474.
17. Berndt AL, Harty M. Transchondral fractures (osteochondritis dissecans) of the talus. *J Bone Joint Surg* 1959; 41A: 988-1020.

18. Baker C L, Morales RW. Arthroscopic treatment of transchondral talar dome fractures: A long-term follow-up study. *Arthroscopy: J Arthrosc Rel Surg* 1999; 15: 197-202.
19. Gielen I, Van Ryssen B, Coopman F, et al. Minimally invasive treatment of canine tarsocrural osteochondritis dissecans: A Long-Term Follow-Up Study of 30 Dogs. *Vet Surg* 2003; Submitted.
20. Aron DN, Mahaffey MB, Rowland GN. Free chondral fragment involving the lateral trochlear ridge of talus in a dog. *J Am Vet Med Assoc* 1985; 186: 1095-1096.
21. Sjöström L, Håkanson N. Traumatic injuries associated with the short collateral ligaments of the talocrural joint of the dog. *J Small Anim Pract* 1994; 35: 163-168.
22. Olsson SE, Reiland S. The nature of osteochondrosis in animals. *Acta Radiol (Suppl)* 1978; 358: 299-306.
23. Douglas G, Rang M. The role of trauma in the pathogenesis of the osteochondrosis. *Clin Orthop* 1981; 158: 28-33.
24. Duthie RB, Houghton CR. Constitutional aspects of the osteochondrosis. *Clin Orthop* 1981; 158: 19-27.
25. Pool RR. Difficulties in definition of equine osteochondrosis, differentiation of developmental and acquired lesions. *Equine Vet J (Suppl)* 1993; 16: 5-12.
26. Canale ST, Belding RH. Osteochondral lesions of the talus. *J Bone Joint Surg* 1980; 62A: 97-102.
27. Stone. Osteochondral Lesions of the Talar Dome. *J Am Acad Orthop Surg* 1996; 4: 63-73.
28. Gielen I, van Bree H. Computerized tomography (CT) compared with radiography in the diagnosis of tarsocrural osteochondrosis of the lateral trochlear ridge in the dog. *Vet Comp Orthop Traumatol* 2003; Accepted.
29. Brinker W, Piermattei D, Flo G. Fractures and other orthopedic injuries of the tarsus, metatarsus and phalanges. In: Brinker W, Piermattei D, Flo G, eds. *Handbook of Small Animal Orthopedics and Fracture Repair*. Philadelphia: WB Saunders Co, 1997; 607-655.
30. Smith MM, Vasseur PB, Morgan JP. Clinical evaluation of dogs after surgical and nonsurgical management of osteochondritis dissecans of the talus. *J Am Vet Med Assoc* 1985; 187: 31-35.
31. Johnston SA. Overview of pain in the lame patient. *Vet Clin North Am Small Anim Pract* 2001; 31: 39-53.

**MINIMALLY INVASIVE TREATMENT OF CANINE TARSOCRURAL
OSTEOCHONDROSIS: A LONG-TERM FOLLOW-UP STUDY OF 30 CASES**

I. Gielen, B. Van Ryssen, F. Coopman, H. van Bree

Department of Medical Imaging, Faculty of Veterinary Medicine,
Ghent University, Salisburylaan 133, Merelbeke, Belgium

Adapted from:

Veterinary Surgery, submitted.

SUMMARY

Objective-To evaluate the long-term results of minimally invasive treatment of tarsocrural osteochondrosis (TOC) in the dog and the application of computed tomographic (CT) findings in the preoperative planning.

Study Design-A retrospective study.

Sample Population-Thirty dogs (32 joints).

Methods-TOC lesions were treated by minimally invasive treatment including arthroscopy or arthroscopically guided mini-arthrotomy. All dogs were clinically evaluated after treatment and radiographs, made prior to and after surgery, were evaluated for degenerative joint disease (DJD).

Results-A follow up study, 9 to 67 months after surgery, revealed excellent to good results in 75% of the cases. Forty-four percent of the treated joints regained full function. The overall success rate of the procedure was not influenced by the type of minimally invasive treatment. Nevertheless, progression of DJD was observed in the majority of treated joints.

Clinical Relevance-On long-term follow-up, results of minimally invasive treatment of TOC surpassed reported results of arthrotomy. CT findings were useful for treatment planning: the puncture sites were determined from the CT mapping and the type of minimally invasive treatment was determined from the size of the defect. Minimally invasive treatment of TOC did not stop the progression of DJD. A high level of pre-operative arthrosis (could) affect the clinical outcome in a negative way.

INTRODUCTION

Although tarsocrural osteochondrosis (TOC) is a well known but uncommon cause of hind limb lameness, it is not an uncommon cause of hock lameness in immature large-breed dogs. TOC represents 9% of all cases of osteochondrosis (OC). Of all joints the tarsocrural joint is the third most commonly affected joint.^{1,2}

The TOC defect involves the medial or the lateral trochlear ridge of the talus and results in instability, pain, lameness, and progressive degenerative joint disease (DJD).²

Treatment options for TOC include conservative treatment (restricted exercise, weight management and medical treatment) and surgery. Surgical treatment consists of TOC fragment removal, with or without curettage of the defect, allowing healing by ingrowing fibrocartilage from the underlying subchondral bone.^{3,4} Fragment removal can be done by arthrotomy,^{1,5,6,7,8} arthroscopy^{9,10} or mini-arthrotomy.⁹

The majority of reports support the idea that dogs with TOC benefit from early surgical removal of the TOC fragment using a minimally invasive technique,^{2,7,8,11} but the prognosis for full use of the affected limb is said to be poor.^{12,13}

Review of cases with long-term evaluation, indicates that lameness may resolve only in 20 to 25 % of the affected dogs, regardless the treatment.^{4,6,7,14,15} The joint function after arthrotomy was improved when compared to conservative treatment,^{1,5,8} but this opinion is not unanimously supported.^{6,7}

The short-term results of arthroscopic treatment look promising,¹⁰ but long-term follow-up studies of large numbers are lacking.

In humans, the arthroscopic treatment for OC defects of the talus is well documented and the long-term results are good to excellent,^{16,17,18} and CT findings are used in preoperative planning and are also helpful in evaluating the follow-up after treatment. By CT the size and location of the lesion can be determined accurately.^{19,20,21,22} In the dog, CT information is helpful to determine the puncture site in arthroscopy and provides accurate information enabling fragment removal in a minimally invasive way.²³

The aims of this study were to determine whether arthroscopic treatment of TOC could be consistently performed in all affected joints. Furthermore, the long-term results after minimally invasive treatment were compared with those reported in the literature after arthrotomy. It was evaluated whether the size of the TOC fragment, as measured on CT,

could determine the type of minimally invasive treatment (arthroscopy or arthroscopically guided mini-arthrotomy). Finally, the possible progression of DJD on follow-up radiographs was evaluated.

MATERIALS AND METHODS

Animals and clinical examination

Thirty dogs (32 joints) (Table 1) with TOC, were included in this study. These dogs were available for follow-up periods longer than 9 months. A questionnaire regarding the status of each dog was available and they were all physically re-examined at the Ghent University. Criteria to be included in this study were a complete radiographic study (including an extended and flexed mediolateral, a flexed dorsoplantar skyline projection, a plantarodorsal and two oblique views), a CT study of both tarsocrural joints (including transverse scans of the tarsocrural region and reconstructions of both talar ridges) and an arthroscopic examination of the clinically affected joints.

Table 1: Breed and sex distribution of 30 dogs with TOC

Breed	Male	Female	Total
Labrador Retriever	4	5	9
Rottweiler	5	3	8
Golden Retriever		3	3
Staffordshire Bull Terrier	1	1	2
Bull Terrier	2		2
Pitbull	1		1
Irish Wolfhound	1		1
Chow Chow	1		1
Kings Poodle	1		1
Beagle	1		1
Belgian Shepherd	1		1
Total	18	12	30

The location of the lesions was classified according to the CT findings, described in a previous study.²³ The CT mapping was used as a guideline to determine the puncture sites. All 32 defects were measured (length, width and depth) using the CT software (Fig 1).

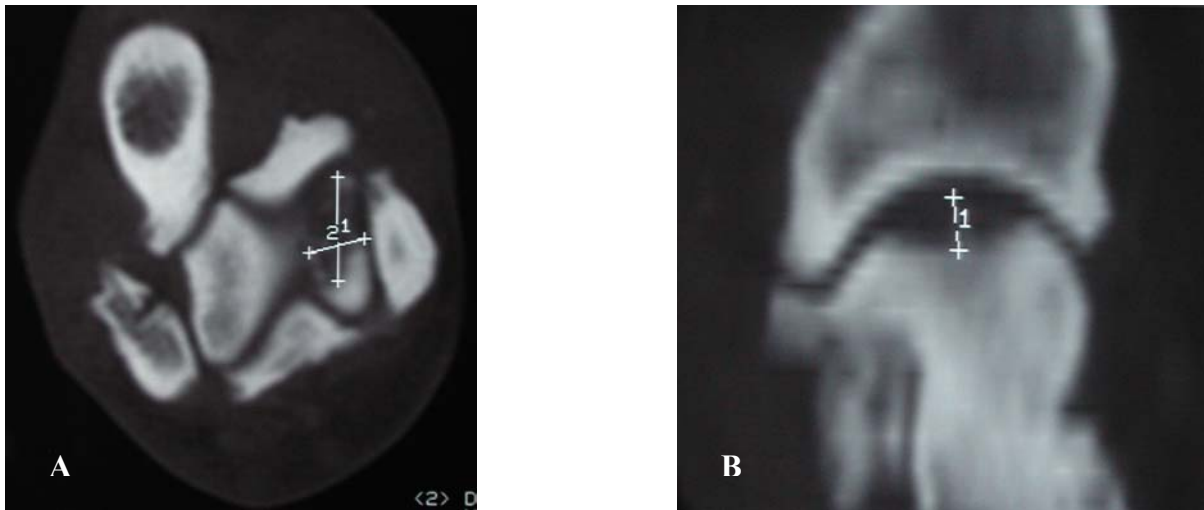


Figure 1. CT measurements:

1A: Transverse CT image through the right tarsocrural joint of a dog with an OCD defect involving the medial tarsal ridge. Using the CT software the length (1) and width (2) of the defect are measured.

1B: Sagittal reconstruction through the medial ridge of the talus of the same joint. On this image the depth (1) of the defect is measured.

After these measurements, the length, depth and width of the defect are multiplied with one another to estimate its volume.

The volume of the defect was estimated by multiplying length, width and depth. In all 32 joints, arthroscopic treatment was attempted by one single surgeon (BVR) using previously described approaches.²⁴ If arthroscopic fragment removal was impossible, the arthroscopic procedure was converted into a mini-arthrotomy and the fragment was removed under arthroscopic guidance as previously described.⁹

During the follow-up examinations, detailed histories were obtained from the owners and referring veterinarians. Special attention was given to the type and amount of exercise by the dog and whether or not lameness was associated with activity.

Functional evaluation of each dog was performed by one single investigator (IG). The patients' functional results were evaluated using a rating scheme that assessed results of a clinical examination (pain, swelling, range of motion), and functional results (postoperative improvement, lameness, and activity) (Table 2). The clinical outcome was graded using a grading scale: 0 = excellent, 1 = good, 2 = fair and 3 = poor. The patient's results were categorised per joint, based on its worst rating in any area.¹⁶

Table 2: Subjective and functional assessment of treatment (modified according to Baker and Morales 1999)

	Excellent (0)	Good (1)	Fair (2)	Poor (3)
Clinical examination				
Pain	None	Mild	Moderate	Severe
Swelling	None/minimal	+	++	+++
Range of motion	No/minimal impaired	mild deficit	moderate def	severe def
Crepitus	Absent	Absent	Present	Present
Muscular atrophy	Absent	Absent	mild	moderate/severe
Functional				
Postoperative improvement	Normal	Greatly improved	Improved	Unchanged/worse
Lameness	None	Slight	Moderate	Severe
Activity	No limits	Minor limits	Moderate lim	Severe limits

NOTE: Patients were assigned a final rating based on the lowest rating in any category

Lameness was assessed during leash walking and a period of unrestricted movement. Pain and presence of crepitus was assessed when manipulating the joint through a normal range of flexion and extension and a range of motion during which the joint was stressed. Tarsal joint range of motion, medial-to-lateral joint stability, and muscular atrophy were subjectively assessed by using the contralateral side for comparison.

The initial and follow-up radiographs of both tarsocrural joints were evaluated for the presence and location of DJD: the presence and size of osteophytes and subchondral sclerosis. The amount of DJD was evaluated using a grading system with normal radiographs for comparison; no evidence of degenerative changes (0), minimal degenerative changes: early osteophyte production and subchondral sclerosis (1), moderate degenerative changes: osteophyte production and bone remodelling (2), severe degenerative changes: excessive osteophyte production and bone remodelling (3) (Fig 2). These evaluations were done by one single examiner (HvB) without any knowledge of the functional outcome.



Figure 2. Degenerative joint disease grading system.

The amount of DJD changes is evaluated; no evidence of degenerative changes (Gr 0), minimal degenerative changes: early osteophyte production and subchondral sclerosis is present (Gr I), moderate degenerative changes: osteophyte production present and bone remodeling apparent (Gr II), and severe degenerative changes: excessive osteophyte production and bone remodeling present (Gr III).

Surgical Technique

The procedure was performed under general anaesthesia. The patients were in supine or lateral position depending on the location of the TOC defect. The puncture sites for the arthroscopic procedure were determined from the CT mapping results. Because many of the lesions were localised in the proximal region the plantar approach was chosen most of the time. A 19-gauge needle was used to distend the joint with 15 ml of fluid before the arthroscope was introduced. A 1.9-mm (Dr. Fritz, Tuttlingen, Germany) or 2.4-mm (Richard Wolf GmbH, Knittlingen, Germany), 30° angled scope was used. Other operative instruments used included a probe, a small-joint grasping forceps, various arthroscopic curettes, and a hand-burr (Richard Wolf GmbH, Knittlingen, Germany). By using a cannula system with a guiding rod (Richard Wolf GmbH, Knittlingen, Germany) to perform the triangulation procedure, the need for multiple punctures was eliminated and soft tissue damage caused by inserting and removing the surgical instruments, was prevented. Diagnostic arthroscopy confirmed the location and stage of the lesion. The findings with regard to the visibility of the fragment determined whether it could be arthroscopically excised or whether a mini-arthrotomy was necessary. Curettage of the remaining subchondral

bed was not performed. In some patients, a partial synovectomy was necessary to improve visualisation. The lesion was explored with a probe to determine the extent of disrupted articular cartilage. When the decision was made to remove the fragment, a probe and various curettes were used to scoop out the lesion. Larger fragments were fractioned using curettes and a hand drill. A small grasping forceps was used to remove the fragment (Fig 3). After completion of the procedure, the joint was thoroughly flushed under pressure and the skin was closed with one or more sutures.

Postoperatively a bandage was applied on the limb for 1 to 4 days, and weight bearing was allowed but restricted to leash exercise for a period of six weeks after surgery. The dog was then turned progressively into full function. Most animals were clinically examined 6 weeks after surgery. The owners were contacted three months and regular times after surgery for a full clinical and radiographic examination.



Figure 3. Arthroscopic image of removal of an TOC fragment using a small grasping forceps.

Statistical analysis

SPSS 10.0 for Windows was used to analyse the data. Correlations between clinical outcome and pre-surgical arthrosis, post-surgical arthrosis and increase in arthrosis were determined. Also the correlations between pre-surgical arthrosis, post-surgical arthrosis and increase in arthrosis were looked for. Relevant differences between the arthroscopic procedure and the mini-arthrotomy were explored by an independent samples t-test (length, width, depth and clinical outcome) or a non-parametric 2 independent samples test (L*W*D). To see whether

the location of the defect (lateral or medial) has an influence on the clinical outcome, an independent samples t-test was performed.

RESULTS

Eighteen of the 30 dogs were male, 12 were female. Their age at initial diagnosis ranged from 5 to 47 months with a mean of 17 months, with 16 dogs older than 12 months. Body weight ranged from 11 to 60 kg with a mean of 30 kg. Duration of lameness at the time of diagnosis ranged from 1 to 24 months with a mean of 5 months. Ten dogs were bilaterally affected but only two of these were bilaterally lame at the time of presentation and bilaterally treated as well. In 25 joints, the lesions were localised on the medial- and in 7 on the lateral talar ridge. The mean follow-up period after initial examination was 34 months (range = 9 to 67 months). All dogs had more than one follow-up examination. The average number of follow-ups was 3.4 (range 2 to 6).

Preoperatively, degenerative changes were present in the majority of the affected joints (24 out of 32). These changes ranged from minimal (17), moderate (6) to severe (1).

Sixteen joints out of 32 could be arthroscopically treated. In 3 out of these 16 joints, a depression of the articular cartilage without real fragments was the only finding. These joints were flushed with 0.9% saline solution. In one of these cases with moderate preoperative DJD, the outcome was only fair. In the two other cases with minimal degenerative changes, the outcome was excellent and good. In one joint the TOC lesion was localised in the distal part of the lateral talar ridge. The 2 fragments were not removed because of their disadvantageous position and they seemed not to interfere with the flexion and extension of the joint as arthroscopically evaluated. This particular dog made an uneventful recovery with a good functional outcome. In the other 12 cases, the fragments could be arthroscopically removed through the instrumental portal.

In 16 out of the 32 joints fragment removal through the surgical portal appeared to be impossible. The instrumental portal was then enlarged and converted into a mini-arthrotomy. The fragments were removed using a grasping forceps, if necessary, under arthroscopic guidance.

The clinical outcome was not influenced by the type of minimally invasive procedure used ($P < 0.05$).

Postoperative complications were not observed in any patient. All dogs were weight bearing the next day and although lameness improved, most dogs were still lame 6 weeks after treatment. The patients returned to full activities at an average of 3 months after surgery. In 5 patients it took 6 to 12 months before they returned to full function of the limb. At an average follow-up period of 34 months, there were 14 excellent, 10 good, 7 fair and 1 poor results. The CT size of the TOC defects ranged from 2 to 7 mm in width (average 4.25) and 8 to 1750 mm³ (average 239 mm³). Significant differences ($p < 0.05$) in width and volume exist between both surgical techniques. When defects with a width of 3.5 mm or smaller and a volume of less than 60 mm³ are diagnosed, arthroscopy is expected to be the best surgical technique. Having defects with widths between 3.5 and 5.0 mm and volumes between 60 and 300 mm³, makes both surgical techniques equally good. With widths of 5.0 mm or more and volumes of 300 mm³ or more, a mini-arthrotomy might be finally necessary.

In 3 dogs, the owner did not consented in follow-up radiographs. In follow-up radiographs of the other 29 affected joints a progression of the degenerative changes in all but 1 dog was observed, regardless the type of minimally invasive treatment. In 10 joints the increase was less than one degree. In 17 joints there was an increase of one degree and in 1, an increase of two. Response to treatment was only fair in the latter.

The correlations indicate clinical outcome to be influenced by the degree of pre-surgical arthrosis ($r = 0.48$; $p < 0.01$), the increase of arthrosis over time ($r = 0.40$; $p < 0.05$) but especially by the degree of post-surgical arthrosis ($r = 0.70$; $p < 0.001$). The higher the degree of pre-surgical arthrosis, the higher the amount of post-surgical arthrosis ($r = 0.78$; $p < 0.001$) and increase of arthrosis over time ($r = 0.51$; $p < 0.01$).

The localisation (lateral or medial) of the TOC defect does not seem to affect the clinical outcome.

DISCUSSION

Diagnostic and therapeutical arthroscopic techniques in dogs for evaluation of the tarsocrural joint have been described.^{24, 10, 11} In the experience of the authors, arthroscopic treatment of TOC lesions is a difficult procedure because of the associated synovitis and the small size of the joint. In this study, only half of the fragments could be visualised well enough to be arthroscopically removed because of the extensive synovial inflammation and/or the disadvantageous position of the fragments. The size of the fragment, assessed by CT, seemed to be the determinant factor for a successful removal. Due to the small size of the tarsocrural joint, it was practically impossible to get a complete overview of the very large fragments (Fig 4).



Figure 4. Arthroscopic image of a large TOC fragment. The fragment is too large to obtain a complete overview making its arthroscopic removal impossible. In this case the arthroscopic procedure is converted into a mini-arthrotomy.

The short-term outcome of arthroscopic treatment of TOC in two dogs has been reported to be excellent¹⁰ and the reported long-term results in these series of cases are encouraging although complete functional healing is less than 50%. In these series, lameness was resolved in 14 out of 32 joints, which means 44% of full recovery. Another 53% improved after minimally invasive treatment and only 3% had a poor outcome. These results are much better than the reported 20% - 25% excellent results.^{4, 6, 7, 14, 15} The overall success of the procedure was not influenced by the type of minimally invasive treatment. In all cases, it was easy to convert the arthroscopic procedure into a mini-arthrotomy if necessary. None of the patients had any post-surgical complication as often reported after arthrotomy.⁷

In humans, however, the reported long-term results are better than in the dog. The overall success rate is about 85% - 90%.^{16, 17, 25} The reason for this difference is probably due to the

fact that these lesions are diagnosed earlier than in the dog. Studies in humans have also shown better results with earlier treatment.²⁷ Another reason could be the different treatment used in humans depending on the stage of the lesions. Stage III and IV lesions are treated with reduction and fixation with absorbable pins in the acute stage²⁵ although long-term studies regarding their outcome are lacking.²⁶ This technique results in less joint incongruity and instability.²⁶ In humans, physiotherapy may be favourable to regain full range of motion and strength.²¹

In these series, stage II to IV fragments were excised, which probably results, in larger fragments, in more incongruity. Fixation of fragments was attempted in the dog but was difficult or even impossible.^{28, 29}

Several complications after tarsal arthrotomy have been reported.^{6, 7} Performing a medial malleolus osteotomy to improve visualisation of the lesions, might increase post-surgical instability.⁶ Disruption of the medial collateral ligament complex following an arthrotomy could create post-surgical instability as well.⁶ In the elbow, experimental work has proved that any arthrotomy technique results in various degrees of joint instability, increasing the risk of progressive DJD.³⁰ There is some evidence that the arthrotomy procedure itself creates degenerative changes within a sound joint.³¹ These negative effects are probably minimised with arthroscopy.

In humans, associated treatments of the TOC lesions including shaving, drilling, debridement and micro-fracture technique have been described.^{25, 32} In this study, the lesions were only thoroughly lavaged because the merits of all these other techniques are still questioned³² and could further compromise joint congruity and stability.

In the majority of the treated joints (95%), degenerative changes progressed in time despite the minimally invasive treatment. Although the majority of dogs in this study had improved limb function and were considered to have good to excellent results, most of the joints used in this study showed an increase in number and size of osteophytes. These changes were also reported in the literature when the joints were treated via arthrotomy.^{6, 7} In most instances, even with a maximal functional healing, some degree of DJD or osteoarthritis (OA) will develop after surgical treatment.^{33, 34} Contrary to other studies,^{6, 7} the amount of DJD was related to the function of the affected joints in this study. In these series, the prognosis was influenced by the pre-surgical arthrosis. A prognosis for an individual patient is difficult. Although osteophyte formation is not necessarily a sign of degenerative changes in the joint

cartilage, it is used routinely as a major criterion for diagnosis and progression of osteoarthritis.^{35, 36, 37} Degenerative changes measured as the size of osteophytes or increased subchondral bone density are known to correlate poorly with cartilage and synovial changes.^{38, 39} The development of osteophytes is often explained as a defensive mechanism to instability; by increasing the joint surface the pressure on the joint will decrease.⁴⁰ This might be possible in TOC, after the removal of larger fragments and a subsequent increase of osteophytosis.

Arthroscopic treatment, unlike any other treatment, will not transform an abnormal joint into a completely normal one. Progressive joint deterioration as seen in this (and other studies) implies that the surgical or arthroscopic procedure does not restore normal joint function or that the pathological process(es) that initially contributed to the disease still were active. It is suggested that increase of degenerative changes after treatment may not be purely biomechanical in origin, but also biochemical. The results in one study reveal a persistent and evolving disturbance in cytokine and keratan sulphate profiles within the anterior cruciate ligament-deficient knee, suggesting an important biochemical dimension to the development of osteoarthritis there.⁴¹

It may be worthwhile to treat these dogs post-surgically with carprofen. In an OA dog model treated with carprofen, a reduction of osteophytes, a decrease of cartilage lesions, and reduction in the remodelling of subchondral bone were observed.⁴²

CT enables a detailed examination of the tarsocrural joint surface⁴³ and determination of the exact location, the size and number of all TOC fragments.²³ These CT findings were useful for treatment planning to choose the puncture site. The information concerning the number of fragments allowed verifying that all fragments were removed. The size of the lesion allowed choosing the type of minimally invasive technique to be used in an individual case.

It can be concluded that minimally invasive treatment of TOC lesions is technically feasible and a better option than arthrotomy because of a better long-term prognosis. As in humans, the CT findings can be used for treatment planning, for the choice of the puncture sites and the type of minimally treatment. In most cases, degenerative joint disease will continue to progress and can interfere with functional healing. In a high degree of pre-operative arthrosis, clinical outcome may be disappointing, but this finding is not consistent.

REFERENCES

1. Montgomery RD, Hathcock JT, Milton JL, et al: Osteochondritis dissecans of the canine tarsal joint. *Compend Cont Educ Pract Vet* 16: 835-845, 1994
2. Fitch RB, Beale BS: Osteochondrosis of the canine tibiotarsal joint. *Vet Clin North Am: Small Anim Pract* 28: 95-113, 1998
3. Olsson SE: Osteochondrosis in the dog, in Kirk RW (ed): *Current veterinary therapy VII*. Philadelphia, PA, Saunders, 1980, pp 807-815
4. Olson NC, Mostosky UV, Flo GL, et al: Osteochondritis dissecans of the tarsocrural joint in three canine siblings. *J Am Vet Med Assoc* 176: 635-637, 1980
5. Johnson KA, Howlett CR, Pettit GD: Osteochondrosis in the hock joints in dogs. *J Am Anim Hosp Assoc* 16: 103-113, 1980
6. Smith MM, Vasseur PB, Morgan JP: Clinical evaluation of dogs after surgical and nonsurgical management of osteochondritis dissecans of the talus. *J Am Vet Med Assoc* 187: 31-35, 1985
7. Breur GJ, Spaulding KA, Braden TD: Osteochondritis dissecans of the medial trochlear ridge of the talus in the dog. *Vet Compar Orthop Traumatol* 4: 168-176, 1989
8. Beale BS, Goring RL, Herrington J, et al: A prospective evaluation of four surgical approaches to the talus of the dog used in the treatment of osteochondritis dissecans. *J Am Anim Hosp Assoc* 27: 221-229, 1991
9. van Bree H, Van Ryssen B: Diagnostic and Surgical Arthroscopy in Osteochondrosis Lesions. *Vet Clin North Am Small Anim Pract* 28: 161-189, 1998
10. Cook J L, Tomlinson M R, Stoll D T, et al: Arthroscopic removal and curettage of osteochondrosis lesions on the lateral and medial trochlear ridges of the talus in two dogs. *J Am Anim Hosp Assoc* 37: 75-80, 2001
11. Van Ryssen B, van Bree H: Arthroscopic evaluation of osteochondrosis lesions in the canine hock joint: a review of two cases. *J Am Anim Hosp Assoc* 28: 295-299, 1992
12. Smith, CW: Osteochondrosis in the dog - Diagnosis, Treatment, and Prognosis. *Canine Pract* 16: 15-22, 1991
13. Bloomberg MS, Lewis DD: Osteochondrosis of sporting and working dogs, in Bloomberg MS, Dee JF and Taylor RA (eds): *Canine sports medicine and surgery*. Philadelphia, PA, Saunders, 1998, 234-250.
14. Rosenblum GP, Robins GM, Carlisle CH: Osteochondritis dissecans of the tibio-tarsal joint in the dog. *J Small Anim Pract* 19: 759-767, 1978
15. Mason RA, Lavelle RB: Osteochondritis dissecans of the tibial tarsal bone in dogs. *J Small Anim Pract* 20: 423-432, 1979
16. Baker C L, Morales RW: Arthroscopic treatment of transchondral talar dome fractures: A long-term follow-up study. *Arthroscopy: J Arthrosc Rel Surg* 15: 197-202, 1999
17. Tol JL, Struijs PA, Bossuyt PM, et al: Treatment strategies in osteochondral defects of the talar dome: a systematic review. *Foot Ankle Int* 21: 119-126, 2000
18. Schuman L, Struijs PA, van Dijk CN: Arthroscopic treatment for osteochondral defects of the talus. Results at follow-up at 2 to 11 years. *J Bone Joint Surg Br* 84: 364-368, 2002

19. Zinman C, Reis ND: Osteochondritis dissecans of the talus: use of the high resolution Computed Tomography Scanner. *Acta Orthop Scand* 53: 697-700, 1982
20. Zinman C, Wolfson N, Reis ND: Osteochondritis dissecans of the dome of the talus. Computed tomography scanning in diagnosis and follow-up. *J Bone Joint Surg Am* 70: 1017-1019, 1988
21. Ogilvie-Harris DJ, Sarrosa EA: Arthroscopic treatment of osteochondritis dissecans of the talus. *Arthroscopy: J Arthrosc Rel Surg* 15: 805-808, 1999
22. Stroud CC, Marks RM; Imaging of osteochondral lesions of the talus. *Foot Ankle Clin* 5: 119-133, 2000
23. Gielen I, van Bree H, Van Ryssen B, et al: Radiographic, computed tomographic and arthroscopic findings in 23 dogs with osteochondrosis of the tarsocrural joint. *Vet Rec* 150: 442-447, 2002
24. Van Ryssen B, van Bree H, Vyt Ph: Arthroscopy of the canine hock joint. *J Am Anim Hosp Assoc* 29: 107-115, 1993
25. Simpson MB: Talar osteochondral injuries in athletes. *Operat Techn Sports Med* 9: 8-13, 2001
26. Farmer JM, Martin DF, Boles CA, et al: Chondral and osteochondral injuries. Diagnosis and management. *Clin Sports Med* 20: 299-320, 2001
27. Pettine KA, Morrey BF: Osteochondral fractures of the talus. *J Bone Joint Surg Br* 69: 89-92, 1987
28. Aron DN, Mahaffey MB, Rowland GN: Free chondral fragment involving the lateral trochlear ridge of the talus in a dog. *J Am Vet Med Assoc* 186: 1095-1096, 1985
29. van Ee RT, Gibson K, Roberts ED: Osteochondritis dissecans of the lateral ridge of the talus in a dog. *J Am Vet Med Assoc* 193: 1284-1286, 1988
30. Suess RP, Trotter EJ, Konieczynski D, et al: Exposure and postoperative stability of three medial surgical approaches to the canine elbow. *Vet Surg* 23: 87-93, 1994
31. Järvinen M, Jozsa L, Johnson RJ, et al: Effect of anterior cruciate ligament reconstruction with patellar tendon or prosthetic ligament on the morphology of other ligaments of the knee joint. An experimental study in dogs. *Clin Orthop Rel Res* 311: 176-181, 1995
32. Hunziker EB: Articular cartilage repair: basic science and clinical progress. A review of the current status and prospects. *Osteoarthr Cartil* 10: 432-463, 2001
33. Roy R, Wallace L, Johnston G, et al: A retrospective evaluation of stifle osteoarthritis in dogs with bilateral medial patellar luxation and unilateral surgical repair. *Vet Surg* 21: 475-479, 1992
34. Vasseur P, Berry C: Progression of stifle osteoarthritis following reconstruction of cranial cruciate ligament in 21 dogs. *J Am Anim Hosp Assoc* 28: 129-136, 1992
35. Kellgren J, Lawrence J: Radiological assessment of osteoarthritis. *Ann Rheum Dis* 16: 494-501, 1957
36. Bennet D, Tennant B, Lewis DG, et al: A reappraisal of anterior cruciate ligament disease in the dog. *J Small Anim Pract* 29: 275-297, 1988
37. Widmer WR, Buckwalter KA, Braunstein EM, et al: Radiographic and magnetic-resonance-imaging of the stifle joint in experimental osteoarthritis of dogs. *Vet Radiol Ultrasound* 35: 371-383, 1994
38. Reichel H, Hein M: Histologic changes of cartilage and subchondral bone in varus gonarthrosis: comparison with radiographic and macroscopic findings, in Grifka J, Ogilvie-Harris DJ (eds): *Osteoarthritis*. Berlin, Heidelberg, New York, NY, Springer-Verlag, 2000, pp 82-92

-
39. Muehleman C, Berzins A, Koepf H, et al: Bone density of the human talus does not increase with the cartilage degeneration score. *Anat Rec* 266: 81-86, 2002
 40. Sokoloff L: The pathology of osteoarthritis and the role of ageing, in Nuki G (ed): *The aetiopathogenesis of osteoarthritis*. Tunbridge Wells, Kent, Pitman, 1980, pp 1-15
 41. Cameron M, Buchgraber A, Passler H, et al: The natural history of the anterior cruciate ligament-deficient knee. Changes in synovial fluid cytokine and keratan sulfate concentrations. *Am J Sports Med* 25: 751-754, 1997
 42. Pelletier JP, Lajeunesse D, Jovanovic DV, et al: Carprofen simultaneously reduces progression of morphologic changes in cartilage and subchondral bone in dog osteoarthritis. *J Rheumatol* 27: 2893-2902, 2000
 43. Gielen I, De Rycke L, van Bree H, et al: Computed tomography of the tarsal joint in clinically normal dogs. *Am J Vet Res* 62: 1911-1915, 2001

**THE VALUE OF COMPUTED TOMOGRAPHY IN THE CLINICAL COURSE
OF CANINE TARSOCRURAL OSTEOCHONDROSIS**

I. Gielen, H. van Bree, F. Coopman, B. Van Ryssen

Department of Medical Imaging, Faculty of Veterinary Medicine,
Ghent University, Salisburylaan 133, Merelbeke, Belgium

Adapted from:

I. Gielen, H. van Bree, B. Van Rijssen, F. Coopman. Prognostic value of CT findings in minimally invasive treatment of tarsocrural OCD in the dog. Abstract 9th Annual Conference EAVDI (European Association of Veterinary Diagnostic Imaging). 24-27th July 2002, Archena (Murcia), Spain. p 75.
Veterinary Radiology & Ultrasound 2003; 44: p 253.

SUMMARY

Objective- To evaluate whether clinical data of the affected animals (age, gender, weight, duration of symptoms, and number of affected joints) and morphological data of the lesions obtained by computed tomography CT (size, site, location, “Berndt and Harty” classification, and number of fragments) can be used to predict long-term functional outcome (excellent, good, fair or poor) after minimally invasive treatment of tarsocrural osteochondrosis (TOC).

Animals- Thirty-two joints (30 dogs) with clinical TOC were considered.

Procedure- All clinical data of these 30 dogs were registered. All 32 TOC defects were measured (length, width and depth) using the CT software. Similar to a method used in humans, the volume (= length x width x depth) and surface (= length x width) were used to compare the size of the different defects. The radiographs of all treated tarsocrural joints were evaluated pre- and post-treatment for the presence and amount of degenerative joint disease (DJD) changes. The correlation between the functional outcome and the clinical and morphological data of the medial (MTOC) and lateral (LTOC) TOC lesions was statistically evaluated.

Results- No significant correlation has been found between the clinical data and the functional outcome of the treated animals, but the size of the clinical lesions has an influence on the long long-term prognosis. Larger lesions tend to give worse long-term results. Although it remains difficult to predict the functional outcome for each individual dog, significant differences have been found between an acceptable outcome (excellent or good) and an unacceptable outcome (fair or poor) in MTOC, and between an excellent and a good clinical outcome in LTOC. The results also indicate that an unacceptable clinical outcome may be caused by post-surgical arthrosis.

Conclusions and Clinical Relevance- Besides the fact that CT can help in the diagnosis of TOC and in the planning of treatment for TOC lesions, the technique can also be used to predict a long-term acceptable functional outcome more accurately.

INTRODUCTION

Osteochondrosis (OC) has been defined as a disturbance in the ossification of articular or physal cartilage into subchondral bone, due to genetic and environmental (trauma, nutrition) factors. As a consequence, the cartilage thickens and the deeper layers are not sufficiently nourished and become weaker. This stage is called “osteochondrosis” (OC), and is usually not accompanied by lameness. When a flap or fragment is formed, clinical signs are usually present, and from this stage on the affection is called “osteochondritis dissecans” (OCD).^{1,2,3} Although several confusing synonyms for this disease have been used in the literature – including osteochondritis dissecans, osteochondrosis dissecans, and dyschondroplasia – the term osteochondrosis (OC) is the most widely accepted term in both the veterinary and human literature (Ekman & Carlson 1998).

In the dog, tarsocrural osteochondrosis (TOC) is a well-known but uncommon cause of hind limb lameness: it comprises 9% of all OC cases. The tarsocrural joint is the third most commonly affected joint.^{4,5,6} Approximately 50% of reported cases of TOC are bilateral.^{4,7} The TOC defect can involve the medial or lateral trochlear ridge of the talus and results in instability, pain, lameness, and progressive degenerative joint disease (DJD).⁶ Both conservative and surgical (arthrotomy) management of TOC have been recommended.^{8,9,10,11,12} Review of the cases reported, which contain long-term (> 2 months) evaluation, indicates that joint lameness may resolve in less than 20% of the affected dogs, regardless of the therapeutic modality chosen.^{10,11,13,14,15,16,17} Recently, arthroscopic treatment of these lesions has yielded promising short-term¹⁸ and long-term¹⁹ results. Although the results of minimally invasive treatment of TOC are better than those of treatment by arthrotomy, the chances for full return to function remain less than 50%.¹⁹ Any affected dog is considered to be a poor candidate for any type of work.²⁰ Therefore, it would be beneficial if the functional outcome could be predicted for the individual patient, thus managing the expectations of the owner. Besides the type of surgical therapy, many factors affect the prognosis of TOC, including the age of the dog, the size and location of the TOC defect, post-surgical joint stability, the number of joints affected, the presence of degenerative joint disease, and the timing of surgical treatment.⁴

6, 20, 10, 11, 12. However, the influence of all these factors has not yet been scientifically or statistically evaluated in a group of patients.

In humans, CT findings are used in pre-operative planning, for an accurate determination of the size and location of the lesion^{21, 22, 23}, and for evaluating the follow-up after treatment.²⁴ In the dog, previous studies have shown that CT enables a detailed examination of the tarsocrural joint surface,²⁵ assesses the exact size, location and number of the OC fragments,²⁶ and can be used for treatment planning.¹⁹ In addition, a four-stage classification system comparable to the one used for humans, called the “Berndt and Harty” classification,²⁷ has been established for the dog.²⁶ For humans, this classification system has been used for treatment planning.^{28, 29}

The aim of this study is to see whether clinical data of the affected animals (age, gender, weight, duration of symptoms, and number of affected joints) and morphological data of the lesions obtained by CT (size, site, location, “Berndt and Harty” classification, and number of fragments) can be used to predict long-term functional outcome (excellent, good, fair or poor).

MATERIAL AND METHODS

Data-collection

Thirty-two joints (30 dogs) with clinical TOC were used for this retrospective study. Only clinical TOC lesions were treated using minimally invasive surgery (arthroscopy or mini-arthrotomy) and all dogs were available for a follow-up period of more than 9 months. Clinical data (age, gender, weight, duration of clinical symptoms) from these 30 dogs were registered. A questionnaire regarding their physical status was available for all the dogs, and they were all re-examined at Ghent University at different time intervals. All dogs had more than one follow-up examination (2 to 6). The patients’ functional outcome was evaluated using a rating scheme that assessed the results of a clinical examination (pain, swelling, range of motion), and the functional results (post-operative improvement, lameness, and activity). The results of their functional outcome (excellent, good, fair or poor) have been published elsewhere.¹⁹

In addition to adequately documented clinical records and a radiographic examination pre- and post-treatment, a CT study of the clinically affected tarsocrural joints (including transverse scans of the tarsocrural region and reconstructions of both talar ridges) was required for this report. The location of the lesions was classified according to the CT findings, as described in a previous study.²⁶ To describe the exact location of the tarsocrural lesions, a map was used in which the medial and lateral trochlear ridges were divided into a proximal, a dorsal, and a distal area. Each area was subdivided into a medial (or lateral) and a central area. If a lesion involved both medial (or lateral) and central areas, it was considered to be presenting total ridge involvement. Using this mapping system, a lesion could be located at 18 different locations.²⁶

All 32 clinical defects were measured – length (L), width (W), and depth (D) – using the CT software. The surface (= length x width) and volume (= length x width x depth) were used to compare the sizes of the various defects. Similar to a method used in humans³⁰ and in a previous study,³¹ all measurements were related to the cross-section of the talus, just below the ridges. This allows dogs of various body weights and sizes to be compared. This new set of data is referred to as relative length (L-rel), relative width (W-rel), relative depth (D-rel), relative surface (Surf-rel), and relative volume (Vol-rel).

Depending on the status of the trochlear ridge and the associated fragment, the lesions were also classified using a four-stage classification system. This system, comparable to the one used in humans (the “Berndt and Harty” classification), has been published previously.^{26, 27} The number of visible fragments on CT was recorded as well.

The initial and follow-up radiographs of both tarsocrural joints were evaluated for the presence and amount of DJD changes. The radiographic signs evaluated were the presence and size of osteophytes and subchondral sclerosis. DJD changes were evaluated using a subjective grading system (used previously¹⁹) ranging from 0 to 3. Subjective assessment of osteophyte formation and subchondral sclerosis, using normal radiographs for comparison, was completed by one of the investigators (HvB) without knowledge of the functional outcome.

Statistical analysis

SPSS 11.0 for Windows was used to explore and analyze the data from this study.

Because medial and lateral OC are different types of disorders,³¹ the data set was split in two. The means, standard deviations, and ranges of all traits were calculated for the various clinical outcomes. A univariate analysis was used to see whether traits (alone or combined) could significantly predict the clinical outcome.

For the group of **medial TOC** (MTOC), an independent samples Student T-test was used to see whether the excellent outcome group differed from the non-excellent (= good, fair, poor) outcome group and to find differences between the acceptable (= excellent and good) outcome group and the non-acceptable (= fair and poor) outcome group. This was done because, in some cases (especially in working dogs), the clinician must be able to predict an excellent outcome. In some cases (companion dog), an excellent to good outcome is acceptable to the owner. Most owners consider a fair or poor outcome to be non-acceptable.

For the group of **lateral TOC** (LTOC), a 2 independent samples test (non-parametric) was used in order to find significant differences between excellent and good clinical outcomes. Looking at the overall ranges for the significantly different traits, strict border values as well as sub-ranges were sought for the various clinical outcomes for both MTOC and LTOC.

RESULTS

Twelve of the 30 dogs were female. Their age at the time of diagnosis ranged from 5 to 47 months with a mean of 17 ± 12 months. Body weight ranged from 11 to 60 kg with a mean of 30 ± 13 kg. Duration of lameness ranged from 1 to 24 months with a mean of 5 ± 5 months. The mean follow-up period was 34 ± 18 months (range = 9 to 67 months) and the average number of follow-ups was 3.4 (range = 2 to 6). In 25 joints, the lesions were localised on the medial talar ridge; and in 7 joints, on the lateral talar ridge (Table 1). Fifteen out of 25 medial lesions were localised proximally (Fig 1) and 10 dorsally (Fig 2).

No lesions were found at the distal part. Five out of the 7 lateral OC lesions were localised proximally, 1 dorsally and 1 distally.

Table 1: Detailed CT location of 32 TOC lesions in 30 dogs.

LOCATION	Medial		Lateral		
Proximo-medial	5		Proximo-lateral	4	<u>Proximal 20</u>
-central	5		-central	0	
-total ridge	5		-total ridge	1	
Dorso-medial	5		Dorso-lateral	1	<u>Dorsal 11</u>
-central	4		-central	0	
-total ridge	1		-total ridge	0	
Disto-medial	0		Disto-lateral	0	<u>Distal 1</u>
-central	0		-central	0	
-total ridge	0		-total ridge	1	
TOTAL	25		7		32

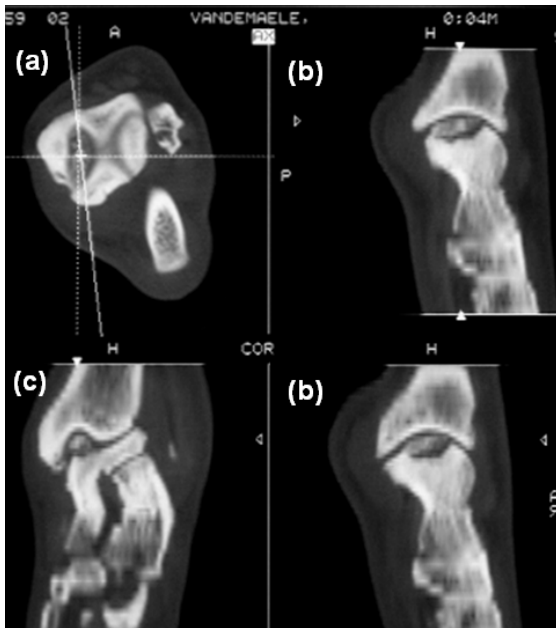


Figure 1: Transverse (a), sagittal (b), and dorsal (c) images of a tarsocrural OC lesion located in the proximal area of the medial trochlear ridge.

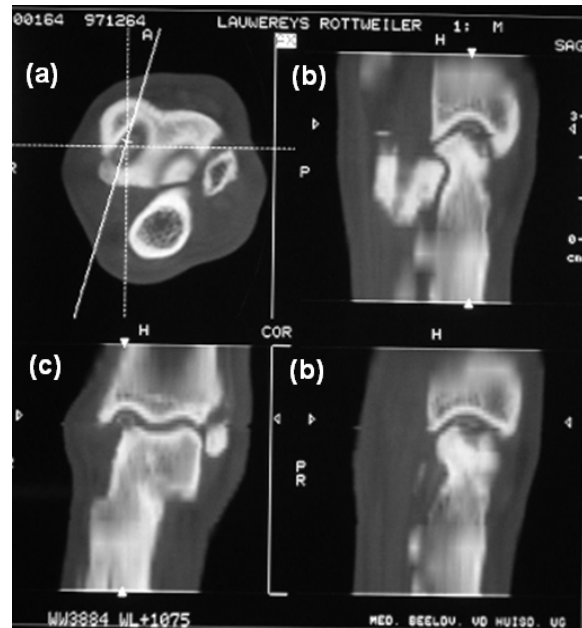


Figure 2: Transverse (a), sagittal (b), and dorsal (c) images of a tarsocrural OC lesion located in the dorsal area of the medial trochlear ridge.

Medial TOC

In Table 2, the characteristics of the clinical and morphological traits for the four different clinical outcomes are listed. The univariate analysis shows that length, surface, D-rel and W-rel of the defect influence the clinical outcome significantly ($p < 0.05$). In addition, the degree of arthrosis after the treatment influences the outcome significantly ($p < 0.001$). The post-treatment arthrosis itself is influenced significantly ($p < 0.05$) by the volume of the defect and the degree of the arthrosis before the treatment. No indications were found to explain why more or less pre-treatment arthrosis is seen. Predicting clinical outcome from one significant predictor (or even a combination of several significant predictors) is not reliable.

Table 2: Characteristics of the clinical and morphological traits for the various clinical outcomes of MTOC (n = 25).

FUNCTIONAL OUTCOME:	Excellent (0)	Good (1)	Fair (2)	Poor (3)
	Mean \pm SD	Mean \pm SD	Mean \pm SD	Mean \pm SD
Age (Months)	19.91 \pm 12.25	12.00 \pm 3.08	28.25 \pm 20.54	13.00 \pm 9.64
Weight (Kg)	29.45 \pm 8.32	18.6 \pm 5.50	35.00 \pm 9.62	34.00 \pm 3.46
Lameness (Months)	6.91 \pm 6.56	2.80 \pm 1.78	7.5 \pm 5.9	3.33 \pm 2.51
Pre-surgical arthrosis (0-3)	0.73 \pm 0.46	1.20 \pm 0.20	1.75 \pm 0.95	0.67 \pm 1.15
Post-surgical arthrosis (0-3)	1.18 \pm 0.40	1.40 \pm 0.54	2.75 \pm 0.50	2.33 \pm 1.15
L (mm)	5.36 \pm 2.58	5.40 \pm 2.79	6.25 \pm 0.5	10.33 \pm 2.88
W (mm)	3.82 \pm 1.53	3.40 \pm 1.34	4.00 \pm 0.81	5.67 \pm 1.15
D (mm)	4.00 \pm 1.00	3.80 \pm 1.48	5.50 \pm 1.29	5.67 \pm 1.15
Surface (mm ²)	23.55 \pm 17.94	21.20 \pm 15.84	25.25 \pm 7.08	59.67 \pm 24.50
Volume (mm ³)	105 \pm 89.23	94.80 \pm 82.36	141 \pm 58.07	354.33 \pm 211.79
L-rel	26.46 \pm 12.58	30.40 \pm 15.75	31.75 \pm 3.77	44.33 \pm 12.89
W-rel	19.18 \pm 6.82	19.20 \pm 7.46	20.00 \pm 1.1	24.33 \pm 3.21
D-rel	20.27 \pm 5.72	21.4 \pm 8.73	27.50 \pm 5.50	26.33 \pm 2.8
Surf-rel	1.15 \pm 0.82	1.18 \pm 0.89	1.24 \pm 0.15	2.53 \pm 0.93
Vol-rel	5.16 \pm 4.06	5.34 \pm 4.75	6.85 \pm 1.79	14.92 \pm 8.03
Number of fragments	1.73 \pm 1.10	1.60 \pm 1.14	1.00 \pm 1.41	2.67 \pm 0.57

The excellent outcome group does not differ significantly from the non-excellent outcome group. The acceptable outcome group differs significantly ($p < 0.05$) from the non-acceptable outcome group for length, surface, depth, volume, D-rel and Vol-rel. Border values, drawing a strict line between acceptable and non-acceptable, were not found. An acceptable outcome is very likely when the defect has a length of 5 mm or less,

a surface of 17 mm² or less, a depth of less than 4 mm, a volume 89 mm³ or less, a D-rel of 20 or less, and a Vol-rel of less than 5.05. A non-acceptable outcome is very likely when $L > 9$ mm, $D > 6$ mm, surface > 56 mm², volume > 280 mm³, D-rel > 35 , and Vol-rel > 12.17 . For the values between these minimum and maximum values, clinical outcome can be either acceptable or non-acceptable. Three sub-ranges can therefore be identified.

Lateral TOC

The characteristics of the clinical and morphological traits for the excellent and good clinical outcomes are listed in Table 3.

Table 3: Characteristics of the clinical and morphological traits for the various functional outcomes of LTOC (n = 7).

FUNCTIONAL OUTCOME:	Excellent (0) Mean ± SD	Good (1) Mean ± SD
Age (Months)	9.50 ± 2.38	10.00 ± 3.46
Weight (Kg)	27 ± 6.272	49.00 ± 19.05
Lameness (Months)	1.5 ± 0.57	3 ± 1.73
L (mm)	7.75 ± 4.64	19.67 ± 9.23
W (mm)	5 ± 2.16	6.33 ± 1.15
D (mm)	7 ± 2.70	9 ± 1.73
Surface (mm²)	44.25 ± 31.67	131.67 ± 75.05
Volume (mm³)	364 ± 273.35	1271.67 ± 828.49
L-rel	38.25 ± 21.93	84.33 ± 34.06
W-rel	25 ± 10.36	27.67 ± 2.30
D-rel	35 ± 12.08	39.67 ± 4.04
Surf-rel	2.18 ± 1.55	5.6 ± 2.9
Vol-rel	17.89 ± 13.37	53.86 ± 33
Number of fragments	1.5 ± 0.57	1.67 ± 0.57

The clinical outcome was fair in only one case. No poor outcome was seen in this type of TOC. No specific predictors of the clinical outcome were found. No significant differences in the mean between excellent and good were seen.

No strict borderlines between excellent and good are available – there is a clear overlap. Nevertheless, focusing on the traits L, volume, L-rel, Surf-rel, and Vol-rel, it is obvious that the larger the defect the less positive the clinical outcome may be. For body weight

and duration of clinical symptoms, larger values are also seen for the worst clinical outcome.

DISCUSSION

Although it has been reported that the results of minimally invasive treatment of canine TOC lesions are better than those of treatment by classic arthrotomy, the long-term results are not as good as in humans. Less than 50% of the treated animals regain full function of the affected limb¹⁹ – which is much less than the 85% to 90% reported in humans.^{28, 32, 33} The aim of this study was to see whether clinical data of the affected animals (age, gender, weight, duration of symptoms, and number of affected joints) and morphological data of the lesions obtained by CT (size, site, location, “Berndt and Harty” classification, and number of fragments) can be used to predict long-term functional outcome (excellent, good, fair or poor).

In this study, no significant correlation has been found between the clinical data (age, gender, weight, duration of symptoms, and number of affected joints) and the functional outcome of the treated animals. These results contradict the statements of other authors, who cite many clinical data that could have an influence on the eventual functional outcome.^{16, 17, 10, 11, 12}

This leads us to several conclusions:

- First of all, adult animals can be treated successfully as well. This is important, because more than half of the animals are older than 12 months of age,¹⁹ an observation also made by others.⁴
- Secondly, bilaterally affected dogs do not have a worse prognosis than unilaterally affected dogs, and chronically lame animals can be successfully treated as well using minimally invasive techniques.

It has been shown in a previous study that the size of MTOC lesions correlates with symptoms of pain and lameness and that clinical lesions are significantly larger than non-clinical lesions.³¹ The results of the present study show that the size of the clinical lesions has an influence on the long-term prognosis. Although some morphologic data obtained

by CT have a significant influence on the functional outcome, it remains difficult to predict the functional outcome for each individual dog. However, the significant differences found in MTOC between an acceptable outcome (excellent or good) and a non-acceptable outcome (fair or poor) and the different ranges in LTOC for excellent and good clinical outcomes show that the sizes of the initial lesions have an influence on the long-term prognosis. Larger lesions tend to give worse long-term results. Deciding whether a patient should be treated or not can be simplified with the help of the defined sub-ranges (the figures presented in Tables 2 and 3) and the degree of pre-treatment arthrosis. Furthermore, the owner can be informed more accurately about the clinical outcome.

There seems to be a difference in clinical outcome between MTOC and LTOC:

- A defect on the medial ridge, having a volume of 588 mm³ or more, is very likely to have a poor outcome; but when the defect is located on the lateral ridge, an excellent outcome is still possible.
- For a defect with a length of 12 mm or more in MTOC, a potentially poor outcome is expected; whereas in LTOC the outcome is most often excellent.
- Heavier dogs seem less likely to have an excellent outcome in LTOC, whereas in MTOC this makes no difference.

These observations confirm the assertion that MTOC and LTOC are different disorders and should be handled differently, also when predicting possible long-term clinical outcome.

A poor clinical outcome may also be the consequence of progressive post-treatment arthrosis. Neither surgical treatment via arthrotomy^{11, 12} nor via minimally invasive treatment¹⁹ seems to stop the progression of DJD. Because post-treatment arthrosis correlates significantly with pre-treatment arthrosis, it is logical to conclude that affected animals should be treated as soon as possible, preferably before the development of DJD. Studies in humans have also shown better results with earlier treatment.³⁴ Furthermore, post-surgical treatment – with carprofen or another anti-inflammatory drug proven to slow down degenerative joint changes.³⁵ – should also be considered, especially for dogs with large defects. Post-surgical treatment could influence the long-term functional outcome in a positive way.

The significant correlation between the volume of the defect and the post-surgical arthrosis is a logical finding, because large defects are likely to produce joint incongruity and instability.^{29, 36} Congruity of a joint is important to assure joint stability. Poor joint congruity causes tension in, or pressure on, the joint capsule, resulting in pain and lameness.³⁷ Although there are differing views concerning curettage of the lesions after fragment removal,^{4, 6, 9, 10, 16, 17, 18, 20} the results of this study lead to the conclusion that curettage of the defects should be avoided, because this increases the size of the post-surgical defect and, consequently, results in even more incongruity³⁶ and post-surgical arthrosis. The ideal treatment would be a technique that restores joint congruity or at least minimises post-surgical incongruity. In general, only removal of the TOC fragments is considered in the treatment of dogs, although fixation of larger OC fragments has been performed experimentally.³⁸ Several authors claim that the re-attachment of OC fragments would be preferable to removal^{12, 14, 39, 40} – especially when the lateral talar ridge is involved.⁴¹ Re-attachment of these fragments may be less successful because of degenerative changes in the fragment and an imperfect “fit” of the fragment in the subchondral bone defect.¹¹ In humans, “Berndt and Harty” Stage III and IV lesions are treated with reduction and fixation with absorbable pins in the acute stage.²⁸ This technique, when successful, should result in less joint incongruity and instability.²⁹ Unfortunately, long-term studies regarding their outcome are as yet lacking.²⁹ It has been shown in humans that there is a lack of correlation between the radiographic appearance of the lesions and the quality of the overlying cartilage, as well as the extension of the osseous defect.⁴² Therefore, CT or MRI data are used for proper treatment planning.^{21, 43} In the dog as well, the benefit of the use of CT in the diagnosis and treatment of TOC lesions has been proven. Besides the fact that CT can help in the diagnosis of lateral tarsocrural OD⁴⁴ and the treatment planning of TOC lesions,^{19, 26} the technique can also be used to predict a long-term acceptable functional outcome more accurately.

REFERENCES

1. Olsson SE, Reiland S. The nature of osteochondrosis in animals. *Acta Radiol (Suppl)* 1978; 358: 299-306.
2. Olsson SE. Pathophysiology, morphology, and clinical signs of osteochondrosis (chondrosis) in the dog. In: *Pathophysiology of small animal surgery*. Ed M.J. Bojrab. Lea & Febiger, Philadelphia, 1981; 604-617.
3. Lenehan TM, Van Sickle DC. Canine osteochondrosis. In: *Textbook of small animal orthopedics*. Eds CD Newton and DM Nunamaker. JB Lippincott Co, Philadelphia, 1985; 981-997.
4. Montgomery RD, Hathcock JT, Milton JL, et al: Osteochondritis dissecans of the canine tarsal joint. *Compend Cont Educ Pract Vet* 1994;16: 835-845.
5. Van Ryssen B, van Bree H, Verschooten F: Osteochondritis dissecans of the tarsal joint in the dog: a review. *Vlaams Diergeneesk Tijdsch* 1991; 60: 197-2002.
6. Fitch RB, Beale BS. Osteochondrosis of the canine tibiotarsal joint. *Vet Clin North Am: Small Anim Pract* 1998; 28: 95- 113.
7. Weinstein MJ, Mongil CM, Rhodes WH, Smith GK. Orthopedic conditions of the Rottweiler – Part II. *Comp Cont Ed Pract Vet* 1995; 17: 925-939.
8. Olsson SE: Osteochondrosis in the dog, in Kirk RW (ed): *Current veterinary therapy VII*. Philadelphia, PA, Saunders, 1980; 807-815.
9. Johnson KA, Howlett CR, Pettit GD: Osteochondrosis in the hock joints in dogs. *J Am Anim Hosp Assoc* 1980; 16: 103-113.
10. Smith MM, Vasseur PB, Morgan JP: Clinical evaluation of dogs after surgical and nonsurgical management of osteochondritis dissecans of the talus. *J Am Vet Med Assoc* 1985; 187: 31-35.
11. Breur GJ, Spaulding KA, Braden TD: Osteochondritis dissecans of the medial trochlear ridge of the talus in the dog. *Vet Compar Orthop Traumatol* 1989; 4: 168-176.
12. Beale BS, Goring RL, Herrington J, et al: A prospective evaluation of four surgical approaches to the talus of the dog used in the treatment of osteochondritis dissecans. *J Am Anim Hosp Assoc* 1991; 27: 221-229.
13. Olson NC, Mostosky UV, Flo GL, et al: Osteochondritis dissecans of the tarsocrural joint in three canine siblings. *J Am Vet Med Assoc* 1980; 176: 635-637.
14. Smith, CW: Osteochondrosis in the dog - Diagnosis, Treatment, and Prognosis. *Canine Pract* 1991; 16: 15-22.
15. Bloomberg MS, Lewis DD: Osteochondrosis of sporting and working dogs, in Bloomberg MS, Dee JF and Taylor RA (eds): *Canine sports medicine and surgery*. Philadelphia, PA, Saunders, 1998; 234-250.
16. Rosenblum GP, Robins GM, Carlisle CH: Osteochondritis dissecans of the tibio-tarsal joint in the dog. *J Small Anim Pract* 1978; 19: 759-767.
17. Mason RA, Lavelle RB: Osteochondritis dissecans of the tibial tarsal bone in dogs. *J Small Anim Pract* 1979; 20: 423-432.

18. Cook J L, Tomlinson M R, Stoll D T, et al: Arthroscopic removal and curettage of osteochondrosis lesions on the lateral and medial trochlear ridges of the talus in two dogs. *J Am Anim Hosp Assoc* 2001; 37: 75-80.
19. Gielen I, Van Ryssen B, Coopman F, et al. Minimally invasive treatment of canine tarsocrural osteochondritis dissecans: A Long-Term Follow-Up Study of 30 Dogs. *Vet Surg* 2003; Submitted.
20. Morgan JP, Wind A, Davidson AP. Osteochondrosis of the talus. In: Hereditary bone and joint disease in the dog: Osteochondroses-Hip dysplasia-Elbow dysplasia. Eds JP Morgan, A Wind and AP Davidson. Schlutersche GmbH, Hannover 2000; 239-245.
21. Schenck, RC, Goodnight, JM. Current concept review: Osteochondritis dissecans. *J Bone Joint Surg* 1996; 78A: 439-456.
22. Zinman C, Reis ND: Osteochondritis dissecans of the talus: use of the high resolution Computed Tomography Scanner. *Acta Orthop Scand* 1982; 53: 697-700.
23. Ogilvie-Harris DJ, Sarrosa EA: Arthroscopic treatment of osteochondritis dissecans of the talus. *Arthroscopy: J Arthrosc Rel Surg* 1999; 15: 805-808.
24. Zinman C, Wolfson N, Reis ND: Osteochondritis dissecans of the dome of the talus. Computed tomography scanning in diagnosis and follow-up. *J Bone Joint Surg Am* 1988; 70: 1017-1019.
25. Gielen I, De Rycke L, van Bree H, et al: Computed tomography of the tarsal joint in clinically normal dogs. *Am J Vet Res* 2001; 62: 1911-1915.
26. Gielen I, van Bree H, Van Ryssen B, et al: Radiographic, computed tomographic and arthroscopic findings in 23 dogs with osteochondrosis of the tarsocrural joint. *Vet Rec* 2002; 150: 442-447.
27. Berndt AL, Harty M. Transchondral fractures (osteochondritis dissecans) of the talus. *J Bone Joint Surg* 1959; 41A: 988-1020.
28. Simpson MB: Talar osteochondral injuries in athletes. *Operat Techn Sports Med* 2001; 9: 8-13.
29. Farmer JM, Martin DF, Boles CA, et al: Chondral and osteochondral injuries. Diagnosis and management. *Clin Sports Med* 2001; 20: 299-320.
30. Lotke PA, Ecker ML. Current concept review: Osteonecrosis of the knee. *J Bone Joint Surg* 1988; 70A: 470-473.
31. Gielen I, van Bree H, Coopman F. Comparison of morphological and clinical features between medial and lateral, and clinical and non-clinical canine tarsocrural osteochondrosis lesions. *Am J Vet Res* 2003; Submitted.
32. Baker C L, Morales RW. Arthroscopic treatment of transchondral talar dome fractures: A long-term follow-up study. *Arthroscopy: J Arthrosc Rel Surg* 1999; 15: 197-202.
33. Tol JL, Struijs PA, Bossuyt PM, et al. Treatment strategies in osteochondral defects of the talar dome: a systematic review. *Foot Ankle Int.* 2000; 21: 119-126.
34. Pettine KA, Morrey BF: Osteochondral fractures of the talus. *J Bone Joint Surg* 1987; Br 69: 89-92.

35. Pelletier JP, Lajeunesse D, Jovanovic DV, et al: Carprofen simultaneously reduces progression of morphologic changes in cartilage and subchondral bone in dog osteoarthritis. *J Rheumatol* 2000; 27: 2893-2902.
36. Brinker W, Piermattei D, Flo G. Fractures and other orthopedic injuries of the tarsus, metatarsus and phalanges. In: *Handbook of Small Animal Orthopedics and Fracture Repair*. WB Saunders, Philadelphia, 1997; 607-655.
37. Johnston SA. Overview of pain in the lame patient. *Vet Clin North Am Small Anim Pract* 2001; 31: 39-53.
38. Dew TL, Martin RA. Functional, radiographic, and histologic assessment of healing of autogenous osteochondral grafts and full-thickness cartilage defects in the talus of dogs. *Am J Vet Res* 1992; 53: 2141-2152.
39. van Ee RT, Gibson K, Roberts ED. Osteochondritis dissecans of the lateral ridge of the talus in a dog. *J Am Vet Med Assoc* 1988; 193: 1284-1286.
40. Aron DN, Mahaffey MB, Rowland GN: Free chondral fragment involving the lateral trochlear ridge of the talus in a dog. *J Am Vet Med Assoc* 1985; 186: 1095-1097.
41. Sjöström L, Håkanson N. Traumatic injuries associated with the short collateral ligaments of the talocrural joint of the dog. *J Small Anim Pract* 1994; 35: 163-168.
42. Lahm A, Erggelet C, Steinwachs M, Reichelt A. Arthroscopic management of osteochondral lesions of the talus: Results of drilling and usefulness of magnetic resonance imaging before and after treatment. *Arthroscopy* 2000; 16: 299-304.
43. Bachmann G, Jurgensen I, Rominger M, Rau WS. The value of magnetic resonance imaging in the clinical course of osteochondrosis dissecans in the knee and ankle joints. *Rofu Fortschr Geb Rontgenstr Neuen Bildgeb Verfahr* 1999; 171: 372-379.
44. Gielen I, van Bree H. Computed tomography (CT) compared with radiography in the diagnosis of tarsocrural osteochondrosis of the lateral trochlear ridge in the dog. *Vet Compar Orthop Traumatol* 2003: Accepted.

Osteochondrosis (OC) is a disturbance of endochondral ossification affecting humans and several animal species and does not always exhibit clinical signs. There is considerable confusion regarding the definition and pathogenesis of OC (Ekman & Carlson, 1998). In the literature on humans, several conditions are grouped under the heading of OC, including osteochondral fractures, osteonecrosis, accessory centres of ossification, osteochondrosis, and hereditary epiphyseal dysplasia (Schenck & Goodnight, 1996). In addition, in all species there are several synonyms for the disease, including osteochondritis dissecans, osteochondrosis dissecans, and dyschondroplasia. However, the term “osteochondrosis” is the most widely accepted term in both the veterinary and human literature (Ekman & Carlson, 1998) and therefore this term has been used throughout the present study.

The aetiology of OC is considered to be multi-factorial, with no single factor accounting for all aspects of the disease. Trauma, hereditary factors and rapid growth, nutritional factors, and ischemia have been suggested as the most important factors (Ekman & Carlson, 1998).

In the dog, OC can affect several joints, but the condition is diagnosed most frequently in the elbow and shoulder joints, and to a much lesser degree in the tarsocrural and stifle joints (Alexander, 1981; Montgomery et al., 1989; Smith, 1991; Fox & Walker, 1993; Montgomery et al., 1994; Boulay, 1998; Harari, 1998; Johnston, 1998). OC is diagnosed more frequently in males than in females, and especially in fast growing dogs of large and giant breeds. The condition appears at certain predilection sites of increased biomechanical stress and is bilateral in a very large percentage of affected dogs (Ekman & Carlson, 1998). The radiographic diagnosis of shoulder and knee OC is usually straightforward (Johnston, 1998; Harari, 1998). On the contrary, the radiographic diagnosis of elbow and tarsocrural OC is often challenging (Boulay, 1998; Montgomery et al, 1994), because these joints are both small and complex.

Tarsocrural osteochondrosis (TOC) has been reported in several species, including humans, horses, cattle, pigs – and in dogs, in which it was first reported in 1975 and comprises 9% of all OC cases (Montgomery et al, 1994, Fitch & Beale, 1998). In the dog, the most common location for TOC lesions is the medial trochlear ridge of the talus,

whereas involvement of the lateral trochlear ridge is less common and occurs in 25% of the cases (Denny, 1981; Breur et al, 1989; Wisner et al, 1990; Van Ryssen et al, 1991; Montgomery et al, 1994). TOC eventually results in joint instability, pain, lameness, and progressive degenerative joint disease (DJD) (Fitch & Beale, 1998).

The radiographic diagnosis of TOC can be difficult, due to the complexity of the tarsocrural joint and the superimposition of various bony structures hiding its articular surface. When the lateral ridge is involved, there is the additional superimposition of the calcaneus, which is probably the reason why reports on lateral TOC appeared later than on medial TOC (Morgan et al, 2000). In 10% of all TOC cases, the radiographic diagnosis can be negative, even after an extended protocol that includes six views: extended and flexed mediolateral, flexed dorsoplantar skyline, plantarodorsal, and two oblique views (plantaromedial-dorsolateral and plantarolateral-dorsomedial) (Chapter 2). When the same protocol is used for diagnosing only lateral TOC lesions, 27% of the lesions can be missed. In practice, the radiographic protocol is usually limited to two standard views (extended mediolateral and extended dorsoplantar), but then 72% of the lateral TOC lesions can be missed (Chapter 3).

Computed tomography (CT), a cross-sectional imaging technique, is useful in displaying the joint surface of the elbow (De Rijcke et al, 2002) and the tarsocrural joint (Chapter 1), without any superimposition of surrounding bony structures. The bony parts can be examined in detail and, by using the right window, soft tissue parts such as joint capsule, muscles and tendons, and larger blood vessels can be examined as well (Chapter 1, De Rijcke et al, 2002). Therefore, CT is superior to radiography in the diagnosis of medial and lateral TOC (Chapters 2 and 3). Using TOC-CT data, a four-stage classification system, similar to a system used in human beings, was established, which is useful for describing the lesions in a standardised way (Chapter 2). This “Berndt and Harty classification” has been widely accepted to classify tarsocrural lesions into four different stages depending on the status of the trochlear ridge and the associated fragment (Berndt & Harty, 1959; Baker & Morales, 1999).

There are significant differences between lateral and medial TOC lesions. Dogs with lateral TOC lesions are significantly younger than those with medial lesions; the duration of symptoms is shorter, and the lesions are more acute (Chapter 4). This distinction is

similar in human beings, where lateral lesions of the talus are presumed to be acute osteochondral fractures, whereas medial lesions are thought to be chronic lesions (Kelberine & Frank, 1999). Lateral TOC lesions are significantly larger than medial lesions (Chapter 4). Medial and lateral TOC lesions probably have different aetiologies, as suggested by some authors (Aron et al, 1985; Sjöström & Håkanson, 1994). In human beings, trauma has been suggested as the initiating factor in lateral lesions (Frank, 2001), and similarly in dogs the majority of the cases have a history of trauma (Chapter 3). The theory that lateral lesions are avulsion fractures of the short lateral collateral ligaments (Sjöström & Håkanson, 1994) appears to be unlikely, because the majority of lateral TOC fragments are large, and 25% of them are situated in the dorsal or distal part of the lateral ridge which is not the site where these ligaments attach to the bone (Chapter 3). Avulsion fractures of ligaments in young dogs, as for instance, of the origin of the cranial cruciate ligament, are normally associated with smaller bony fragments (Stuart, 1998). The attachment of the short lateral collateral ligaments to these fragments is probably coincidental. The fact that lateral TOC lesions, although larger than the medial ones, are not associated with much more severe DJD is probably due to the fact that they are diagnosed in an earlier phase and DJD has had no time to develop.

The reported incidence of bilateral TOC in the tarsocrural joint is approximately 50% of dogs with TOC (Montgomery et al, 1994; Weinstein et al, 1995). Although clinical lameness in these cases is rarely symmetrical (Smith et al, 1985; Wisner et al, 1990; Beale et al, 1991), 30% of the dogs presenting bilateral lesions are bilaterally lame (Chapter 4). The lameness is more manifest in the joint with the largest defects. The “non-clinical” TOC lesions are significantly smaller than the “clinical” ones (Chapter 4), similar to an observation made in shoulder OC lesions as well (van Bree, 1994).

Both conservative and surgical management (arthrotomy) have been recommended for treating TOC lesions (Johnson et al, 1980; Olsson, 1980; Smith et al, 1985; Breur et al, 1989; Beale et al, 1991). Long-term evaluation of cases indicates that joint lameness resolves in not even 25% of the affected dogs, regardless of the therapeutic modality chosen (Rosenblum et al, 1978; Mason & Lavelle, 1979; Olson et al, 1980; Smith et al, 1985; Breur et al, 1989; Smith, 1991; Bloomberg & Lewis, 1998). Minimally invasive treatment yields excellent long-term results in 44% of the cases, which compares

favourably to the results of arthrotomy (Chapter 5). The same observation has been made in humans (Van Buecken et al, 1989). The reason for these better results is probably multi-factorial. The minimally invasive treatment itself allows the TOC fragments to be excised with minimal soft tissue trauma as compared to arthrotomy (Chapter 5). Besides possible post-surgical complications (Smith et al, 1985; Breur et al, 1989), the arthrotomy procedure has different consequences, including the induction of instability (Smith et al, 1985; Brinker et al, 1997) and degenerative changes (Järvinen et al, 1995). In combination with minimally invasive treatment, CT data were used for treatment planning. Apart from a precise diagnosis, CT allows determination of the location, number and size of the TOC fragments (Chapters 2, 3 and 5). When minimally invasive techniques, including arthroscopy or mini-arthrotomy (van Bree & Van Ryssen et al, 1998), are applied to remove TOC fragments, the exact location is useful for determining the best approach to the lesion. The choice between arthroscopy and arthroscopically guided mini-arthrotomy can be determined in advance by using CT to measure the size of the TOC defects (Chapter 5). CT can also be used to determine the exact number of TOC fragments to be removed. More than 75% of the TOC defects are associated with more than 2 fragments (Chapter 2). Smaller fragments, in particular, can be missed in conventional arthrotomy – and even in a minimal exposure arthrotomy technique or arthroscopy – due to a limited overview. This might explain the relatively poor outcome in some cases after conventional surgical treatment (Smith, 1991; Bloomberg & Lewis, 1998; Morgan et al, 2000).

Arthroscopic treatment of TOC lesions remains technically difficult and requires a high level of expertise (Chapters 2 and 5). In addition, only half of the lesions can be treated arthroscopically. Whenever necessary, the arthroscopic procedure can easily be converted into a mini-arthrotomy with minimal trauma without having any effect on the functional outcome – there is no difference in long-term results between the two minimally invasive techniques (Chapter 5).

Comparison of reported results can be biased. The evaluation criteria should be clear and similar. In the present study, the patients' functional outcomes were evaluated using a rating scheme that assessed the results of a clinical examination (pain, swelling, range of motion) and functional results (post-operative improvement, lameness, and activity). The

outcomes were rated as excellent, good, fair or poor. The patients' outcome was categorised per joint, based on the lowest rating in any area (Chapter 5). This scaling system is very strict and is comparable to a rating scheme used in humans for the evaluation of post-surgical results of talar dome fractures (Baker & Morales, 1999). The definition of "long-term" and the number of cases included in a study are important as well. In the follow-up study described in Chapter 5, 30 dogs (32 joints) were evaluated during a mean follow-up period of 34 months. "Long-term" was defined as a follow-up period of more than 9 months. These numbers compare favourably to those available in the literature (Rosenblum et al, 1978; Mason & Lavelle, 1979; Olson et al, 1980; Smith et al, 1985; Breur et al, 1989; Smith, 1991; Bloomberg & Lewis, 1998).

Although the long-term functional outcomes of minimally invasive treatment are better than those reported after treatment by arthrotomy, return to full function is less than 50% (Chapter 5). These results are inferior to the reported 85% - 90% excellent long-term results in humans (Baker & Morales, 1999; Tol et al, 2000; Simpson, 2001). The better results in humans are partially explained by the fact that lesions are diagnosed in an earlier phase than they are in dogs. Studies in humans show better results as a consequence of earlier treatment (Pettine & Morrey, 1987). The "Berndt and Harty" classification is used by some surgeons to determine the therapeutic regime in talar dome lesions (Farmer et al, 2001; Simpson, 2001), although its value has been questioned because it might not accurately reflect the integrity of the articular cartilage (Stone, 1996; Jarde et al, 2000). Stage III and IV lesions are often treated with reduction and fixation with absorbable pins in the acute stage (Simpson, 2001), resulting in less joint incongruity and instability (Farmer et al, 2001). In the dog, no correlation has been found between the several "Berndt and Harty" stages and the long-term functional outcome, nor could this classification be used in treatment planning (Chapter 6). In this study, fragments in Stages II to IV were excised (Chapter 5), probably resulting in more incongruity in larger fragments. Several treatments have been reported for humans. Because the success rate by excision alone was 38%, this technique is no longer recommended (Tol et al, 2000). In the dog, fixation of larger TOC fragments has been performed experimentally (Dew & Martin, 1992), and several authors claim that, in clinical cases, reattachment of TOC fragments is preferable to removal (Aron et al, 1985;

van Ee et al, 1988; Beale et al, 1991; Smith, 1991) especially when the lateral talar ridge is involved (Sjösström & Håkanson, 1994). However, reattachment of these fragments may be less successful due to degenerative changes in the fragment and an imperfect “fit” of the fragment in the subchondral bone defect (Breur et al, 1989). In the majority of cases, the presence of more than 2 fragments associated with the OC defects further complicates the issue (Chapters 2 and 5). In humans, lateral lesions carry a better prognosis than medial lesions (Kelberine & Frank, 1999; Shearer et al, 2002), but this could not be statistically confirmed in the dog (Chapters 5 and 6), probably because the number of lateral TOC cases is relatively small.

Minimally invasive treatment of TOC did not stop the progression of DJD in the majority of treated joints. This might be partially explained by the resulting incongruity after fragment removal (Chapter 5; Brinker et al, 1997). The long-term functional outcomes are influenced by the size of the fragment and the post-surgical arthrosis, which itself is significantly influenced by the volume of the defect and the degree of the arthrosis before the treatment (Chapters 5 and 6). The significant correlation between the volume of the defect and the post-surgical DJD is a logical finding, because large defects likely produce joint incongruity and instability (Farmer et al, 2001; Brinker et al, 1997). Poor joint congruity causes tension in, or pressure on, the joint capsule, resulting in pain and lameness (Johnston, 2001). This contrasts with observations made in humans, where usually only mild radiographic DJD changes develop, which do not correlate with the clinical outcome (Shearer et al, 2002).

Theoretically, the ideal treatment would be a technique that restores joint congruity or at least minimises post-surgical incongruity. In our opinion, curettage of the lesions should be avoided to prevent increased post-surgical incongruity. In humans, the long-term results of curettage, drilling, and bone grafting favour the latter (Draper & Fallat, 2000). The usefulness of curettage, although often performed, has been questioned in humans as well (Draper & Fallat, 2000; Hunziker, 2001). On the other hand, lavage after arthroscopic treatment could be beneficial, because inflammatory substances are washed out of the joint (Hunziker, 2001).

Although it is difficult to give a prognosis for every individual patient, the size of the lesion and the pre- and post-surgical arthrosis are important prognostic factors (Chapter

6). Larger defects tend to give poorer post-surgical results (Chapter 6). CT measurements make it possible to predict acceptable – and even more importantly, non-acceptable – outcomes. An owner will be delighted with full recovery (excellent result), but a good result (minimal lameness after exercise) will be very acceptable as well. Minimal improvement (fair result) or no improvement at all (poor result) will hardly be tolerated. A negative correlation, reported in the literature, between functional outcome and age, weight, duration of symptoms, and bilateral involvement (Breur et al, 1989; Beale et al, 1991; Montgomery et al, 1994; Morgan et al, 2000; Fitch & Beale, 1998) could not be confirmed by this study (Chapter 6). Adult dogs (more than 1 year old), an important group of patients, can be treated with an acceptable functional outcome.

The application of CT in canine TOC is extremely beneficial in the diagnosis of both lateral and medial TOC. CT can be used in treatment planning and gives a more accurate prognosis in individual cases. Therefore, we can conclude that CT examination, although costly and requiring general anaesthesia, can be fully justified in dogs with TOC.

REFERENCES

- Alexander JW, Richardson DC, Selcer BA. Osteochondritis dissecans of the elbow, stifle, and hock - a review. *J Am Anim Hosp Assoc* 1981, 17, 51-56.
- Aron DN, Mahaffey MB, Rowland GN. Free chondral fragment involving the lateral trochlear ridge of talus in a dog. *J Am Vet Med Assoc* 1985; 186: 1095-1096.
- Baker C L, Morales RW. Arthroscopic treatment of transchondral talar dome fractures: A long-term follow-up study. *Arthroscopy: J Arthrosc Rel Surg* 1999; 15: 197-202.
- Beale BS, Goring RL, Herrington J, et al. A prospective evaluation of four surgical approaches to the talus of the dog used in the treatment of osteochondritis dissecans. *J Am Anim Hosp Assoc* 1991; 27: 221-229.
- Berndt AL, Harty M. Transchondral fractures (osteochondritis dissecans) of the talus. *J Bone Joint Surg* 1959; 41A: 988-1020.
- Bloomberg MS, Lewis DD. Osteochondrosis of sporting and working dogs. In: *Canine sports medicine and surgery*. Eds Bloomberg MS, Dee JF and Taylor RA. Saunders, Philadelphia 1998; 234-250.
- Boulay JP. Fragmented medial coronoid process of the ulna in the dog. *Vet Clin North Am: Small Anim Pract* 1998; 28: 51-74.
- Breur GJ, Spaulding KA, Braden TD. Osteochondritis dissecans of the medial trochlear ridge of the talus in the dog. *Vet Compar Orthop Traumatol* 1989; 4: 168-176.
- Brinker W, Piermattei D, Flo G. Fractures and other orthopedic injuries of the tarsus, metatarsus and phalanges. In: *Handbook of Small Animal Orthopedics and Fracture Repair*. WB Saunders, Philadelphia, 1997; 607-655.
- Denny HR. Osteochondritis dissecans of the hock joint in the dog. *Vet Annual* 1981; 21: 224-228.
- De Rycke LM, Gielen IM, van Bree H, et al. Computed tomography of the elbow joint in clinically normal dogs. *Am J Vet Res* 2002; 63:1400-1407.
- Dew TL, Martin RA. Functional, radiographic, and histologic assessment of healing of autogenous osteochondral grafts and full-thickness cartilage defects in the talus of dogs. *Am J Vet Res* 1992; 53: 2141-2152.
- Draper SD, Fallat LM. Autogenous bone grafting for the treatment of talar dome lesions. *J Foot Ankle Surg* 2000; 39: 15-23.
- Ekman S, Carlson CS. The pathophysiology of osteochondrosis. *Vet Clin North Am: Small Anim Pract* 1998, 28, 17- 32.
- Farmer JM, Martin DF, Boles CA, et al. Chondral and osteochondral injuries. Diagnosis and management. *Clin Sports Med* 2001; 20: 299-320.
- Fitch RB, Beale BS. Osteochondrosis of the canine tibiotarsal joint. *Vet Clin North Am: Small Anim Pract* 1998; 28: 95-113.
- Fox SM, Walker AM. Identifying and treating the primary manifestations of osteochondrosis of the elbow. *Vet Med* 1993; 2: 132-146.

- Frank A. Arthroscopic treatment of osteochondral lesions of the talar dome. *Orthopäde* 2001; 30:37-46.
- Harari J. Osteochondrosis of the femur. *Vet Clin North Am: Small Anim Pract* 1998, 28, 87-94.
- Hunziker EB. Articular cartilage repair: basic science and clinical progress. A review of the current status and prospects. *Osteoarthr Cartil* 2001; 10: 432-463.
- Jarde O, Trinquier-Lautard JL, Garate F, et al. Osteochondral lesions of the talar dome: surgical treatment in a series of 30 cases. *Rev Chir Orthop Reparatrice Appar Mot* 2000; 86: 608-615.
- Järvinen M, Jozsa L, Johnson RJ, et al. Effect of anterior cruciate ligament reconstruction with patellar tendon or prosthetic ligament on the morphology of other ligaments of the knee joint. An experimental study in dogs. *Clin Orthop Rel Res* 1995; 311: 176-181.
- Johnston SA. Overview of pain in the lame patient. *Vet Clin North Am: Small Anim Pract* 2001; 31: 39-53.
- Johnson KA, Howlett CR, Pettit GD. Osteochondrosis in the hock joints in dogs. *J Am Anim Hosp Assoc* 1980; 16: 103-113.
- Johnston SP. Osteochondritis dissecans of the humeral head. *Vet Clin North Am: Small Anim Pract* 1998; 28: 33-49.
- Kelberine F, Frank A. Arthroscopic treatment of osteochondral lesions of the talar dome: a retrospective study of 48 cases. *Arthroscopy: J Arthrosc Rel Surg* 1999; 15: 77-84.
- Mason RA, Lavelle RB. Osteochondritis dissecans of the tibial tarsal bone in dogs. *J Small Anim Pract* 1979; 20: 423-432.
- Montgomery RD, Milton JL, Henderson, RA, et al. Osteochondritis dissecans of the canine stifle. *Compend Cont Educ Pract* 1989; 11: 1199-1210.
- Montgomery RD, Hathcock JT, Milton JL, et al: Osteochondritis dissecans of the canine tarsal joint. *Compend Cont Educ Pract* 1994; 16: 835-845.
- Morgan JP, Wind A, Davidson AP. Osteochondrosis of the talus. In: *Hereditary bone and joint disease in the dog: Osteochondroses-Hip dysplasia-Elbow dysplasia*. Eds JP Morgan, A Wind and AP Davidson. Schlutersche GmbH, Hannover 2000; 239-245.
- Olson NC, Mostosky UV, Flo GL, et al: Osteochondritis dissecans of the tarsocrural joint in three canine siblings. *J Am Vet Med Assoc* 1980; 176: 635-637.
- Olsson SE. Osteochondrosis in the dog. In: *Current veterinary therapy VII*. Ed RW Kirk. Saunders, Philadelphia 1980; 807-815.
- Pettine KA, Morrey BF. Osteochondral fractures of the talus. *J Bone Joint Surg* 1987; 69B: 89-92.
- Rosenblum GP, Robins GM, Carlisle CH. Osteochondritis dissecans of the tibio-tarsal joint in the dog. *J Small Anim Pract* 1978; 19: 759-767.
- Schenck, RC, Goodnight, JM. Current concept review: Osteochondritis dissecans. *J Bone Joint Surg* 1996; 78A: 439-456.
- Shearer C, Loomer R, Clement D. Nonoperatively managed stage 5 osteochondral talar lesions. *Foot Ankle Int* 2002; 23:651-654.
- Simpson MB: Talar osteochondral injuries in athletes. *Operat Techn Sports Med* 2001; 9: 8-13.

- Sjösström L, Håkanson N. Traumatic injuries associated with the short collateral ligaments of the talocrural joint of the dog. *J Small Anim Pract* 1994; 35: 163-168.
- Smith, CW: Osteochondrosis in the dog - Diagnosis, Treatment, and Prognosis. *Canine Pract* 1991; 16: 15-22.
- Smith MM, Vasseur PB, Morgan JP. Clinical evaluation of dogs after surgical and nonsurgical management of osteochondritis dissecans of the talus. *J Am Vet Med Assoc* 1985; 187: 31-35.
- Stone JW. Osteochondral Lesions of the Talar Dome. *J Am Acad Orthop Surg* 1996; 4: 63-73.
- Stuart C. Fractures in skeletally immature animals. In: *Manual of small animal fracture repair and management*. Eds Coughlan A, Miller A. British Small Animal Veterinary Association, Hampshire, UK, 1998; 103-111.
- Tol JL, Struijs PA, Bossuyt PM, et al: Treatment strategies in osteochondral defects of the talar dome: a systematic review. *Foot Ankle Int* 2000; 21: 119-126.
- van Bree H. Evaluation of subchondral lesion size in osteochondrosis of the scapulohumeral joint in dogs. *J Am Vet Med Assoc* 1994; 204: 1472-1474.
- van Bree H, Van Ryssen B: Diagnostic and Surgical Arthroscopy in Osteochondrosis Lesions. *Vet Clin North Am: Small Anim Pract* 28: 161-189, 1998.
- Van Buecken K, Barrack RL, Alexander AH, et al. Arthroscopic treatment of transchondral talar dome fractures. *Am J Sports Med* 1989; 17: 350-355.
- van Ee RT, Gibson K, Roberts ED. Osteochondritis dissecans of the lateral ridge of the talus in a dog. *J Am Vet Med Assoc* 1988; 193: 1284-1286.
- Van Ryssen B, van Bree H, Verschooten F. Osteochondritis dissecans of the tarsal joint in the dog: a review. *Vlaams Diergeneesk Tijdsch* 1991; 60: 197-202.
- Weinstein MJ, Mongil CM, Rhodes WH, et al. Orthopedic conditions of the Rottweiler – Part II. *Comp Cont Ed Pract Vet* 1995; 17: 925-939.
- Wisner ER, Berry CR, Morgan JP, et al. Osteochondrosis of the lateral trochlear ridge of the talus in seven Rottweiler dogs. *Vet Surg* 1990; 19: 435-439.

Osteochondrosis (OC) is a developmental joint and bone disease in humans and in a variety of animal species. OC lesions are highly prevalent in pigs, horses, large breed dogs and poultry, but they do not always result in clinical signs. In dogs, OC is diagnosed more frequently in males than in females, and especially in fast-growing dogs of large and giant breeds. In a high percentage of the cases, the condition is bilateral, although the affected dogs are rarely bilaterally lame. OC can affect several different joints, but it is diagnosed most frequently in the elbow and shoulder, and much less often in the tarsocrural and stifle joints. OC of the tarsus has been reported in several species, including dogs, horses, cattle, pigs and humans. Tarsocrural OC (TOC) was first reported in the dog in 1975 and comprises 9% of all OC cases. The TOC defect can involve the medial or the lateral trochlear talar ridge and results in instability, pain, lameness, and progressive degenerative joint disease (DJD).

Diagnosing TOC is not always obvious and some authors advocate exploratory arthrotomy as a reasonable diagnostic option. But this is somewhat drastic and should be considered as the last resort.

Although a detailed study on the radiographic anatomy of the canine tarsocrural joint exists, the radiographic evaluation of this region remains difficult due to the superimposition of the tibia, fibula and calcaneus. The small size and complexity of the tarsocrural joint – especially in the young dog – is such that, even with an adequate number of appropriate projections, subtle changes involving both talar ridges can be missed. Therefore, the radiographic diagnosis of TOC can often be challenging. OC lesions are found in the medial or lateral aspect of the talus in humans as well, and although plain radiographs are usually sufficient to diagnose this condition, computed tomography (CT) is beneficial in pre-operative planning to accurately determine the size and location of the lesion.

CT is becoming more available to veterinarians, but it is only rarely used to diagnose orthopaedic disorders in small animals. A few reports exist on the use of CT in the imaging of fragmented ulnar coronoid processes. CT offers several advantages over

conventional radiography, including elimination of superimposed structures, thereby decreasing the complexity of the image. In addition, CT images can be displayed in various grey-scale formats, which can enhance visualisation of specific structures, and the images can be reconstructed in multiple anatomic planes. These features could provide useful additional information, not only in diagnosing OC in complex joints such as the tarsocrural joint, but also in identifying the exact extent and location of the lesion, which is necessary for selection of an appropriate surgical approach.

Since no data are yet available on CT of the canine tarsus, in the first part of this study we have provided a technical protocol for CT examination of the canine tarsal joint and a detailed description of the normal canine tarsus as revealed by CT. The dogs must be anaesthetised and positioned in ventral recumbency on the CT-scanning table with the tarsal joints in extension. This position allows a perfect symmetry and comparison of both tarsi at the same level. A lateral scout view is made to confirm correct positioning and 1 and 2 mm contiguous slices are made. Individual images are reviewed using both a bone (WW = 3500 HU; WL = 500 HU) and a soft tissue window (WW = 400 HU; WL = 66 HU). CT-image technique includes 120 kVp and 300 mAs. Image acquisition time using a third generation CT scanner is approximately 10 minutes. Afterwards, CT-reconstructions of the tarsocrural joint in a sagittal and dorsal plane are made. The entire tarsocrural joint surface can be evaluated from these reconstructed images, without superimposition of any bony structures. Besides full anatomic detail of the bony structures, some soft tissues such as tendons and large blood vessels can also be evaluated. However, it is not possible to identify nerves and smaller blood vessels. The results of this study can be used as a basis for the interpretation and exact evaluation of CT images of dogs with tarsal joint injuries. The area of the tarsocrural joint is of particular interest in dogs suspected of having TOC.

In the second part of this study, the CT, radiographic, and arthroscopic features in 23 dogs with TOC were evaluated. The radiographic procedure included extended and flexed mediolateral views, a plantarodorsal view, a flexed dorsoplantar skyline view, and plantaromedial-dorsolateral and plantarolateral-dorsomedial views (two oblique views).

CT revealed a total of 31 lesions on the 46 joints that were examined. The arthroscopic exploration was performed using either a plantar or a dorsal puncture, depending on the CT localisation of the lesion. Arthroscopy gave us information concerning synovial inflammation and joint cartilage damage.

The lateral trochlear ridge was involved in 6 cases and the medial in 17 cases. The results of this study show that, although survey radiographs are sufficient for making the diagnosis in most cases, CT is beneficial for determining the exact location, number, and size of the fragments, which could be of use in selecting an appropriate surgical approach.

A four-stage classification system was established (comparable to the “Berndt and Harty” system used for humans). This classification system classifies the lesion into four separate stages, depending on the status of the trochlear ridge and the associated fragment:

- Stage I – a subchondral bone defect without an associated fragment;
- Stage II – a partially detached osteochondral fragment;
- Stage III – a completely detached osteochondral fragment remaining in the crater; and
- Stage IV – a completely detached and displaced fragment.

The conclusion of this study was that CT reveals TOC lesions more thoroughly and provides information that might have a prognostic value. CT is helpful as well in making decisions about the timing and type of arthroscopic treatment.

The third part of this study was a retrospective study conducted on 11 tarsocrural joints with lateral OC. The radiographic diagnosis of lateral TOC (LTOC) is especially difficult due to the superimposition of not only the tibia and fibula but the calcaneus as well. As CT allows inspection of the talar ridges without superimposition of any bony structures, the capabilities of CT in diagnosing LTOC were compared with those of radiography. The flexed dorsoplantar skyline and the plantarolateral-dorsomedial (lateral oblique) projection were the most successful views for detecting the LTOC defect (in 7 out of 11 cases). Radiography failed to detect the fragment in 3 out of the 11 LTOC lesions, whereas with the help of CT the fragments could be visualised and exactly localised in all cases. In 6 joints, 2 fragments, and in 5 only 1 fragment was detected. This information is

quite useful when minimally invasive techniques are used to treat the lesions. The conclusion of this study was that CT is superior to radiography for diagnosing LTOC in the dog.

In the fourth part of this study, 49 joints (35 dogs) with TOC were used to evaluate whether significant differences exist between medial TOC (MTOC) and lateral TOC (LTOC), and between clinical and non-clinical lesions in dogs showing bilateral MTOC of the tarsus. This was done by comparing the morphological data of the lesions obtained by CT, the clinical features of the affected dogs, and the amount of radiographic DJD at the time of presentation. The differences between the data on LTOC and MTOC and on clinical and non-clinical lesions were statistically evaluated. Clinical data (breed, age, gender, weight, duration of clinical symptoms) were registered for these 35 dogs. The defects were measured (length, width and depth) using the CT software. Similar to a method used in humans, the volume (= length x width x depth) and surface (= length x width) were used to compare the size of the different defects. The radiographs of all affected tarsocrural joints were evaluated for the presence of DJD changes. Dogs with LTOC appeared to be significantly younger than those with MTOC, and the duration of lameness before admittance to the clinic appeared to be shorter. LTOC lesions are significantly larger than MTOC lesions, and clinical lesions are larger than non-clinical lesions. The difference in length between clinical and non-clinical lesions was statistically significant. These results support the view of some authors that LTOC has a different aetiology than MTOC and, therefore, must be considered as a different disorder. As in humans, a traumatic fragmentation of the lateral talar ridge could be the cause of the OC lesions. As in shoulder OC, there is probably a correlation between the size of tarsocrural lesions and the symptoms of pain and lameness.

In the fifth part of this study, a retrospective study of 30 dogs (32 joints) was conducted to evaluate the long-term results of minimally invasive treatment of TOC in the dog and the usefulness of CT findings in pre-operative planning. The TOC lesions were treated using minimally invasive treatment including arthroscopy or arthroscopically guided mini-arthrotomy. All dogs were clinically evaluated after treatment, and radiographs

(made before and after the procedure) were evaluated for signs of DJD. A follow-up study ranging from 9 to 67 months revealed excellent or good results in 75% of the cases. Forty-four percent of the treated joints regained full function. The overall success rate of the procedure was not influenced by the type of minimally invasive treatment. Progression of DJD was observed in the majority of the affected joints.

The conclusion was that, over the long term, minimally invasive treatment of TOC yields better results than those reported after arthrotomy. CT findings can be used to good advantage for treatment planning: the puncture sites can be determined from the CT mapping and the type of minimally invasive treatment can be determined from the size of the defect as measured on the CT images. Minimally invasive treatment of TOC does not stop the progression of DJD. A high level of pre-operative arthrosis may affect the clinical outcome negatively.

In the last part of this study, it was evaluated whether clinical data of the affected animals (age, gender, weight, duration of symptoms, and number of affected joints) and morphological data of the lesions obtained by CT (size, site, location, "Berndt and Harty" classification, and number of fragments) could be used to predict the long-term functional outcome (excellent, good, fair or poor) after minimally invasive treatment of TOC. The clinical data were registered for 30 dogs (32 joints) with TOC. All 32 defects were measured (length, width and depth) using the CT software. Similar to a method used in humans, the volume (= length x width x depth) and surface (= length x width) were used to compare the size of the different defects. The radiographs of all treated tarsocrural joints were evaluated pre- and post-treatment for the presence and amount of DJD changes. The correlation between the functional outcome and the clinical and morphological data of the MTOC and LTOC lesions was statistically evaluated. No significant correlation has been found between the clinical data and the functional outcome of the treated animals, but the size of the clinical lesions has an influence on the long-term prognosis. Larger lesions tend to give poorer long-term results. Although it remains difficult to predict the functional outcome for each individual dog, significant differences have been found in MTOC between acceptable (excellent or good) and non-

acceptable (fair or poor) outcomes and different ranges in LTOC for excellent and good clinical outcomes. The results also indicate that a poor clinical outcome may be caused by post-surgical arthrosis. Besides the fact that CT can help in the diagnosis of TOC and in the treatment planning of TOC lesions, the technique can also be used to predict a long-term acceptable functional outcome more accurately.

Osteochondrose (OC) is een ontwikkelingsstoornis van gewricht en bot die bij de mens en een hele reeks diersoorten voorkomt. OC letsels komen vrij veel voor bij varkens, paarden, grote hondenrassen en gevogelte. Deze letsels geven niet altijd aanleiding tot symptomen. Bij de hond komt OC meer voor bij mannelijke dieren, vooral bij snelgroeïende grote en reuzenrassen. In veel gevallen is er een bilaterale aantasting van de gewrichten. OC kan verschillende gewrichten aantasten maar komt toch het meest voor in elleboog en schouder. De knie en sprong zijn in mindere mate aangetast. Sprong OC komt bij verschillende diersoorten voor waaronder hond, paard, rund, varken en ook bij de mens. Bij de hond is de aandoening in 1975 voor het eerst beschreven en maakt 9% van alle OC gevallen uit. In de sprong kan OC aan de mediale of de laterale kam van de talus voorkomen. Het resultaat is meestal instabiliteit in het gewricht wat aanleiding geeft tot pijn en kreupelheid en op lange termijn osteoartrose (OA) veroorzaakt.

De diagnose van sprong OC is niet altijd evident en soms wordt een exploratieve artrotomie als diagnostisch alternatief aangeraden. Dit is echter een vrij drastische oplossing die best wordt vermeden.

Hoewel er bij de hond een gedetailleerde studie over de röntgenanatomie van de sprong bestaat, blijft het toch een uiterst moeilijke streek om radiografisch te evalueren door superpositie van de distale tibia, fibula en calcaneus. De kleine afmetingen en complexiteit van het spronggewricht, vooral bij de jonge hond, maakt dat zelfs met een hele reeks van uitprojecties subtiele veranderingen aan de taluskammen over het hoofd kunnen worden gezien. Het gevolg hiervan is dat de diagnose van sprong OC een uitdaging blijft. Ook bij de mens kan sprong OC aan de mediale en laterale taluskam voorkomen. Hoewel radiografie gewoonlijk voldoende is om deze aandoening te diagnosticeren, wordt computer tomografie (CT) gebruikt bij de preoperatieve planning. Aan de hand van CT wordt de grootte van het letsel en zijn juiste lokalisatie bepaald. CT wordt ook in de diergeneeskunde meer en meer gebruikt maar wordt slechts zelden in de veterinaire orthopedie ingezet. Er bestaan enkele publicaties over het gebruik van CT in de diagnose van losse processus coronoideus medialis in de elleboog van de hond. CT heeft, vergeleken met conventionele radiografie, een aantal voordelen. Onder andere wordt superpositie van botstructuren geëlimineerd waardoor de interpretatie van het beeld eenvoudiger wordt. Een ander voordeel is dat CT beelden verschillende grijswaarden

kunnen bevatten wat het mogelijk maakt om bepaalde structuren beter te kunnen zien. Ook kan men met CT, beelden in andere vlakken reconstrueren. Al deze kenmerken maken van CT een interessante techniek om OC in een klein complex gewricht, zoals de hondentarsus, te diagnosticeren. Verder kan zij informatie geven over de exacte uitbreiding en lokalisatie van letsels hetgeen essentieel is voor het plannen van de gepaste behandeling.

Tot hiertoe bestonden er bij de hond geen gegevens over CT onderzoek van het spronggewricht. Het eerste deel van het onderzoek bestond er dan ook in om een technisch protocol van onderzoek op te stellen en een gedetailleerde beschrijving te geven van de normale CT anatomie van de sprong bij de hond. Het CT onderzoek wordt onder algemene anesthesie uitgevoerd met het dier in buikligging. De beide sprongen worden perfect parallel gestrekt op de CT tafel om doorsneden te verkrijgen die met elkaar kunnen vergeleken worden. Eerst wordt er een overzichtsbeeld (scout view) gemaakt om de positionering te controleren en te bepalen waar de doorsneden worden gemaakt. Vervolgens worden er doorsneden doorheen het gewricht gemaakt van 1 en 2 mm. Op het einde van het onderzoek worden de transversale beelden individueel bekeken met een botvenster (WW = 3500 HU; WL = 500 HU) en een weke delenvenster (WW = 400 HU; WL = 66 HU). De beelden worden gemaakt met 120 kVp en 300 mAs. Het volledige onderzoek met een derde generatie scanner duurt ongeveer 10 minuten. Nadien worden er sagittale en dorsale reconstructies van het gewricht gemaakt. Op deze reconstructies kan het hele gewrichtsooppervlak geëvalueerd worden zonder superpositie van andere botstructuren. Naast alle anatomische details van de botstructuren kunnen ook weke delen structuren zoals pezen en grote bloedvaten worden onderzocht. Kleinere bloedvaten en zenuwen blijven echter ook met CT onzichtbaar. De resultaten van dit onderzoek kunnen als basis gebruikt worden voor de interpretatie van beelden van honden met tarsale traumata. Het op deze manier in beeld brengen van beide tarsale kammen is vooral interessant bij honden die verdacht worden van OC.

In het tweede deel van dit onderzoek werden de CT-, radiografische en artroscopische beelden van 23 honden met sprong OC geëvalueerd en vergeleken. Van beide

spronggewrichten werden radiografische opnamen gemaakt (mediolaterale opnamen in extensie en flexie, voorachterwaartse gestrekte en raaklijnopnamen en twee schuine opnamen). Met CT werden er in 46 gewrichten 31 OC letsels gedetecteerd. Daarna werden de gewrichten artroschopisch onderzocht via een plantaire of dorsale punctie, afhankelijk van de CT lokalisatie van de OC letsels, en konden de synovitis en kraakbeenletsels geëvalueerd worden. Bij 17 honden werden er letsels aan de mediale taluskam vastgesteld en bij 6 aan de laterale kam. De resultaten van deze studie wezen uit dat radiografie meestal volstaat voor de diagnose van sprong OC maar dat CT bijkomende informatie levert voor wat betreft de exacte lokalisatie van de letsels en het aantal en de grootte van de OC fragmenten. Dit zijn gegevens die kunnen helpen bij het plannen van de chirurgische ingreep. Aan de hand van de CT gegevens kunnen de letsels ingedeeld worden in 4 categorieën analoog naar een systeem dat bij de mens bestaat. Deze classificatie heet de “Berndt en Harty” indeling en deelt de letsels in afhankelijk van de toestand van het defect van de taluskam en het fragment: Groep I – een subchondraal defect waarbij geen los fragment te zien is; Groep II – een fragment dat nog gedeeltelijk vastzit; Groep III – een fragment dat volledig loszit maar nog in zijn subchondrale krater zit; Groep IV – een volledig los fragment dat verplaatst is. De conclusie van deze studie was dat CT een nauwkeurige inschatting van de OC letsels toelaat en informatie hierover geeft die misschien een prognostische waarde kan hebben en kan helpen bij het plannen van de artroschopische behandeling.

Het derde deel bestaat uit een retrospectief onderzoek op 11 spronggewrichten met OC letsels aan de laterale taluskam. De diagnose van laterale OC wordt bemoeilijkt door superpositie van de calcaneus. Aangezien CT de laterale taluskam in beeld kan brengen zonder deze superpositie werd in deze studie de vergelijking gemaakt tussen de radiografische - en CT diagnose van laterale sprong OC. Uit dit onderzoek bleek dat de voorachterwaartse raaklijn-opname en de schuine projectie waarbij het laterale compartiment van de sprong wordt uitprojecteerd, het meest efficiënt waren om een lateraal defect te detecteren (in 7 van 11 letsels). Met radiografie werden er echter 3 van de 11 letsels niet gezien. Met CT werden alle 11 letsels gedetecteerd en exact gelokaliseerd. In 6 gewrichten werden er 2 fragmenten en in 5 slechts 1 fragment

vastgesteld. Deze informatie is belangrijk indien men deze letsels minimaal invasief wenst te behandelen. De conclusie van deze studie was dat CT superieur is ten opzichte van radiografie voor de diagnose van laterale sprong OC bij de hond.

In het vierde deel van de studie werd er bij 49 gewrichten (35 honden) met sprong OC nagegaan of er significante verschillen bestaan tussen mediale en laterale OC letsels. Ook werd onderzocht of er significante verschillen bestaan tussen klinische en niet-klinische mediale OC letsels bij een groep honden met bilaterale aantasting maar slechts unilaterale kreupelheid. Hiervoor werden morfologische CT gegevens van de letsels, klinische gegevens van de honden en de radiografische artroseletsels van de gewrichten met elkaar vergeleken. De verschillen tussen mediale en laterale letsels en tussen klinische- en niet klinische letsels werden statistisch geëvalueerd op hun relevantie. Alle klinische gegevens (ras, geslacht, gewicht, duur van de klinische symptomen) van de 35 honden werden verzameld. De 49 OC defecten werden opgemeten met de CT software. Daarna werden de oppervlakte (= lengte x breedte) en het volume (= lengte x breedte x diepte) van de defecten berekend. Analoog met een methode beschreven bij de mens werden daarna de afmetingen van de verschillende defecten met elkaar vergeleken. Radiografisch werd bij alle 49 gewrichten de OA veranderingen ingedeeld in een schaal van 0 tot 3. Uit de vergelijkingen bleek dat honden met laterale letsels significant jonger waren dan deze met mediale letsels en ook in een vroeger stadium in de kliniek werden aangeboden. Laterale letsels bleken ook significant groter te zijn dan mediale. Klinische letsels bleken ook groter te zijn dan niet klinische. Vooral de lengte van de letsels bleek significant verschillend. De resultaten van deze studie schijnen de mening van sommige auteurs te onderschrijven dat laterale letsels een andere etiologie zouden hebben dan de mediale en als een andere aandoening moeten beschouwd worden. Zoals bij de mens, worden laterale letsels door sommigen als een traumatische fragmentatie van de laterale taluskam beschouwd. Een andere gevolgtrekking die kan gemaakt worden is dat er waarschijnlijk een correlatie bestaat tussen de afmeting van sprong OC letsels en de symptomen van pijn en kreupelheid. Een analoge correlatie werd gevonden bij schouder OC.

In het vijfde deel van dit onderzoek werd een retrospectief onderzoek uitgevoerd bij 30 honden (32 gewrichten) waarbij de lange termijn follow-up na minimaal invasieve behandeling van de OC letsels werd nagegaan. Eveneens werd de waarde van de CT gegevens voor de preoperatieve planning nagegaan. Alle letsels werden behandeld met een minimaal invasieve techniek: artroscoopisch of via een mini-artrotomie onder artroscoopische begeleiding. Alle honden werden klinisch geëvalueerd na de behandeling en OA werd radiografisch voor en na behandeling eveneens geëvalueerd. De follow-up periode varieerde van 9 tot 67 maanden. Bij 75% waren de resultaten goed tot uitstekend. Vierenveertig procent van alle gewrichten kenden een volledig functioneel herstel. Het succespercentage werd niet beïnvloed door het type van minimaal invasieve behandeling. Bij bijna alle gewrichten was een vooruitgang van de OA veranderingen vast te stellen. De conclusie van deze studie was dat de lange termijn resultaten van minimaal invasieve behandeling van sprong OC beter zijn dan na klassieke artrotomie. De CT gegevens kunnen gebruikt worden in de preoperatieve planning: de punctieplaatsen kunnen aan de hand van de CT lokalisatie bepaald worden en het type van behandeling kan worden afgeleid van de afmetingen van de defecten gemeten op de CT beelden. Minimaal invasieve behandeling van de letsels stopt echter niet de vooruitgang van de OA letsels. Preoperatieve OA letsels kunnen een negatieve invloed hebben op het functionele herstel.

In het laatste deel van de studie werd bij 30 honden (32 gewrichten) de correlatie nagegaan tussen de klinische gegevens van de honden en de morfologische CT gegevens van de OC letsels en het functionele herstel op lange termijn. Alle aangetaste gewrichten werden behandeld met een minimaal invasieve methode: artroscopie of mini-artrotomie. De 32 defecten werden opgemeten met de software van het CT apparaat. Daarna werden de oppervlakte (= lengte x breedte) en het volume (= lengte x breedte x diepte) van de defecten berekend. Analoog met een methode beschreven bij de mens werden daarna de afmetingen van de verschillende defecten met elkaar vergeleken. De klinische gegevens en de CT metingen werden daarna vergeleken met het resultaat van de behandeling en statistisch geëvalueerd op hun significantie. Radiografisch werd bij alle 32 gewrichten de OA veranderingen ingedeeld in een schaal van 0 tot 3 en bekeken voor - en na behandeling. Deze gegevens werden eveneens met het resultaat van behandeling

vergeleken. Uit de vergelijkingen bleek dat er geen significante correlatie kon aangetoond worden tussen de klinische gegevens van de patiënten en het functionele herstel. Wel bleek er een significante correlatie te bestaan tussen de grootte van de letsels en hun functionele herstel. Hoe groter de letsels hoe slechter de klinische afloop na behandeling. Een individuele prognose voor elke patiënt voorop te stellen blijft een moeilijke zaak hoewel het mogelijk bleek grenswaarden voorop te stellen voor mediale letsels die na behandeling een aanvaardbaar resultaat opleveren voor hond en eigenaar en deze die een niet aanvaardbare afloop kennen. Er werd ook een significant verband aangetoond tussen de postoperatieve OA letsels, geëvalueerd aan de hand van radiografie, en het functionele herstel van deze letsels na minimaal invasieve behandeling. Het bleek mogelijk om met de hulp van CT onderzoek de prognose van sprong OC op lange termijn nauwkeuriger in te schatten.

Nooit had ik kunnen denken dat ik de kans zou krijgen om onderzoek te doen en een proefschrift te schrijven.

Een doctoraat afleggen is niet eenvoudig en voor mij vergelijkbaar met een avontuurlijke reis. Het vergt studie, planning en doorzettingsvermogen om het uiteindelijke doel te bereiken. Gelukkig ontmoet je onderweg mensen zonder wie je het niet zou redden. Daarom wil ik hier iedereen hartelijk bedanken die me op één of andere manier geholpen heeft in het tot stand komen van dit proefschrift.

In de eerste plaats dank ik mijn promotor Prof. Dr. H. van Bree uit de grond van mijn hart voor het vertrouwen dat hij mij schonk en de kans die hij mij geboden heeft om dit onderzoek aan te vatten. Ook kreeg ik van hem de vorming in de beeldvorming en de orthopedie gedurende de jaren dat ik werkzaam ben in de vakgroep. Het zijn leerzame jaren geweest, en dit niet alleen wetenschappelijk maar ook op vriendschappelijk vlak. Dankzij zijn eindeloos geduld, zijn aanmoediging en zijn vooropgestelde deadline is deze thesis uiteindelijk een feit geworden.

Prof. Dr. Y. Palmers wil ik bedanken voor het aanvaarden om copromotor te zijn van deze studie, voor het enthousiasme waarmee hij hieraan meegewerkte en zich verdiept heeft in dit toch eerder diergeneeskundig thema. In zijn dienst heb ik van al de collega's radiologen mijn vak kunnen leren. Steeds ben ik er welkom in de weekends wanneer ik weer met "gevallen" om raad kom vragen. Bedankt aan het ganse team radiologen van de Ziekenhuizen Oost Limburg voor hun enthousiasme en interesse.

Ik dank Prof. Dr. B. Van Ryssen voor de samenwerking en haar steun in soms moeilijke omstandigheden. Samen met Prof. van Bree heeft zij mij ingewerkt in de boeiende gewrichtspathologie bij honden. Zij zijn mijn directe maatjes en naast onze wetenschappelijke samenwerking ook echte vrienden.

Dr. J. Vandevenne bedank ik voor zijn raadgevingen en kritische zin. Dank je Jan, voor je hulp in het comparatieve aspect met de humane geneeskunde, je aanvullingen over humane osteochondrose en de interessante en positieve discussies. Bedankt ook om meerdere weekends op te offeren om met ons onderzoeken te doen.

Prof. Dr. L. Brunberg ben ik dankbaar voor het aanvaarden om te zetelen in mijn begeleidingscommissie. De jarenlange contacten met hem hebben mij geholpen de pathologie van mijn onderzoeksthema beter te begrijpen.

Prof. Dr. F. Verschooten bedank ik voor het nauwkeurige verbeteren van de teksten en voor het enthousiasme waarop hij mij inwijdde in de OC pathologie van het paard. Hij heeft me steeds van in mijn studententijd aangemoedigd, mij opgepept in moeilijke momenten en op de gepaste tijden het vertrouwen gegeven.

Dank aan Prof. Dr. P. Simoens voor zijn positieve en aanmoedigende commentaren van in het begin van dit onderzoek. Zijn zeer nauwkeurig corrigeren van het manuscript heeft mij veel geholpen.

Verder gaat mijn dank naar de andere leden van de begeleidings- en examencommissie Prof. K. Dik, Prof. F. Gasthuys en Prof. M. Kramer. Zij leverden allen een bijdrage bij het tot stand komen van dit werk.

Dr. L. De Rycke apprecieer ik ten zeerste voor het delen van haar anatomische kennis, niet alleen bij de tarsus maar bij tal van andere comparatieve onderzoeken.

Dr. F. Coopman bedank ik voor de vele tijd die hij investeerde om mij als leek een beetje in te wijden in de toch moeilijke materie van de statistiek. Hoewel hij zelf aan een doctoraat werkt vond hij steeds tijd voor mij.

Speciale dank aan Dr. A. Van Caelenberg voor de hulp bij het uitvoeren van de radiografische- en CT onderzoeken van de patiënten en ook bij de follow-ups. Annemie, bedankt voor de aanmoediging en voor het regelmatig overnemen van mijn klinieken gedurende het laatste halve jaar.

Dank aan alle collega's van de Vakgroep Medische Beeldvorming voor de fijne samenwerking en werksfeer, welwillende hulp en vriendschap. Extra dank ook aan mijn collega's Dr. P. Verleyen voor de aanmoedigingen, en aan Dr. J. Saunders voor het zeer kritisch lezen en verbeteren van het manuscript, dit terwijl hij zelf ook genoeg werk had met zijn eigen doctoraat.

Een dank- je- wel aan Marleen Goethals voor het steeds terugvinden van verloren patiëntendossiers, en aan Frank De Smet voor het verzamelen van artikels. Een welverdiende pluim aan Jeanine Van den Meersschant en Anne Guillaume voor het op orde houden van de chaos op mijn bureautje. Een woord van dank ook voor Claudine Van Sante voor de fijne samenwerking bij het vele werk voor het PUO.

Verder wil ik de residents Dr. O. Taeymans en Dr. B. Vandevelde bedanken voor hun bereidwillige hulp bij het uitvoeren van de radiografische onderzoeken en de follow-ups. Ook de anesthesisten, Dr. Y. Hoybergs, Dr. T. Waelbers en Dr. I. Polis die er zonder aflatende inzet voor zorgden dat de honden "stil" bleven liggen, leverden hun bijdrage tot dit proefschrift. Ook een woord van dank aan Stijn Van Gils voor de hulp tijdens de follow-ups en aan alle andere collega's die hebben meegewerkt.

De heer Verachtert ben ik zeer erkentelijk voor het tot beschikking stellen van een draagbaar radiografieapparaat, zodat ik ook "in the field" follow-up foto's kon gaan nemen.

Dr. T. De Clercq ben ik erkentelijk voor de jarenlange fijne samenwerking. Menige avond hebben we beiden op de dienst gesleten en het is jammer dat hij andere paden is gaan bewandelen. Samen hebben we de pionierstijd van de CT beleefd en inzicht gekregen in de technische werking ervan. Ook Lieven Annys en Patrick Versonnen, bedankt voor jullie praktische tips en technische hulp in de beginperiode van de CT onderzoeken.

Marnix Verdonck, my dear en redder in nood! Bedankt voor je logistieke en technische steun. Altijd kom je ter hulp als ik weer in gevecht ben met mijn computer en op het punt sta “hem” weer uit het raam te keilen.

Dr. A. Van Waes ben ik erkentelijk voor de interesse die hij betoonde sinds mijn studententijd en de periode dat ik mijn eerste stappen in de vakgroep zette.

Eveneens wens ik mijn vrienden te bedanken voor hun oprechte steun al die jaren: Ann Claes, Martine Kellens en Filip Moermans, Celle Martens, Anne Olaerts, Vera Reumers, Annick Vandereycken, Niki Vandermeulen, Luc Verschuere, en Annelies Castermans die de omslag van dit werk heeft ontworpen.

Hierbij gaat mijn dank uit naar mijn nonkels die tijdens mijn studie steeds interesse hebben betoond in de goede afloop.

Mijn speciale dank gaat ook naar mijn broers Marc en Francis en naar mijn schoonzus Reinilde en de kindjes Hannah en Emmeline. Marc, bedankt voor de aanmoediging en voor onze gesprekjes die me steeds een hart onder de riem steken.

En ten slotte wil ik mijn mama en papa bedanken voor hun onvoorwaardelijke steun, aanmoediging en vertrouwen. Mama, bedankt voor je geduld, aandacht en luisterend oor elke avond.

Het laatste woord van dank gaat naar mijn papa, aan wie ik dit werk opdraag. Helaas heeft hij het voltooiën van dit proefschrift, waarop hij ongetwijfeld even trots zou zijn als ik, niet mogen meemaken.

Ingrid

Ingrid Gielen behaalde het diploma hoger secundair onderwijs aan het Onze Lieve Vrouw Lyceum te Genk. Daarna begon zij met de studie Diergeneeskunde aan het RUCA en behaalde het diploma van dierenarts aan de Universiteit Gent in 1995.

Onmiddellijk daarna trad zij in dienst bij de Vakgroep Medische Beeldvorming van de Huisdieren. Haar voornaamste taak bestaat uit CT-onderzoeken bij kleine en grote huisdieren, mankonderzoek bij kleine huisdieren en minimaal invasieve chirurgie.

Sinds eind 1996 is zij “course secretary” en medeorganisator van de “International Workshop for Small Animal Arthroscopy”, opgericht door de vakgroep. Vanaf 1997 is zij coördinator en programmaverantwoordelijke van het Post Universitair Onderwijs Diergeneeskunde van de Kleine Huisdieren en Bijzondere Dieren. In 2000 behaalde ze een Masters Degree in Laboratory Animal Science, met grote onderscheiding. In 2001 werd haar het getuigschrift van de doctoraatsopleiding in de diergeneeskundige wetenschappen uitgereikt.

Haar interesse voor de tarsocrurale aandoeningen bij de hond ontstond vanuit klinische ervaring in de vakgroep dat de diagnosestelling als ook de behandeling van deze letsels niet evident was. Het eigenlijke onderzoek begon in 1998 en heeft uiteindelijk tot dit proefschrift geleid.

Ingrid Gielen is auteur of medeauteur van 16 publicaties in internationale en nationale tijdschriften en van een hoofdstuk over CT in een chirurgieboek. Zij was spreker op 12 internationale congressen, waarvan verschillende op uitnodiging. In 2000 ontving zij op het wereldcongres voor veterinaire radiologie in Japan de prijs voor de beste presentatie.

PUBLICATIONS

I. Gielen, L. De Rycke, B. Van Ryssen, H. van Bree.

Die Thoracoscopie beim Hund.

Kleintiermedizin 1999; 3: 114-117.

M. Risselada, J. Saunders, S. Bhatti, I. Gielen, L. Van Ham, H. van Bree.

CT-guided biopsy of an infected intervertebral disk - CT geleid aspiratiebiopt van een geïnfecteerde tussenwervelschijf.

Vlaams Diergeneeskundig Tijdschrift 2001; 70: 59-64.

I. Gielen, L. De Rycke, H. van Bree, P. Simoens.

Computed tomography (CT) of the tarsal joint in clinically normal dogs.

American Journal of Veterinary Research 2001; 62: 1911-1915.

K. Peremans, P. De Bondt, K. Audenaert, K. Van Laere, I. Gielen, M. Koole, J. Versijpt, H. van Bree, F. Verschooten, R. Dierckx.

Regional brain perfusion in 10 normal dogs measured with technetium-99m ethylcysteinate dimmer SPECT.

Veterinary Radiology and Ultrasound 2001; 42: 562-568.

L. De Rycke, I. Gielen, I. Polis, B. Van Ryssen, H. van Bree, P. Simoens.

Thoracoscopic Anatomy of dogs positioned in Lateral Recumbency.

Journal of American Animal Hospital Association 2001; 37: 543-548.

J.H. Saunders, J. Zonderland, C. Clercx, I. Gielen, F. R. Snaps, M. Sullivan, H. van Bree, R. F. Dondelinger.

Canine nasal aspergillosis: Computed tomographic findings in 35 dogs with nasal aspergillosis.

Veterinary Radiology and Ultrasound 2002; 42: 5-9.

I. Gielen, H. van Bree, B. Van Ryssen, T. De Clercq.

The use of computerized tomography (CT) in tarsocrural OCD in the dog: a comparison with radiography and arthroscopy.

The Veterinary Record 2002; 150: 442-447.

I. Polis, F. Gasthuys, I. Gielen, B. Van Ryssen, H. van Bree, H. Laevens, L. De Rycke.

The effects of intrathoracic pressure during continuous two-lung ventilation for thoracoscopy on the cardiorespiratory parameters in sevoflurane anaesthetized dogs.

Journal of Veterinary Medicine A 2002; 49: 113-120.

H. van Bree, I. Gielen, B. Van Rijssen, J. Saunders, M. Kramer, K. Peremans, F. Snaps.
Comparative joint imaging in small animals.
The European Journal of Companion Animal Practice 2002; 12: 25-36.

M. Risselada, M. Kramer, J. Saunders, L. Verhaert, I. Gielen.
Partial maxillectomy as a possibility to treat tumors in the upper jaw - Tumoren van de
bovenkaak en partiële maxillectomy als behandelingsmogelijkheid.
Vlaams Diergeneeskundig Tijdschrift 2002; 71: 378-395.

L. De Rycke, I. Gielen, H. van Bree, P. Simoens.
Computed tomography of the elbow joint in clinically normal dogs.
American Journal of Veterinary Research 2002; 63: 1400-1407.

I. Gielen, A. Van Caelenberg, H. van Bree.
Computed tomography (CT) in small animals: Part 1: Technical aspects.
Vlaams Diergeneeskundig Tijdschrift. In press 2003.

I. Gielen, H. van Bree.
Computed tomography (CT) in small animals: Part 2: Clinical applications.
Vlaams Diergeneeskundig Tijdschrift. In press 2003.

Saunders J.H., van Bree H., Gielen I., de Rooster H.
Computed tomography in dogs with chronic nasal disease.
Veterinary Radiology and Ultrasound. In press 2003.

Lieve M. De Rycke, Jimmy H. Saunders, Ingrid M. Gielen, Henri J. van Bree.
Magnetic resonance imaging, computed tomography and cross sectional anatomy of the
normal canine nasal cavities and paranasal sinuses in the mesaticephalic dog.
American Journal of Veterinary Research. In press 2003.

I. Gielen, H. van Bree.
Computed tomography compared with radiography in the diagnosis of tarsocrural
osteochondrosis of the lateral trochlear ridge in the dog.
The Veterinary and Comparative Orthopaedics and Traumatology. Accepted 2003.

CHAPTER/BOOK

Kompendium der allgemeinen Veterinärchirurgie, Kramer (Hrsg.)
3. Bildgebende Verfahren, 3.3 Computertomographie (CT), I. Gielen und H. van Bree.
Kramer M. (ed.), Schlütersche Verlag, Hannover, Deutschland. In press 2003.

COMMUNICATIONS/PROCEEDINGS PRESENTED DURING INTERNATIONAL SCIENTIFIC MEETINGS

H.van Bree, B.Van Ryssen, I.Gielen.

Diagnostic imaging of the canine shoulder, including arthrography, magnetic resonance imaging (MRI), computerized tomography (CT) and arthroscopy.

Proceedings Seventh Annual Meeting of the European College of Veterinary Surgery, June 26-28, 1998, Pörschach, Austria, 107-110.

H. van Bree, I. Gielen, L. De Rycke, B. Van Ryssen. .

Computerized tomography (CT) of the canine tarsal joint.

Proceedings 3e Berliner Kleintiersymposium, Erkrankungen der Hintergliedmasse und Therapie, 7-8 November 1998, Berlin University, Germany, 94-95.

I. Gielen, B. Van Ryssen, H. van Bree. .

Thoracoscopy: normal thoracoscopic anatomy in the dog.

Proceedings 5th MIS, European Surgical Institute, 10 November 1998, Norderstedt (Hamburg), Germany.

B. Van Ryssen, H. van Bree, I. Gielen.

Arthroscopy in the dog: elbow and shoulder.

Proceedings Fourth International Workshop for Small Animal Arthroscopy, basic course and advanced course January 2000, Ghent University, Belgium.

B.Van Ryssen, H.van Bree, I.Gielen.

Arthroscopy in the canine elbow and shoulder.

Proceedings Bewegungsstörungen der Vordergliedmasse bei Hund und Katze.

VIII. BPT-Intensivfortbildung Kleintierpraxis. 25-27 Februar 2000, Stadthalle Bielefeld, Deutschland, 79-87.

H. van Bree, B. Van Ryssen, I. Gielen.

Diagnostic and Surgical Arthroscopy in Small Animals.

Proceedings: Dusseldorf 46. Jahreskongress der FK-DVG. 9-12 November 2000, CCD, Düsseldorf, Germany, 83-88 and 57-60.

H. van Bree, B.Van Ryssen, I.Gielen.

Nutzungen von Arthroscopie bei Diagnose und Behandlung von Schulter OCD.

Proceedings V Berliner Kleintiersymposium: Lahmheiten der Vordergliedmasse und Therapie, Kleintierklinik der FU Berlin, 25-26 November 2000, University of Berlin, Germany, 16-17 and 80-81.

H.van Bree, B.Van Ryssen, I.Gielen.

Diagnostische und therapeutische Arthroscopie des Ellenbogengelenks.

Proceedings V Berliner Kleintiersymposium: Lahmheiten der Vordergliedmasse und Therapie, Kleintierklinik der FU Berlin, 25-26 November 2000, Berlin, Germany, 33-34 and 78-79.

B.Van Ryssen, H.van Bree, I.Gielen.

Ellbogen und Schulterarthroscopie. Proceedings V Berliner Kleintiersymposium: Lahmheiten der Vordergliedmasse und Therapie, Kleintierklinik der FU Berlin, 25-26 November 2000, Berlin, Germany, 29-32 and 82-85.

B. Van Ryssen, H. van Bree, I. Gielen.

Diagnostic and Surgical Arthroscopy in Small Animals. Proceedings Fifth International Workshop for Small Animal Arthroscopy, basic course, January 26-27th, 2001, Ghent University, Belgium.

H. van Bree, I. Gielen.

The use of computed tomography (CT) in hind limb disorders in the dog.

Proceedings IX BPT Intensivfortbildung Kleintierpraxis: Bewegungsstörungen der Hintergliedmasse bei Hund und Katze, 23-25 Februar 2001, Stadthalle Bielefeld, Deutschland, 20-25. Einsatz der Computer Tomographie (CT) bei Erkrankungen der Hinterhand des Hundes, 189-194.

H. van Bree, I. Gielen, B. Van Ryssen, J. Saunders, K. Peremans, F. Snaps.

Comparative imaging in joint disease including radiology, CT, MRI and arthroscopy. Proceedings FECAVA 2001, 25-28 October, Berlin, Germany, p 51-53.

H. van Bree, B. Van Ryssen, I. Gielen .

Progression of degenerative joint disease after arthroscopic treatment of OCD
Proceedings FECAVA 2001, 25-28 October, Berlin, Germany, p 54-56.

H. van Bree, B. Van Ryssen, I. Gielen.

Progression of degenerative joint disease after arthroscopic treatment of OCD. Proceedings Sixth International Workshop for Small Animal Arthroscopy, advanced course, January 18-19th, 2002, Ghent University, Belgium.

H. van Bree, I. Gielen, K. Peremans, J. Saunders, F. Snaps.

Brain Imaging in Older Dogs.

Proceedings: Hill's European Symposium on Canine Brain Ageing. Barcelona, Spain, 11-13 March, 2002, p 18-21.

I. Gielen, H van Bree.

CT-examination of the canine elbow: Techniques and normal anatomy.

Proceedings 1. Düsseldorf Vet-Imaging-Day. 1. Düsseldorf Symposium für "Bildgebende Diagnostik in der Kleintiermedizin" Saturday, 1st of June 2002, Düsseldorf, Germany, p23-24.

I. Gielen, H van Bree.

Computerized tomography (CT) in canine elbow disease.

Proceedings 1. Düsseldorf Vet-Imaging-Day. 1. Düsseldorf Symposium für "Bildgebende Diagnostik in der Kleintiermedizin" Saturday, 1st of June 2002, Düsseldorf, Germany, p27-28.

I. Gielen, I. Polis, B. Van Ryssen, L. De Rycke, H van Bree.

Thoracoscopy beim hund: Material, Technik und normale Anatomie.

Berliner Kleintierforum, Endoskopie Seminar I, 22-23 Juni 2002, Kleintierklinik der FU, Universität Berlin, Berlin, Deutschland.

B. Van Ryssen, I. Gielen, H van Bree.

Arthroscopy in the dog. Berliner Kleintierforum, Endoskopie Seminar I, 22-23 Juni 2002, Kleintierklinik der FU, Universität Berlin, Berlin, Deutschland.

H. van Bree, B. Van Ryssen, I. Gielen.

Progression of DJD after arthroscopic treatment of OCD, a surgical complication?

Proceedings 11th Annual Scientific Meeting ECVS. University of Veterinary Medicine, Vienna, Austria, 5-7 July, 2002, p 295-297.

B. Van Ryssen, H. van Bree, I. Gielen.

Elbow and Shoulder Arthroscopy: Second looks and Special cases. Old diseases thru new eyes, ACVS San Diego, USA, 17-21 October, 2002.

H. van Bree, B. Van Ryssen, I. Gielen.

Arthroscopy of The Canine Hock joint. Old diseases thru new eyes, ACVS San Diego, USA, 17-21 October, 2002.

H. van Bree, B. Van Ryssen, I. Gielen.

Incongruity of the Elbow joint. Old diseases thru new eyes, ACVS San Diego, USA, 17-21 October, 2002.

I. Gielen, B. Van Ryssen, H. van Bree.

Incongruity of the elbow joint. "Eleventh International Workshop for Small Animal Arthroscopy, basic course", January 17-18th, 2003, Department of Medical Imaging of Animals, Faculty of Veterinary Medicine, Ghent University, Merelbeke, Belgium.

B. Van Ryssen, H. van Bree, I. Gielen.

Elbow and shoulder arthroscopy: Second looks and special cases. "Twelfth International Workshop for Small Animal Arthroscopy, refresher course", January 31st-February 1st, 2003, Department of Medical Imaging of Animals, Faculty of Veterinary Medicine, Ghent University, Merelbeke, Belgium, p 31-32.

I. Gielen, B. Van Ryssen, H. van Bree.

Computerized tomography (CT) related to arthroscopy in canine elbow disease. "Twelfth International Workshop for Small Animal Arthroscopy, refresher course", January 31st-February 1st, 2003, Department of Medical Imaging of Animals, Faculty of Veterinary Medicine, Ghent University, Merelbeke, Belgium, p 33-35.

H. van Bree, B. Van Ryssen I. Gielen.

Arthroscopy of the canine hock joint. "Twelfth International Workshop for Small Animal Arthroscopy, refresher course", January 31st-February 1st, 2003, Department of Medical Imaging of Animals, Faculty of Veterinary Medicine, Ghent University, Merelbeke, Belgium, p 36-40.

COMMUNICATIONS/ABSTRACTS PRESENTED DURING INTERNATIONAL SCIENTIFIC MEETINGS

I. Gielen, T. De Clercq, B. Van Ryssen, H. van Bree.

The use of computerised tomography (CT) in tarsocrural OCD in the dog. European Association of Veterinary Diagnostic Imaging (EAVDI), 5th Annual Conference, August 26-29, 1998, Balsta, Sweden, 0915-014. Veterinary Radiology and Ultrasound 1999; 40: 190.

I. Gielen, L. De Rycke, T. De Clercq, H. van Bree.

Computerized tomography of the normal tarsal joint in a dog. EAVDI, 5th Annual Conference, August 26-29, 1998, Bälsta, Sweden, 31. Veterinary Radiology and Ultrasound 1999; 40: 190.

B. Van Rysen, I. Gielen, H. van Bree.

Erfolg nach diagnostischer Arthroscopie und Gelenkspüllung bei FCP im Ellbogengelenk.. 44. Jahrestagung der FK-DVG, 19-22 November 1998, Stuttgart, Deutschland, 84.

V. Biourge, I. Gielen, M.R. Slater, H. van Bree.

Evaluation of diet and exercise as risk factors for osteochondrosis dissecans in dogs. European College of Veterinary Surgery, July 2-4, 1999, Brugge, Belgium, 93.

I. Gielen, B. Van Ryssen, T. De Clerq, H. van Bree.

The use of computerized tomography (CT) in tarsocrural OCD in the dog.

8th Annual Scientific Meeting, European College of Veterinary Surgery, July 2-4, 1999, Brugge, Belgium, 95-97.

L. De Rycke, I. Gielen, B. Van Ryssen, H. van Bree, P. Simoens.

Thoracoscopy: normal intrathoracic anatomy in the dog.

European College of Veterinary Surgery, July 2-4, 1999, Brugge, Belgium, 108.

Zonderland J.L., Saunders J.H., Gielen I., Clercx C., Snaps F.R., Dondelinger R.F.

Relationship between disease duration, physical examination, rhinoscopic and computed tomographic findings in canine nasal aspergillosis.

6th Annual Conference of the European Association of Veterinary Diagnostic Imaging (EAVDI), July 5-9, 1999, Vienna, Austria, 21.

Veterinary Radiology and Ultrasound 1999; 40: 533-534.

B. Van Ryssen, I. Gielen, A. Moritz, T. Spillmann. 1999.

Rhinoscopy: Experiences with rostral and retrograde rhinoscopy.

45. Jahrestagung der DVG-FK, 7-10 October 1999, Giessen, Germany.

B. Van Ryssen, H. van Bree, I. Gielen. 2000.

Arthroscopic treatment of elbow dysplasia (FCP): the Belgian experience.

Advanced arthroscopy in dogs: current experiences in Belgium;

10th Annual European Society of Veterinary Orthopaedics and Traumatology Congress (ESVOT), March 24-26th, 2000, Munich, Germany, 99.

JH. Saunders, JL. Zonderland, I. Gielen, C. Clercx, FR. Snaps, H. van Bree, RF. Dondelinger. 2000.

Canine nasal aspergillosis: CT findings in 25 patients.

43rd Annual Congress, British Small Animal Veterinary Association, April 6-9, 2000 Birmingham, UK, 281.

I. Gielen, B. Van Ryssen, H. van Bree.

The use of computerized tomography (CT) in tarsocrural OCD in the lateral ridge of the dog.

12th Meeting International Veterinary Radiology Association, Obihiro University of

Agriculture and Veterinary Medicine, August 21-25, 2000, Obihiro, Hokkaido, Japan, 29.

Veterinary Radiology and Ultrasound 2001; 42: 174.

- K.Peremans, P. De Bondt, K. Audenaert, K. Van Laere, I. Gielen, M. Koole, J. Versijpt, H. van Bree, F. Verschooten, R. Dierckx.
Normal database of canine regional perfusion measured with technetium-99m ethylcysteinate dimer. 12th Meeting International Veterinary Radiology Association, Obihiro University of Agriculture and Veterinary Medicine, August 21-25, 2000, Obihiro, Hokkaido, Japan, 30.
Veterinary Radiology and Ultrasound 2001; 42: 175.
- K.Peremans, P. De Bondt, K. Audenaert, I. Gielen, K. Van Laere, M. Koole, J. Versijpt, C. De Cupere, F. Verschooten, H. van Bree, R. Dierckx.
Regional analysis and inter-subject variability of perfusion in normal canine brain measured with ^{99m}Tc-ECD-brain SPECT.
EANM congress Parijs, September 2-6, 2000, Paris, France, 1103.
European Journal of Nuclear Medicine 2000; 27: 1103.
- J.H. Saunders, F.R. Snaps, C.K. Störk, I. Gielen, C. Clerx, T. Schwarz, H. van Bree, R.F. Dondelinger.
Computed Tomographic features of canine nasal aspergillosis.
American College of Veterinary Radiology, 2000 Annual Scientific Meeting Chicago, Illinois, USA, November 29th- December 2nd, 2000.
Veterinary Radiology and Ultrasound 2000; 41: 579.
- I. Gielen, B. Van Ryssen, J. Buijtels, R. Lückerrath, H. van Bree.
Canine elbow incongruity evaluated with Computed tomography (CT), Radiography and Arthroscopy. 7th Annual Conference, European Association for Veterinary Diagnostic Imaging, July 18-21, 2001, Paris, France, p 22.
- J. H.Saunders, H. van Bree, I. Gielen.
Comparison between radiography and computed tomography for diagnosis of canine nasal aspergillosis. Voorjaarsdagen, 26-28 april 2002, Amsterdam, The Netherlands, p 251.
- I. Gielen, H. van Bree, B. Van Rijssen, F. Coopman.
Prognostic value of CT findings in minimal invasive treatment of tarsocrural OCD in the dog. 9th Annual Conference EAVDI (European Association of Veterinary Diagnostic Imaging), 24-27th July 2002, Archena (Murcia), Spain. p 75.
Veterinary Radiology and Ultrasound 2003; 44: 253.
- L. De Rycke, J. Saunders, I. Gielen, H. Van Bree, P. Simoens.
Computerized tomography (CT) and magnetic resonance (MR) anatomy of the normal canine nasal cavity and frontal sinuses. 9th EAVDI (European Association of Veterinary Diagnostic Imaging) Annual Conference, Archena (Murcia), Spain, 24-27 July, 2002. p 100.
Veterinary Radiology and Ultrasound 2003; 44: 233.

L. De Rycke, I. Gielen, H. Van Bree, P. Simoens.

Computerized tomography (CT) and magnetic resonance imaging (MRI) of the normal canine elbow. 9th EAVDI (European Association of Veterinary Diagnostic Imaging) Annual Conference, Archena (Murcia), Spain, 24-27 July, 2002. p 101.

Veterinary Radiology and Ultrasound 2003; 44: 233.

Gielen I., van Bree H., Coopman F.

Comparison of morphological and clinical features between medial and lateral canine tarsocruralosteochondrosis lesions. Tri-Annual Meeting International Veterinary Radiology Association, South Africa. Accepted 2003.

van Bree H., Gielen I., Van Ryssen B., Saunders J.

Computed tomographic (CT) features of elbow OCD compared with radiography and arthroscopy. Tri-Annual Meeting International Veterinary Radiology Association, South Africa. Accepted 2003.

INVITED SPEAKER AT INTERNATIONAL MEETINGS

Thoracoscopy: normal thoroscopic anatomy in the dog, 5th MIS, European Surgical Institute, November 10th, 1998, Norderstedt (Hamburg), Germany.

The application of computer tomography (CT) in small animals, Mai 8th, 2000, Justus-Liebig-Universität Giessen, Germany.

Computed tomography in the diagnosis of joint pathology in the dog. Mai 10th, 2000, Justus-Liebig- Universität Giessen, Germany.

Computerized tomography (CT) in canine elbow disease. I. Gielen, H. van Bree.

Dusseldorfer Vet-Imaging-Day. 1. Dusseldorfer Symposium für "Bildgebende Diagnostik in der Kleintiermedizin" Saturday, 1st of June 2002, Dusseldorf, Germany.

Thoracoscopie beim Hund: Material, Technik und normale Anatomie. I. Gielen, B. Van Rijssen, H. van Bree. Berliner Kleintierforum, Endoskopie Seminar I, 22-23 Juni 2002, Kleintierklinik der FU, Universität Berlin, Deutschland.

Computed tomography of the canine shoulder joint. Dusseldorfer Vet-Imaging-Day.

Dusseldorfer Symposium für "Bildgebende Diagnostik in der Kleintiermedizin" Dusseldorf, Germany, October 2003.

SCIENTIFIC AWARDS

Award for best oral presentation: The use of computerized tomography (CT) in tarsocrural OCD in the lateral ridge of the dog, I. Gielen, B. Van Ryssen, H. van Bree. 12th Meeting International Veterinary Radiology Association, Obihiro University of Agriculture and Veterinary Medicine, Obihiro, Hokkaido, Japan, August 21-25, 2000.

Genomineerd voor “The IAMS Compagny Award 2002”: The use of computerized tomography (CT) in tarsocrural OCD in the dog: a comparison with radiography and arthroscopy. I. Gielen, H. van Bree, B. Van Ryssen, T. De Clercq.